FIRST LASING OF THE IR FEL AT THE FRITZ-HABER-INSTITUT, BERLIN

W. Schöllkopf, S. Gewinner, W. Erlebach, G. Heyne, H. Junkes, A. Liedke, V. Platschkowski, G. von Helden, W. Zhang, G. Meijer, Fritz-Haber-Institut der Max-Planck-Gesellschaft, Berlin, Germany
H. Bluem, M. Davidsaver*, D. Dowell*, K. Jordan*, R. Lange*, H. Loos*, J. Park, J. Rathke, A.M.M. Todd, L.M. Young*, Advanced Energy Systems, Medford, NY, USA
U. Lehnert, P. Michel, W. Seidel, R. Wünsch, HZDR, Rossendorf, Germany
S.C. Gottschalk, STI Optronics, Bellevue, WA, USA

Abstract

A new mid-infrared FEL has been commissioned at the Fritz-Haber-Institut in Berlin. The oscillator FEL operates with 15 – 50 MeV electrons from a normal-conducting S-band linac. Calculations of the FEL gain and IR-cavity losses predict that lasing will be possible in the wavelength range from less than 4 to more than 50 µm. First lasing was achieved at a wavelength of 16 µm with an electron energy of 28 MeV. At these conditions, lasing was observed over a cavity length scan range of 100 µm.

INTRODUCTION

At the Fritz-Haber-Institut in Berlin, Germany, a new IR and THz FEL has been commissioned for applications in gas-phase spectroscopy of (bio-)molecules, clusters, and nano-particles, as well as in surface science [1-3]. To cover the wavelength range of interest from about 4 to 500 µm, the system design, shown in Fig. 1, includes two FELs; a mid-infrared (MIR) FEL for wavelengths up to about 50 µm and a far-infrared (FIR) FEL for wavelengths larger than about 40 µm. A normal conducting S-band linac provides electrons of up to 50 MeV energy to either FEL.

As of August 2012, installation of the accelerator and electron-beam transport system (designed and installed by Advanced Energy Systems, Inc.) [4,5], the MIR undulator (STI Optronics) [6], and the MIR oscillator mirror optical equipment (Bestec GmbH) is complete and commissioning is ongoing, whereas the FIR FEL has not yet been installed. In this paper, after a brief summery of the electron accelerator, we describe the design of the MIR FEL and report on results from first lasing achieved on February 14th, 2012.

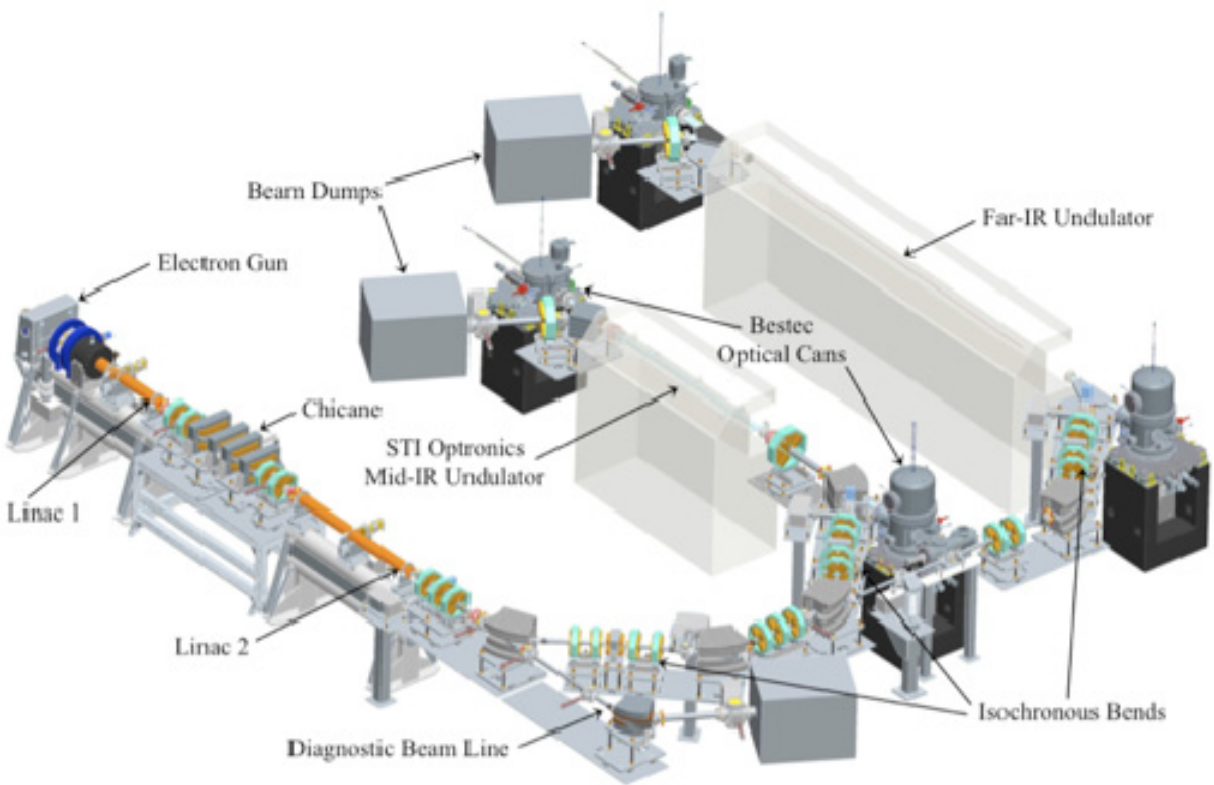

Figure 1: Schematic overview of the infrared free-electron laser at the Fritz-Haber-Institut.

* Consultants to AES

ISBN 978-3-95450-123-6

PROGRESS IN SACLA OPERATION

Toru Hara#, Kazuaki Togawa, Hitoshi Tanaka
RIKEN SPring-8 Center/XFEL Research and Development Division, Hyogo 679-5148, Japan

Abstract

In March 2012, SACLA was open to public users. Currently, 100-400 μJ laser pulses in a photon range between 5 and 15 keV are provided to the user experiments. Since SACLA employs variable-gap in-vacuum undulators, users can freely change the undulator gap to finely adjust the photon energy.

While the first lasing was achieved at 10 keV after several months of machine commissioning, the pulse energy was about 30 μJ, which was lower than a design value. In the autumn of 2011, we intensively worked on the reduction of a projected emittance, then 120 μJ was routinely obtained at 10 keV. After cathode replacement in the winter shutdown, we re-tuned the accelerator using higher energy beams with increased undulator K-values. Currently the pulse energy at 10 keV reaches 250 μJ. The stability of the accelerator, particularly the injector section, has been improved. Intensity fluctuations of 10-20 % (σ) are achieved during day-to-day operation. Since the floor of the undulator hall still moves by 50 μm in 2 months, the beam orbit at the undulator section is realigned every two weeks to maintain the FEL performance.

In this paper, we will report the recent progress of the SACLA laser performance and operation.

INTRODUCTION

Since March 2012, SACLA has provided intense X-rays to public user experiments. Fig. 1 is a schematic of the SACLA facility. 18 undulators are installed in the center beamline (BL3) as an XFEL light source in the present phase [1].

The accelerator has been operated using a basic parameter set determined from a 1-D model and 3-D simulations. However, final optimization of the parameters with observing FEL outputs is indispensable, since there are errors on RF parameters, component alignments and the limitations of simulation accuracy, like space charge and CSR effects.

In this paper, the improvement of the SACLA electron beam performance since the beginning of the beam commissioning is described.

OPTIMIZATION OF A PROJECTED EMITTANCE

The pulse energy obtained at the time of the first lasing in June 2011 was around 30 μJ at 10 keV with 7 GeV beams and K=1.8, which was lower than the expected value [2]. The main reason for this low pulse energy was supposed that only a small number of electrons contribute to the FEL amplification in the entire electron bunch.

Different from a photo-cathode based RF gun system, the injector of SACLA uses a traditional buncher-booster system with a thermionic high-voltage pulsed gun. The thermionic cathode electron gun of SACLA has advantages over an RF photo-cathode gun, such as uniform emission, a long cathode lifetime and maintenance-free operation [3]. On the other hand, the emission current is small as 1 A. In order to increase a peak current, the electron bunch is compressed in the injector by velocity bunching. For that, it is required to transport a low-energy electron bunch having a large energy chirp more than 5 m in the SACLA injector. Since the divergence of this low-energy beam due to the space charge is compensated by magnetic lenses, chromatic aberration varies a betatron phase inside the bunch resulting in the increase of a projected emittance. Although a slice emittance, which is directly connected to the FEL gain, maintains its small initial value, the increased projected emittance degrades the transverse envelope matching inside the undulator section and consequently limits the number of electrons contributing to the FEL amplification. The normalized projected emittance measured at the time of the first lasing was about 2~3 mm-mrad, which is about 5 times larger than the initial emittance of the gun.

In September 2011, the bunch charge was first augmented from 130 pC to 280 pC to increase the total number of electrons. Then the injector parameters are tuned to decrease the projected emittance.

In SACLA, the projected emittance is measured by a Q-magnet scan method using a single YAG screen. To avoid the contamination of coherent OTR, which degrades measurement reliability, a spatial mask is inserted in the focusing optics, and its shape, size and position were optimized. Also a focal length was carefully adjusted using a real beam profile. Fig. 2 is the observed beam size as a function of the CCD camera position. The CCD position was initially determined by an offline alignment using a reference plate placed at the position of the YAG screen. However the result of the online alignment using an electron beam profile revealed that the offline alignment was out of focus by a few hundreds of microns. After the improvements of the Q-magnet scan system, the measurements of the projected emittance became accurate and reliable with a reproducibility of ±10 %.

The projected emittances were measured after the first bunch compressor (BC1) and the final bunch compressor (BC3). After the optimization of the injector parameters, the normalized emittance was reduced to around 1.5 mm-mrad, which is almost half of the previous values before optimization, with a higher bunch charge.

#toru@spring8.or.jp

ISBN 978-3-95450-123-6

SWISSFEL, THE X-RAY FREE ELECTRON LASER AT PSI

H.H. Braun on behalf of the SwissFEL team
Paul Scherrer Institut, Villigen-PSI, Switzerland

Abstract

PSI prepares the construction of an X-ray free-electron laser, SwissFEL, as its next major research facility. The baseline design consists of a 5.8 GeV linear accelerator and two FEL lines covering the wavelength range from 0.1-0.7 nm and 0.7-70 nm, respectively. SwissFEL features a linear accelerator in C-band technology, a novel design of variable gap in-vacuum undulators for the hard X-ray FEL and Apple II undulators with full polarization control for the soft X-ray FEL. The two FELs are operated independently and simultaneously with 100 Hz pulse rate each. In addition to the FEL performance goals SwissFEL aims for low overall energy consumption. Linac parameters as well as the cooling systems are optimized towards this goal. For the whole facility a staged construction is planned, with groundbreaking in spring 2013. The commissioning of the linear accelerator and the hard X-ray FEL will start in 2016. An overview of SwissFEL goals, status, and plans is given and the SwissFEL R&D activities are reviewed.

OVERVIEW

Since the last status reports at FEL conferences [1,2], the SwissFEL design has matured and stabilized towards construction of the facility. Preparation of the building site and procurement of major components has begun, with groundbreaking for the buildings scheduled for early 2013. All key parameters and most modifications have been included in a final update of the design report [3]. The design is driven by the following requirements

- wavelength coverage from 1-70 Å with very good timing resolution and stability in the order of 10 fs for the range of science as described in [4,5]
- a tight overall budget frame
- construction site in the vicinity of PSI with less than 800 m facility length
- constraints for power consumption and power dissipation

Figure 1 shows an overview of the facility and table 1 the project schedule until first operation of the hard X-ray FEL (1-7Å) named "ARAMIS". The building has all necessary provisions for the second, soft X-ray FEL "ATHOS" with 7-70Å wavelength range. The procurement of ATHOS components will happen in a later budget phase after 2016.

INJECTOR

A test version of the SwissFEL injector consisting of a photocathode RF gun, 4 S-band RF cavities, an X-band harmonic cavity, the first bunch compressor, and a diagnostics section for the characterisation of projected emittance, slice emittances and longitudinal phase space has been set-up at PSI and is used for SwissFEL beam dynamics studies and component development [6]. All components are now operational with the exception of the RF power source for the harmonic cavity [7]. Commissioning of this power source is expected for early autumn this year. Very good emittance figures, compliant with the SwissFEL design, have been measured, covering the two extremes of the SwissFEL bunch charge range [8,9]. A summary of the results is listed in table 2.

A new RF gun capable of running at 100 Hz with improved beam dynamics properties [10] will be installed in the course of 2013. Further plans for the facility include a test of a full fledged undulator prototype with beam.

The injector test facility will be dismantled in late 2014 for reuse of its components in SwissFEL. To mitigate effects of microbunching instability [11], a laser heater will be will be integrated in the final injector configuration for SwissFEL with an undulator designed by ASTeC/Daresbury. Two more S-band and one more X-band structure will be added for a beam energy of 350 MeV in BC1.

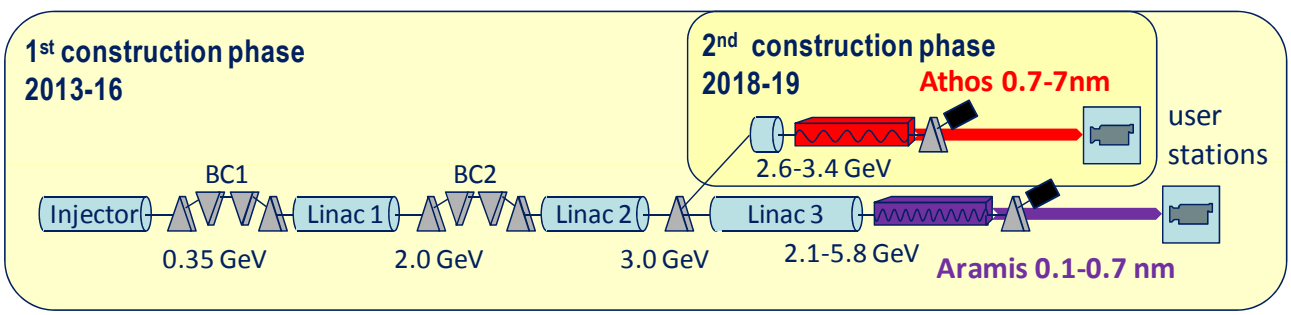

Figure 1: Schematic of SwissFEL.

ISBN 978-3-95450-123-6

FIRST LASING OF FERMI FEL-2 (1° STAGE) AND FERMI FEL-1 RECENT RESULTS*

L. Giannessi[1,7], E. Allaria[1], L. Badano[1], D. Castronovo[1], P. Cinquegrana[1], P. Craievich[1,6], M. B. Danailov[1], G. D'Auria[1], A. Demidovitch[1], G. De Ninno[1,2],S. Di Mitri[1], B. Diviacco[1], W. M. Fawley[1], E. Ferrari[1,2], L. Froehlich[1], G. Gaio[1], R. Ivanov[1], E. Karantzoulis[1], B. Mahieu[1,2,3], N. Mahne[1], I. Nikolov[1], F. Parmigiani[1,5], G. Penco[1], L. Raimondi[1], C. Serpico[1], P. Sigalotti[1], S. Spampinati[1,2], C. Spezzani[1], M. Svandrlik[1], C. Svetina[1], M. Trovò[1], M. Veronese[1], D. Zangrando[1], M. Zangrando[1,4]

[1] Sincrotrone Trieste S.C.p.A., Area Science Park, S.S. 14 Km 163.5, I-34149 Trieste, Italy
[2] University of Nova Gorica, Nova Gorica, Slovenia
[3] DSM/DRECAM/SPCSI, CEA, Saclay F-91191 Gyf sur Yvette, Cedex, France
[4] IOM-CNR, Trieste, Italy, [5] Università degli Studi di Trieste, Trieste, Italy
[6] PSI, Villigen, Switzerland, [7] ENEA C.R. Frascati, Via E. Fermi 45, 00044 Frascati, Italy

Abstract

The FERMI@Elettra seeded Free Electron Laser (FEL) is based on two complementary FEL lines, FEL-1 and FEL-2. FEL-1 is a single stage cascaded FEL delivering light in the 80-20 nm wavelength range, while FEL-2 is a double stage cascaded FEL where the additional stage should extend the frequency up-conversion to the spectral range of 20-4 nm. The FEL-1 beam line is in operation since the end of 2010, with user experiments carried on in 2011 and 2012. During 2012 the commissioning of the FEL-2 beam line has started and the first observation of coherent light from the first stage of the cascade has been demonstrated. In the meanwhile, the commissioning of a number of key components of FERMI, as the laser heater, the X-Band cavity for the longitudinal phase space linearization and the high energy RF deflector, has been completed. The additional control on the longitudinal phase space and a progressive improvement in the machine optics optimization, had a significant impact of FEL-1 performances, which has reached the expected specifications. In addition, emission of radiation at very high order conversion factors (up to 29th) has been observed from FEL-1 and schemes based on double stage cascades have been preliminarily tested, with the observation of coherent radiation up to the 65th harmonic of the seed drive laser, at about 4.1 nm in the water window.

INTRODUCTION

FERMI@Elettra (Fermi) is a fourth generation light FEL source, under commissioning at the Elettra laboratory in Trieste. The scientific case driving the design of the FEL is based on three experimental programs, namely *Diffraction and Projection Imaging* (DiProI), *Elastic and Inelastic Scattering* (EIS), *Low Density Matter* (LDM). The experiments require high peak brightness, fully coherent, narrow and stable bandwidth photon pulses, wavelength tunability and variable polarization: circular and linear [1]. The FEL, constructed to accomplish those requests, is based on two separated beam lines, FEL-1 and FEL-2 and will produce photons in the ultraviolet and soft X-ray range, between 15 eV and 310 eV. The first beam line, FEL-1, is a single stage cascaded FEL delivering light in the 80-20 nm wavelength range [2]. It is in operation since the end of 2010, with user experiments carried on during 2011 and 2012. The second beam line, FEL-2, is a double stage cascaded FEL where the additional stage should extend the wavelength operation range, down to 20-4 nm. The source of electrons is based on a high brightness photocathode RF gun. The electron beam is then accelerated in a normal conducting, traveling wave linac, working at 3 GHz RF frequency and 10 Hz (will be upgraded to 50 Hz in 2013) repetition rate [3]. The electron beam energies for FEL-1 and FEL-2 are respectively 1.2 and 1.5 GeV. Two stages of magnetic compression are used to get extremely short electron bunches (less than 1 ps) with high peak current. During 2012 a number of important components of the machine have been commissioned, as the laser heater [4], the fourth harmonic RF structure (12 GHz, X-band) [5] providing the longitudinal phase space linearization needed to optimize the compression process and the high energy RF-deflector [6], allowing to monitor the beam longitudinal phase space at the end of the linac. The FEL is seeded by an external UV laser in the range 230-260 nm. Frequency tuning of the drive laser ensures a continuous tuning of the FEL output wavelength, around a given, desired order of harmonic conversion. The first stage of the two FEL lines is made up by a modulator, where the electron beam is seeded by the UV external laser, a dispersive bunching section, where energy modulation is converted into density modulation, and by a radiator made by six undulator for FEL-1, and two undulators for FEL-2. In FEL-2 a second stage of modulator-dispersive section-radiator follows the first. The two stages of FEL-2 are separated by a chicane for shifting the radiation emitted in the first stage onto fresh

*Work supported in part by the Italian Ministry of University and Research under grants FIRB-RBAP045JF2 and FIRB-RBAP06AWK3

ISBN 978-3-95450-123-6

GROWTH RATES AND COHERENCE PROPERTIES OF FODO-LATTICE BASED X-RAY FREE ELECTRON LASERS

S. Reiche and E. Prat *
Paul Scherrer Institute, Villigen, Switzerland

Abstract

Most hard X-ray Free Electron Lasers are designed with a super-imposed FODO lattice to focus the electron beam for optimum performance of the FEL. Theory predicts an optimum value of the beta-function, where the induced axial velocity spread starts to counteract the increased Pierce-parameter due to higher electron density. However in a FODO lattice the electron beam envelope varies significantly and disrupts the coupling of the electron beam to the radiation field. This is particularly relevant for hard X-ray FELs, where the radiation mode is smaller than the electron beam size. In this presentation we study the impact of the FODO cell length and the beta-function variation on the FEL gain length and growth of the coherence properties for SASE FELs.

INTRODUCTION

Free-electron lasers in the soft and hard X-ray regime require a sufficiently high electron density for the shortest gain length and an overall reasonable requirement for the undulator length. This cannot be provided by the natural focusing of the undulator field [1], which vanishes with higher beam energies. Therefore all operating and planned X-ray FELs [2] utilize quadrupoles in a FODO lattice to focus the beam. Because the beam orbit is much more sensitive to quadrupole misalignment than undulator misalignment, the quadrupoles are placed in drift sections between undulators. It is easier to align the quadrupoles alone than entire undulator modules with integrated quadrupoles.

The variation in the beam size along the undulator violates the assumption of a rigid beam in most 3D FEL theories [3]. It is impossible to obtain a fully analytical solution because the length of the FODO cell can be comparable or shorter than the characteristic length of the FEL amplification: the gain length. However simulations, which derive their results on a more basic set of equations with less assumptions on the beam transport, can give an insight on the effect of the explicit focusing on the FEL performance.

We ran simulations with Genesis 1.3 [4] to study this effect. While similar studies have been done for the FEL output power [5, 6], none of these publications include the aspect of coherence growth for SASE FELs. We studied the impact of the FEL power and the coherence for operation at 1 and 10 Ångstrom, based on SwissFEL facility layout[7]. The latter case exhibits stronger diffraction and any fine structure in the transverse electron beam distribution will be washed out stronger, implying less impact from the FODO lattice than for the former case.

* sven.reiche@psi.ch

3D FEL THEORY AND FEL MODES

In the 3D theory the FEL equations are scaled differently, resulting in a definition of the FEL parameter [3], which deviates from the standard 1D FEL parameter ρ [8]. In addition, a new independent parameter is introduced, expressing the ratio between the characteristic scaling length and the length of diffraction (Rayleigh length). It is called the Diffraction parameter [3], where a large value indicates negligible effects from diffraction.

The FEL equation is transformed into a form very similar to that of a 2D field equation in quantum mechanics, except that the system is not hermite. The transverse current profile plays the role of the quantum mechanical potential and for a well-defined solution the FEL wavefront has to drop faster than $\propto r^{-2}$ to avoid unphysical infinite radiation power.

The different solutions (modes) can be grouped by their number of azimuthal and radial nodes, each yielding their own dispersion equation to determine the growth rate. In a system with strong diffraction the growth rate of the fundamental mode is the strongest and the radiation mode is larger than the electron beam. With vanishing diffraction the growth rates and gain curves of all modes collapse into the one of the 1D FEL model and even a distorted wavefront is preserved during amplification. Low diffraction causes problems for SASE FELs reducing the overall transverse coherence of the FEL pulse.

In all 3D models the beam is treated radially symmetric and rigid and the effect of the betatron oscillation is expressed by any effective shift in the beam electron energy [9] . However this is not the case if a FODO based focusing structure is used to keep the beam size small along the undulator. Typically, the beam exhibits a sawtooth like variation in its beam size with its variation proportional to the spacing of the quadrupoles. Fig. 1 shows the variation in the beam size as a function for different FODO cell lengths, based on the hard X-ray FEL Aramis of the SwissFEL facility. Because the FEL eigenmode is also imprinted into the bunching profile of the electron beam any variation in the electron distribution reduces the overlap of radiation field and bunching profile. We expect a reduction in the growth rate of the mode, however it is very difficult to calculate it analytically. For this we present the numerical calculation with Genesis 1.3

ISBN 978-3-95450-123-6

ON QUANTUM EFFECTS IN SPONTANEOUS EMISSION BY A RELATIVISTIC ELECTRON BEAM IN AN UNDULATOR

G. Geloni, European XFEL GmbH, Hamburg, Germany
V. Kocharyan and E. Saldin, DESY, Hamburg, Germany

Abstract

Robb and Bonifacio (2011) claimed that a previously neglected quantum effect results in noticeable changes in the evolution of the energy distribution associated with spontaneous emission in long undulators. They revisited theoretical models used to describe the emission of radiation by relativistic electrons, and claimed that in the asymptotic limit for a large number of undulator periods the evolution of the electron energy distribution occurs as discrete energy groups according to Poisson distribution. These novel results are based on a one-dimensional model of spontaneous emission and assume that electrons are sheets of charge. However, electrons are point-like particles and the bandwidth of the angular-integrated spectrum of undulator radiation is independent of the number of undulator periods. The evolution of the energy distribution studied with a three-dimensional theory is consistent with a continuous diffusive process. We also review how quantum diffusion of electron energy in an undulator with small undulator parameter can be analyzed using the Thomson cross-section expression, unlike the conventional treatment based on the expression for the Lienard-Wiechert fields.

INTRODUCTION

In a recent article [1] it is stated that quantum effects in spontaneous emission by a relativistic electron beam in an undulator can be described by a drift-diffusion equation only when the parameter

$$\epsilon = \frac{N_w \hbar \omega}{\gamma m c^2} \,, \tag{1}$$

is much smaller than unity, where N_w is the number of undulator periods, $\hbar$ is the reduced Planck constant, ω is the photon frequency, γ the relativistic Lorentz factor, m the electron rest mass and c the speed of light. In that work it is argued that when $\epsilon \geq 1$, a drift-diffusion equation is no more sufficient to describe the the evolution of the distribution of electron momenta, which "occurs as discrete momentum groups according to a Poisson distribution".

In this paper we will show that results in [1] are incorrect, because they are based on a one-dimensional model of the spontaneous radiation emission. This model does not account for the angular distribution of the radiation, but only for the emission on axis, which is characterized by an overall relative bandwidth $\sim 1/N_w$. In contrast to this, the electron recoil related with the quantized nature of photons depends on the entire angular distribution of the radiation, which is fundamentally linked to the Thomson scattering phenomenon in the case for a small undulator parameter $K \ll 1$, [2, 3]. When the angular distribution of radiation is properly accounted for, the overall, angle-integrated relative bandwidth is independent on the number of undulator periods. As a result, it turns out that a three-dimensional drift-diffusion model is valid when the parameter

$$\zeta = \frac{\hbar \omega}{\gamma m c^2} \,, \tag{2}$$

is much smaller than unity. This means that a Fokker-Planck approach is always valid in all cases of practical interest.

In this work we will first review the spectral-angular characteristics of undulator radiation. For reasons of simplicity, from the very beginning we will consider the limit for $N_w \gg 1$ and $K \ll 1$. Our considerations can easily be applied to arbitrary values of N_w and K, but the choice of $N_w \gg 1$ and $K \ll 1$ easily allows one to underline the fundamental point that the angle-integrated spectrum of radiation does not depend on the number of undulator periods N_w. Using a Fokker-Planck equation we will derive the diffusion coefficient in agreement with [4]. Finally, the diffusion coefficient will also be derived by exploiting the relation between undulator radiation and Thomson scattering, which stresses once more the intrinsic three-dimensional nature of the radiation pattern.

The aim of this article is not that of changing, or adding anything to previous theory, but rather to defend the previous theory against the thesis formulated in[1].

SPONTANEOUS EMISSION PROCESS AND ASSOCIATED QUANTUM EFFECTS

Spectral-Angular Distribution of Radiation

As is well-known, spontaneous radiation emission from an ultrarelativistic electron in an undulator can be modeled fully classically as long as the energy of the emitted photons $\hbar\omega$ is much smaller than the electron energy γmc^2. In this case, the knowledge of the classical characteristics of radiation can easily be used to discuss quantum effects on the electron motion integrated along the trajectory.

Characteristics of spontaneous radiation have been studied long time ago in [5, 6]. In this section, we briefly review them, focusing on the particular case of a planar undulator, and following notations introduced in previous works of us [7]. In order to do so, we first call with $\vec{\tilde{E}}(\omega)$ the transverse component of the electric field generated by an electron in

ISBN 978-3-95450-123-6

GROWING MODES OF THE FREE-ELECTRON LASER AND THEIR BANDWIDTH*

G. Wang#, V. N. Litvinenko, BNL, Upton, NY 11973, U.S.A.
S. D. Webb, Tech-X Corporation, Boulder, CO 80303, U.S.A.

Abstract

We studied in detail the FEL dispersion relation for a spatially uniform electron beam, taking into account energy spread and the effects of space charge. We derived the maximum number of growing modes and the upper frequency cut-off for energy distributions satisfying a few constraints. Since the FEL dispersion relation for an infinite electron beam can be reduced to the 1D FEL dispersion relations when the radiation propagates along the undulation's axis, our analyses and findings directly are applicable to 1D FELs.

INTRODUCTION

We previously introduced a method of determining the number of growing modes and calculating their high frequency cut-off for the 1D FEL dispersion relation in the absence of the space- charge effects [1]. By allowing the radiation fields to propagate at an angle with respect to the undulator's axis, while assuming that the electrons move along constrained helical trajectories parallel with the undulator's axis, we were able to derive a dispersion relationship for a spatially uniform electron beam [2]; furthermore, it is reducible to the 1D FEL dispersion relation provided that the radiation propagates along the undulator's axis.

In this work, we started with the FEL dispersion relation we derived earlier [2] for a spatially uniform electron-beam, and investigated the number of growing modes and their high frequency cut-off , taking into account the space-charge effects. In section II, for an unspecified energy distribution satisfying certain constraints, we derive the formula for determining the maximal number of growing modes and their high frequency cut-off. Section III contains some examples where we apply the formula to several frequently encountered energy distributions and compare our results with direct numerical solutions of the dispersion relations. We summarize our findings in Section IV.

MAXIMAL NUMBER OF GROWING MODES

Assuming that electrons have a uniform spatial distribution and move along helical trajectories in parallel with the undulator's axis, the FEL dispersion relation is [2]

$$s = \left(1 + is\hat{\Lambda}_p^2\right)D(s), \qquad (1)$$

where s is the Laplace transformation-variable of the normalized longitudinal location $\hat{z} \equiv \Gamma z$,

$$\hat{\Lambda}_p \equiv \frac{1}{\Gamma}\left[\frac{4\pi j_0}{\gamma_z^2 \gamma I_A}\right]^{1/2}$$

is the space-charge parameter,

$$\Gamma \equiv \left[\frac{\pi j_0 \theta_s^2 \omega}{c\gamma_z^2 \gamma I_A}\right]^{1/3},$$

is the 1D FEL gain parameter, $I_A \equiv m_e c^3/e$ is the Alfven current, ω is the radiation frequency, v_z is the longitudinal velocity of electrons, γ_z is the Lorentz parameter for v_z, and $\hat{\Delta}_{3d} \equiv \hat{\Delta} + \hat{k}_\perp^2$ is the normalized detuning parameter defined for the radiation field propagating with a transverse angle,

$$\hat{\Delta} \equiv -\frac{1}{\Gamma}\left[k_w + \frac{\omega}{c} - \frac{\omega}{v_z}\right]$$

is the normalized detuning parameter, $k_w = 2\pi/\lambda_w$ is the undulator's wave number, $\rho = \gamma_z^2 \Gamma c/\omega$ is the Pierce parameter, and the normalized transverse wave-vector is defined as

$$\vec{\hat{k}}_\perp \equiv \sqrt{\frac{\rho}{2}}\frac{\vec{k}_\perp}{\gamma_z \Gamma}.$$

The dispersion integral in eq. (1) is defined as

$$D(s) \equiv \int_{-\infty}^{\infty} d\hat{P}\frac{d\hat{F}(\hat{P})}{d\hat{P}}\frac{1}{s + i\left(\hat{P} - \hat{\Delta}_{3d}\right)}, \qquad (2)$$

for any root of eq. (1) with $\mathrm{Re}(s) > 0$ to correspond to an exponential growing FEL instability. To explore the roots of eq. (1) with $\mathrm{Re}(s) > 0$, we define a complex function

$$w(s) \equiv s - is\hat{\Lambda}_p^2 D(s) - D(s) \qquad (3)$$

and consider a mapping from the complex s plane to the complex $w(s)$ plane along the contour $\mathcal{C}$, which comprises a vertical straight line parallel to the imaginary axis, $\mathcal{C}_1$, and a semi-circle in the right half complex plane, $\mathcal{C}_2$, as illustrated in fig. 1 (a). Fig. 1 (b) shows the map of $\mathcal{C}$ in the complex $w(s)$ plane, $\mathcal{D}$, with $\mathcal{D}_1$ and $\mathcal{D}_2$ being, respectively, the map of $\mathcal{C}_1$ and $\mathcal{C}_2$. For an energy distribution $\hat{F}(\hat{P})$ falling faster than Lorentzian distribution, we previously proved that the map from $\mathcal{C}_2$ to $\mathcal{D}_2$ has the asymptotic property

$$\lim_{|s|\to\infty}\left|\hat{D}(s)\right| \le \sqrt{2}\pi\hat{q}\hat{F}_{\max}\lim_{|s|\to\infty}\frac{1}{|s|^2}\left[1 + \frac{\hat{q}}{\mathrm{Re}(s)}\right], \qquad (4)$$

* Work supported by Brookhaven Science Associates, LLC under Contract No.DE-AC02-98CH10886 with the U.S. Department of Energy.
#gawang@bnl.gov

ISBN 978-3-95450-123-6

LASER PHASE ERRORS IN SEEDED FELS

D. Ratner, A. Fry, G. Stupakov, W. White, SLAC, Menlo Park, California 94025, USA

Abstract

Harmonic seeding of free electron lasers has attracted significant attention as a method for producing transform-limited pulses in the soft X-ray region. Harmonic multiplication schemes extend seeding to shorter wavelengths, but also amplify the phase errors of the initial seed laser, and may degrade the pulse quality and impede production of transform-limited pulses. In this paper we consider the effect of seed laser phase errors in high gain harmonic generation and echo-enabled harmonic generation. We use simulations to confirm analytical results for the case of linearly chirped seed lasers, and extend the results for arbitrary seed laser envelope and phase.

INTRODUCTION

The recent success of Self-Amplified Spontaneous Emission (SASE) Free Electron Lasers (FELs) has led to x-ray sources of unprecedented brightness [1, 2]. However, some applications still require higher power (e.g. [3, 4]), and the poor longitudinal coherence of SASE FELs can inhibit x-ray optimization and degrade experimental results. To improve control over the spectral and temporal x-ray properties, there is strong interest in seeding FELs at high harmonics of optical or UV lasers. Beamline users are particularly interested in the minimal bandwidth and simple temporal structure of transform-limited x-ray pulses.

One potentially serious issue for the seeding process is how properties of the seed laser can affect the production of transform-limited x-ray pulses. In Ref. [5] we presented a detailed study of how laser phase errors affect the final pulse characteristics. Here we present a summary of those results.

There are numerous challenges for seeding schemes, and previous theoretical and experimental studies have focused on a wide variety of accelerator and FEL requirements. In particular, it is well known that harmonic seeding schemes must contend with increasingly strict electron beam tolerances as the harmonic number increases. Initial errors that are insignificant compared to the seed wavelength may be large relative to a much shorter wavelength harmonic. For example, harmonic multiplication amplifies electron shot noise, which can overwhelm the external seeding source [6, 7, 8, 9]. More recently attention has turned to errors from the seed laser itself [5, 10, 11, 12, 13]. Without sufficient control of the initial seed laser phase, the x-ray pulse acquires longitudinal structure; if sufficiently far from the transform-limit, seeding may have little or no benefit compared to SASE FELs.

This paper focuses on the effects of laser phase errors on the seeded electron density, using both analytical methods [12] and simulations [5]. We also consider several potential techniques for measuring and controlling laser phase in the UV spectrum.

SCHEMATIC DESCRIPTION OF HARMONIC PHASE MULTIPLICATION

As a simple example of seeding, we consider a High Gain Harmonic Generation (HGHG) scheme driven by a temporally flat-top laser pulse of wavelength, λ_L. The seeding scheme bunches the electrons both at the fundamental wavevector, $k_1 = 2\pi/\lambda_L$, as well as at higher harmonics $k_H = Hk_1$, for harmonic number H.

In a non-ideal laser pulse, the wavelength varies as a function of time; i.e. the pulse has non-flat phase. As the wavelength changes, the resulting separation of electron density spikes also shifts from the central wavelength, as illustrated in Fig. 1. Because the relative shift in frequency is the same at all harmonics, an increase in the fundamental frequency of Δk_1 will grow the harmonic bandwidth by $\Delta k_H \approx H\Delta k_1$.

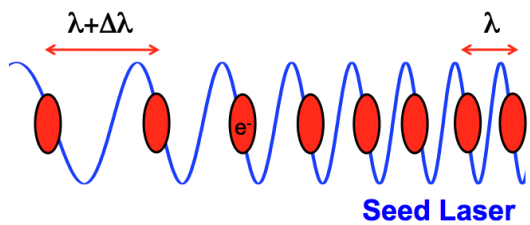

Figure 1: Cartoon illustrating the effect of seed phase errors on HGHG electron bunching. A time-varying wavelength in the seed laser (blue line) results in a varying separation of the bunched electrons (red bunches).

To quantify the effect of wavelength variation in the seed laser, we calculate the FEL's Time-Bandwidth Product (TBP), $\mathrm{TBP} = c\Delta T_{\mathrm{FEL}}\Delta k_{\mathrm{FEL}}$, from the pulse duration, ΔT_{FEL}, bandwidth, Δk_{FEL} and speed of light, c. For a given spectral distribution, the minimal TBP corresponds to a transform-limited pulse. As the TBP grows, the seeded FEL characteristics revert to those of a SASE pulse. For a flat-top seed laser with a small linear variation in wavelength, all harmonics have the same pulse length, so we the TBP grows linearly with harmonic number.

HGHG WITH SPECTRAL PHASE ERRORS

Laser Phase Definition

Experimental laser measurements are predominantly spectral, so it is convenient to describe the laser pulse using

ISBN 978-3-95450-123-6

STATUS OF THE FLASH FACILITY

S. Schreiber*, B. Faatz, J. Feldhaus, K. Honkavaara, R. Treusch, M. Vogt, DESY, Hamburg, Germany†

Abstract

FLASH at DESY, Hamburg is a soft X-ray free-electron laser user facility. After a 3.5 months shutdown in autumn 2011 required for civil construction for a second undulator beamline, beam operation started as scheduled in January 2012. FLASH shows again an improvement in performance with even higher single and average photon pulse energies, better stability, and significant improvements in operation procedures. The fourth user period started end of March 2012. A four months shutdown is scheduled spring 2013 to connect the second undulator beamline to the FLASH accelerator.

INTRODUCTION

FLASH [1–5], the free-electron laser (FEL) user facility at DESY, delivers high brilliance XUV and soft x-ray FEL radiation for photon experiments since summer 2005.

Besides the user operation, FLASH beam time is dedicated to improve its overall performance as an FEL user facility, e.g. on developments on the automation and stabilization, including, for example, sophisticated beam based feedbacks. Time is also reserved to set-up the photon beamlines prior to the user experiments, and to advance the photon diagnostics. In addition, part of the yearly study time is allocated for general accelerator physics experiments and developments related to future projects, in particular the European XFEL and the International Linear Collider (ILC).

In parallel to the growing user demand, the FLASH facility has been constantly upgraded. Key developments are to provide higher electron beam energies to achieve shorter photon wavelengths, improved photon beam quality as well as better stability in terms of photon pulse energy, wavelength, spectral width, pulse duration, arrival time, pointing, and wavefront quality. Synchronization of the FEL photon pulses with pump probe lasers to better than 10 fs and a reliable tool to measure photon pulse duration from 1 to 100 fs remain a hot R&D issue.

The next major upgrade underway is the construction of a second undulator beamline, the FLASH II project [6].

In this paper we summarize the present status of the FLASH facility and outline its midterm plans. Part of the material discussed here has already been presented in [5].

FLASH FACILITY

Figure 1 shows an overview of FLASH including the second undulator beamline under construction. Some of the main electron and photon beam parameters are listed in Table 1. These parameters are not all achieved simultaneously, but indicate the overall span of the performance.

Table 1: Some FLASH parameters. They are not all achieved simultaneously, but indicate the overall span of the performance.

Electron beam		
Energy (max)	MeV	1250
Peak current	kA	1 - 2
Emittance, norm. (x,y)	μm	1 - 2
Bunch charge	nC	0.06 - 1.5
Bunches / train		1 - 600
Bunch spacing	μs	1 - 25
Rep. rate	Hz	10
FEL radiation		
Wavelength (fundamental)	nm	4.2 - 45
Average single pulse energy	μJ	10 - 500
Pulse duration (fwhm)	fs	50 - 200
Spectral width (fwhm)	%	0.7 - 2
Peak power	GW	1 - 3
Photons per pulse		10^{11} - 10^{13}
Peak brilliance	*	10^{29} - 10^{31}
Average brilliance	*	10^{17} - 10^{21}

* photons / (s mrad^2 mm^2 0.1 % bw)

Trains of up to 800 high quality electron bunches are produced by a laser driven normal conducting RF-gun. Since 2010, problems have occurred related to the RF-gun and its RF-window. These issues are discussed in more detail later in this paper. The photocathode laser system is based on a mode-locked pulse train oscillator with a chain of fully diode pumped Nd:YLF amplifiers [7, 8]. The cathode is a thin film of Cs_2Te on molybdenum plugs [9].

The electron beam is accelerated up to 1.25 GeV by seven superconducting TESLA type accelerating modules. Each module has eight 1.3 GHz 9-cell niobium cavities. Downstream the first module, four 3.9 GHz (third harmonics) superconducting cavities are installed. They are used to linearize the longitudinal phase space, thus allowing operation with more regular longitudinal shaped electron bunches. The peak current required for the lasing process is achieved by compressing the electron bunches by two magnetic chicane bunch compressors at beam energies of 150 MeV and 450 MeV.

FEL radiation is produced based on the SASE (Self Amplified Spontaneous Emission) process by six undulator modules. Each of them consists of a 4.5 m long fixed gap undulator (K=1.23, period 27.3 mm, 12 mm gap) with

* siegfried.schreiber@desy.de
† for the FLASH team

ISBN 978-3-95450-123-6

PULSE-FRONT TILT CAUSED BY THE USE OF A GRATING MONOCHROMATOR AND SELF-SEEDING OF SOFT X-RAY FELS

G. Geloni, European XFEL GmbH, Hamburg, Germany
V. Kocharyan and E. Saldin, DESY, Hamburg, Germany

Abstract

Self-seeding is a promising approach to significantly narrow the SASE bandwidth of XFELs to produce nearly transform-limited pulses. The development of such schemes in the soft X-ray wavelength range necessarily involves gratings as dispersive elements. These introduce, in general, a pulse-front tilt, which is directly proportional to the angular dispersion. Pulse-front tilt may easily lead to a seed signal decrease by a factor two or more. Suggestions on how to minimize the pulse-front tilt effect in the self-seeding setup are given. More details and references can be found in [1].

INTRODUCTION

The longitudinal coherence of X-ray SASE FELs is rather poor. Self-seeding schemes have been studied to reduce the bandwidth of SASE X-ray FELs. A self-seeding setup consists of two undulators separated by a photon monochromator and an electron bypass, normally a four-dipole chicane. Recently, a very compact soft X-ray self-seeding scheme was designed at SLAC, based on a grating monochromator. We studied the performance of this compact scheme for the European XFEL upgrade elsewhere (see [1] for references). Limitations on the performance of the self-seeding scheme related with aberrations and spatial quality of the seed beam have been extensively discussed in literature and go beyond the scope of this paper. Here we will focus our attention on the spatiotemporal distortions of the X-ray seed pulse. Numerical results provided by ray-tracing algorithms applied to grating design programs give accurate information on the spatial properties of the imaging optical system of grating monochromator. However, in the case of self-seeding, the spatiotemporal deformation of the seeded X-ray optical pulses is not negligible: aside from the conventional aberrations, distortions as pulse-front tilt should also be considered (see [1] for references). The propagation and distortion of X-ray pulses in grating monochromators can be described using a wave optical theory. Most of our calculations are, in principle, straightforward applications of conventional ultrafast pulse optics. Our paper provides physical understanding of the self-seeding setup with a grating monochromator, and we expect that this study can be useful in the design stage of self-seeding setups.

THEORETICAL BACKGROUND

Pulse-front Tilt from Gratings

Ultrashort X-ray FEL pulses are usually represented as products of electric field factors separately dependent on space and time. The assumption of separability of the spatial (or spatial frequency) dependence of the pulse from the temporal (or temporal frequency) dependence is usually made for the sake of simplicity. However, when the manipulation of ultrashort X-ray pulses requires the introduction of coupling between spatial and temporal frequency coordinates, such assumption fails. The direction of energy flow -usually identified as rays directions- is always orthogonal to the surface of constant phase, that is to the wavefronts of the corresponding propagating wave. If one deals with ultrashort X-ray pulses, one has to consider, in addition, planes of constant intensity, that is pulse fronts. Fig. 1 shows a schematic representation of the electric field profile of an undistorted pulse and one with a pulse-front tilt. A distortion of the pulse front does not affect propagation, because the phase fronts remain unaffected. However, for most applications, including self-seeding applications, it is desirable that these fronts be parallel to the phase fronts, and therefore orthogonal to the propagating

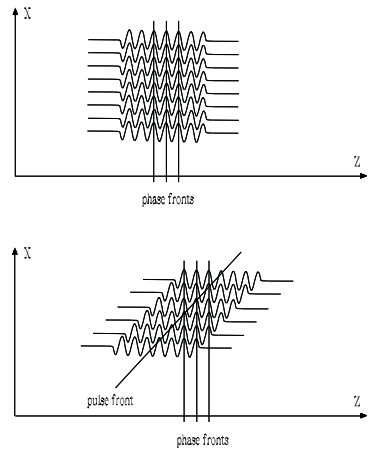

Figure 1: An undistorted pulse beam (left) and a beam with pulse front tilt (right) (adapted from literature, see [1] for references).

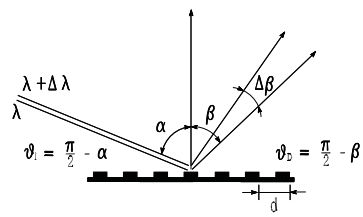

Figure 2: Geometry of diffraction grating scattering.

ISBN 978-3-95450-123-6

HARMONIC LASING IN X-RAY FELS

E.A. Schneidmiller, M.V. Yurkov, DESY, Hamburg, Germany

Abstract

Contrary to nonlinear harmonic generation, harmonic lasing in a high-gain FEL can provide much more intense, stable,and narrow-band FEL beam which is easier to handle if the fundamental is suppressed. We performed thorough study of the problem withing framework of 3D model taking into account all essential effects. We found that harmonic lasing is much more robust than usually thought, and can be widely used in the existing or planned X-ray FEL facilities. LCLS after a minor modification can lase at the 3rd harmonic up to the photon energy of 25-30 keV providing multi-gigawatt power level. At the European XFEL the harmonic lasing would allow to extend operating range ultimately up to 100 keV.

INTRODUCTION

Harmonic lasing in single-pass high-gain FELs [1–4], i.e. the radiative instability at an odd harmonic of the planar undulator developing independently from lasing at the fundamental wavelength, might have significant advantages over nonlinear harmonic generation [1,2,5–9] providing much higher power, much better stability, and smaller bandwidth.

Thorough revision of the parameter space for harmonicds lasing has been performed recently within framework of 3D FEL theory and taking into account all essential effects [10]. It has been found that harmonic lasing can be of interest in many practical cases. In fact, gain at higher harmonics can be higher than that at the fundamental for diffraction limited electron beams with small ratio of emittance to radiation wavelength $2\pi\epsilon/\lambda$. This parameter space corresponds to the operating range of soft X-ray beamlines of X-ray FEL facilities. For $2\pi\epsilon/\lambda \gtrsim 1$ (hard x-ray FELs are in this parameter range) the properties of saturated harmonic lasing at a given wavelength are approximately the same as those of the retuned fundamental.

In this paper we consider a possible application of harmonic lasing to different X-ray FEL facilities, and conclude that they can strongly profit from this option. In particular, LCLS [11] can significantly extend its operating range towards shorter wavelengths making use of the third harmonic lasing with the help of the intra-undulator spectral filtering and phase shifters. In the case of the European XFEL [12], the harmonic lasing can allow to extend the operating range, to reduce FEL bandwidth and increase brilliance. Similar improvements can be realized in other X-ray FEL facilities with gap-tunable undulators like FLASH II [13], SACLA [14], LCLS II [15], etc.

FEL GAIN

In the linear regime of a SASE FEL operation the fundamental frequency and harmonics grow independently with gain lengths $L_g^{(h)}$ (here the superscript denotes harmonic number). In the case of the simultaneous lasing in the parameter range $2\pi\epsilon/\lambda \gtrsim 1$ the fundamental mode always has the shortest gain length., i.e. it saturates first. Let us formulate the problem differently. We can produce radiation at a target wavelength λ by two ways. First option is tuning of FEL amplifier to the fundamental wavelength λ. Second option is tuning of FEL amplifier to the fundamental wavelength λ/h and generate h-th harmonic with wavelength λ. The question is which option provides shortest gain length.

Tuning of the FEL amplifier can be peroformed either by increasing electron energy, or reducing the undulator parameter K as it is is implemented in x-ray facilities. For the case when we can neglect energy spread effects, and assuming that the beta-function is tuned to the optimum value corresponding to maximum gain for each case we have [10]:

$$\begin{aligned} \frac{L_g^{(1K)}}{L_g^{(h)}} &= \frac{h^{1/2} K A_{JJh}(K)}{K_{re} A_{JJ1}(K_{re})}\,, \\ \frac{L_g^{(1\gamma)}}{L_g^{(h)}} &= \frac{h^{5/6} A_{JJh}(K)}{A_{JJ1}(K)}\,. \end{aligned} \qquad (1)$$

The superscripts $(1K)$ and (1γ) refer to retunig of the undulator parameter and electron energy, respectively. A_{JJh} is coupling factor defined in a standard way [2, 4, 10]. The retuned undulator parameter K_{re} is given by $K_{re}^2 = (1+K^2)/h - 1$ (obviously, K must be larger than $\sqrt{h-1}$). For large K the ratio in the first line of Eq. (1) is reduced to hA_{JJh}/A_{JJ1}, so that the gain length of the retuned fundamental mode is larger by a factor of 1.41 (1.65) than that of the third (fifth) harmonic. For an arbitrary K we plot in Fig. 1 the ratio of gain lengths (1). It is seen that the third harmonic always has an advantage (in case of negligible energy spread), i.e. its gain length is shorter for any value of K.

In the case of boosting electron energy for lasing at three times reduced fundamental wavelength, the advantage of using the 3rd harmonic is not that obvious (since an increase of electron energy at the same wavelength leads to a decrease of the parameter $2\pi\epsilon/\lambda$ thus improving FEL properties, in general). However, even in this case, the gain length for the third harmonic is shorter if rms value of K is larger than 1.4.

Let us present a numerical example for the European XFEL. New baseline parameters [16–18] assume operation

ISBN 978-3-95450-123-6

FITTING FORMULAS FOR HARMONIC LASING IN FEL AMPLIFIERS

E.A. Schneidmiller, M.V. Yurkov, DESY, Hamburg, Germany

Abstract

One of the most important subjects of the high-gain FEL engineering is the calculation of the gain length, and fitting formulas are frequently used for this purpose. Here we refer to Ming Xie fitting formulas [1] and fitting formulas for optimized FEL written down in an explicit form in terms of the electron beam and undulator parameters [2]. In this paper we perform generalization of these fitting formulas to the case of harmonic lasing.

INTRODUCTION

In order to calculate FEL gain length (and, therefore, saturation length) one has to solve an eigenvalue equation. Eigenvalue equation for harmonic lasing was derived in the framework of one-dimensional (1D) model in [3, 4], and a thorough 1D analysis can be found in [5]. Usually, more realistic 3D model is required to make conclusions on a possibility of practical realization of some option. Three-dimensional analysis was done in [6], where an eigenvalue equation was derived based on an approach developed in [1] for the fundamental frequency. However, this eigenvalue equation is rather complicated and can be solved only numerically. One can correctly calculate the gain length for a specific set of parameters, but it is very difficult to trace general dependencies and perform analysis of the parameter space.

In this paper we perform a parametrization of the solution of the eigenvalue equation for lasing at odd harmonics [6], and present explicit (although approximate) expressions for FEL gain length, optimal beta-function, and saturation length taking into account emittance, betatron motion, diffraction of radiation, energy spread and its growth along the undulator length due to quantum fluctuations of the undulator radiation. Considering 3rd harmonic lasing as a practical example, we come to the conclusion that it is much more robust than usually thought, and can be widely used at the present level of accelerator and FEL technology. We surprisingly find out that in many cases the 3D model of harmonic lasing gives more optimistic results than the 1D model. For instance, one of the results of our studies is that in a part of the parameter space, corresponding to the operating range of soft X-ray beamlines of X-ray FEL facilities, harmonics can grow faster than the fundamental mode.

EIGENVALUE EQUATION

In Ref. [1] the eigenvalue equation for a high-gain FEL was derived that includes such important effects as diffraction of radiation, betatron motion of particles and longitudinal velocity spread due to emittance, energy spread in the electron beam, frequency detuning. The eigenvalue equation is an integral equation which can be evaluated numerically for any particular parameter set with a desirable accuracy. The generalization of this eigenvalue equation to the case of harmonic lasing was done in [6]. Here we present the latter result for the growth rate of TEM_{nm} mode in a dimensionless form accepted in [7]:

$$\bar{\Phi}_{nm}(p) = -\frac{h^2 A_{JJh}^2}{A_{JJ1}^2(2\,\mathrm{i}\,hB\hat{\Lambda} - p^2)} \int_0^\infty \mathrm{d}\,p' p' \bar{\Phi}_{nm}(p')$$
$$\times \int_0^\infty \frac{\zeta\,\mathrm{d}\,\zeta}{(1 - \mathrm{i}\,hB\hat{k}_\beta^2\zeta/2)^2} \exp\left[-\frac{h^2\hat{\Lambda}_\mathrm{T}^2\zeta^2}{2} - (\hat{\Lambda} + \mathrm{i}\,\hat{C})\zeta\right]$$
$$\times \exp\left[-\frac{p^2 + p'^2}{4(1 - \mathrm{i}\,hB\hat{k}_\beta^2\zeta/2)}\right] I_n\left[\frac{pp'\cos(\hat{k}_\beta\zeta)}{2(1 - \mathrm{i}\,hB\hat{k}_\beta^2\zeta/2)}\right] \quad (1)$$

where $h = 1, 3, 5, ...$ is harmonic number, I_n is the modified Bessel function of the first kind. The normalized growth rate $\hat{\Lambda} = \Lambda/\Gamma$ has to be found from numerical solution of the integral equation. The following notations are used here: $\hat{r} = r/(\sigma\sqrt{2})$, $B = 2\sigma^2\Gamma\omega_1/c$ is the diffraction parameter, ω_1 is the fundamental frequency, $\sigma = \sqrt{\epsilon\beta}$ is the transverse rms size of the matched Gaussian beam, emittance ϵ is simply given by $\epsilon = \epsilon_n/\gamma$ with ϵ_n being normalized rms emittance, $\hat{k}_\beta = k_\beta/\Gamma$ is the betatron motion parameter, $k_\beta = 1/\beta$ is the betatron wavenumber, β is the beta-function, $\hat{\Lambda}_\mathrm{T}^2 = \sigma_\gamma^2/(\bar{\rho}\gamma)^2$ is the energy spread parameter, $\hat{C} = \left[k_\mathrm{w} - \omega_h/(2hc\gamma_z^2)\right]/\Gamma$ is the detuning parameter, $\omega_h \simeq h\omega_1$, $\Gamma = \left[A_{\mathrm{JJ}1}^2 I\omega_1^2\theta_\mathrm{s}^2\left(I_\mathrm{A}c^2\gamma_z^2\gamma\right)^{-1}\right]^{1/2}$ is the gain factor, $\bar{\rho} = c\gamma_z^2\Gamma/\omega_1$ is the efficiency parameter, $\theta_\mathrm{s} = K/\gamma$, K is the rms undulator parameter, γ is relativistic factor, $\gamma_z^{-2} = \gamma^{-2} + \theta_\mathrm{s}^2$, k_w is the undulator wavenumber, I is the beam current, $I_\mathrm{A} = 17$ kA is the Alfven current, $A_{\mathrm{JJh}} = J_{(h-1)/2}(hK^2/2(1+K^2)) - J_{(h+1)/2}(hK^2/2(1+K^2))$. The coupling factors for the 1st, 3rd, and 5th harmonics are shown in Fig. 1. When the rms undulator parameter K is large, the coupling factors are $A_{JJ1} \simeq 0.696$, $A_{JJ3} \simeq 0.326$, $A_{JJ5} \simeq 0.230$. Asymptotically for large h we have $A_{JJh} \simeq 0.652\,h^{-2/3}$. Note that the scaling factors (Γ, $\bar{\rho}$) reflect the growth rate of the fundamental harmonic. The efficiency parameter $\bar{\rho}$ is related to the corresponding parameter ρ [8] of the one-dimensional model as follows: $\bar{\rho} = \rho B^{1/3}$.

One can observe that the equation (1) can be rewritten such that it looks the same for all harmonics:

ISBN 978-3-95450-123-6

HARMONIC LASING OF THIN ELECTRON BEAM

E.A. Schneidmiller, M.V. Yurkov, DESY, Hamburg, Germany

Abstract

For a typical operating range of hard X-ray FELs the condition for ratio of the electron beam emittance to radiation wavelength $2\pi\epsilon/\lambda \simeq 1$ is usually a design goal for the shortest wavelength. In the case of the simultaneous lasing the fundamental mode has shorter gain length than harmonics. If the same electron beam is used to drive an FEL in a soft X-ray beamline, the regime with $2\pi\epsilon/\lambda \ll 1$ is realized which corresponds to the case of a small value of diffraction parameter. Here we present a detailed study of this regime. We discover that in a part of the parameter space, corresponding to the operating range of soft X-ray beamlines of X-ray FEL facilities (like SASE3 beamline of the European XFEL), harmonics can grow faster than the fundamental wavelength. This feature can be used in some experiments, but might also be an unwanted phenomenon, and we discuss possible measures to diminish it.

INTRODUCTION

Once pronounced harmonic of the beam current density exists in the electron beam, it allows to produce powerful coherent radiation. Two mechanisms are usually considered providing electron beam modulation at higher harmonics. Bunching at higher harmonics always takes place when FEL apmplification process driven by the fundamental frequency reaches saturation regime. This mechanism is referred to as nonlinear harmonic generation [1–7]. In the case of planar undulator there always exists also an amplification of odd harmonics due to FEL instability. This mechanism is usually referred as linear harmonic generation [1,3,8–14]. It is generally accepted that self-consistent amplification of the radiation at higher harmonics is weaker than that of the fundamental. This is true in the framework of one-dimensional approximation (or, in a wide beam limit) as it has been show in early studies. However, situation changes qualitatively for diffraction limited electron beams with small value of diffraction parameter. This parameter range refers to as thin beam limit [21]. Our studies have shown that there exists range of parameters when gain at higher harmonics exceeds the gain at the fundamental. This range of parameters is not of pure academical interest, but can be experimentally realized for long wavelength FELS driven by high energy electron beams. Free electron laser at SASE3 beam line of the European XFEL falls in this parameter range.

FEL gain length is calculated from solution of an eigenvalue equation. Eigenvalue equation for harmonic lasing was derived in the framework of one-dimensional (1D) model in [1, 13], and a thorough 1D analysis can be found in [14]. An eigenvalue equation for three-dimensional case has been derived in [3]. However, this eigenvalue equation is rather complicated and can be solved only numerically. One can correctly calculate the gain length for a specific set of parameters, but it is very difficult to trace general dependencies and perform analysis of the parameter space. In paper [23] we performed a parametrization of the solution of the eigenvalue equation for lasing at odd harmonics [3], and presented explicit expressions for FEL gain length, optimal beta-function, and saturation length taking into account emittance, betatron motion, diffraction of radiation, energy spread and its growth along the undulator length due to quantum fluctuations of the undulator radiation. Considering 3rd harmonic lasing as a practical example, we come to the conclusion that it is much more robust than usually thought, and can be widely used at the present level of accelerator and FEL technology. We surprisingly find out that in many cases the 3D model of harmonic lasing gives more optimistic results than the 1D model. For instance, one of the results of our studies is that in a part of the parameter space, corresponding to the operating range of soft X-ray beamlines of X-ray FEL facilities, harmonics can grow faster than the fundamental mode.

SIMULTANEOUS LASING IN THE CASE OF A THIN ELECTRON BEAM

For a typical operating range of hard X-ray FELs the condition $2\pi\epsilon/\lambda \simeq 1$ is usually a design goal for the shortest wavelength. In the case of the simultaneous lasing the fundamental mode has shorter gain length than harmonics, as it was shown above in paper [23]. However, if the same electron beam is supposed to drive an FEL in a soft X-ray beamline, the regime with $2\pi\epsilon/\lambda \ll 1$ can be realized. Here we present a detailed study of this regime. In this Section we assume that beta-function is much longer than FEL field gain length, $\beta \gg L_g^{(h)}$. Here subscript h denotes harmonic number. In this case we can use the model of parallel beam (no betatron oscillations), and can also neglect an influence of longitudinal velocity spread due to emittance on FEL process. If in addition the energy spread is negligibly small, then the normalized FEL growth rate at the fundamental frequency is described by the only dimensionless parameter, namely the diffraction parameter B [21]. The generalized diffraction parameter $\tilde{B}$, that can be used for harmonics, is written as follows [23]:

$$\tilde{B} = 2\epsilon\beta\tilde{\Gamma}\omega_h/c\,. \qquad (1)$$

Here $\omega_h = 2\pi c/\lambda_h$, ω_h (λ_h) is frequency (wavelength) of the hth harmonic, c is velocity of light, and $\tilde{\Gamma}$ is the gain factor that also depends on harmonic number:

ISBN 978-3-95450-123-6

SPATIAL PROPERTIES OF THE RADIATION FROM SASE FELS AT THE EUROPEAN XFEL

E.A. Schneidmiller, M.V. Yurkov, DESY, Hamburg, Germany

Abstract

Recently DESY and the European XFEL GmbH performed revision of the baseline parameters for the electron beam and undulators. Operating range of bunch charges has been extended from 20 pC to 1 nC. Different modes of FEL operation become possible with essentially different properties of the radiation. This paper is devoted to the analysis of spatial properties of the radiation (fundamental and harmonics), an important subject for design of photon beam lines and planning user's experiments.

INTRODUCTION

Early version of the European XFEL project implemented operation of the facility with fixed bunch charge of 1 nC and rather conservative value for the emittance 1.4 mm-mrad [1]. Recent success of FLASH and Linac Coherent Light Source (LCLS) demonstrated feasibility for reliable production, compression, and acceleration of electron beams with small emittance [2,3]. Results of the Photo Injector Test Facility in Zeuthen (PITZ) demonstrated the possibility to generate electron beams with smaller charge and emittance [4, 5]. Intensive work on revision of electron beam parameter space of the European XFEL has been performed [6–9] which resulted in a new set of baseline parameters. Parameter space has been significantly extended in terms of the bunch charge and electron energy [10]. In parallel there was also revision of the undulator parameters based on user's requirements. It has been decided that SASE1 and SASE2 undulators will have period of 4 cm, and SASE3 undulator will have period 6.8 cm [11]. As a result, different modes of FEL operation become possible with essentially different properties of the radiation. Variation of the bunch charge will allow to control radiation pulse duration in wide limits. An important factor related to emittance reduction is significant change of angular divergence of the radiation with new baseline parameters. This forced corresponding revision of the photon distribution system [12].

In paper [13] we presented a comprehensive overview of radiation properties of SASE FEL radiators driven by electron beam with new baseline parameters. An important missed topic was spatial properties of the higher harmonic radiation. This paper fills the gap. Present study makes use of fitting formulae based on application of similarity techniques to the results of extended numerical simulations [14–17, 19]. As a result, it becomes possible to describe complicated phenomena with simple parametric dependencies.

BASIC RELATIONS

Design of the focusing system of XFEL assumes nearly uniform focusing of the electron beam in the undulator, so we consider axisymmetric model of the electron beam. It is assumed that transverse distribution function of the electron beam is Gaussian, so rms transverse size of matched beam is $\sigma = \sqrt{\epsilon\beta}$,where $\epsilon = \epsilon_{\rm n}/\gamma$ is rms beam emittance, γ is relativistic factor, and β is focusing beta-function. In the following we apply similarity techniques to the analysis of the FEL amplifier operation. Key notions of the three-dimensional theory of the FEL amplifier which we use here are is the gain parameter Γ and diffraction parameter B [20, 21]:

$$\begin{aligned} \Gamma &= \left[\frac{I}{I_{\rm A}}\frac{8\pi^2 K^2 A_{\rm JJ1}^2}{\lambda\lambda_{\rm w}\gamma^3}\right]^{1/2}, \\ B &= 2\Gamma\sigma^2\omega/c\,. \end{aligned} \tag{1}$$

Here I is the beam current, $I_{\rm A} = 17$ kA is Alfven's current, λ is radiation wavelength, $\omega = 2\pi c/\lambda$, $\lambda_{\rm w}$ is undulator period, and K is rms undulator parameter. Coupling factor is $A_{\rm JJ1} = 1$ for helical undulator, and $A_{\rm JJh} = J_{(h-1)/2}(K^2/2(1+K^2)) - J_{(h+1)/2}(K^2/2(1+K))$ for planar undulator. J_n is the Bessel function of the first kind.

With given parameters of electron beam and undulator period the only parameter remaining for optimization of the FEL gain is focusing beta function. In the parameter range $1 \lesssim \hat{\epsilon} = 2\pi\epsilon/\lambda \lesssim 5$ optimum beta function is given explicitly by expression [14]:

$$\begin{aligned} \beta_{\rm opt} &\simeq 11.2\left(\frac{I_A}{I}\right)^{1/2}\frac{\epsilon_n^{3/2}\lambda_{\rm w}^{1/2}}{\lambda K A_{JJ1}}\,(1+8\delta)^{-1/3}, \\ \delta &= 131\,\frac{I_A}{I}\,\frac{\epsilon_n^{5/4}}{\lambda^{1/8}\lambda_{\rm w}^{9/8}}\,\frac{\sigma_\gamma^2}{(KA_{JJ1})^2(1+K^2)^{1/8}}, \end{aligned} \tag{2}$$

where $\sigma_\gamma = \sigma_{\rm E}/m_{\rm e}c^2$. When energy spread is not important for amplification process, diffraction parameter for optimized x-ray FEL (with optimum beta function given by (2) yields in a simple relation:

$$B \simeq 12.5 \times \hat{\epsilon}^{5/2}\,. \tag{3}$$

FUNDAMENTAL HARMONIC

We start illustration of spatial properties with specific numerical example for SASE1 and SASE3 operating with bunch charge 100 pC. Other parameters of SASE1 (SASE3) are energy 14 GeV (17.5 GeV), radiation wavelength 0.25 nm (1.6 nm) [13]. Evolution along the undulator of the spot size of the radiation and angular divergence of the radiation is shown in Fig. 1. Simulations have

ISBN 978-3-95450-123-6

ON DISRUPTION OF THE FUNDAMENTAL HARMONIC IN SASE FEL WITH PHASE SHIFTERS

E.A. Schneidmiller, M.V. Yurkov, DESY, Hamburg, Germany

Abstract

A method to disrupt the fundamental harmonic with phase shifters installed between undulator modules (while keeping the lasing at the third harmonic undisturbed) was proposed in [1]. If phase shifters are tuned such that the phase delay is $2\pi/3$ (or $4\pi/3$) for the fundamental, then its amplification is disrupted. At the same time the phase shift is equal to 2π for the third harmonic, i.e. it continues to get amplified without being affected by phase shifters. We note that simulations in [1] were done for the case of a monochromatic seed, and the results cannot be applied for a SASE FEL. The reason is that in the latter case the amplified frequencies are defined self-consistently, i.e. there is frequency shift (red or blue) depending on positions and magnitudes of phase kicks. This leads to a significantly weaker suppression effect. In particular, we found out that a consecutive use of phase shifters with the same phase kicks $2\pi/3$ (as proposed in [1] is inefficient, i.e. it does not lead to a sufficiently strong suppression of the fundamental wavelength. In the present report we propose a modification of phase shifters method that can work in the case of a SASE FEL.

INTRODUCTION

When the saturation is achieved at the fundamental frequency, the nonlinear harmonic generation occurs, i.e. the radiation of the bunched beam at odd harmonics of the undulator [2–7]. This radiation has a relatively low power (for the 3rd harmonic it is on the order of a per cent of the saturated power of the fundamental wavelength), and its relative bandwidth is about the same as that of the fundamental [8]. Intensity of harmonics is subjected to much stronger fluctuations than that of the fundamental frequency [4,8,9]. Linear amplification of a harmonic does not proceed due to a strong impact of the saturation at the fundamental mode on the longitudinal phase space of the electron beam.

If, however, we disrupt the lasing at the fundamental frequency such that it stays well below saturation, then the third harmonic lasing proceeds up to saturation resulting in a significant intensity (about 30 % of the saturated power of the fundamental mode in 1D limit), narrow relative bandwidth (also about 30 % of that at the fundamental in 1D case). In other words, the brilliance can be by two orders of magnitude higher than in the case of nonlinear harmonic generation (for the 5th harmonic the improvement can reach three orders of magnitude). Intensity fluctuations of a harmonic are about the same as those at the fundamental wavelength of a SASE FEL since statistics is the same. Moreover, if the fundamental harmonic is strongly suppressed in the undulator, the users of X-ray facilities do not need filters which are in most cases required if one uses nonlinear harmonic generation. Note that the filters suppress the fundamental wavelength but may also partially suppress harmonics. Thus, harmonic lasing up to its saturation has decisive advantages over nonlinear harmonic generation, so one should have good methods to disrupt the fundamental mode.

DESCRIPTION OF THE METHOD

A method to disrupt the fundamental harmonic (while keeping the lasing at the third harmonic undisturbed) was proposed in [1]. The undulators for X-ray FELs consist of many segments. In case of gap-tunable undulators, phase shifters are foreseen between the segments. If phase shifters are tuned such that the phase delay is $2\pi/3$ (or $4\pi/3$) for the fundamental, then its amplification is disrupted. At the same time the phase shift is equal to 2π for the third harmonic, i.e. it continues to get amplified without being affected by phase shifters. However, the simulations in [1] were done for the case of a monochromatic seed, and the results cannot be applied for a SASE FEL. The reason is that in the latter case the amplified frequencies are defined self-consistently, i.e. there is frequency shift (red or blue) depending on positions and magnitudes of phase kicks. This leads to a significantly weaker suppression effect. In particular, we found out that a consecutive use of phase shifters with the same phase kicks $2\pi/3$ (as proposed in [1]) is inefficient, i.e. it does not lead to a sufficiently strong suppression of the fundamental wavelength. In a realistic 3D case, the radiation is diffracted out of the electron beam, and the density and energy modulations within this frequency band are partially suppressed due to emittance and energy spread while the beam is passing the second part of the undulator (although the suppression effect is often small). We propose here a modification of phase shifters method that can work in the case of a SASE FEL. We define phase shift in the same way as it was done in [1] in order to make our results compatible with the previous studies. For example, the shift $2\pi/3$ corresponds to the advance[1] of a modulated electron beam with respect to elec-

[1] In a phase shifter (like a small magnetic chicane) the beam is, obviously, delayed with respect to electromagnetic field. One can, however, always add or subtract 2π, so that the shift is kept between 0 and 2π. Therefore, a delay in the phase shifter by $2\pi/3$ corresponds to the phase

ISBN 978-3-95450-123-6

COHERENCE PROPERTIES OF THE ODD HARMONICS OF THE RADIATION FROM SASE FEL WITH PLANAR UNDULATOR

E.A. Schneidmiller, M.V. Yurkov, DESY, Hamburg, Germany

Abstract

We present analysis of coherence properties of odd harmonics radiated from a SASE FEL with planar undulator. Nonlinear mechanism of harmonic generation is under study. Temporal and space correlation functions, coherence time and degree of transverse coherence are calculated by means of numerical simulations with the code FAST. Similarity techniques have been used to derive general coherence properties of the radiation from optimized x-ray FEL operating in the saturation regime.

INTRODUCTION

We consider free electron laser (FEL) amplifier - device in which electron bunch amplifies electromagnetic radiation during single pass of an undulator. The FEL collective instability in the electron beam produces an exponential growth (along the undulator) of the radiation and the modulation of the electron density on the scale of undulator resonance radiation wavelength. Amplification process in a Self Amplified Spontaneous Emission (SASE) FEL [1] starts from the shot noise in the electron beam. When the electron beam enters the undulator, the presence of the beam modulation at frequencies close to the resonance frequency initiates the process of radiation. The fluctuations of current density in the electron beam are uncorrelated not only in time but in space, too. A big number of transverse mode is excited. TEM_{00} mode with highest gain dominates when undulator length progresses. Coherence time and degree of transverse coherence grow in the exponential amplification stage, and reach maximum values near the saturation point. Saturation length is limited from nine to eleven field gain length for VUV and x-ray FELs which fundamentally define coherence properties of the radiation [2–6]. Poor longitudinal coherence also affects transverse coherence [2, 3].

Radiation from SASE FEL with planar undulator contains visible contribution of odd harmonics. Parameter range where intensity of higher harmonics is defined mainly by nonlinear beam bunching in the fundamental harmonic has been intensively studied in refs. [7–16]. Comprehensive studies of nonlinear harmonic generation have been performed in [16] in the framework of the one-dimensional model. General features of harmonic radiation have been determined. It was found that coherence time at saturation falls inversely proportional to harmonic number, and relative spectrum bandwidth remains constant with harmonic number. In this paper we extend studies of higher harmonics taking into account diffraction effects. We consider parameter range when intensity of higher harmonics is mainly defined by nonlinear harmonics generation mechanism. The results have been obtained with time-dependent, three-dimensional FEL simulation code FAST [17] performing simulation of the FEL process with actual number of electrons in the beam. Using similarity techniques we present universal dependencies for the main characteristics of the SASE FEL covering all practical range of optimized X-ray FELs. Present studies are limited with the third harmonic.

OPTIMIZED XFEL

Design of the focusing system of XFEL assumes nearly uniform focusing of the electron beam in the undulator, so we consider axisymmetric model of the electron beam. It is assumed that transverse distribution function of the electron beam is Gaussian, so rms transverse size of matched beam is $\sigma = \sqrt{\epsilon\beta}$,where $\epsilon = \epsilon_{\mathrm{n}}/\gamma$ is rms beam emittance and β is focusing beta-function. In the case of negligibly small effects of the space charge and energy spread, operation of the FEL amplifier is described by the diffraction parameter B and the betatron motion parameter $\hat{k}_\beta$: [18]:

$$B = 2\Gamma\sigma^2\omega/c\,, \qquad \hat{k}_\beta = 1/(\beta\Gamma)\,, \tag{1}$$

where $\Gamma = \left[I\omega^2\theta_{\mathrm{s}}^2 A_{\mathrm{JJ1}}^2/(I_{\mathrm{A}}c^2\gamma_{\mathrm{z}}^2\gamma)\right]^{1/2}$ is the gain parameter. When describing shot noise in the electron beam, one more parameter appears, the number of electrons in the volume of coherence: $N_{\mathrm{c}} = I/(e\omega\rho)$, where $\rho = c\gamma_{\mathrm{z}}^2\Gamma/\omega$ is the efficiency parameter. The following notations are used here: I is the beam current, $\omega = 2\pi c/\lambda$ is the frequency of the electromagnetic wave, $\theta_{\mathrm{s}} = K_{\mathrm{rms}}/\gamma$, K_{rms} is the rms undulator parameter, γ is relativistic factor, $\gamma_z^{-2} = \gamma^{-2} + \theta_{\mathrm{s}}^2$, $k_{\mathrm{w}} = 2\pi/\lambda_{\mathrm{w}}$ is the undulator wavenumber, $I_{\mathrm{A}} = 17$ kA is the Alfven current. Coupling factor is $A_{\mathrm{JJ1}} = 1$ for helical undulator and $A_{\mathrm{JJh}} = J_{(h-1)/2}(K_{\mathrm{rms}}^2/2(1 + K_{\mathrm{rms}}^2)) - J_{(h-1)/2}(K_{\mathrm{rms}}^2/2(1 + K_{\mathrm{rms}}^2))$ for planar undulator. Here J_n are the Bessel functions of the first kind, and h is harmonic number.

Target value of interest for XFEL optimization is the field gain length of the fundamental mode. For this practically important case the solution of the eigenvalue equation for the field gain length of the fundamental mode and optimum beta function are rather accurately approximated by [19]:

$$\begin{aligned} L_{\mathrm{g}} &= 1.67\left(\frac{I_A}{I}\right)^{1/2}\frac{(\epsilon_n\lambda_{\mathrm{w}})^{5/6}}{\lambda^{2/3}}\,\frac{(1+K^2)^{1/3}}{KA_{JJ1}} \\ \beta_{\mathrm{opt}} &\simeq 11.2\left(\frac{I_A}{I}\right)^{1/2}\frac{\epsilon_n^{3/2}\lambda_{\mathrm{w}}^{1/2}}{\lambda K A_{JJ1}}\,, \end{aligned} \tag{2}$$

It follows from (1) and (2) that diffraction parameter B and parameter of betatron oscillations, $\hat{k}_\beta$ are functions of the

ISBN 978-3-95450-123-6

NONLINEAR HARMONIC SELECTION IN AN FEL UNDULATOR SYSTEM

Sandra Biedron, Luca Giannessi*, Karen Horovitz, Stephen Milton
Electrical and Computer Engineering, Colorado State University, Fort Collins, CO 80523, USA
*ENEA C.R. Frascati Via E. Fermi 45, 00044 Roma, Italy

Abstract

Both fundamental and higher order harmonics are produced within the synchrotron radiation emitted during the free electron laser (FEL) process. These harmonics are not always wanted and at times can be detrimental to the overall operation of the FEL; furthermore, they can have a negative effect on user operations. Thus, the ability to control the harmonics is an important area of research. In this paper we discuss some possible means of controlling the harmonics and use PERSEO simulations to reduce the 5th harmonic of a test FEL system to acceptable levels.

CONCEPT

FEL Basics

In an FEL's undulator, the electron oscillations and its synchrotron radiation are phase matched, allowing energy exchange between the electrons and the EM radiation. This energy exchange causes the electrons to bunch at the resonant wavelength and subsequently emit coherently at this wavelength and its harmonics (Eqn. 1).

$$\lambda_{Rn} = \frac{\lambda_{und}}{2n\gamma^2}\left(1 + K^2/2\right) \tag{1}$$

Here, λ_{und} is the period of the undulator, K is the normalized maximum field strength of the undulator magnet, n is the harmonic number, γ is the normalized electron beam energy, and λ_{Rn} is the output wavelength for harmonic number n ($n = 1$ implies the fundamental). K can be interpreted in a different manner. It is the ratio of the maximum angle of oscillation of the electron beam within the undulator field, $x_{\max}$, to the opening angle of the radiation, θ_r (Eqn. 2).

$$K = \frac{x_{\max}}{\theta_r} = x_{\max}\gamma \tag{2}$$

Harmonics

The primary origin of harmonics generated by a single particle can be seen graphically in Figure 1. As K gets larger than about 1, the radiation pulse gets richer in harmonics and more intense.

The strengths of the on-axis fundamental and harmonics generated for a single electron traveling through an undulator have been calculated [1] and are directly proportional to the following function,

$$F_n(K) = \frac{n^2K^2}{\xi^2}\left\{J_{\frac{n-1}{2}}\left[\frac{nK^2}{4\xi}\right] - J_{\frac{n+1}{2}}\left[\frac{nK^2}{4\xi}\right]\right\}^2 \tag{3}$$
$$\left(n = 1,3,5,\ldots\right) \qquad \xi = \left(1 + K^2/2\right)$$

where n is the harmonic number and the J's are Bessel functions. The function $F_n(K)$ is plotted in Figure 2. It is clear that emission from a single particle is dominated by the harmonics for K values larger than about 1.5.

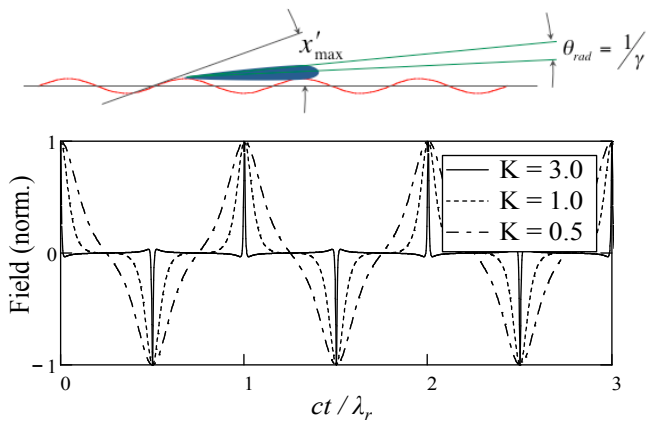

Figure 1: Graphical depiction of the impact of K on the harmonic content of the synchrotron radiation.

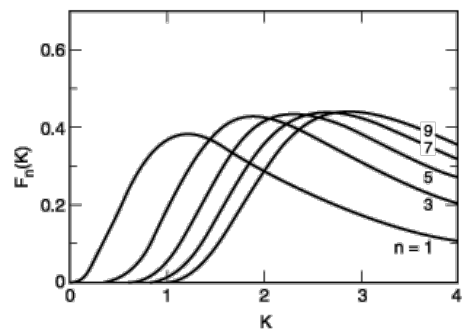

Figure 2: Strengths of the on-axis fundamental and harmonics as a function of K.

In an FEL we have coherent emission of a large number of electrons. Consider the case of a train of single electrons spaced exactly at the resonant wavelength of the undulator/beam system. The phases of fundamental and harmonic fields generated from the electron train along the direction of propagation overlap perfectly and a coherent build up of the field occurs. Adding N electrons

ISBN 978-3-95450-123-6

PUFFIN: A THREE DIMENSIONAL, UNAVERAGED FREE ELECTRON LASER SIMULATION CODE

L.T. Campbell and B.W.J. M^{c}Neil
SUPA, Department of Physics, University of Strathclyde, Glasgow, UK

Abstract

The broadband, 3D FEL code Puffin is presented. The analytical model is derived in absence of the Slowly Varying Envelope Approximation, and can model undulators of any polarization. Due to the enhanced resolution, the memory and processing requirements are greater than equivalent averaged codes. The numerical code to solve the system of equations is therefore written for a parallel computing environment utilizing MPI. An example simulation is presented.

INTRODUCTION

Most analytical and numerical models of the FEL use the Slowly Varying Envelope Approximation [1] (SVEA) on the radiation field. This assumes a slow temporal and spatial evolution of the field envelope at the scale of the radiation wavelength, and allows an averaging of the field envelope and some electron phase-space parameters over at least one radiation period, removing the need to model any fast oscillatory terms at the radiation frequency. Most of the commonly used multi-dimensional FEL simulation codes (e.g. MEDUSSA [2], GINGER [3], GENESIS 1.3 [4] and FAST [5]), are based on averaged SVEA models. While these have been used successfully to model basic FEL operation, and have been extensively benchmarked against experiment, SVEA means that resolution of sub-resonant wavelength scale processes are not possible. The particles used to simulate the electrons are confined to localised regions of one radiation period within the electron pulse, so that transport of particles over many radiation wavelengths, such as may occur as a result of the FEL interaction or e.g. a pre-imposed electron energy chirp, cannot be modelled easily. Furthermore, the correct simulation of electron shot-noise is only valid for a limited radiation wavelength range [6]. The minimum sampling period of the field envelope imposed by SVEA also limits the range of radiation frequencies able to be modelled without numerical aliasing effects to $\omega_r/2 < \omega < 3\omega_r/2$, where ω_r is the radiation resonant frequency [7]. Thus, using SVEA, it is not possible to model effects with a broader bandwidth using the same radiation field envelope. Such issues with SVEA constrain the effective modelling of several more advanced FEL methods including designs to achieve shorter radiation wavelengths and pulse durations [8].

This paper presents what the authors believe to be the first 3D unaveraged, broadband FEL computer simulation code, named Puffin (Parallel Unaveraged Fel INtegrator). The primary aim of this code is to provide a flexible research resource that can be adapted to test new ideas and methods for future FEL development. It is not intended, at least initially, as a design tool for FEL facility development.

The radiation field is modelled using the Finite Element method [9] and the electrons by a distribution of charge weighted macroparticles that can model the effects of electron shot-noise across a broad frequency bandwith [6]. Electrons are not confined to localised regions of the beam so that electron transport throughout the beam is correctly modelled. The main approximations applied are the neglect of the backward (counterpropagating) radiation field and the paraxial approximation. Furthermore, space-charge effects in the electron beam are neglected.

The resulting parallelised numerical code is able to simulate both CSE and spontaneous emission arising from electron shot-noise. The advantages are an enhanced and broadband resolution of the radiation including a self-consistent modelling of variable radiation polarisation. The disadvantages are the increased computer memory requirements and processing time when compared to the averaged numerical models.

In the following, the derivation of the final working equations and subsequent numerical solution is outlined and the operation of the code is demonstrated using different FEL configurations.

MATHEMATICAL MODEL

The electromagnetic field is given by:

$$\mathbf{E} = \frac{1}{\sqrt{2}}\left(\hat{\mathbf{e}}\xi_0 e^{i(k_r z-\omega_r t)} + c.c.\right), \tag{1}$$

where the vector basis

$$\hat{\mathbf{e}} = \frac{1}{\sqrt{2}}(\hat{\mathbf{x}} + i\hat{\mathbf{y}}) \tag{2}$$

and $\xi_0(x,y,z,t) = |\xi_0(x,y,z,t)|\exp(i\psi(x,y,z,t))$ is the complex field envelope, with k_r and ω_r, the field wavenumber and angular frequency respectively, of a resonant wave.

It is assumed the field propagates in vacuum and that the paraxial approximation applies, so that $\omega_r = ck_r$ and $\partial/\partial z \approx \partial/c\partial t$.

The undulator magnetic field is defined as:

$$\mathbf{B}_u = \frac{B_u}{2}\left(\mathbf{u}e^{ik_u z} + c.c.\right) \tag{3}$$

where $k_u = 2\pi/\lambda_u$ is the undulator wavenumber, λ_u is the undulator wavelength and B_u is the peak magnetic field

ISBN 978-3-95450-123-6

NONLINEAR EFFECTS IN FEL THEORY AND THEIR ROLE IN COHERENT ELECTRON COOLING*

Andrey Elizarov†, Vladimir Litvinenko, Stony Brook University, Stony Brook, NY 11794, USA, BNL, Upton, NY 11973, USA

Abstract

The novel cooling technique, the coherent electron cooling [1] relies on the amplification of the interaction between hadrons and electrons by an FEL. The linearity of the amplification process is essential for operation of such cooler. In this paper we propose a theoretical method of taking into account nonlinear effects in computation of evolution of charge perturbation in an FEL. This will allow to explore the limits of the FEL gain with special attention to the smearing of the phase caused by nonlinear and saturation effects.

INTRODUCTION

The coherent electron cooling (CeC) is a realization of the stochastic cooling where an electron beam copropagating with a hadron beam being cooled serves as a pick-up and a kicker being amplified by an FEL on its way, the schematic layout of the device is depicted in Fig. 1. Pick-up or modulator stores the information about the hadron beam as a perturbation of a charge density in the electron beam, then this perturbation is amplified by an FEL, and then goes to the kicker where its field accelerates slow moving hadrons and decelerates the fast ones. The detailed theoretical investigation of all these steps is required to build a working device. Now the modulator section is described in an infinite beam approximation in [2] and the study for the finite realistic beam is started in [3]. In the CeC an FEL is used in a nonstandard way, i.e. as an amplifier of the electron density perturbation. This facet of the FEL theory is not developed enough and we fill this gap in this article. With the methods presented we plan to analyze possible limitations of the FEL gain in the CeC device by nonlinear effects and saturation. In the next two sections we discuss 1D model for a modulator and the simplest possible initial conditions, i.e. electron density perturbation coming from the modulator. We considered 1D model and cos-like condition. The rest of the paper is devoted to possible ways to compute an evolution of these perturbations in an FEL.

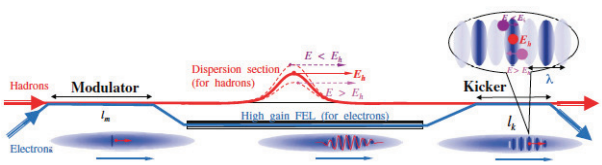

Figure 1: The scheme of the coherent electron cooler.

1D MODULATOR

In 1D case the problem of a shielding of a hadron moving along the trajectory $y(t) = x_0 + tv_0$ in an electron beam is described by the following Maxwell-Vlasov system:

$$\frac{\partial f_1}{\partial t} + v\frac{\partial f_1}{\partial x} = \frac{e}{m_0\gamma}\frac{\partial U}{\partial x}\cdot\frac{\partial f_0}{\partial v}, \quad (1)$$

$$\frac{\partial^2 U(x,t)}{\partial x^2} = -\frac{e}{\epsilon_0}\left(n_1(x,t) - Z\delta(x - y(t))\right), \quad (2)$$

the Maxwell equation can be solved via Fourier transform:

$$k^2\tilde{U}(k,t) = \frac{e}{\epsilon_0}\left(\tilde{n}_1(x,t) - Z\int\delta(x-y(t))\,\mathrm{e}^{-ikx}dx\right). \quad (3)$$

Using this solution the equation (1) can be transformed to

$$\tilde{N}_1(k,s) = -\frac{e}{\epsilon_0}\int_0^\infty \mathrm{e}^{-ts}t\int f_0(v)\,\mathrm{e}^{-ikvt}dvdt\times$$
$$\times\left(\tilde{N}_1(k,s) - Z\int_0^\infty \mathrm{e}^{-iky(t)-ts}dt\right), \quad (4)$$

where $\tilde{N}_1(k,s)$ is a Laplace-Fourier image of $n_1(x,t) \equiv \int f_1 dv$. Assuming the cold electron beam we have

$$\tilde{N}_1(k,s) = Z\rho\frac{\mathrm{e}^{-ikx_0}}{(s+ikv_0)\left((s+ikv_c)^2 + \frac{e\rho}{\epsilon_0}\right)}. \quad (5)$$

The inverse Laplace and Fourier transforms of this expression can be computed by Mathematica analytically, the expression is pretty bulky. It appears to be complex. Looking back to initial equations and assuming complex f_1 we see that equation with $\mathrm{Im}f_1$ corresponds to equation without external charge, while equation with $\mathrm{Re}f_1$ is the equation with it. So as a solution we take

$$n_1(x,t) = \mathrm{Re}\mathcal{F}^{-1}\mathcal{L}^{-1}\left\{\frac{Z\rho\mathrm{e}^{-ikx_0}}{(s+ikv_0)\left((s+ikv_c)^2 + \frac{e\rho}{\epsilon_0}\right)}\right\}. \quad (6)$$

INITIAL CONDITIONS

We change variables in (6) to the ones widely used in FEL theory [4], namely we take $z \equiv x$ as a new independent variable and $\theta = k_w z + \omega\left(\frac{z}{c} - r\right)$ and get:

$$n_1(\theta,z) = \mathrm{Re}\int_{\gamma-i\infty}^{\gamma+i\infty}\frac{-iZ\rho\mathrm{e}^{-ikx_0+ikz+\left(\frac{z}{c}-\frac{\theta-k_w z}{\omega}\right)s}}{(s+ikv_0)\left((s+ikv_c)^2+\frac{e\rho}{\epsilon_0}\right)}dkds, \quad (7)$$

* Work is supported by the U.S. Department of Energy.
† aelizarov@bnl.gov

ISBN 978-3-95450-123-6

A GENERAL METHOD FOR ANALYZING 3-D EFFECTS IN FEL AMPLIFIERS

Panagiotis Baxevanis, Ronald D.Ruth, Zhirong Huang
SLAC National Accelerator Laboratory, Menlo Park, CA 94025, USA

Abstract

FEL configurations in which the parameters of the electron beam vary along the undulator become relevant when considering new aspects of existing FELs or when exploring novel concepts. This paper describes a fully three-dimensional, analytical method suitable for studying such systems. As an example, we consider a seeded FEL driven by a beam with varying transverse sizes. In the context of the Vlasov-Maxwell formalism, a self-consistent equation governing the evolution of the radiation field amplitude is derived. An approximate solution to this equation is then obtained by employing an orthogonal expansion technique. This approach yields accurate estimates for both the amplified power and the radiation beam size. Specific numerical results are presented for two different sets of X-ray FEL parameters.

INTRODUCTION

The standard approach for analyzing the physics of a high-gain FEL in the linear regime is based on formulating and solving the eigenmode problem for the system [1–4]. However, this method is only valid when the electron beam parameters do not depend on the longitudinal position z. In some important cases, this assumption is not satisfied [5]. In this paper, we develop an analytical technique that is applicable even when such a z-dependence is present and use it to study an FEL that is driven by a mismatched or an unfocused beam. For full details, we refer to [6].

THEORY

To begin with, let us assume that the FEL radiation is generated as a relativistic, bunched electron beam passes through a planar, parabolic-pole-face undulator with symmetric focusing. From Ref. [7], the 3-D single particle equations of motion are

$$\frac{d\mathbf{x}}{dz}=\mathbf{p}\,,\quad \frac{d\mathbf{p}}{dz}=-k_\beta^2\mathbf{x}\,, \tag{1}$$

$$\frac{d\theta}{dz}=2k_u\eta-\frac{k_r}{2}[\mathbf{p}^2+k_\beta^2\mathbf{x}^2]\,, \tag{2}$$

$$\frac{d\eta}{dz}=\kappa_1\int_0^\infty d\nu E_\nu(\mathbf{x},z)e^{-i\Delta\nu k_u z}e^{i\nu\theta}+c.c.\,, \tag{3}$$

where $\mathbf{x}$ is the transverse position, k_β is the total focusing strength of the undulator system, $\theta=(k_u+k_r)z-\omega_r t+[k_rK^2/(8k_u\gamma_0^2)]\sin(2k_uz)$ is the electron phase, $\lambda_u=2\pi/k_u$ is the undulator period, $\lambda_r=\lambda_u(1+K^2/2)/(2\gamma_0^2)=2\pi/k_r=2\pi c/\omega_r$ is the resonant wavelength, γ_0 is the average Lorentz factor, K is the undulator parameter, $\eta=(\gamma-\gamma_0)/\gamma_0$ is the relative energy deviation, $\nu=\omega/\omega_r$ is the scaled frequency, $\Delta\nu=\nu-1$, E_ν is the complex amplitude of the radiation field, $\kappa_1=eKJJ/(4\gamma_0^2m_0c^2)$ (e and m_0 are the electron charge and mass, $JJ=J_0[K^2/(4+2K^2)]-J_1[K^2/(4+2K^2)]$) and c.c. stands for complex conjugate. Up to the onset of saturation effects, the operation of the FEL is accurately described by the following set of coupled, frequency-domain, linearized Vlasov-Maxwell equations:

$$\frac{\partial f_\nu}{\partial z}+\mathbf{p}\frac{\partial f_\nu}{\partial\mathbf{x}}-k_\beta^2\mathbf{x}\frac{\partial f_\nu}{\partial\mathbf{p}}+i\theta' f_\nu=-\kappa_1E_\nu e^{-i\Delta\nu k_uz}\frac{\partial f_0}{\partial\eta}\,, \tag{4}$$

$$\left(\frac{\partial}{\partial z}+\frac{\nabla_\perp^2}{2ik_r}\right)E_\nu(\mathbf{x},z)=-\kappa_2e^{i\Delta\nu k_uz}\times\int d^2\mathbf{p}\int d\eta f_\nu(\eta,\mathbf{x},\mathbf{p},z)\,, \tag{5}$$

where $f_\nu=\int d\theta f_1e^{-i\nu\theta}/(2\pi)$ is the amplitude of the perturbation f_1 to the distribution function of the electron beam, f_0 is the background distribution, $\kappa_2=eKJJ/(2\varepsilon_0\gamma_0)$ and $\theta'=d\theta/dz$ is given by Eq. (2). Moreover, the unperturbed distribution f_0 - which we take to be θ-independent - evolves according to the zeroth-order Vlasov equation

$$\frac{\partial f_0}{\partial z}+\mathbf{p}\frac{\partial f_0}{\partial\mathbf{x}}-k_\beta^2\mathbf{x}\frac{\partial f_0}{\partial\mathbf{p}}=0 \tag{6}$$

and its normalization is given by $\int d^2\mathbf{p}\int d^2\mathbf{x}\int d\eta f_0=N_b/l_b$, where l_b and N_b are, respectively, the length of one bunch and the number of electrons it contains. We note that this analysis dose not include space charge or shot noise effects.

Equation for the amplitude of the radiation field

The general solution of Eq. (4) is

$$f_\nu=f_\nu(z=0)\exp\left(-i\frac{d\theta}{dz}z\right)-\kappa_1\frac{\partial f_0}{\partial\eta}\int_0^z d\zeta E_\nu(\bar{\mathbf{x}},\zeta)e^{-i\Delta\nu k_u\zeta}\exp\left(i\frac{d\theta}{dz}\xi\right)d\zeta\,, \tag{7}$$

where $\xi=\zeta-z$ and $\bar{\mathbf{x}}=\mathbf{x}\cos(k_\beta\xi)+(\mathbf{p}/k_\beta)\sin(k_\beta\xi)$. One can also show that Eq. (6) admits solutions of the form $f_0=f_0(\eta,\mathbf{x}\cos\bar{z}-(\mathbf{p}/k_\beta)\sin\bar{z},\mathbf{x}k_\beta\sin\bar{z}+\mathbf{p}\cos\bar{z})$, where $\bar{z}=k_\beta z_0$, $z_0=z-z_e$ and z_e is a constant. We choose a background distribution given by

$$f_0=\frac{N_b}{(2\pi)^{5/2}l_b\sigma^2\sigma'^2\sigma_\eta}\exp\left(-\frac{\eta^2}{2\sigma_\eta^2}\right)\times\exp\left(\frac{k_\beta\Gamma\sin(2k_\beta z_0)}{2\sigma'^2}\mathbf{x}\mathbf{p}-\frac{k_\beta^2[1+\Gamma\cos^2(k_\beta z_0)]}{2\sigma'^2}\mathbf{x}^2-\frac{1+\Gamma\sin^2(k_\beta z_0)}{2\sigma'^2}\mathbf{p}^2\right)\,, \tag{8}$$

ISBN 978-3-95450-123-6

THEORETICAL STUDY OF SMITH–PURCELL FREE-ELECTRON LASERS

D. Li #, K. Imasaki, ILT, Osaka, Japan
M. Hangyo, Osaka University, Osaka, Japan
Z. Yang, Y. Wei, UESTC, Chengdu, China
S. Miyamoto, University of Hyogo, Hyogo, Japan
M. R. Asakawa, Y. Tsunawaki, Kansai University, Osaka, Japan

Abstract

We present an analytical theory for small-signal operation of a Smith–Purcell free-electron laser with a finitely thick electron beam travelling close to the surface of a grating. The dispersion equation is derived from a self-consistent set of small-signal equations describing the dynamics of beam-wave interaction. By solving the dispersion equation carefully, we reveal that the growth rate of the field amplitude holds a finite value at the Bragg point, which is different from previous theoretical predictions.

INTRODUCTION

It is believed that a compact, tunable, and coherent radiation source in the THz domain could be developed using the principles of Smith–Purcell free-electron lasers (SP-FEL)[1-5]. The principle of the beam-wave interaction above an open grating was established in Refs. [1-3], where the authors assumed a uniform electron beam filling the entire space above a lamellar grating and derived the dispersion relation for the evanescent wave on the surface of the grating. The authors pointed out that the device operates as a backward-wave oscillator (BWO) when the interaction with an electron beam occurs on the downward slope of the dispersion relation and as a travelling-wave tube (TWT) when the interaction occurs on the upward slope [2,3]. From their theory, they predicted that the spatial growth rate would be proportional to $I^{1/3} v_g^{-1/3}$, where I is the beam current and $v_g = d\omega/dk$ is the group velocity of the surface wave, and that the growth rate diverges at the Bragg point, where the group velocity vanishes. In evaluating the start current of the SP-FEL, all the authors followed the methods that have been used for analyzing BWOs. Almost the same boundary conditions were used in Refs. [2-4] to establish the equations determining the start current for SP-FEL. One condition, namely, the field

$$g_p = \frac{(e^{2\alpha_{II}d}-1)(\alpha_p^2\varepsilon_z^2(k_p v_0\varepsilon_x-\omega)^2-\alpha_{II}^2(v_0k_p-\omega)^2)}{e^{2\alpha_p s}((\alpha_p\varepsilon_z(k_p v_0\varepsilon_x-\omega)+\alpha_{II}(v_0k_p-\omega))^2 e^{2\alpha_{II}d}-(\alpha_p\varepsilon_z(k_p v_0\varepsilon_x-\omega)-\alpha_{II}(v_0k_p-\omega))^2)}$$

vanishes at the downstream end of the grating, is used.

However, we know that it is possible for the surface wave to interact with the electron beam even at the Bragg point, so the prediction that the growth rate diverges at the Bragg point cannot be true. Also, the behavior that occurs at the ends of a grating, which will be addressed later, and the effect of this behavior in determining start current implies that the condition of a vanishing electromagnetic field at the downstream end is less reasonable. Therefore, it is necessary to reexamine the theoretical analysis.

DISPERSION

In the Cartesian coordinate system, the electrons initially move in the z direction with velocity v_0 in the vacuum above a lamellar grating along the trajectories $s \le x \le s+d$, and are coupled with the TM mode of an electromagnetic wave. The grating is ruled parallel to the y direction, and it has a period length L, groove width A, and groove depth H. The grating is assumed to be a perfect conductor, which means that the losses from the surface current can be ignored. The component of magnetic-flux density above the grating B_y can be expanded in the form

$$B_y = \sum_{p=-\infty}^{\infty} B_p(x) e^{-jk_p z}, \quad (1)$$

Where, $k_p = k + 2\pi p/L$, and p is an integer. The wave equation is obtained below:

$$\frac{\partial^2}{\partial x^2} B_p(x) - (k_p^2 - \frac{\omega^2}{c^2} + \frac{\omega_p^2}{c^2}) B_p(x) = 0 \quad (2)$$

Following the methods using in Ref.[2,3], it is straightforward to get the dispersion equation

$$\sum_{p=-\infty}^{\infty} \Re_p \frac{\alpha_{g,0}\tan(\alpha_{g,0}d) S_{1,p} S_{2,p}}{LA\alpha_p} = 1, \quad (3)$$

Where,

$$\Re_p = \frac{1+g_p}{1-g_p}, \qquad S_{1,q} = \int_0^A e^{jk_q z} dz$$

$$S_{2,p} = \int_0^A e^{jk_p z} dz, \qquad \varepsilon_x = \frac{\omega - v_0 k_p - \frac{v_0\omega_p^2}{c^2 k_p}}{\omega - v_0 k_p - \frac{\omega_p^2}{\omega}}$$

#dazhi_li@hotmail.com

ISBN 978-3-95450-123-6

INJECTOR OPTIMIZATION FOR A HIGH-REPETITION RATE X-RAY FEL

Christos Frantzis Papadopoulos *, John Corlett, Paul J. Emma, Daniele Filippetto, Gregory Penn, Ji Qiang, Matthias Reinsch, Fernando Sannibale, Marco Venturini
Lawrence Berkeley National Lab, Berkeley, CA, 94704

Abstract

In linac driven free electron lasers, the final electron beam quality is constrained by the low energy (<100 MeV) beam dynamics at the injector. In this paper, we present studies and the optimized design for a high-repetition (> 1 MHz) injector in order to provide a high brightness electron beam. The design effort is also extended to multiple modes of operation, in particular different bunch charges. The effects of space charge and low energy compression on the electron beam brightness are also discussed for the different modes.

INTRODUCTION

The Next Generation Light Source (NGLS) is a proposed fourth generation soft xray FEL facility at Lawrence Berkeley National Lab, based on a high repetition rate, superconducting linear accelerator. In this paper, we present the beam dynamics studies and optimization results for the NGLS injector, defined as the low energy (< 100 MeV) part of the accelerator. For this, a photoinjector based on a VHF frequency electron gun is used. The constraints imposed by the high repetition rate (> 1 MHz) lead to a design that includes compression at low energy, in addition to the emittance compensation process used in other facilities.

A schematic of the injector, showing only the components directly affecting the beam dynamics studies, is shown in Fig. 1.

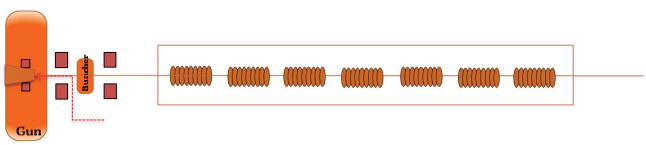

Figure 1: Conceptual design of the high rep. rate injector.

Injector Beamline

The basis of the photoinjector setup is a normal conducting electron gun, operating at a continuous wave (CW) mode at 186 MHz. A more detailed description of the injector subsystems is given in [1]. For our current purposes of beam dynamics optimization, the electron gun is defined by the on-axis z component of the electric field. In contrast to higher frequency and lower repetition rate systems, the peak value of E_z at the cathode is limited to 20 MV/m, which is sufficient to guarantee good transverse beam emittance. The cathode-to-anode gap of the gun is 4 cm, leading to a final beam energy of 750 keV at the gun exit.

* Corresponding authos:cpapadopoulos@lbl.gov

Using a load-lock system, different cathodes can be used, as described in [1]. In our simulations, we assume an initial distribution compatible with a Cs_2Te cathode, that is we assume an initial emittance given by $\epsilon_{nx}[mm-mrad] = c_e[mrad] * \sigma_x[mm]$, where σ_x is the rms beam size at the cathode and c_e a factor experimentally measured to be 0.8 [2] and conservatively estimated to be 1 in the simulations.

Downstream of the gun, 2 solenoids are present in order to perform the emittance compensation process [3]. In addition to those, a bucking coil is present behind the cathode, in order to cancel any residual magnetic field on the cathode, which would lead to an effective emittance growth. Also present, is a single cell normal conducting cavity at 1.3 GHz. This is used at 0 crossing in order to compress the beam longitudinally.

In addition to this, the simulations follow the beam across the first 7 TESLA cavities of the linac, corresponding to 1 cryomodule and about 100 MeV of energy gain. The energy gain in the TESLA cavities is limited to 16 MV/m, in order to minimize the cost of the cryoplant and the generation of dark current. The simulations show that this limit is sufficient to accelerate the beam and manipulate it longitudinally while maintaining the six dimensional brightness.

Beam Dynamics Considerations

In the case of the VHF electron gun, the relativistically correct transit time t across the gap is given by the formula $t = \sqrt{(d/c)^2 + 2d/a}$, where d is the gap length, c the speed of light and $a = eE/m$ is the acceleration of an electron of charge e, mass m under and electric field E, assumed to be constant. We can thus estimate the transit time to be $t \simeq$0.2 ns, a value much smaller than the period of the RF field given by $\tau_{RF} = 1/187MHz \simeq$5.35ns. Comparing these time scales, we can see that the dynamics in our case are conceptually closer to a DC gun than an LCLS-type cavity with RF frequency $\simeq$ 2.85 GHz.

The other dynamically important quality of the gun is the peak field at the cathode. In order to minimize dark current and power dissipation requirements this is kept at the relatively low value of $20MV/m$. This is sufficient for keeping the transverse emittance low, but requires longer bunches in order to overcome the space charge limit, as well as to minimize transverse space charge effects that may dilute the beam quality.

This constraint leads to low beam current at the injector, unless some compression is done at low energy. For this reason, we employ the single cell buncher at 0 crossing, in

ISBN 978-3-95450-123-6

THEORY OF THE QUANTUM FEL IN A NUTSHELL

P. Preiss*, Helmholtz-Zentrum Dresden-Rossendorf eV, D-01328 Dresden, Germany
and Institut für Quantenphysik, Universität Ulm, D-89069 Ulm, Germany
R. Sauerbrey, Helmholtz-Zentrum Dresden-Rossendorf eV, D-01328 Dresden, Germany
M. S. Zubairy, Institute for Quantum Science and Engineering,
Department of Physics and Astronomy, Texas A&M University, College Station, Texas 77843, USA
R. Endrich, E. Giese, P. Kling, M. Knobl and W. P. Schleich,
Institut für Quantenphysik and Center for Integrated Quantum Science and Technology (IQST),
Universität Ulm, D-89069 Ulm, Germany

Abstract

A new regime of the free-electron laser arises when the recoil of the electron due to its scattering in the wiggler and laser field cannot be neglected any more. In such a quantum free-electron laser the discreetness of the momenta becomes visible and leads to novel effects. We present a quantum mechanical theory in this domain.

INTRODUCTION

Classical electrodynamics combined with classical statistical mechanics are sufficient [1] to describe today's free-electron laser (FEL) devices. However, new developments in accelerator and laser physics raise hope for the experimental realization of a quantum free-electron laser (QFEL). In this paper we outline a theory of the QFEL guided by techniques of quantum optics developed in the context of the one-atom maser [2]. For an earlier and different approach towards the QFEL we refer to [3][4].

We start by recalling the Hamiltonian [5] corresponding to a one-dimensional, single-particle description of the FEL in the co-moving Bambini-Renieri frame where the electrons move with a non-relativistic velocity. Based on the classical free-electron laser (CFEL) and introducing recoil effects by hand we illustrate the emergence of the quantum mechanical regime of the FEL from the pendulum equation. Moreover, a perturbation theory in which these effects are fully taken into account illustrates in a vivid way the characteristic features of the QFEL. Here, the electron can emit or absorb only a single photon leading to a two-level dynamics. In this way we obtain an analytically solvable model for the QFEL. The resulting gain function confirms the applicability of the two-level QFEL model. Finally, we establish the key experimental requirements for realizing a QFEL device. Our conditions are in agreement with the ones put forward in [4].

QUANTUM MODEL OF FEL

The interaction of a single electron in the FEL with the wiggler field and the emitted laser field, when described in the co-moving Bambini-Renieri frame where the frequencies $\omega = ck$ of both fields coincide, is determined [5] by the Hamiltonian $\hat{H} \equiv \hat{H}_{\rm F} + \hat{H}_{\rm I}$ consisting of the free part

$$\hat{H}_{\rm F} \equiv \frac{\hat{p}^2}{2m} + \hbar\omega \left(\hat{a}_{\rm L}^\dagger \hat{a}_{\rm L} + \hat{a}_{\rm W}^\dagger \hat{a}_{\rm W} \right) \tag{1}$$

and the interaction part

$$\hat{H}_{\rm I} \equiv \hbar\tilde{g} \left(\hat{a}_{\rm L}^\dagger \hat{a}_{\rm W} e^{-i2k\hat{z}} + \hat{a}_{\rm L} \hat{a}_{\rm W}^\dagger e^{i2k\hat{z}} \right) \tag{2}$$

with the coupling strength $\tilde{g}$. The creation or annihilation operators $\hat{a}_{\rm L}^\dagger$ or $\hat{a}_{\rm L}$ and $\hat{a}_{\rm W}^\dagger$ or $\hat{a}_{\rm W}$ of the laser and wiggler field, respectively, obey the familiar commutation relation $[\hat{a}_j, \hat{a}_j^\dagger] = 1$, where $j = {\rm L}$ and W. Moreover, $\hat{z}$ and $\hat{p}$ denote the position and momentum operator of the electron in the Bambini-Renieri frame obeying $[\hat{z}, \hat{p}] = i\hbar$ and $m \equiv m_e(1 + a_0^2)$ represents the shifted mass of the electron where a_0 is the wiggler parameter, $k \equiv 2\pi/\lambda$ the wave number of the laser and wiggler field with wavelength λ and m_e the rest mass of the electron. The exponential $e^{\pm i2k\hat{z}}$ in Eq. (2) indicates a shift in the momentum of the electron by the recoil $q \equiv 2\hbar k$ when one photon of the wiggler scatters into the laser field or vice versa.

In the interaction picture $\hat{H}$ transforms into

$$\hat{H}_{\rm I}^{(\rm I)} \equiv \hbar g \left(\hat{a}_{\rm L}^\dagger e^{-i2k\hat{z}} e^{-i2k(\hat{p}-q/2)t/m} + {\rm h.c.} \right) \tag{3}$$

where we have used the semiclassical approximation $\hat{a}_{\rm W}^\dagger \approx \hat{a}_{\rm W} \approx \sqrt{n_{\rm W}}$ for the wiggler field.

Assuming circularly polarized vector potentials

$$\hat{\mathbf{A}}_{\rm L} \equiv \mathcal{A}_{\rm L} \left(\mathbf{e} \hat{a}_{\rm L} e^{-i(\omega t - k\hat{z})} + {\rm h.c.} \right) \tag{4}$$

and

$$\hat{\mathbf{A}}_{\rm W} = \mathcal{A}_{\rm W} \left(\mathbf{e} \hat{a}_{\rm W} e^{-i(\omega t + k\hat{z})} + {\rm h.c.} \right) \tag{5}$$

for the laser field, and the wiggler field in Weizsäcker-Williams approximation of strengths $\mathcal{A}_{\rm L}$ and $\mathcal{A}_{\rm W}$, respectively, and polarization vectors that obey the relation $\mathbf{e}^2 = \mathbf{e}^{*2} = 0$, we obtain the coupling constant

$$g = \frac{e_0^2}{\hbar m} \mathcal{A}_{\rm L} \mathcal{A}_{\rm W} \sqrt{n_{\rm W}} \tag{6}$$

with the elementary charge e_0.

* p.preiss@hzdr.de

ISBN 978-3-95450-123-6

SATURATION IN FREE ELECTRON LASER WITH QUADRUPOLE WIGGLER AND AXIAL MAGNETIC FIELD

P. Yahyaee, A. Kordbacheh, IUST, Tehran, Iran

Abstract

In this paper, we study the nonlinear evolution of a helical quadrupole wiggler FEL, in Raman regime and in the presence of space-charge field. By using Maxwell's equations and nonwiggler averaged equation of motion of electron beam, a set of nonlinear first-order differential equations describing the evolution of the helical quadrupole FEL is derived in the slowly varying amplitude and wave number approximation and solved numerically by the Runge–Kutta method. The beam is cold and propagates with a relativistic velocity. The amplitude of wiggler field increases adiabatically from zero to a constant level. To focus the electron beam, we apply an axial magnetic field. Finally, the results of helical quadrupole wiggler are compared to an equivalent dipole wiggler.

INTRODUCTION

There are two principle directions for FEL development activities. One is to generate high coherent X-ray pulses, and the other is to generate high average power at infrared wavelength. A FEL which works at millimeter wavelengths has many applications such as telecommunication and measurement of solid state materials and semi conductor's properties.

In order to generate a quadrupole wiggler magnetic field, one can use a helical winding of four wires, with a current flow in in two wires in one direction, and in the oder two wires in the opposite direction. First works on quadrupole wiggler FEL were done by Levush *et al.* [1]. They proposed this kind of wiggler and showed that it can represent a new concept to obtain high power, coherent radiation in millimeter and sub millimeter regime. They examined the near axis orbit properties of a quadrupole wiggler without an axial guide field but including the effects of space charge and showed that it had improved beam stability when compared to a dipole wiggler. The effect of an axial guide field on the nonlinear stage of the dipole wiggler FEL interaction studied by Freund [2]

Antonsen *et al.* [6] examined the nonlinear theory of a quadrupole free-electron laser when the betatron frequency is close to the mismatch frequency and found that it can reduced the three-dimensional equations to an integrable one-dimensional equation. CHANG *et al.* examined the characteristics of a Compton regime quadrupole magnetic wiggler for a FEL amplifier neglecting space charge effects. They showed that Optimum efficiencies for the quadrupole case occur for lower beam voltages, larger guide radii, and shorter total wiggler lengths than for a comparable dipole case [7].

The purpose of this study is to consider a FEL with a helical quadrupole wiggler in Raman regime at millimeter wavelengths.

This code is based on the equations in which the space-charge effect is presented and then, there are some additional terms in the equations to show this effect. This is an improvement of CHANG *et al.* Formulation in which this effect is neglected [7]. In fact, we modified Freund *et al.* formulation [2], to examine the evolution of radiation amplitude for a helical quadrupole wiggler and finally we compare its results with an equivalent helical dipole case.

FIELDS STRUCTURE AND POTENTIAL EQUATIONS

The idealized, one dimensional helical quadrupole wiggler magnetic field may be described as [7]

$$\mathbf{B_W}(z) = B_W(z)k_W\mathbf{e}_x\left[x\cos(2k_W z) + y\sin(2k_W z)\right] + B_W(z)k_W\mathbf{e}_y\left[-y\cos(2k_W z) + x\sin(2k_W z)\right] \quad (1)$$

$$B_w(z) = \begin{cases} B_w \sin^2\left(\dfrac{k_w z}{4N_w}\right), & 0 \le z \le N_w\lambda_w \\ B_w, & N_w\lambda_w \le z \end{cases} \quad (2)$$

Where B_W refers to the wiggler amplitude which presents an adiabatic injection of the electron beam and $k_W = 2\pi/\lambda_W$ is the wiggler wave number.

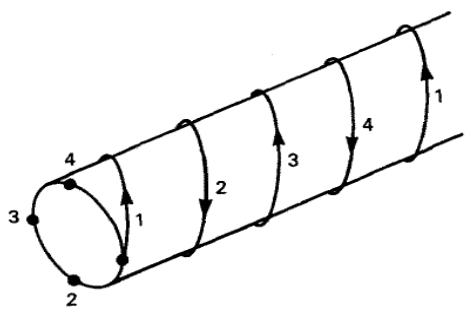

Figure 1: Quadrupole wiggler configuration

In addition to the wiggler filed, an axial magnetic field is used to focus the beam,

$$\mathbf{B}_0 = B_0 e_z \quad (3)$$

The vector and scalar potentials of radiation and space charge may be in the form of [2], [5]

$$\delta\mathbf{A}(z,t) = \delta A(z)\left[\mathbf{e}_x\cos\alpha_+(z,t) - \mathbf{e}_y\sin\alpha_+(z,t)\right] \quad (4)$$

$$\delta\phi(z,t) = \delta\rho(z)\cos\alpha(z,t) \quad (5)$$

$$\alpha_+(z,t) = \int_0^z dz' k_+(z') - \omega t \quad (6)$$

$$\alpha(z,t) = \int_0^z dz' k(z') - \omega t \quad (7)$$

ISBN 978-3-95450-123-6

DETAILED MODELING OF SEEDED FREE-ELECTRON LASERS

S. Reiche – Paul Scherrer Institute, Villigen, Switzerland
M. Carlà – Università degli Studi di Firenze, Florence, Italy

Abstract

Seeding schemes for Free Electron Lasers have mostly a strong impact on the electron distribution by either a conversion of an energy modulation into a current modulation with high harmonic content (HGHG seeding) or an overcompression of this energy modulation to induce energy bands (EEHG seeding) or smear out any bunching in the electron beam (self-seeding).

Most codes follow an approach using thin electron slices, which are carefully generated to provide the correct shot-noise but which also prevents them from mixing and resorting the macro-particle distribution. The FEL code Genesis 1.3 has been modified to allow resolution of each individual electron. Using this approach the correct shot noise at all frequencies is provided and permits re-binning of the particles to the 3D radiation grid at any time. The results for self-seeding and HGHG seeding are discussed.

INTRODUCTION

Most FEL programs, such as Genesis [1] and Ginger [2], run with less particles than the number of electrons to be simulated for fast and efficient calculations. To simulate the correct shot noise in the electron distribution they rely on quiet loading algorithms [3] to suppress the inherent fluctuation in the macro particle distribution and to randomize the particle positions in a controlled manner. A common approach is to group macro particles into ”beamlets” [4], where the group is evaluated as a whole when used in the source term of the Maxwell equation.

However these codes are required to keep these beamlets together at the same grid location of the radiation field. While this is fully sufficient for single pass SASE FEL simulations strong electron beam manipulations can spread electrons over many wavelength. Most prominent are advanced methods such as echo-enabled harmonic generation [5] and the debunching effect in a self-seeding scheme [6]. The beamlets cannot be split, redistributed over the radiation grid and then recombined with other macro particles. Therefore both schemes cannot be modeled self-consistently with the existing codes.

On the other hand it has to be noted that for X-ray FELs the number of electrons per radiation wavelength is relatively low (e. g. a 3 kA beam contains only 1500 electrons per wavelength at 1 Å) and lies within the capability of FEL simulation codes which progress sequentially through the electron beam keeping only a few radiation slices in memory at any time. A direct representation of each individual electron would simplify the preparation of the particle distribution a lot. Therefore Genesis 1.3 has been modified to model all electrons.

This paper describes the simulation strategy to resolve each individual electron in the bunch and the adaptation in the algorithm to sort particles after some radical changes in the particle distribution such as magnetic chicanes or conversion to a higher harmonic. Based on the modified code, sample problems for self-seeding [7] and HGHG FELs [8] are calculated and discussed in the following sections.

SIMULATION STRATEGY

Because Genesis propagates electron slices sequentially through the undulator the sorting among slices cannot be integrated directly into the source code. Instead the electron distribution is dumped after the first stage and an external program sorts and rebins the electrons to generate a new particle file, which is then imported into Genesis for the second stage of the FEL. The sorting program utilizes a parallel computer using MPI, which allows to hold the entire particle distribution of about 40 GByte of size in memory. Because the sorting in the longitudinal position is a one dimensional problem the MPI algorithm is structured very similar to the bubble sort algorithm [9]. The very efficient algorithm is briefly described in the following.

All nodes are arranged in a 1D topology, where each node corresponds to a slice in the longitudinal bunch frame. Each node reads a section of the particle distribution and splits them into three distributions: particles which are located ahead of the given time-window, particles behind the time window and particles which fall into the time-window. The particles, which are not in the correct time window, are then exchanged with adjacent nodes, pushing them in the correct direction within the 1D topology. Each node gathers particles from two neighbor nodes and the sorting process is repeated until each node indicates that no more electrons need to be transmitted. Then each node bins the electrons within its time-window into the individually radiating slices and writes out the particle distribution.

It is foreseen that in a future release Genesis will hold the entire particle distribution in memory. Then the algorithm, described above, can be integrated into the code for a single execution of a multi-stage FEL.

SELF-SEEDING

The simulations for self-seeding are modeled after the layout of the SwissFEL hard X-ray FEL beamline Aramis

ISBN 978-3-95450-123-6

DARK CURRENT STUDIES FOR SWISSFEL

F. Le Pimpec, R. Zennaro, S. Reiche, A. Adelmann
Paul Scherrer Institut, 5232 Villigen, Switzerland
B. Grigoryan
CANDLE Yerevan, Armenia

Abstract

Activation of the surrounding of an accelerator must be quantified and those data provided to the official agencies. This is a necessary step in obtaining the appropriate authorization to operate such accelerator. The SwissFEL, being a 4^{th} generation light source, will produce more accelerated charges, which are dumped or lost, than any conventional 3^{rd} generation light source, like the Swiss Light Source. We have simulated the propagation of a dark current beam produced in the photoelectron gun using tracking codes like ASTRA and Elegant for the current layout of the SwissFEL. Detailed experimental study have been carried out at the SwissFEL test facilities at PSI (C-Band RF Stand and SwissFEL Injector Test Facility), in order to provide necessary input data for detailed study of components using the simulation code OPAL. A summary of these studies are presented.

DARK CURRENT SIMULATIONS FOR SWISSFEL

The dark current is initially generated by field emission from the photocathode, in an RF gun, and around the irises of the cavities for all accelerating RF structures. The direction of propagation of the electrons obviously depends on the RF phase and the efficiency of propagation depends of the type of cavity, traveling or standing wave (TW, SW). Impinging electrons to the surrounding walls of the cavity will produce secondaries which can also be transported along the beam line and add to the dark current.

ASTRA Simulations

We have simulated the dark current of the SwissFEL [1] S-band standing wave photogun to the end of the second 4 m long S-band traveling wave structure, by using the tracking code ASTRA [2]. The initial electron bunch was produced by using the SwissFEL nominal bunch, spreading its dimension in time and space. The emission time was limited to 120 ps which is only covering one RF bucket $\pm 60^{\circ}$ around the on-crest phase. We turned off the space charge option. The dark current is in reality emitted at some threshold and at every RF bucket. This simple approximation is sufficient as every other dark current bucket propagating downstream of the RF gun will be transported identically by the machine optics. From the initial 300 k particles of the bunch, $\sim$22% are lost on the cathode. The losses on the walls (in percent) are quantified along the first 13 m of the machine using the remaining $\sim$234 k particles, Fig.1. Only 9.7% of those remaining particles reach the beginning of the third S-band accelerating structures. As shown in Fig.1, more than 90% of the bunch is lost before even reaching the first S-band structure with a $\sim$7 MeV kinetic energy. The 9.7% remaining particles are concentrated in the core of the initial bunch. The output distribution was reused as an input for the elegant tracker [3] starting from the beginning of the third S-band structure.

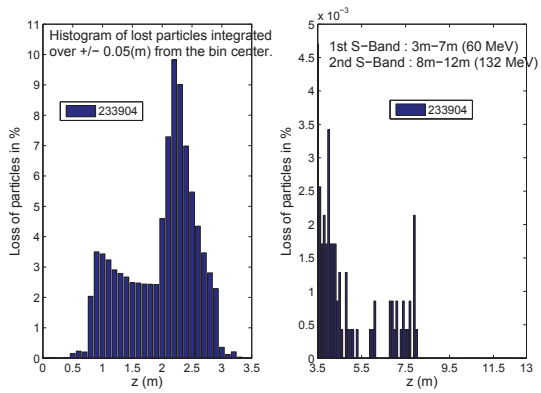

Figure 1: Histogram of the particle losses at the walls of the accelerator up to the end of the second S-band cavity (132 MeV)

Elegant Simulations

The leftover particles from the ASTRA simulation were not numerous enough to do a proper elegant simulation. We have multiplied the input distribution by cloning every particle with a small change in their positions and momenta. We hence produced 2.2 million particles. The tracking was done using the SwissFEL Elegant model which includes the physical apertures of the machine and by adding collimators toward the end of the Aramis beam line [1]. The space charge and wake field options were turned off. Fig.2 (bottom plot) and Fig.3 show the location where particles are lost and with which energy and energy spread. The energy spread for the lost particles is small, less than 1%, as can be seen by the small error bars displayed in the bottom plot of Fig.2. Losses are concentrated before the first bunch compressor (s$\sim$50 m) and at the second bunch compressor (s$\sim$200 m), as shown by Fig.3. No other losses are recorded after the second bunch compressor. The transverse collimators placed at the end of the machine (s $>$ 400 m) induce dark current losses only for apertures

ISBN 978-3-95450-123-6

SWITCHYARD DESIGN: ATHOS

N. Milas* and S. Reiche, PSI, Villigen 5232, Switzerland

Abstract

The SwissFEL facility will produce coherent, ultrabright and ultra-short photon pulses covering a wavelength range from 0.1 nm to 7 nm, requiring an emittance of 0.43 mm mrad or better. In order to provide electrons to the soft X-ray beam line a switchyard is necessary. This beamline will switch the electron bunch coming from the SwissFEL linac, with an energy of 3.0 GeV, and transport it to Athos. The switchyard has to be designed in such a way to guarantee that beam properties like low emittance, high peak charge and small bunch length will not be spoiled. In order to keep the switchyard as versatile as possible it can work for a range of values of R_{56} from isochronous up to 6 mm, when the bunch is stretched by a factor two, and also be able to transport the beam in the so called "large bandwidth" [1] mode. In this paper we present the schematics for the switchyard, discuss its many modes of operation, sextupole correction scheme and positioning of energy collimator for machine protection.

SWITCHYARD DESCRIPTION

The switchyard for SwissFEL [2] diverts the beam coming from Linac 2, with an energy of 3.0 GeV, to thesoft X-ray undulator (Athos beamline). At the Switchyard entrance a set of 3 fast resonant kickers [3] followed by a lambertson magnet will deviate the second of the two bunches accelerated in the Linac. This second bunch will then be further transported towards Athos beamline while the first bunch continues straight towards Aramis. In order to allow some flexibility in Athos and to accommodate possible different working configurations, it is possible to setup the switchyard for a range of values of R_{56}.

The switchyard has a total length of 65 m and the separation between the Athos and Aramis beamlines is 3.75 m, with a net bending angle equal to zero, making the two beamlines parallel to each other, as shown in Figure1. This design has one triple-bend (TBA) and one double-bend (DBA) achromat sections; and each section has a total bending angle of 5 degrees. To make the full setup of the switchyard easier, specially during commissioning, it was divided into 4 sections, having each one a specific function:

Section 1 (TBA): The central dipole in the triple bend is weaker and is situated in a high dispersive area, by changing the dispersion function in this magnet we can choose the value of R_{56}, making the sector go from isochronous (no variation on the bunch length) to a value of R_{56} = 6 mm (relative to a bunch lengthening factor of 1.9).

Section 2: Since the kickers deviate the beam vertically it is also required that in the switchyard the beam is brought back to level with respect to the rest of the machine, this is performed by a set of 2 vertical dipoles right after the triple-bend. In this section also, 4 quadrupoles are responsible for closing the vertical dispersion created by the kickers.

Section 3: The phase advance between the two bends (TBA and DBA) is adjustable by changing the settings of the quadrupoles in the transport line (5 quadrupoles after the second vertical dipole). The lattice functions on the dipoles of the switchyard are set to the minimum value possible so that kicks due to coherent synchrotron radiation (CSR) are minimized and by adjusting the phase advance between them, we can compensate for the projected emittance dilution caused by CSR. A de-chirper is also foreseen to be installed in this section.

Section 4 (DBA): Finally, the second bend set is setup in order to accommodate the energy collimators.

KICKER AND SEPTUM

SwissFEL will work in double bunch mode with a bunch time separation of 28 ns and a repetition rate of 100 Hz. In order to separate the beam for the soft x-ray beamline 3 resonant kickers will deflect the beam in the vertical direction and a DC Lambertson magnet will separate it horizontally, this setup has the advantage of introducing much less noise on the beam but on the other hand creates vertical dispersion that must be taken care of in the switchyard.

Given the requirements of the undulators the maximum orbit jitter acceptable due to pulsed elements at the switchyard is $0.05\sigma_{x,y}$ and for the Athos beamline, a maximum acceptable projected emittance growth of 5%. In order to estimate the shot-to-shot jitter for the kicker and lambertson we used the following expression

$$\frac{\Delta\theta_{rms}}{\theta} < \frac{0.05}{\theta}\sqrt{\frac{\epsilon_N}{\beta\gamma}} \qquad (1)$$

where $\Delta\theta$ is the angle fluctuation, θ the total bending angle, ϵ_N the normalized emittance, β the beta function at the element position and γ the Lorentz factor. From this expression, and considering the most extreme case of 10 pC operation [2], we find that $\Delta\theta_K < 86$ ppm and $\Delta\theta_L < 3.5$ ppm, for the kickers and lambertson respectively. Those jitter requirements, specially for the kickers, are very tight and are under study.

* natalia.abreu@psi.ch

ISBN 978-3-95450-123-6

INVESTIGATION OF NON-RECTANGULAR RF PULSE INFLUENCE IN EMITTED ELECTRON BEAM OF THE THERMIONIC RF-GUN AT THE LINAC-BASED THZ FACILTY IN THAILAND

K. Damminsek*, S. Rimjaem, Department of Physics and Materials Science,
Faculty of Science, Chiang Mai University, Chiang Mai, 50200, Thailand

Abstract

An electron gun of a linac-based THz radiation source at the Plasma and Beam Physics (PBP) Research Facility at Chiang Mai University (CMU) in Thailand is a 1-1/2 cell S-band standing wave RF cavity with an Os/Ru coating tungsten dispenser cathode. The electron current density of a few A/cm^2 can be achieved from zero-field thermionic emission using this cathode type at a desired operating temperature. However, non-rectangular RF pulse shape has a significant influence on the acceleration of electrons inside the RF cavity, which leads to the properties of the output electron beam from a thermionic RF-gun. Numerical and experimental studies on the contribution of the effect have been carried out. Results of the investigations are presented and discussed in this contribution.

INTRODUCTION

A thermionic cathode RF-gun is widely used as a promising electron source for a linac-based accelerator due to its compact, economical and easy operation system. It can produce output electron bunches with higher brightness than DC electron guns with no additional buncher system. It also does not require an expansive high power laser system like in the case of a photo-cathode RF-gun. However, due to the high accelerating gradient at the cathode surface some fraction of electrons emitted late in the RF oscillating cycle feel a decreasing accelerating field and do not exit from the gun before the RF field reverses its direction. These electrons are decelerated back to hit the cathode at high energies leading to a serious disadvantage of the thermionic RF-gun called electron back-bombardment effect.

For an RF-gun of a linac-based THz radiation source at the PBP facility, the electron back-bombardment limits a stable operation with an RF pulse length longer than a few microseconds. The RF pulse length has been shortened in order to reduce the influence of this effect to achieve a more stable beam operation. The drawback of the shortened RF pulse length at our facility is a non-rectangular RF pulse shape. The influence of the non-rectangular RF pulse on the electron beam properties have been investigated in order to improve the performance of the thermionic RF-gun and to accumulate the information for the future upgrade of the RF system.

* kantaphon.damminsek@gmail.com

THERMIONIC EMISSION IN RF-GUN

The thermionic cathode of the RF-gun at the PBP-linac facility is a tungsten dispenser cathode with Os/Ru coating model 101207, which is commercially available from the HeatWaves Lab Company [1]. Pure tungsten has a work function of 4.5 eV. After the proper activation by heating the cathode to have a temperature above 1050 °C, the work function of the cathode material lowers from 4.5 eV to 2.1 eV [2]. Applying an Os/Ru coating at the cathode surface leads to the lower work function of 1.9 eV. Specifications of the thermionic RF-gun at the PBP-linac facility are listed in Table 1.

Table 1: Specifications of the Thermionic Cathode

Parameter	Value
Emitting surface diameter	6 mm
Os/Ru coating thickness	0.3-0.5 μ m
Cathode work function	1.9 eV
Emissivity at λ=0.65 μm	0.44
Cold resistance at 20°C	0.54 Ω
Hot resistance in operation	2.2-2.3 Ω
Nominal filament power in operation	13.4-13.8 W
Operating temperature	~950 °C

When the electricity power is provided to the cathode filament the heat is transferred to the cathode. As a result, the cathode temperature increases (Fig. 1) leading to an increasing of the kinetic energy of electrons at the cathode surface to be higher than the Fermi energy and the work function of the cathode material. Then, the electrons escape from the cathode surface to become free electrons in the vacuum chamber of the RF-gun. At zero-field, the kinetic energy (KE) of electrons depends on the temperature (T) of the heating cathode as $KE = (3/2)kT$, where k is the Boltzmann constant. In experiment, the cathode surface temperature at various filament powers can be measured using a heated-wire comparative type optical Pyrometer. The measured results show that there is a proportional relationship between the filament power and the cathode temperature as showed in Fig. 1. In the measured range of cathode temperature between 770°C to 1065°C, the kinetic energies of the free electrons are 0.22 eV to 0.27 eV.

ISBN 978-3-95450-123-6

SIMULATION FOR NEW INJECTOR TEST FACILITY OF PAL-XFEL*

M. Chae#, I.S. Ko, POSTECH, Pohang, 790-784, S.Korea
J. Hong, J.H Han, S.J. Park, PAL, Pohang, 790-784, S.Korea

Abstract

For the preparation of PAL-XFEL, Injector Test Facility (ITF) has been constructed and required beamline components are being installed for the test of the injector system. ITF components include an RF gun, two accelerating columns, solenoids and basic diagnostic components such as spectrometers, quad scan system, BPMs, a wire scanner. Passing through the two accelerating columns an electron beam is accelerated up to 139 MeV with a charge of 200 pC and an emittance under 0.5 μm. For optimization of operation modes and precise diagnostics simulation for ITF beamline has been carried out with the ASTRA code. In this paper simulation results and discussion related to emittance measurements will be shown.

INTRODUCTION

ITF consists of an S-band 1.6-cell photocathode RF gun, two S-band accelerating columns, solenoids and diagnostic components. In particular, quadrupoles will be installed downstream of the 2nd accelerating column for quad scan. And also a laser heater system and an RF deflector for longitudinal phase space measurement will be installed next year. Assembling all components except the laser heater system and the deflector will be ready by the end of August. Beam commissioning will be started soon and the generation of a beam with an emittance under 0.5 μm is the first plan for this year. A schematic layout of the ITF beamline is shown in Fig. 1.

Diagnostics for ITF

Diagnostics for ITF will be conducted mainly in two energy regions, i.e. the Low Energy (LE) region with an energy of 6 MeV and the High Energy (HE) region with an energy of 139 MeV. Detailed diagnostic components are as follows:

- LE dipole & HE dipole for energy measurement.
- ICTs & Faraday cup.
- BPMs & phase monitors.
- quadrupoles for quad scan.
- wire scanner.
- RF deflector.

Quad scans will be carried out by one HE quadrupole and two LE quadrupoles. The LE quadrupoles, HE quadrupole and screen are located at 9.15 m, 9.55 m, 13.22 m and 15.86 m from the cathode respectively. Two LE quadrupoles are not mainly installed for quad scan and the locations of them are not optimized for quad scan. Thus additional quadrupoles will be installed upstream of the existing HE quadrupole if necessary. Detailed specification of the quadrupoles are listed in Table 1.

Table 1: Specification of the Quadrupoles for Quad Scan

Component	effective length	Max. quadrupole strength
LE quadrupole	8 cm	7.21 /m^2
HE quadrupole	14.7 cm	27.97 /m^2

QUAD SCAN

Quadrupole scan is mostly used for emittance measurement of a beam with high energy. It is non beam destructive way to measure and can be affected by the nonlinear field of the quadrupole thus the quadrupoles should be properly arranged, say, they should have enough drift space longer than their focal length.

Let's consider a beam transfer matrix as follows:

$$M = \begin{pmatrix} m_{11} & m_{12} \\ m_{21} & m_{22} \end{pmatrix} \quad (1)$$

This matrix is generally a product of various matrices describing drifts, quadrupoles, etc. In our case each element is the function of focal length, that is, the strength and effective length of quadrupole and distance between components of beam optics we consider and also we already know. For 2nd moments of a certain position of the beamline there exist beamsize which corresponds to certain focal length and distance. Therefore if someone measure at least three different beamsize corresponding to different beam optic functions 2nd moments in phase space can be calculated by numerical method. This can be expressed as follows [1],[2]:

$$\begin{pmatrix} x_0^2 \\ x_0 x_0^{'} \\ x_0^{'2} \end{pmatrix} = \begin{pmatrix} m_{11(1)}^{\ 2} & 2m_{11(1)}m_{12(1)} & m_{12(1)}^{\ 2} \\ m_{11(2)}^{\ 2} & 2m_{11(2)}m_{12(2)} & m_{12(2)}^{\ 2} \\ \vdots & \vdots & \vdots \\ m_{11(N)}^{\ 2} & 2m_{11(N)}m_{12(N)} & m_{12(N)}^{\ 2} \end{pmatrix}^{-1} \begin{pmatrix} x_{(1)}^2 \\ x_{(2)}^2 \\ \vdots \\ x_{(N)}^2 \end{pmatrix} \quad (2)$$

Here subscript stands for number of cases with different beam optics, that is, the number of combinations of quadrupoles with different strength or position. Calculation will be more accurate for more measurement conducted. From calculated 2nd beam moments normalized transverse beam emittance can be evaluated by a formula as:

*Work supported by the National Research Foundation of Korea (NRF) funded by the Ministry of Education, Science and Technology (MEST) (Grant No. 2008-0059842).
#cmswill@postech.ac.kr

ISBN 978-3-95450-123-6

LOW EMITTANCE INJECTOR DEVELOPMENT FOR THE PAL-XFEL PROJECT*

J.-H. Han†, J. Hong, I. Hwang, M. S. Chae, S.-J. Park, H.-S. Kang, I. S. Ko,
Pohang Accelerator Laboratory (PAL), Pohang, 790-784, Republic of Korea

Abstract

An injector for low emittance electron beam generation as well as high repetition rate and more reliable operation is under development at PAL. Here, we introduce the design of the S-band photocathode gun using a coaxial coupler for the PAL-XFEL project. The gun will be able to provide a low emittance electron beam for ultimate X-ray FEL performance. Injector beam dynamics optimization using this gun is shown. Various injector operating conditions are studied numerically.

INTRODUCTION

The Pohang Accelerator Laboratory X-ray Free electron Laser (PAL-XFEL) project [1] started in 2011. This project aims at the generation of X-ray FEL radiation in the range of 0.1 to 10 nm for users. The machine consists of a 10 GeV linear accelerator and soft and hard X-ray undulator beamlines. The accelerator will operate at a repetition rate of 60 Hz. Building construction starts in September 2012.

The PAL-XFEL baseline injector [2] was designed for satisfying the PAL-XFEL beam requirements. The baseline injector adopts the GTF gun [3, 4] developed at PAL over the last six years and two 3 m long S-band traveling-wave tubes. The injector has been installed in the Injector Test Facility (ITF) and first beam generation is foreseen in September 2012. RF conditioning of the gun cavity and accelerator tubes is being started. Numerical simulations using the baseline injector shows 0.26 mm mrad normalized transverse rms emittance at 200 pC are achievable [2]. The experimental target is 0.4 mm mrad as first phase. For emittance measurements, three quadrupole magnets and a screen will be used [5].

Transverse emittance of an electron beam has a crucial role in hard X-ray SASE FEL. For the PAL-XFEL hard X-ray case, a 50% emittance reduction will result in 30 to 50% FEL power increase as well as 20 to 50% FEL saturation length reduction depending on other parameters [6]. Even though the baseline injector will fully satisfy the PAL-XFEL beam parameter, a low emittance injector will allow better FEL performance with reduced undulator length.

The low emittance injector has two major changes compared with the baseline injector. The RF gun with a side coupler is replace with a gun with coaxial coupler. Three accelerator tubes will be used for acceleration instead of two tubes in the baseline injector. Possible future installation of the low emittance injector in the PAL-XFEL main linac will be also discussed.

* Work supported by The Ministry of Education, Science and Technology of the Korean Government

† janghui_han@postech.ac.kr

LOW EMITTANCE GUN

The PAL-XFEL low emittance gun is similar as the Diamond S-band (2.998 GHz) gun which was developed for high repetition rate operation and low emittance beam generation [7]. By adopting a coaxial RF coupler connected at the gun exit as for the DESY PITZ gun [8], the gun solenoid can be positioned at an optimum location for low emittance and cooling water channels can fully surround the gun cavity cylinder for maximizing cooling capacity and allowing uniform temperature distribution over the gun body. With an exchangeable photocathode plug, high quantum efficiency cathodes can be used for reducing drive-laser power requirement and a damaged cathode can be easily replaced with a fresh one under ultra-high vacuum. Since the PAL-XFEL gun should operate at 2.856 GHz, the Diamond gun cavity was enlarged by about 5% and cooling channel was adjusted. The first technical design is ready.

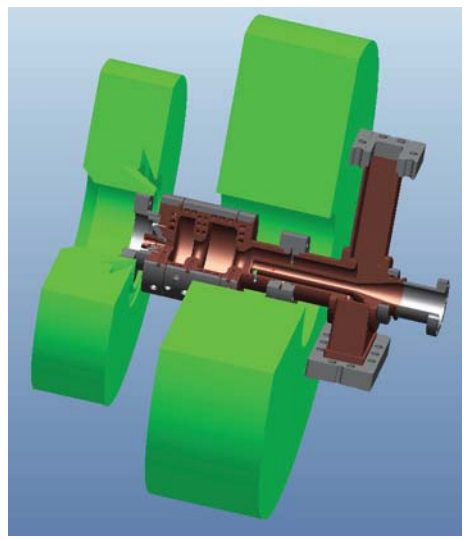

Figure 1: Low emittance gun cavity and solenoids. A cathode exchange system is connected at the rear of the gun.

In this gun design, the center of the solenoid is at 0.105 m from the cathode. For magnetic field compensation at the cathode, a bucking solenoid is placed immediate upstream of the gun.

Maximum repetition rate required for the PAL-XFEL gun is 120 Hz even considering future upgrade [1]. At the first gun design, no RF pick-up probed was included as for

ISBN 978-3-95450-123-6

MICROBUNCHING INSTABILITY STUDY FOR THE PAL-XFEL LINAC*

J.-H. Han†, I. Hwang, H.-S. Kang,
Pohang Accelerator Laboratory (PAL), Pohang, 790-784, Republic of Korea

Abstract

PAL-XFEL is designed to generate X-ray FEL radiation in a range of 0.1 and 10 nm for users. The machine consists of a 10 GeV linear accelerator and five undulator beamlines. An electron beam is generated at a low emittance S-band photoinjector and accelerated through an S-band normal conducting linac. Microbunching instability may occur when the beam goes through magnetic bunch compressors and beam spreaders. We show preliminary microbunching instability simulation study for the PAL-XFEL linac.

INTRODUCTION

For the generation of fully coherent hard X-ray laser, the PAL-XFEL linac will deliver a high brightness electron beam from the injector to the undulator beamlines [1]. Small transverse emittance and high peak current of an electron bunch is essential for SASE FEL; however such a high brightness beam may suffer from collective effects. Microbunching instability may impair electron beam quality and make beam image measurements with screen difficult. The PAL-XFEL linac uses three magnetic chicanes for bunch compression for flexible and independent operation of the soft and hard X-ray beamines [2]. Microbunching may amplify significantly through the chicanes. The linac has a beam branch to the soft X-ray beamlines at the 3 GeV point from the 10 GeV main linac. The branch has a large deflection angle, $3^\circ + 3^\circ$, therefore that is a potential instability source. The electron beam spreaders for three hard and two soft X-ray beamlines are also concerned.

In this preliminary study, the Elegant code [3] is used for beam tracking through the linac including the chicanes. A simplified laser heater model in Elegant is used for simulation including a magnetic chicane, a small undulator and a heat laser. The soft X-ray branch and the beam spreaders are not considered yet in this study.

MODEL LAYOUT

A few model layouts of the linac were studied for beam tracking including microbunching effect. One model showing best electron beam shapes after the linac was chosen for this simulation study. The model layout is shown in Fig. 1.

Beam Tracking with Laser Heater Off

Three initial beam distributions from the injector were used for Elegant tracking simulation: A 200 pC nominal bunch and a 20 pC low charge bunch from the baseline injector [4] and a 200 pC nominal bunch from the low emittance injector [5]. The simulation result using a 200 pC bunch from the baseline injector is shown in Fig. 2 when heater laser is off. For this simulation, 2M macroparticles was tracked using 200 bins for longitudinal space charge (LSC) and CSR calculation.

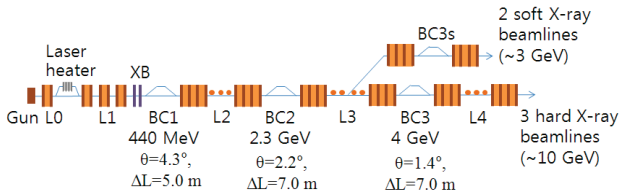

Figure 1: Model layout of the PAL-XFEL linac used for this simulation study.

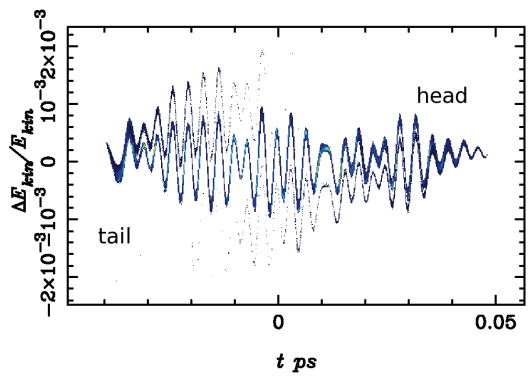

Figure 2: Time-energy phase space at the linac end for a 200 pC beam from the baseline injector. Heater laser is off.

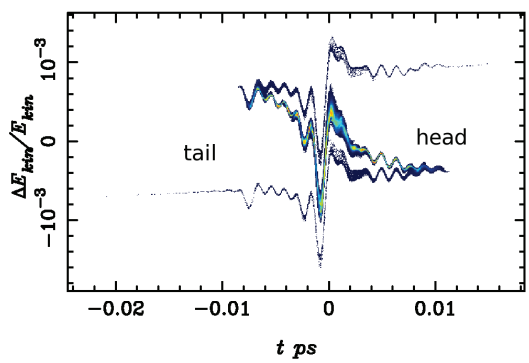

Figure 3: Time-energy phase space at the linac end for a 20 pC beam from the baseline injector. Heater laser is off.

* Work supported by The Ministry of Education, Science and Technology of the Korean Government

† janghui_han@postech.ac.kr

ISBN 978-3-95450-123-6

NEW RF-GUN DESIGN FOR THE PAL-XFEL*

J. Hong†, J.-H. Han, S.-J. Park, H.-S Kang, K. Gil, PAL, Pohang, Kyungbuk
M. S. Chae, I. S. Ko, POSTECH, Pohang, Kyungbuk

Abstract

We are developing an S-band photocathode RF-gun for the X-ray free electron laser (XFEL) at the Pohang Accelerator Laboratory (PAL). This RF-gun is a 1.6-cell RF-gun with dual-feed waveguide ports and two pumping ports. We have done the complete RF and thermal analysis of a new gun. The new RF-gun is designed to operate at a maximum field gradient of 130 MV/m with a RF pulse width of 3 μs, a repetition rate of 120 Hz. In this paper we present features and RF simulation results and thermal analysis results of the new RF-gun.

INTRODUCTION

In 2005 the first photocathode RF-gun has been fabricated at the PAL. The lowest normalized transverse rms emittance at the position from the cathode of 1.4 m was attained 1.7 mm-mrad with 300-pC beam charge, 3.7-MeV beam energy and 0.79-mm beam spot size. This was the first RF-gun fabricated with high-brightness in the country. However, there are a lot of dark current and electric discharges [1]. To avoid such problems of the first RF-gun we modified the design and fabricated the second rf gun in 2007. There were several improvements on the vacuum seals and the tuning methods. This RF-gun was operated with a peak accelerating field of 110 MV/m and achieved a maximum beam energy of up to 5.2 MeV for a laser injection phase of 34° [2]. For PAL-XFEL we have proposed and fabricated the third RF-gun with two RF ports and two pumping ports which called Four-port RF-gun in 2010. From 2010 to 2011 the Four-port RF-gun was successfully fabricated and finished its low-power test. In 2011 the RF gun had been installed at the GTF in PAL for high-power beam test [3, 4]. The RF-gun was operated with maximum field gradient of 126 MV/m and has achieved a maximum beam energy of up to 5.6 MeV for a laser injection phase of 34°. The relative beam energy spread is about 0.1% rms. Measured transverse emittances are $\epsilon_x = 0.74 \pm 0.15$ mm-mrad and $\epsilon_y = 1.32 \pm 0.30$ mm-mrad [5]. Now the goal of the photocathode RF-gun for PAL-XFEL is to produce the electron beam with transverse emittance of 0.5 mm-mrad, beam charge of 200 pC and its repetition rate of 60 Hz. This paper gives brief summary of the new RF-gun design.

FEATURES OF NEW RF-GUN

The design has been optimized to allow good performance of an RF-gun. The features incorporated into the new RF-gun are as follows:

- To increase 0 and π-mode separation relatively large coupling iris radius and short coupling iris length are introduced.
- To reduce the shunt impedance rounded cell profile is seclected.
- To reduce the maximum surface electric field iris shape are changed by elliptical.
- To probe the full-cell field two probing ports are added.
- To lower the vacuum level two additional pumping ports are added.
- To be uniform the RF heating cooling channels are modified.

The three dimensional drawing of new photocathode RF-gun is shown in Fig. 1.

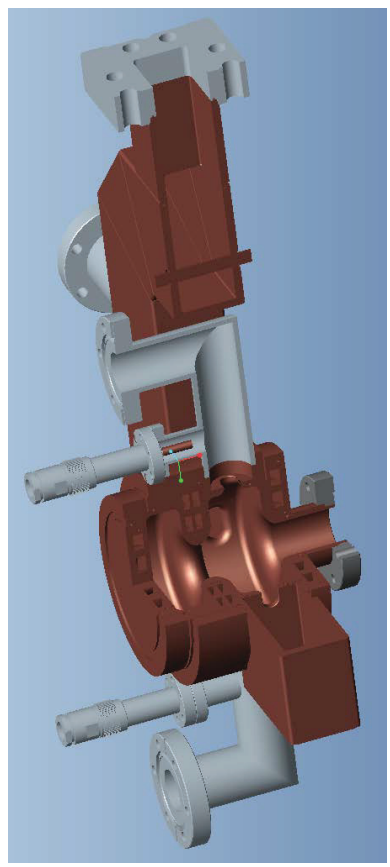

Figure 1: Three dimensional model of new photocathode RF-gun.

* Work supported by The Ministry of Education, Science and Tehnology of the Korean Government
† npwinner@postech.ac.kr

ISBN 978-3-95450-123-6

DESIGN OF MAGNETS FOR PAL-XFEL

H.S. Suh, Y. G Jung, K.H Park, H.S. Han, S.T. Jung, H.G. Lee, H.S. Kang, T.Y. Lee, D.E. Kim, J.Y. Huang, I.S. Ko, M.H. Cho, PAL, Pohang, Kyungbuk, Republic of Korea

Abstract

Pohang Accelerator Laboratory (PAL) is starting the X-ray Free Electron Laser of 10 GeV from 2011. PAL-XFEL has the hard X-ray and soft X-ray branches. This accelerator contains several kinds of magnets such as dipole magnets, quadrupole magnets, kicker magnets, and so on. In this presentation, we describe the preliminary design and the classification of the magnets.

INTRODUCTION

The PAL-XFEL is a 0.1-nm hard X-ray FEL project starting from 2011. Two FEL beamlines, one hard X-ray (HX1) and one soft X-ray (SX1) will be prepared in the first phase. The flexibility of beam control for these two lines will be done by the switching system of a kicker and a septum magnet at 3 GeV point.

This facility for the first phase contains 484 electro-magnets. The magnets are composed of dipole magnets, quadrupole magnets, corrector magnets, kicker magnets, and septum magnet. They are used for the bunch compressors, acceleration section, diagnostic section, beam switch line, beam transport line, undulator hall, and dump section, and so on.

The lattice requirements called for a lot of different types of magnets, many efforts have been dedicated to reduce the total number of the magnet families. We are designing all magnets on our own physically and mechanically, and will search for the domestic and foreign manufacturers.

Corrector magnet and septum magnet are left out of this presentation because they are not determined exactly yet.

Table 1: Summary of Magnets for HX1 and SX1

Magnet	Number of magnet
Dipole	35
Quadrupole	222
Corrector	222
Kicker	3
Septum	1
Sum	484

DIPOLE MAGNET

The dipole magnets for the HX1 and SX1 are classified into four kinds according to the effective magnetic length and the maximum magnetic field.

They are used in the bunch compressor, linac tunnel, BTL, undulator hall, and dump. All dipole magnets have pole gap of 30 mm.

Table 2: Four kinds of Dipole Magnets for HX1 and SX1

Family name	Effective length [m]	Max. field [T]	Magnet number
D3	0.3	0.8	7
D8	0.8	0.9	15
D10A	1.0	0.8	7
D10B	1.0	1.2	6
Sum			35

D8 dipole magnet for the bunch compressors was designed preliminary. The main parameters are listed in Table 3, and the magnetic profile is shown in Fig. 1.

Table 3: Main Parameters of D8 Dipole Magnet

Parameter	Value
Number of magnets	15
Max. field	0.9 T
Max. current	109 A
Pole gap	30.0 mm
Effective length	800 mm
Core length	753 mm
Number of turns	100
Coil size (hollow)	6.5x 6.5 (ϕ4) mm
Cooling system	water
Temperature rise ΔT	22 deg
Field uniformity (ΔB/B)	< 3E-4 (at x=±30mm)

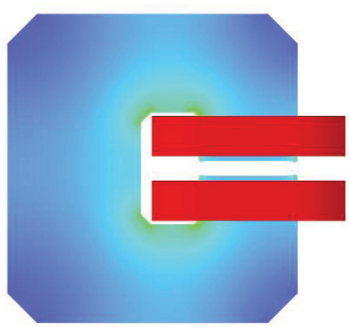

Figure 1: Cross section of dipole magnet (D8) and the field profile.

ISBN 978-3-95450-123-6

PRESENT STATUS OF THERMIONIC RF-GUN FOR TERAHERTZ SOURCE PROJECT AT TOHOKU UNIVERSITY*

F. Hinode#, H. Hama, N.Y. Huang, S. Kashiwagi, M. Kawai, X. Li†, T. Muto, I. Nagasawa, K. Nanbu, Y. Shibasaki, K. Takahashi, Tohoku University, Sendai, Japan.

Abstract

A thermionic RF gun for an accelerator-based terahertz source has been commissioned at Electron Light Science Centre, Tohoku University. Recently we constructed the measurement system to obtain the momentum distribution of the extracted beam from the RF gun. The system consists of the analyser magnet, tungsten beam slit followed by a Faraday cup and a Hall probe for the real-time magnetic field measurement. The momentum resolution of the spectrometer is estimated to be about 0.15 %, which will be sufficient to analyse the detailed distribution of highest energy part for the extracted electrons from the gun. The preliminary results of measured momentum spectrum and the current status of the terahertz source project are presented.

INTRODUCTION

Coherent radiation from a very short electron bunch can be considered as a candidate of the bright source in the terahertz frequency region. In Tohoku University, a test accelerator for the coherent terahertz source (t-ACTS) is now being constructed, in which a specially designed thermionic RF gun is equipped in the injector [1, 2]. The RF gun consisting of two independently-tunable cells (ITC RF-gun) can be operated so as to optimize the longitudinal phase space distribution of the extracted electrons for the further manipulation in an alpha magnet and a 3 m accelerating structure toward the short pulse generation. Tracking simulations show that very short electron pulse less than 100 fs with a bunch charge of about 20 pC can be obtained by means of the velocity bunching in the accelerating structure [3].

In the early result of the gun commissioning with higher current density of about 50 A/cm^2, it was shown that the back-bombardment (B-B) effect seemed to be rather serious for the beam quality in spite of the operation with the short pulse length and slow repetition rate. The simulation study for the B-B effect with the 2D heat transfer model turned out that low energy electrons coming back in the cathode cell have the significant contribution for the additional cathode heating rather than the higher energy electrons. This is the reason why an attempt of simple dipole field on the cathode cannot avoid sufficiently hitting the cathode by back-streaming electrons [4]. At the moment, the other cathode with a little bit larger diameter is going to be employed for a new RF gun in order to mitigate the B-B effect. On the other hand, it is very important to investigate the actual property of the RF gun by measuring the beam quality. Especially a space charge effect will degrade the longitudinal beam distribution significantly, thus the measurement of the energy spectrum is one of the most essential issues for the RF gun in order to realize the very short electron bunch.

*This work is partially supported by the Ministry of Education, Science, Sports and Culture, Grant-in-Aid for Scientific Research (S), Contract #20226003.

#hinode@lns.tohoku.ac.jp

† Present address: Tsinghua University, China

EXPERIMENTAL SETUP FOR MEASUREMENT OF MOMENTUM DISTRIBUTION

Measurement Setup

The energy spectrometer consists of a 45 degree analyzer magnet, tungsten beam slit followed by a Faraday cup (FC) as shown in Fig. 1. Furthermore, the same magnet as analyzer is connected in series, thus it can be anticipated to monitor the magnetic field precisely without vagueness such as instability of power supply and hysteresis. The beam current extracted from the gun is measured by a current transformer (CT) placed at the gun exit. Since the analyzer magnet was diverted from the other attempt, which was originally fabricated as the dipole magnet for the isochronous accumulator ring in t-ACTS, the pole edge has the tilting angle of 17.5 degree at each edge. This tilting angle may help to focus the beam in vertical direction. Since the extracted particles from the gun have different Twiss parameters depending on the RF phase and thus their energy, two quadrupole magnets placed at the gun exit can be used so as to focus the beam on the slit location.

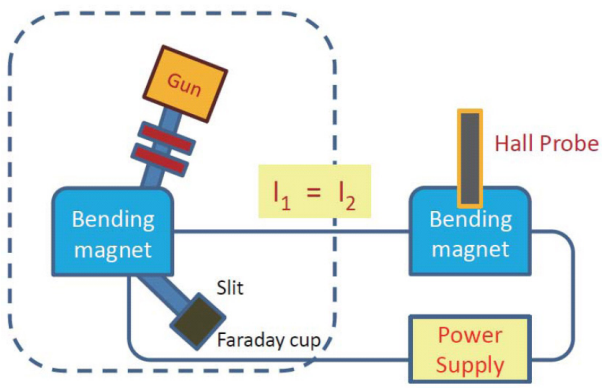

Figure 1: Measurement setup.

Estimation of Momentum Resolution

The momentum resolution for the beam passing through the beam slit is described as

ISBN 978-3-95450-123-6

DESIGN STUDY OF THE LINAC OF THE SHANGHAI SOFT X-RAY FREE ELECTRON LASER FACILITY

Dazhang Huang#, Qiang Gu†, Meng Zhang, Wencheng Fang, Duan Gu, Guoqiang Lin,
SINAP, Shanghai, China

Abstract

Shanghai soft X-ray Free Electron Laser (SXFEL) will be the first X-ray FEL facility in China. In this article, physical study in the design process of the linear accelerator (LINAC) will be given. The study is about how to improve the performance of the LINAC to gain stable operation and control over the possible instabilities such as the microbunching instability [1], which are critical to the success of the FEL facility.

INTRODUCTION

The recent approved Shanghai soft X-ray FEL facility is planned to be built in a few years. It is proposed to be a cascading HGHG FEL facility which will be working at 9 nm soft X-ray band. The main beam parameters at the exit of the LINAC are shown in table 1.

Table 1: Main beam parameters of SXFEL LINAC

Parameter	Value
Electron energy (MeV)	0.84
rms energy spread (%)	0.10 - 0.15
rms normalized emittance (mm-mrad)	2.0 - 2.5
Bunch length (ps, FWHM)	~0.8
Bunch charge (nC)	0.5
Peak current (A)	600
Rep. rate	1 - 10

In order to reach the desired beam quality and match the engineering requirements, the LINAC lattice was designed and optimized. The layout of the LINAC is illustrated in Figure 1. The working parameters of each LINAC components are determined, the jitter analysis and transverse trajectory error correction are given. The mechanism of microbunching instability in SXFEL is also studied.

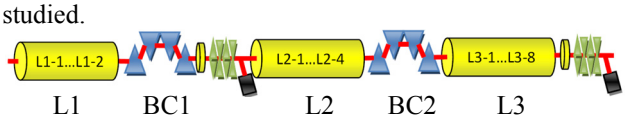

Figure 1 (color): layout of SXFEL linear accelerator (LINAC).

BASIC DESIGN

As shown in Figure 1, the SXFEL LINAC mainly consists of 3 accelerating sections, 2 compressors and 2 diagnostic sections. The 2 bunch compressors (BC1, BC2) provide 10-fold compression rate in total to increase the peak current from ~60 A after the injector to ~ 600 A at the LINAC exit; the 3 accelerating sections includes 2 S-band structures (L1, L2) and a C-band structure (L3). The C-band structure is more compact and able to provide stronger wake field, which is very important to reduce the total size of the LINAC and compensate the beam energy spread after the 2nd bunch compressor. The total length of the LINAC is about 135 m. The longitudinal phase spaces and current profiles at various locations are shown in Figure 2 for comparison.

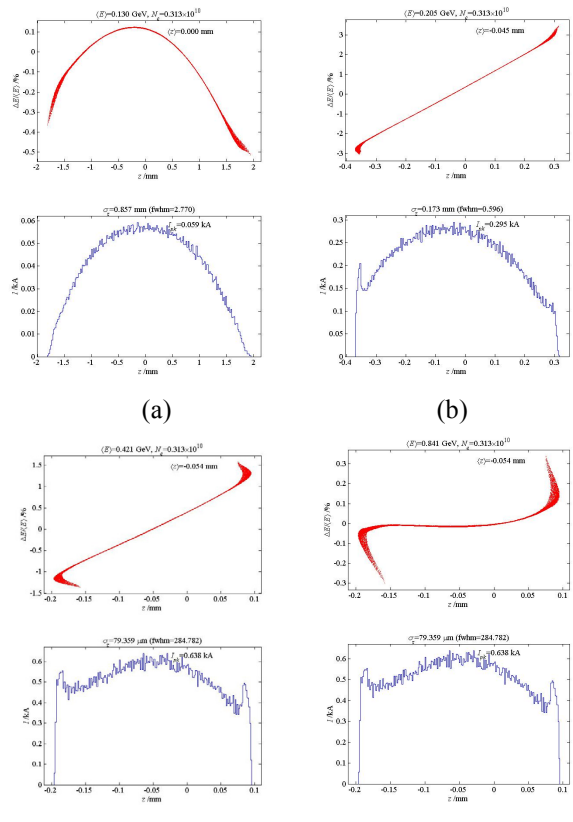

Figure 2 (color): longitudinal phase space (red) and current profile along the bunch (blue) at (a): entry of injector; (b)exit of injector; (c)exit of BC2; (d) exit of L3.

The FODO focusing structures are used at the exit of BC1 and L3 to make the transverse emittance measurement and beam tomography. A number of quadruple magnets are also used in between each section to do transverse matching. The betatron functions and the transverse beam

#huangdazhang@sinap.ac.cn
†guqiang@sinap.ac.cn

ISBN 978-3-95450-123-6

ENHANCEMENT OF THE ELECTRON ENERGY BY USING A LINEARLY TAPERED DENSITY IN THE LASER WAKEFIELD ACCELERATION

Jaehoon Kim#,
Korea Electrotechnology Research Insititute, Sadong, Ansan, Gyeonggido, Rep. Korea

Abstract

Due to the capability of making a compact accelerator and the ability to generate an ultra-short bunch electron beam, a laser wakefield acceleration (LWFA) is widely studied. In LWFA, a dephasing effect is the main limitation of the electron energy. To overcome the dephasing effect and increase the electron energy, we studied the linearly tapered density. Experimental results show that with linearly tapered density, we could increase the electron energy with the same laser power.

INTRODUCTION

By using an ultra high power femtosecond laser and plasma, it is possible to accelerate the electron to high energy in short distance, which is called a laser wakefield accelerator (LWFA) [1,2]. When the high intensity laser propagates inside the plasma, a plasma wakewave is generated due to the Ponderomotive force. Acceleration field generated by this wakewave, the electron can be accelerated. The acceleration field strength is almost thousand times higher than the conventional RF linac, a compact electron accelerator can be made. LWFA scheme also generate a femtosecond electron bunch due to the narrow acceleration region. Such short electron bunch can be used to time resolved x-ray probing experiment.

In LWFA, the acceleration length is limited due to the dephasing effect, which means that the electron accelerated high energy can go out from the acceleration phase to deceleration phase. The dephasing length is determined by the plasma density (dephasing length $\mu\ n_e^{-3/2}$). Due to this dephasing effect, the energy of the electron is determined by the electron density of the plasma. To overcome the limitation of the energy due to the dephasing, a tapered density as an acceleration medium is proposed. In which the plasma density increases along the laser propagation direction [3]. In this work, we studied the effect of the tapered density on the energy.

EFFECT OF THE TAPERED DENSITY

In LWFA, a plasma density is an important parameter, because the density determines the maximum acceleration field strength limited by the wavebreaking, given as $E_{\max}[\mathrm{V/m}] = 0.96\sqrt{n_e[\mathrm{cm}^{-3}]}$, and the dephasing length given as $L_d = l_p(w/w_p)^2$, where l_p the plasma wavelength, w laser frequency, and w_p the plasma frequency [4]. The maximum electron energy is determined by the plasma density because the electron energy can be estimated by the product of the field strength and the acceleration length.

If the plasma density increases along the laser propagation direction, the plasma wavelength decreases. The size of the acceleration region decreases due to the size of the plasma wavelength. The laser position is almost the same because the group velocity of the laser does not change much. The overall effect of the density increment is that the region of acceleration (acceleration phase) go ahead compared with the uniform density. Using this effect, the electron can be accelerated in longer distance. The acceleration field strength also increases along the laser propagation direction. Due to these effects, the electron can be accelerated higher energy by using a tapered density.

EXPERIMENT AND RESULTS

The effect of the linearly tapered density was studied by using a square nozzle and a high power femtosecond laser. To generate a linearly tapered density structure, a square shape nozzle was made. The measured gas density profile shows that the gas density linearly decreases along the normal direction of the nozzle. Simply tilting the nozzle, the gas density along the laser propagation direction increases linearly because the distance between the laser and the nozzle linearly decreases. The size of the nozzle out is 3 mm long and 1 mm wide. The gas density was controlled by the back pressure of the gas nozzle and the laser beam height from the nozzle.

Figure 1 shows the experimental setup. A 20 TW laser was used. The pulse duration of the laser was 40 fs which was measured by using a single shot autocorrelator before the experiment. For the experiment, the laser energy was 500 mJ. The laser beam was focused using on axis parabolic mirror with f/#=17.

The plasma density was measured by using a biprism interferometer for each laser shot. A small part of the laser beam was used for the interferometer. The frequency was converted to second harmonic frequency by using a BBO crystal. The delay between the laser pulse and the probe light was controlled by the optical delay line of the probe light. In the experiment the delay was set as the main pulse is at the edge of the nozzle.

A Lanex film was used to measure the electron beam position. The fluorescence light from the Lanex film was imaged on the ICCD camera. For the electron energy measurement, a permanent magnet was inserted between the Lanex and the nozzle. The magnetic field of the magnet was 1 T. After the magnet, an integrated current transformer (ICT) was used to measure the bunch charge.

#jkim@keri.re.kr

ISBN 978-3-95450-123-6

OVERALL PERFORMANCE COMPARISON OF S-BAND C-BAND, AND X-BAND BASED COMPACT XFEL FACILITIES

Yujong Kim[1,2,3*], S. Setiniyaz[1], M. Titberidze[1], and K. H. Jang[4]
[1]Department of Physics, Idaho State University, Pocatello, ID 83209, USA
[2]Idaho Accelerator Center, Idaho State University, Pocatello, ID 83201, USA
[3]Thomas Jefferson National Accelerator Facility, Newport News, VA 23606, USA
[4]Korea Atomic Energy Research Institute, Daejeon 305-353, Korea

Abstract

Recently, there were several activities to build much more compact XFEL facilities, which are based on C-band and X-band RF linac technologies. But up to now, there was no detailed research to compare the performance of S-band, C-band, and X-band RF linac based compact XFEL facilities. To compare the performance, recently, Idaho State University Next-generation advanced Accelerators & ultrafast Beams Lab (ISU NABL) members have designed three different XFEL facilities where the S-band, C-band, and X-band RF linac technologies are used for the main FEL driving linacs. In this paper, we describe layouts, start-to-end simulations, and comparison of overall performance of those three XFEL facilities. In addition, we also describe control of energy chirp, RF jitter tolerances, alignment and transverse wakefield issue, and bandwidth of XFEL photon beam in C-band or X-band based compact XFEL facilities.

INTRODUCTION

Recently, several leading national laboratories around world have constructed or plans to construct new XFEL facilities. Among them, SPring-8 Angstrom Compact free electron LAser (SACLA) of SPring-8 in Japan was constructed by using the C-band RF linac technology due to the limitation in available site for their XFEL facility [1]. After considering the performance of the XFEL driving linac and an available site for the facility, similarly, PSI in Switzerland also determined to build their SwissFEL facility with the same C-band RF linac technology [2]. After the successful XFEL lasing at SACLA, demand on compact XFEL facilities becomes much stronger. Recently, there were several activities to build much more compact XFEL facilities with a higher RF frequency. However, there are merits and demerits when we use a higher RF frequency for the XFEL driving main linac. To compare overall performance of the various XFEL driving linacs, ISU NABL members have designed three different XFEL facilities where the S-band, C-band, and X-band RF linac technologies are used in the XFEL driving main linacs after the second bunch compressor (BC2). Here, to supply the same initial beam conditions up to BC2, a common S-band injector and linac from the gun cathode to BC2 are used in three different XFEL facilities. In this paper, we describe how to control the energy chirp and energy spread at the end of the XFEL driving linac, and compare overall performance of those three XFEL facilities, where RF jitter tolerances, alignment and transverse short-range wakefield issue, and bandwidth of XFEL photon beam are discussed.

* E-Mail: yjkim@ISU.edu

ENERGY CHIRP VS. XFEL BANDWIDTH

Generally, the bandwidth of XFEL photon beams becomes wider, and the brilliance of XFEL photon beams is also dropped if the projected energy spread of the electron bunch is larger at the entrance of undulators where the XFEL photon beams are generated [3]. That means that the energy chirp in the longitudinal phase space of the electron beam should be flat or minimized to obtain the minimum projected energy spread and to get the narrowest bandwidth and the highest brillance of the XFEL photon beams [3].

For a Gaussian electron beam, the rms relative projected energy spread σ_δ after an RF linac is a function of the longitudinal short-range wakefield $W_{||}$, single bunch charge $Q = Ne$, rms bunch length σ_z, RF frequency $f_{\rm rf} = \kappa_{\rm rf} c/2\pi$, RF gradient G, and RF phase $\phi_{\rm rf}$ of the linac, and it is given by

$$\sigma_\delta \simeq \left| \frac{(1+0.25i)3.04\pi\epsilon_0 N r_e W_{||}(1.3\sigma_z)}{2.35G\cos\phi_{\rm rf}} - \sigma_z \kappa_{\rm rf} \tan\phi_{\rm rf} \right|, \quad (1)$$

where ϵ_0 is the permittivity of free space, N is the number of electrons per bunch, e is the single electron charge, $\kappa_{\rm rf}$ is the wave number of the RF linac, and c is the speed of light [3, 4]. Since the longitudinal short-range wakefield $W_{||}$ of a long periodic linac structure is a function of the average iris radius a and the periodic cell length L in the linac structure, the rms relative projected energy spread σ_δ also depends on them, and the minimum σ_δ can be obtained when the real part of Eq. (1) is zero [3–5]. Therefore, the minimum projected energy spread and minimum XFEL bandwidth can always be obtainable by choosing a proper RF gradient G and a proper phase $\phi_{\rm rf}$ of the linac for a given linac structure, a given bunch length, and a given bunch charge [3].

As summarized in Table 1 and as shown in Fig. 1, average geometric parameters a, b, g, and L of common European S-band, C-band, and X-band linac structures are

ISBN 978-3-95450-123-6

DEVELOPMENT OF S-BAND ACCELERATING STRUCTURE

Sadao Miura, MITSUBISHI HEAVY INDUSTRIES, LTD., 1-1, Itozaki Minami 1-chome, Mihara, Hiroshima, 729-0393, JAPAN
Heung-Soo Lee, POHANG ACCELERATOR LABORATORY, San31, Hyoja-dong, Nam-gu, Pohang, Gyeongbuk, 790-784, Republic of Korea
Hiroshi Matsumoto, Hirokazu Maesaka, Takahiro Inagaki, Tsumoru Shintake,
HIGH ENERGY ACCELERATOR RESEARCH ORGANIZATION
1-1 Oho, Tsukuba, Ibaragi, 305-0801, JAPAN

Abstract

In Pohang Accelerator Laboratory (PAL) in Korea construction of XFEL (X-ray Free electron Lazar) institution is under construction aiming at the completion in 2014[1]. Energy 10GeV of the linac part of this institution and main frequency are planned in S-band (2856 MHz), and about 178 S-band 3m accelerating structures are due to be used for this linac.

The oscillation of an X-ray laser requires very low emittance electron beam. On the other hand, since the accelerating structure which accelerates an electron beam has a feed port of microwave (iris), the electromagnetic field asymmetry of the microwave feeding device called coupler worsens the emittance of an electron beam.

MHI manufactured two kinds of S-band accelerating structures with which the electromagnetic field asymmetry of coupler cavity was compensated for PALXFEL linac. We report these accelerating structures.

INTRODUCTION

MHI manufactured two kinds of every two S-band accelerating structures as prototype machine for PALXFEL linac, and supplied them to PAL in June and August 2012 respectively. 1st kind of accelerating structures which MHI manufactured are S-band 3m structure which equipped J-type double feed coupler, and one more kind equips quasi-symmetrical type single feed coupler. Both accelerating structures, J-type and Quasi-symmetrical type, are the structures with which the electromagnetic field asymmetry of coupler cavity was compensated.

TWO TYPE PROTOTYPE S-BAND ACCELERATING STRUCTURE FOR PALXFEL

Fig.1 shows J-type S-band accelerating structure which equipped J-type double feed coupler. Fig.2 shows Quasi-symmetrical type S-band accelerating structure which equipped quasi-symmetrical type single feed coupler.

These are 3m long, constant gradient, S-band 2856MHz accelerating structures. Cell number is 84 regular cells and 2 coupler cells. Material of these structures is oxygen free high conductivity copper. All cell are machined by super-precision lathe, and surface roughness of these cells are suppressed to 0.1 μ m or less. And all cells are assembled by vacuum brazing. Table 1 shows the specifications of these S-band accelerating structures.

Table 1: Specifications of S-band Accelerating Structures

Resonance Frequency	2,856 MHz
Phase Shift	2π/3
Accelerator Type	C.G.
Number of Cells	84+2 coupler cell
Quality Factor	13000
Group Velocity	0.012c (average)
Shunt Impedance	49.3～60.0 MΩ/m
Attenuation Constant	0.56
Filling Time	0.84 μs
Coupler type	J-type
	Quasi-summetry

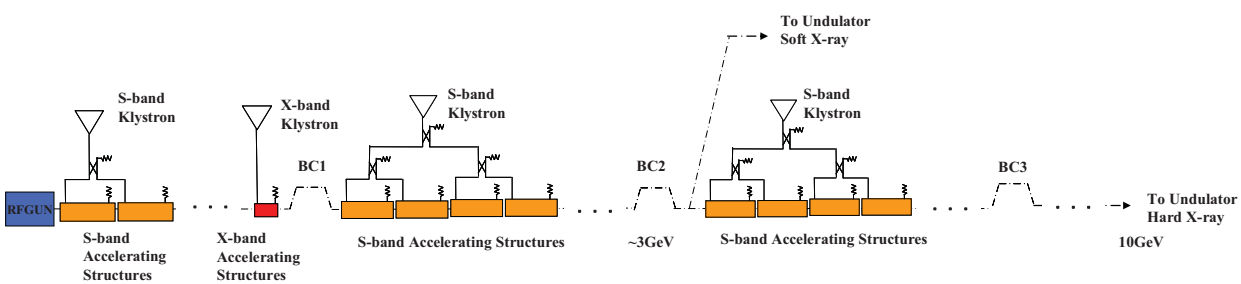

Figure 1: Linac layout of PAL XFEL project.

ISBN 978-3-95450-123-6

BEAM DYNAMICS CALCULATIONS FOR THE SPring-8 PHOTOINJECTOR SYSTEM USING MULTIPLE BEAM ENVELOPE EQUATIONS

A. Mizuno*, H. Dewa, T. Taniuchi, H. Tomizawa and H, Hanaki
JASRI/SPring-8, 1-1-1, Koto, Sayo, Hyogo, 679-5198, Japan
E. Hotta, Department of Energy Sciences, Tokyo Institute of Technology,
Nagatsuta-cho, Midori-ku, Yokohama, Kanagawa, 226-8502, Japan

Abstract

A new semi-analytical method of investigating the beam dynamics for electron injectors was developed. In this method, a short bunched electron beam is assumed to be an ensemble of several segmentation pieces in both the longitudinal and the transverse directions. The trajectory of each electron in the segmentation pieces is solved by the beam envelope equations. The shape of the entire bunch is consequently calculated, and thus the emittances can be obtained from weighted mean values of the solutions for the obtained electron trajectories. Using this method, the beam dynamics calculation for the SPring-8 photoinjector system was performed while taking into account the space charge fields, the image charge fields at a cathode surface, the electromagnetic fields of the rf gun cavity and the following accelerator structure, and the fields of solenoidal coils. In this paper, we discuss applicable conditions for this method by comparing calculation results of this method and those of a particle-tracking simulation code.

INTRODUCTION

The emittance calculation technique is important in the design of electron injectors for x-ray free electron lasers. There have been many analytical solutions for beam dynamics though it is difficult to accurately calculate practical bunch shapes and detailed emittance behavior. Meanwhile, particle-tracking simulation codes are useful to calculate dynamics of practical beams. However, the calculated emittances often depend on the number of particles.

To overcome the above problems and for accurate calculations of short bunched electron beam dynamics, the authors developed a new semi-analytical solution by combining an analytical method and a simulation method [1] using the multiple beam envelope equations.

In this method, a short bunched electron beam is assumed to be an ensemble of several segmentation pieces in both the longitudinal and the transverse directions. The trajectory of each electron in the segmentation pieces is solved by the beam envelope equations. The shape of the entire bunch is consequently calculated, and thus the accurate emittances were successfully calculated from weighted mean values of the solutions for the each obtained electron trajectory.

* mizuno@spring8.or.jp

In Ref [1], the authors discussed the semi-analytical solution method of beam dynamics mainly about space charge effects. Therefore, only the beam dynamics in an rf gun cavity and free space including image charge effects for a cathode were described. However, to analyze the beam dynamics of practical electron injectors, it is necessary to calculate beam traces with solenoidal coil focusing effects and in accelerator structures.

In this paper, we describe methods for calculating beam traces in solenoidal fields and in accelerator structures using the semi-analytical method described in Ref [1]. We also show the beam dynamics calculation results for the SPring-8 photoinjector system and compare them with results of a particle-tracking simulation code.

OUTLINE OF MULTIPLE BEAM ENVELOPE EQUATIONS

The initial bunch model used for the semi-analytical method in Ref [1] is shown in Fig. 1. The bunch is longitudinally divided into m slices and transversely n parts. The each electron is located at each segmentation boundary and traced by the beam envelope equation.

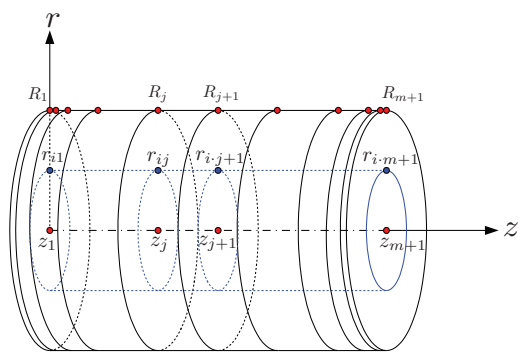

Figure 1: The initial bunch segmentation model for the multiple beam envelope equations.

For the longitudinal envelope equations, the electrons z_j ($j = 1, \ldots, m+1$) are set on the beam axis. For the transverse equations, the electrons r_{ij} ($i = 1, \ldots, n$ and $j = 1, \ldots, m+1$) which represent the parts inside the bunch are set at each transverse segmentation boundary, R_j are set at circumference of the bunch. β_j are also defined as the normalized longitudinal velocity of each elec-

ISBN 978-3-95450-123-6

DEVELOPMENT OF A PHOTOEMISSION DC GUN AT JAEA

N. Nishimori#, R. Nagai, S. Matsuba, R. Hajima, JAEA, Tokai, Naka, Ibaraki 319-1195, Japan
M. Yamamoto, Y. Honda, T. Miyajima, KEK, Oho, Tsukuba, Ibaraki 305-0801, Japan
H. Iijima, M. Kuriki, Hiroshima University, Higashihiroshima, Hiroshima 739-8530 Japan
M. Kuwahara, S. Okumi, T. Nakanishi, Nagoya University, Nagoya464-8602, Japan

Abstract

The next generation light source such as X-ray FEL oscillator requires high brightness electron gun with megahertz repetition rate. We have developed a photoemission DC gun at JAEA. By employing a segmented insulator with guard rings, we successfully applied 500 kV on the ceramics with a central stem electrode for eight hours without any discharge in 2009. In 2011 we reached 526 kV with NEG pumps and electrodes in place, before suffering another field emission problem from the cathode electrode. The problem may be attributed to small dust inside our gun chamber. We also generated high current beam up to 10 mA and obtained charge extracted lifetime of 30 C. In this paper, our current status of development will be presented.

INTRODUCTION

Electron guns which can deliver a high brightness electron beam with emittance lower than 1 mm-mrad and current up to 100 mA are being developed for Energy Recovery Linac (ERL) Light Sources (LS) worldwide [1]. A DC photoemission gun with a GaAs or multi alkali photocathode is one of the most promising candidates, since the JLab FEL photoemission DC gun has provided 9.1 mA beam [2] and the Cornell photoinjector recently demonstrated operation at 20 mA for eight hours [3].The gun high voltage equal to or greater than 500 kV is required to generate low emittance beam by reducing non-linear space charge effects in low energy region [4]. The accelerating field on the cathode surface should also be as high as possible to suppress the space charge effects.

This high brightness gun is anticipated to be used in a 3-GeV ERL based hard X-ray synchrotron light source project in Japan [5], an X-ray FEL oscillator [6], and an ERL based high-flux Compton gamma-ray as a new nondestructive assay method for ^{235}U, ^{239}Pu, and minor actinides in spent nuclear fuel assembly [7,8].

We have developed a 500-kV DC gun for the Japanese ERL light sources [9]. One of technological challenges of high brightness DC guns is to apply DC high voltage on a ceramic insulator with a central stem electrode, since field emission causes discharge or punch through on the ceramic surface. We have employed a segmented insulator with rings to keep the insulator safe from the field emission generated from the stem electrode. Although the emission from backside of the rings may still directly hit the insulator, its maximum electric field is more than three times smaller than that of the stem electrode. In this way, we have successfully applied 500 kV on the ceramics for eight hours in 2009 [10].

A prototype facility of 3 GeV ERL light source called compact ERL (cERL) has been constructed at KEK. Our photoemission DC gun is scheduled to be installed by this fall. Beam generation from the gun is anticipated by the end of this fiscal year. We need to demonstrate high brightness and high current beam generation by this fall. We reached 526 kV with cathode electrode in place and demonstrated 440 kV for eight hours. We also demonstrated 10 mA beam generation. In this paper, our current status of gun development will be presented.

HIGH VOLTAGE CONDITIONING

500-kV Photoemission DC Gun at JAEA

Details of our 500-kV DC gun are described elsewhere [9,10]. A GaAs wafer on a molybdenum puck is used as photocathode. The wafer is atomic hydrogen cleaned and transferred to the preparation chamber where cesium and oxygen are alternatively applied for negative electron

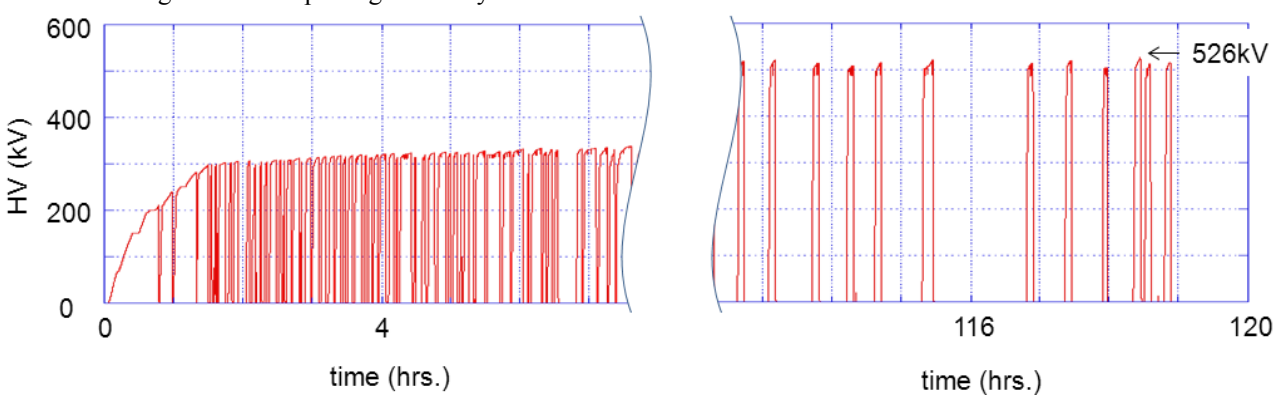

Figure 1: High voltage conditioning of the 500-kV photoemission DC gun with cathode electrode in place.

nishimori.nobuyuki@jaea.go.jp

ISBN 978-3-95450-123-6

RF DESIGN AND HIGH POWER TESTS OF A NEW TSINGHUA PHOTOCATHODE RF GUN*

H. J. Qian, Y. C. Du, L. X. Yan, C. Li, J. F. Hua, W. H. Huang, C. X. Tang#,
Department of Engineering Physics, Tsinghua University, Beijing 100084, China

Abstract

A new photocathode RF gun has been designed and fabricated to meet beam brightness requirements (0.5-1 nC, 1-2 mm mrad) of Tsinghua Thomson scattering project (TTX) and Shanghai soft X-ray free electron laser test facillity (SXFEL). Compared with classical BNL type gun, the new Tsinghua gun features improved cathode sealing structure, 0-mode and multipole field suppression, and higher quality factor. Single RF feed is kept in the new gun for simplicity, and beam dynamics due to single RF feed are investigated theoretically, which predict negligible emittance growth. After high power conditioning, the new gun operates stably with a peak acceleration gradient of ~120 MV/m. Measurements of dark current, Quantum Efficiency (QE), and transverse emittance are presented and discussed in this paper.

INTRODUCTION

Tsinghua University has been developing BNL type photocathode RF gun since 2001, and three generations of RF guns have been fabricated to support Thomson scattering X-ray source project (TTX) and MeV ultrafast electron diffraction (UED) in Tsinghua University, free electron laser projects in Shanghai and so on [1-3]. With progress of TTX and Shanghai soft X-ray free electron laser project (SXFEL), higher beam brightness are required from the RF gun, such as a normalized transverse emittance of 1.5-3 mm mrad for a beam charge of 0.5-1 nC. Besides, MeV UED requires lower dark current for sharper diffraction pattern imaging. RF guns of the first two generations have relatively low acceleration gradient (~75 MV/m) and high dark current (~100 pC/pulse), which are imposing limitations on the above projects, so a third generation RF gun has been developed since 2011 to address the above issues.

Based on the BNL type gun, a lot of RF guns have been developed around the world, which successfully improved gun gradient, RF field properties, gun rep rate and generated lower emittance electron beams. Many modifications in these guns, such as the LCLS gun, UCLA gun, Eindhoven gun, KEK gun, and PAL gun, have been adopted in the third generation Tsinghua photocathode RF gun [4-7].

The new gun has been fabricated, cold tested, and high power conditioned in Tsinghua Univeristy. In the rest of this paper, features of the third generation Tsinghua photocathode RF gun are briefly described [8]; then, impact of single RF feed on beam dynamics is analyzed; finally, the high power conditioning results and emittance measurements are presented.

*This work is supported by the National Natural Science Foundation of China (NSFC), under Grant Nos. 10925523, 11127507.
#tang.xuh@mail.thu.edu.cn

FEATURES OF THE NEW TSINGHUA PHOTOCATHODE RF GUN

The main goal of the new gun is to increase the gun gradient from ~75 MV/m to ~100 MV/m, and the gradients of the previous Tsinghua guns are limited by RF breakdowns, as shown in Fig. 1. The cathode plate sealing structure was improved in many guns, such as knife edge sealing, brazing and Matsumoto gasket, which eliminate gaps exist in Helicoflex seal and successfully increased the gun gradient above 100 MV/m. Matsumoto gasket is adopted in the new Tsinghua gun due to its simplicity and frequency tuning function. Besides structure optimization, the new gun will operate with a shorter RF pulse width (< 2 μs), which is also expected to bring down the RF breakdown rate.

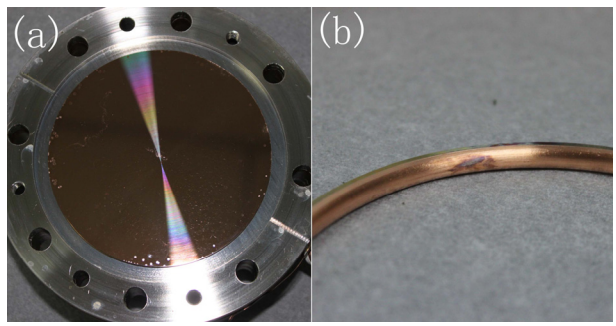

Figure 1: RF breakdown spots in the 2nd generation Tsinghua gun, (a) edge of the cathode plate, (b) Helicoflex seal.

Besides gun gradient, the RF field properties also affect the beam emittance, such as nonaxisymmetry of the acceleration mode and excitation of the non-resonant mode. Nonaxisymmetry of acceleration field (π-mode) contains multipole harmonics, and excitation of non-resonant mode (0-mode) increases beam energy spread, both of which result in beam emittance degrade. The π-mode field symmetry of the BNL gun is further improved by dual RF feed and racetrack full cell shape in LCLS gun and coaxial coupler in Eindhoven gun, both of which require major change of the original structure of BNL gun. For simplicity, single RF feed is reserved in the new gun instead of the dual RF feed. Dipole field component is reduced by asymmetric vacuum port design, while quadruple component is reduced by 4-port design [8]. Compared with the BNL gun, dipole and quadruple are decreased by 10^{-2} and 10^{-3} respectively. Phase asymmetry induced multipoles due to single RF feed are analyzed in the following section, and its impact on beam dynamics is

ISBN 978-3-95450-123-6

DESIGN AND COMMISSION OF THE DRIVEN LASER SYSTEM FOR ADVANCED SUPERCONDUCTING TEST ACCELERATOR*

J. Ruan, J. Santucci, M.Church, Fermi lab, PO Box 500, Batavia, IL 60510, USA

Abstract

Currently an advanced superconducting test accelerator (ASTA) is being built at Fermilab. The accelerator will consist of an photo electron gun, injector, ILC-type cryomodules, multiple downstream beam lines for testing cryomodules and carrying advanced accelerator research. In this paper we will describe the design and commissioning of the drive laser system for this facility. It consists of a fiber laser system properly locked to the master frequency, a multi-pass amplifier, several power amplifier and final wavelength conversion stage. We will also report the initial characterization of the fiber laser system and the current commissioning status of the laser system.

INTRODUCTION

A future superconducting RF accelerator test facility is currently being commisioned at Fermilab in the existing New Muon Lab (NML) building. The designed accelerator will consist of a photoinjector, two booster cavities, beam acceleration section consisting of 3 ILC-type cryomodules, multiple downstream beam lines with various diagnostics to conduct beam tests, and a high power beam dump[1, 2]. In this paper we will describe the design and commissioning of the drive laser system for this facility. One of the goals is to realize a long pulse train operation (up to 1000 individual pulses with 1 μs apart or 3000 pulses with 330 ns apart) which is essential for the newly built ASTA facility in Fermi lab.

Our new laser system is based on the design for the old laser system used at A0 photoinjector[3]. One of the disadvantages of the A0 laser system design is the low efficiency of the gain medium, Nd:Glass, used in the amplifying structure. Couples with the fact of the instability of the flash lamp used to pump the gain medium it's very difficult to realize long pulse train operation as required in the new facility[3]. In order to address those issues we decided to use Neodymium-doped yttrium-lithium fluoride (Nd:YLF) as our new gain medium to replace the Nd:glass used in current A0 laser amplifier chain. Nd:YLF is a very efficient material that can be pumped by either flash lamp or diode laser. In addition the induced emission cross section is large enough to produce a single pass amplification up to 10. At the same time we will also upgrade our flash lamp pump to fiber coupled laser diode pump to get better stability and higher reliability. Using optical fiber to deliver the pump to the end-pumped active medium has several practical advantages:

- The pump beam at the end of the fiber has a high quality, central symmetrical profile.
- The radial size of the beam can be easily scaled up or scaled down with high quality optics.
- A fiber connection provides a simple and virtually lossless interface between the pump source and the active medium.
- Both the pump source and active medium can be changed simply by reconnecting the fiber between them.

In addition to the change of the amplifying chain we also replaced the solid state seed laser used at A0 laser structure with a fiber laser based seed system. Figure 1 is the designed flow chart of the whole photocathode laser system. The top box is a fiber based seed laser locked directly to the master oscillator and the bottom box includes a solid state based amplifier chain and frequency conversion stage.

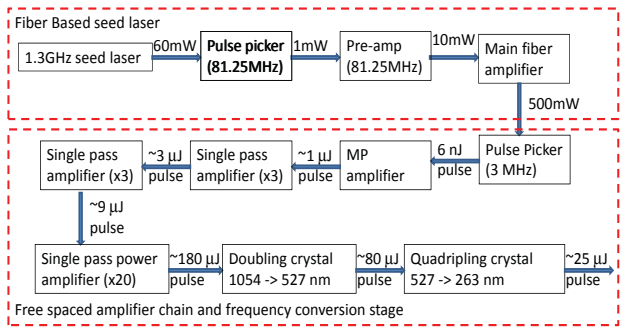

Figure 1: Designed flow chart of the whole photocathode laser system. The number is the expected power level at each stage.The top box is the fiber based seed laser stage and the bottom box is solid state based amplifier chain.

COMMISSIONING AND PRELIMINARY TEST OF THE ASTA LASER SYSTEM

The laser room at ASTA facility is finished at the beginning of the August, 2012. We are in the early stage of commissioning the laser system. In this part we will go over some of the preliminary test done in the fiber based seed laser system and diode pumped multi-pass amplifier system.

* Work supported by U.S. Department of Energy, Office of Science, Office of High Energy Physics, under Contract No. DE-AC02-06CH11357.

ISBN 978-3-95450-123-6

DEVELOPMENT OF MULTI-BUNCH LASER SYSTEM FOR PHOTOCATHODE RF GUN IN KU-FEL

K. Shimahashi#, H. Zen, T. Kii, K. Okumura, M. Shibata, H. Imon, T. Konstantin, H. Negm, M. Omer, K. Yoshida, Y.W. Choi, R. Kinjo, K. Masuda, H. Ohgaki,
Institute of Advanced Energy, Kyoto University, Gokasho, Uji, Kyoto 611-0011, Japan
R. Kuroda, National Institute of Advanced Industrial Science and Technology (AIST),
1-1-1 Umezono, Tsukuba, Ibaraki 305-8568, Japan

Abstract

We have been developing mid-infrared FEL (MIR-FEL) system, Kyoto University-FEL (KU-FEL), which utilizes a 4.5-cell S-band thermionic radio frequency (RF) gun, in Institute of Advanced Energy, Kyoto University. We plan to introduce a Brookhaven National Laboratory (BNL)-type 1.6-cell photocathode RF gun to generate higher peak power MIR-FEL. The purpose of this work is to develop a multi-bunch laser system which excites the photocathode in the RF gun. The target values of the system are bunch number of 300 and micro-pulse energy of 1 μJ in the wavelength of 266 nm. The laser system consists of a mode-locked Nd:YVO_4 laser as the oscillator, an acousto-optic modulator (AOM), a beam alignment feedback system, a laser diode (LD) pumped Nd:YAG amplifier. We could stabilize the laser position within 1 μm at the downstream of the AOM, and achieve to amplify the seed laser up to 1.2 μJ per micro-pulse.

INTRODUCTION

We have been developing our resonator type MIR-FEL to upgrade our user facility to contribute the advanced energy science in Kyoto University. Using a 4.5-cell S-band thermionic RF gun and a 3-m accelerator tube in the present facility, electrons are accelerated up to 40 MeV. We have extended FEL wavelength from 5 to 14.5 μm by the substitution of undulator system [1].

We have planned to introduce a BNL-type 1.6-cell photocathode RF gun to generate more stable and higher peak FEL power which has been showed by our numerical study [2]. Since a photocathode RF gun has already been manufactured [3], we started to develop a multi-bunch laser system for resonator type FEL system with this RF gun. For the laser system, we introduced a beam alignment feedback system, and constructed a multi-pass amplifier in the infrared (IR) wavelength. In this paper we will briefly describe the multi-bunch laser system and the present status of the development.

MULTI-BUNCH LASER SYSTEM

Target Value

Electron charge, Q, from the photocathode is written by formula.

$$Q = \frac{\eta e W \lambda_L}{hc} \quad (1)$$

Here, η is quantum efficiency, e is elementary charge, W is pulse energy of the drive laser, λ_L is wavelength of the drive laser, and h is Planck's constant. Considering the quantum efficiency and the life time, Cs_2Te is the candidate of our photocathode. Because Cs_2Te has the band gap energy of 3.2 eV, a drive laser of the ultraviolet (UV) wavelength is required to excite photoelectrons. In this work, the quantum efficiency was assumed to be 1.5% [4]. Therefore, when the electron charge is assumed to be 1 nC, the pulse energy in the UV wavelength is required to be 0.31 μJ per micro-pulse from the formula (1). Taking into account the optical loss and other issues, the target value of the pulse energy in the UV wavelength was set to be 1 μJ per micro-pulse. Here, we plan to use two non-linear optical crystals to generate the high harmonic generation. The conversion efficiency changing from 1064 nm to 266 nm was assumed to be 10% [5]. Therefore, the target value of the IR wavelength before the wavelength conversion is 10 μJ per micro-pulse. We plan to construct a multi-pass amplifier with optical gain of 40 dB to achieve these values. The main parameters are shown in Table 1.

Table 1: The Main Parameter of the Target Value

electron charge	1 nC / micro-pulse
micro-pulse number in a macro-pulse	more than 300
repetition frequency of macro-pulse	1 ~ 10 Hz
micro-pulse energy (UV)	1 μJ
micro-pulse energy (IR)	10 μJ

System Configuration

We used a mode locked Nd:YVO_4 laser (GE-100-VAN, Time-Bandwidth) as a laser oscillator. This laser's specifications are summarized that wavelength is 1064 nm, repetition frequency is 89.25 MHz (11.2 ns), average output power is 600 mW, and pulse width is 7.5 ps. This repetition frequency is one thirty second of the RF frequency of KU-FEL linac (2856 MHz). The laser system was designed to synchronize the phase timing between the RF signal of KU-FEL and the repetition frequency of the drive laser by controlling the resonator

#kyohei@iae.kyoto-u.ac.jp

ISBN 978-3-95450-123-6

COMMISIONING OF THE FERMI@ELETTRA LASER HEATER*

Simone Spampanati#, Sincrotrone Trieste, Italy,
University of Nova Gorica, Nova Gorica, Slovenia, SLAC, Menlo Park, CA 94025,U.S.A
Enrico Allaria, Laura Badano, Silvano Bassanese, Davide Castronovo, Miltcho B. Danailov,
Alexander Demidovich, Simone Di Mitri, Bruno Diviacco, William M. Fawley, Lars Froelish,
Giuseppe Penco, Carlo Spezzani, Mauro Trovò, Sincrotrone Trieste, Italy
Giovanni DeNinno, Eugenio Ferrari,
Sincrotrone Trieste, Italy, University of Nova Gorica, Nova Gorica, Slovenia
Luca Giannessi, ENEA C.R. Frascati, Frascati (Roma) Italy, Sincrotrone Trieste, Italy.

Abstract

The linac of the FERMI seeded free electron laser includes a laser heater to control the longitudinal microbunching instability, which otherwise is expected to degrade the quality of high brightness electron beam sufficiently to reduce the FEL power. The laser heater consists of a short undulator located in a small magnetic chicane through which an external laser pulse enters to modulate the electron beam energy both temporally and spatially. This modulation, which varies on the scale of the laser wavelength, together with the effective R52 transport term of the chicane increases the incoherent energy spread (i.e., e-beam heating). We present the first commissioning results of this system, and its impact both upon the electron beam phase space, and upon the FEL output intensity and quality.

INTRODUCTION

FERMI@ELETTRA [1] is an user facility based on two seeded FELs in the VUV (FEL-1) and soft x-ray (FEL-2) wavelength regimes. FEL-1 is a single stage HGHG while FEL-2 is a two stage HGHG cascade working in a fresh bunch configuration. One of the main features of both the two FEL lines is their capability to produce output radiation pulses with a very narrow spectrum. The longitudinal high quality of the output FEL pulses originates with the external seed laser. However, the nearly transform-limited single spike spectrum [2] can be spoiled by unwanted modulations and distortions in the longitudinal phase space of the electron beam. The very bright electron beam (*e.g.,* slice emittance <2 mm mrad) and incoherent energy spread (~3KeV) required to drive this FEL is susceptible to a microbunching instability [3] that produces short wavelength (~1-5μm) energy and current modulations. These can both degrade the FEL spectrum and reduce the power by increasing the slice energy spread. This instability is presumed to start at the photoinjector exit growing from a pure density modulation caused by shot noise and/or unwanted modulations in the photoinjector laser temporal profile. As the electron beam travels along the linac to reach the first bunch compressor (BC1), the density modulation leads to an energy modulation via longitudinal space charge. The resultant energy modulations are then transformed into higher density modulations by the bunch compressor. The increased current non-uniformity leads to further energy modulations along the rest of the linac. Coherent synchrotron radiation in the bunch compressor can further enhance these energy and density modulations. To control these degradations, we have installed a laser heater between the photoinjector and the linac. This device can add a small controlled amount of incoherent energy spread to the beam and reduces microbunching instability growth via Landau Damping in the bunch compressor.

LASER HEATER SET UP

The FERMI laser heater [4] consists of a short, planar-polarized undulator located in a magnetic chicane through which an external laser pulse enters to modulate the electron beam both temporally and spatially. The resulting interaction within the undulator produces an energy modulation of the electron beam on the scale of the laser wavelength. The last half of the chicane then time-smears the energy modulation leaving an effective incoherent energy spread increase. Figure 1 shows the FERMI layout with the laser heater positioned between the photoinjector and the linac. Figure 2 illustrates the laser heater system installed in the linac tunnel.

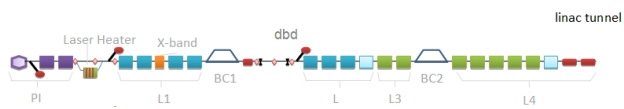

Figure 1: FERMI linac layout.

The laser heater undulator has 12 periods of 4cm. The gap can be changed to find the resonance with the external laser wavelength (783nm) for several beam energy. The relative bandwidth of undulator radiation is ~8% while the gap- K calibration has an error of the order of 0.3%. A nearby spectrometer allows determination of the electron beam energy to within 1%. Consequently it is

*Work supported in part by the Italian Ministry of University and Research under grants FIRB-RBAP045JF2 and FIRB-RBAP06AWK3
spampina@slac.stanford.edu

ISBN 978-3-95450-123-6

PITZ STATUS, RECENT MEASUREMENTS AND TESTS

M. Krasilnikov*, H.-J. Grabosch, M. Gross, I. Isaev, Y. Ivanisenko, M. Khojoyan, G. Klemz, G. Kourkafas, K. Kusoljariyakul#, J. Li†, M. Mahgoub, D. Malyutin, B. Marchetti, A. Oppelt, M. Otevrel, B. Petrosyan, S. Rimjaem#, A. Shapovalov, F. Stephan, G. Vashchenko, DESY, Zeuthen, Germany
D. Richter, HZB, Berlin, Germany
I. Will, MBI, Berlin, Germany

Abstract

The Photo Injector Test facility at DESY, Zeuthen site (PITZ) is dedicated to the development and optimization of a high-brightness electron source for the European XFEL. Recently a significant upgrade has been done at the facility. A new RF system has been installed for the PITZ gun, enabling higher attainable peak power in the cavity which is important for efficient LLRF regulation. First long-term tests for a stable gun operation at high duty cycle have been performed. Two major components for electron beam diagnostics – a transverse deflecting cavity for time resolved electron bunch characterization, and a second high energy dispersive arm for precise longitudinal phase space measurements – have been installed. First results of their commissioning will be reported.

INTRODUCTION

The PITZ facility develops and tests high-brightness electron sources for free-electron lasers, such as FLASH and the European XFEL in Hamburg. The current PITZ setup consists of a photo cathode rf gun, a normal conducting booster cavity and various systems for electron beam diagnostics. The photo cathode laser system is developed and supported by the Max-Born-Institute (MBI, Berlin). One of the major goals of the facility is to minimize the projected normalized emittance for electron beams with different charges. The projected emittance for bunch charges in the range between 20 pC and 2 nC was minimized by multi parametric machine tuning, setting a new benchmark for high-brightness photo injector performance [1, 2]. The challenging time structure of the electron pulse train is one of the important specifications to be demonstrated at PITZ. The photo injector is capable to produce trains with up to 800 micro pulses and 1 µs spacing between the pulses of the train at 10 Hz repetition rate. Demonstration of stable electron beam production supporting the maximum available duty factor is a subject of the so-called long-term tests (LTTs), which were performed at PITZ in 2012.

Being a spare gun for the FLASH user facility, the PITZ gun in May 2012 has replaced the FLASH gun, which was damaged during operation. The installation of a spare gun cavity for PITZ (the gun prototype 3.1) is under preparation. Dry ice cleaning of which is supposed to reduce the field emission significantly has been applied to this cavity.

In parallel, a number of important upgrades have been carried out at PITZ to improve the electron beam diagnostics, namely to characterise the bunch slice properties. The transverse deflecting system (TDS) was built to characterize the temporal properties of electron bunches from the photo injector. The deflecting cavity was developed at the Institute for Nuclear Research (INR, Moscow, Russia) and is planned to be also applied at the European XFEL. A prototype of the system will be tested at PITZ; the final installations are ongoing. Another important diagnostic device recently installed and commissioned is the second high energy dispersive section in the PITZ linac. Besides the beam momentum measurements it can be used for single shot measurements of the longitudinal phase space and the slice energy spread when used together with the TDS cavity.

RF GUN

The PITZ gun is a 1.6 cell normal conducting rf cavity with a Cs_2Te photocathode. It is operated at 1.3 GHz with a maximum rf peak power of ~6 MW in the cavity. The gun cavity is fed using a 10 MW multi-beam klystron with two outputs, the mean length of each waveguide arm is about 40 m. A major part of the waveguides is filled with SF_6 in order to reduce the spark rate. A vacuum T-combiner is located in the gun cavity vicinity isolated from the SF_6-filled waveguide line by two ceramic rf windows. The T-combiner is followed by a 10 MW in-vacuum directional coupler; the feed-forward and the feedback are realized based on signals from the two antennas of the directional coupler. The rf gun cavity operated at the maximum peak power delivers electron bunches with maximum mean momentum of ~7 MeV/c.

The gun cavity (gun prototype 4.1) was conditioned with rf pulses up to 700 µs duration applying the full available peak power, but for emittance optimization [3, 4] a maximum rf pulse duration of 300 µs was used. In order to check the gun trip rate at the full average power performance long-term tests were carried out in 2012 at PITZ. Results of these tests are discussed below.

PITZ rf guns also serve as spare guns for the running FEL user facility FLASH in Hamburg. In May 2012 the rf gun at FLASH (gun prototype 4.2 being also commissioned and characterized at PITZ in 2008-2009 [2]) has shown significant problems during operation at an rf peak power level of ~4 MW, including

* mikhail.krasilnikov@desy.de
# Currently at Chiang Mai University, Chiang Mai, Thailand
† On leave from USTC, Hefei, China

ISBN 978-3-95450-123-6

OPTIMIZATION OF THE TRANSVERSE PROJECTED EMITTANCE OF THE ELECTRON BEAM AT PITZ

G. Vashchenko*, G. Asova†, M. Gross, L. Hakobyan, I. Isaev, Y. Ivanisenko, M. Khojoyan‡, M. Krasilnikov, M. Mahgoub, D. Malyutin, A. Oppelt, M. Otevrel, B. Petrosyan, S. Rimjaem§, A. Shapovalov, F. Stephan, DESY, 15738 Zeuthen, Germany
D. Richter, HZB, 14109 Berlin, Germany

Abstract

High brightness electron sources for linac based free-electron lasers operating at short wavelength such as the Free-Electron Laser in Hamburg at DESY, Hamburg Site (FLASH) and the European X-Ray Laser Project XFEL (European XFEL) are characterized and optimized at the Photo Injector Test Facility at DESY, Zeuthen Site (PITZ). One of the most important parameters influencing the FEL process is the normalized transverse projected emittance of the electron beam. The major part of the experimental program at PITZ is devoted to its optimization. Detailed simulations of the present facility setup are performed for a 1 nC bunch charge in order to optimize the transverse projected emittance of the electron beam. Cathode laser pulse length and transverse spot size at the photo cathode, gun and booster accelerating gradients and their launching phases as well as the main solenoid current are optimized. Simulations results together with experimental data are presented.

INTRODUCTION

Linac based free electron lasers like FLASH [1] and the European XFEL [2], developed to produce high brilliance coherent laser light with wavelength down to nanometers and below, require high quality electron beams with high peak current, small relative energy spread and transverse slice emittance. For the production of the laser light at such FELs the Self Amplified Spontaneous Emission (SASE) process in the undulator is used. Aforementioned parameters of the electron beam define minimum achievable wavelength and brilliance of the emitted laser radiation obtained during the lasing process [3]. Such characteristics like peak current of the electron beam and its energy spread can be improved during the electron beam transport from the gun towards the undulator, while the minimum emittance value of the electron beam at the undulator entrance is a property which is already determined at the output of the photo injector and usually only degrades after the electron beam leaves the photo injector. The research program at PITZ is devoted to the characterization and optimization of the photo injectors which will be used at FLASH and the European XFEL. The description of the PITZ facility setup used for measurements and simulations can be found in [4]. The emittance of the electron beam in the PITZ photo injector is a quantity which depends on several machine parameters such as laser transverse and temporal profiles, gun and booster on-axis peak fields and their launching phases with respect to maximum mean momentum gain phase, hereinafter w.r.t MMMG phase as well as the focusing current of the main solenoid. A detailed set of the simulations was done in order to study the emittance dependence on the aforementioned machine parameters and will be presented together with experimental data obtained during the run period January-June 2011.

* Grygorii.Vashchenko@desy.de
† On leave from INRNE, Sofia, Bulgaria
‡ On leave from ANSL, Yerevan, Armenia
§ Currently at Chiang Mai University, Chiang Mai, Thailand

BEAM DYNAMICS SIMULATIONS AND EXPERIMENTAL RESULTS

A Space charge TRacking Algorithm (ASTRA) code was used for the simulations [5]. The range of parameters used for the emittance simulations is presented in Table.1. The booster launching phase was kept constant during the simulations since the emittance dependence on this parameter is negligible [6]. The normalized transverse projected emittance, hereinafter emittance, of the electron beam was measured at EMSY1 (see [4]), placed directly behind the booster cavity, by using the well established single slit scan technique [4, 7].

Emittance dependence on the gun on-axis peak field

The emittance dependence on the gun on-axis peak field was studied for a fixed laser pulse length with FWHM = 21.5 ps corresponding to an average value measured during the last run period. Other parameters like gun launching phase, main solenoid current, booster on-axis peak field were varied in order to get the minimum emittance values for each gun on-axis peak field. Results of the simulations are presented in Fig.1. An exponential decay fit is applied to the simulation data.

The values of the rms laser spot size on the cathode for which minimum emittance value was found for a given gun on-axis peak field are presented in Fig.2. An allometric fit is applied to the simulation data. Values of the gun launching phase at which minimum emittance value was found for a given gun on-axis peak field are presented in Fig.3. We can consider some weak trend on the phase to the negative direction meaning relative growth of the space-charge induced emittance compared to the RF-induced emittance as the electron beam more compressed for the positive phases. The focusing strength of the main solenoid current deliver-

ISBN 978-3-95450-123-6

LASER PULSE TRAIN MANAGEMENT WITH AN ACOUSTO-OPTIC MODULATOR

M. Gross*, G. Klemz, H.J. Grabosch, L. Hakobyan, I.V. Isaev, Y. Ivanisenko, M. Khojoyan[+], G. Kourkafas, M. Krasilnikov, K. Kusoljariyakul[‡], J. Li[‡+], M. Mahgoub, D.A. Malyutin, B. Marchetti, A. Oppelt, M. Otevrel, B. Petrosyan, A. Shapovalov, F. Stephan, G. Vashchenko,
DESY, 15738 Zeuthen, Germany
H. Schlarb, S. Schreiber, DESY, 22607 Hamburg, Germany
D. Richter, HZB, 12489 Berlin, Germany

Abstract

Photo injector laser systems for linac based Free Electron Lasers (FELs) sometimes have the capability of generating pulse trains with an adjustable length. For example, the currently installed laser at the Photo Injector Test Facility at DESY, Zeuthen Site (PITZ) can generate pulse trains containing up to 800 pulses. Repetition frequencies are 10 Hz for the pulse trains and 1 MHz for the pulses within a train, respectively [1].

Mostly due to thermal effects caused by absorption in amplifier and frequency doubling crystals, pulse properties are changing slightly within a pulse train and also shot-to-shot, depending on the pulse train length. To increase stability and repeatability it is desirable to run the laser under constant conditions. To achieve this while still being able to freely choose pulse patterns a pulse picker can be installed at the laser output to sort out unwanted pulses. A promising candidate for this functionality is an acousto-optic modulator which currently is being tested at PITZ. First experimental results will be presented and discussed towards the possibility of including this device into an FEL photo injector.

INTRODUCTION

A central issue for running high quality experiments with a FEL is the stability of its output, requiring every subsystem including the photocathode laser to meet set specifications. In the case of an FEL with a multi-bunch structure, e.g. FLASH and the European XFEL, where each output event is a pulse train of varying length, the stability criterion has to be met not only shot-to-shot but also within each laser pulse train.

One critical part of the photocathode laser system is the frequency quadrupling where the laser output wavelength is converted from the near infrared (1030 nm) via green (515 nm) into the ultraviolet (UV at 258 nm). This is done in two steps with nonlinear crystals, each doubling the laser wavelength. The second conversion step from green into UV is done with a beta barium borate (BBO) crystal which absorbs a tiny fraction of the converted UV light. The resulting temperature variation in the crystal leads to small but measurable variations of e.g. charge and delay of pulses within a pulse train [2]. Absorption of light in the other conversion crystal and amplifier crystals of the laser adds to this effect.

A possible solution to this problem is to let the laser run constantly to stabilize the temperature of the crystals and define the pulse trains by picking the appropriate pulses behind the laser. Such a pulse picker may be realized using a UV Pockels cell or an acousto-optic modulator (AOM). This improves the situation because of the difference in the physical processes: the wavelength conversion in the BBO crystal is a nonlinear process requiring high light intensity. Small variations in operating conditions have big effects on arrival time and conversion efficiency. The AOM on the other hand is based on the linear acousto-optic effect, making it possible to operate the pulse picker at low intensity, which should, together with the low UV absorption of the AOM material (quartz), reduce the influence of heating enormously.

In order to prove the anticipated advantages experimentally such an AOM is currently being tested at the Photo Injector Test Facility at DESY, Zeuthen Site (PITZ) and in the following we will first explain the function of this device and then present initial experimental results.

THE ACOUSTO-OPTIC MODULATOR

The function of an AOM is based on the acousto-optic effect which is an interaction of light with a sound wave [3]. An AOM is a device which utilizes this effect to deflect a light beam as illustrated in Fig. 1.

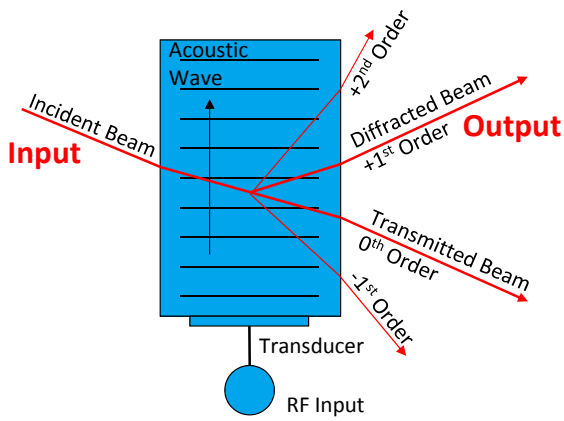

Figure 1: Function of an AOM.

* matthias.gross@desy.de
[+] On leave from ANSL, Yerevan, Armenia
[‡] On leave from Chiang Mai University, Thailand
[‡+] On leave from USTC, Hefei, China

ISBN 978-3-95450-123-6

HIGH-BRIGHTNESS ELECTRON BEAM EVOLUTION IN TIME FOLLOWING LASER-BASED CLEANING OF THE LCLS CATHODE*

F. Zhou+, A. Brachmann, F-J. Decker, P. Emma, R. Iverson, P. Stefan, and J. Turner
SLAC National Accelerator Laboratory, 2575 Sand Hill Road, Menlo Park, CA 94025, USA

Abstract

Laser-based techniques have been widely used for cleaning metal photocathodes to increase quantum efficiency (QE). However, the impact of laser cleaning on cathode uniformity and thereby on electron beam quality are less understood. We are evaluating whether this technique can be applied to revive photocathodes used for electron beam sources in advanced x-ray free electron laser (FEL) facilities, such as the Linac Coherent Light Source (LCLS) at the SLAC. Laser-based cleaning was applied to two separate areas of the current LCLS photocathode on July 4 and July 26, 2011, respectively. QE was increased by 8-10 times upon the laser cleaning. Since the cleaning, routine operation has exhibited a slow evolution of QE improvement and comparatively rapid improvement of transverse emittance, with a factor-of-3 QE enhancement over five months, and a significant emittance improvement over the initial 2-3 weeks following the cleaning. Currently, the QE of the LCLS photocathode is holding constant at about 1.2×10^{-4}, with a normalized injector emittance of about 0.3 μm for a 150-pC bunch charge. With proper procedures, the laser cleaning technique appears to be a viable tool to revive the LCLS photocathode. We present observations and analyses for QE and emittance evolution in time following laser-based cleaning of the LCLS photocathode, and comparison to previous studies, the measured thermal emittance versus QE and comparison to the model.

OVERVIEW

The Linac Coherent Light Source (LCLS), located at the SLAC, has been successfully operated for users for more than three years [1]. Its copper-cathode based photo injector has produced an ultra-low emittance electron beam [2] for the x-ray free electron laser (FEL). To date, three polycrystalline copper photocathodes have been used in LCLS injector operation since its initial commissioning [3]. The first cathode had quantum efficiency (QE), $2\text{-}3\times10^{-5}$ after some processing, sufficient for initial commissioning from early of 2007 to July 2008. The second cathode had a QE of about 5×10^{-5} and was used for about three years of operation, from July 2008 to May 2011. When the LCLS repetition rate was increased from 60 Hz to 120 Hz, its QE quickly decayed to one half its initial value within 7-10 days. For this reason, the transverse position of the drive laser on the cathode had to be moved frequently to find new high-QE spots. This movement and subsequent retuning of the photo injector occupied significant LCLS machine time, and only a limited number of laser locations on the cathode could deliver the desired low emittance electron beam for reasonably good FEL performance. The second cathode was then replaced by a third one in May 2011, but the initial QE of this third cathode was only $\sim5\times10^{-6}$, insufficient for user operations. Eventually, laser-based cleaning was initiated on the third photocathode, in order to boost the QE. Previous cleaning attempts for the third cathode, using in-situ gun hydrogen plasma cleaning [3], failed to achieve adequate QE improvement. Laser-based cleaning techniques have been used in the photo injector community for many years on metal cathodes, such as copper and Mg, to enhance QE [4-6]. A high-intensity laser beam, interacting with the cathode, may ablate the cathode surface and/or remove contamination, thereby resulting in a QE increase. However, the impact of laser cleaning on cathode uniformity and electron beam emittance are unknown at present. We evaluated whether this technique could be used to revive the LCLS photocathode for x-ray FEL facilities, which have stringent requirements on the beam emittance as well as the QE. Laser-based cleaning for the LCLS photocathode was successfully performed in July 2011, and the evolution of the QE and emittance following the cleaning will be presented.

LASER CLEANING PARAMETERS AND PROCEDURES

The applied laser fluence is a key parameter in laser-based cleaning for metal cathodes. The fluence of the refocused UV drive laser (253 nm) needs to be properly chosen so that the laser can effectively remove surface contamination to enhance the QE, but will not destroy the cathode surface quality or change the surface morphology. For this application to the LCLS copper cathode, the laser fluence used for laser cleaning was determined by the "vacuum activity" in the photocathode RF gun [5]. In other words, the applied laser fluence (laser energy for a given laser spot size) had to be gradually increased until a change in vacuum pressure in the RF gun was observed. In the LCLS gun system, the nearest vacuum gauge to monitor the gun vacuum is located at a nearby RF-feed waveguide [7]. The cold cathode ion gauge on the waveguide is about 50 cm away from the cathode. Estimate shows the vacuum pressure on the cathode is 1.3-1.5 times higher than the ion gauge [8].

* Work supported by DOE under grant No. DE-AC02-76SF00515
+ zhoufeng@slac.stanford.edu

ISBN 978-3-95450-123-6

FIRST DIRECT SEEDING AT 38 nm*

C. Lechner†, A. Azima, J. Bödewadt, M. Drescher, E. Hass, U. Hipp, Th. Maltezopoulos, V. Miltchev, M. Rehders, J. Rönsch-Schulenburg, J. Rossbach, R. Tarkeshian‡, V. Wacker, M. Wieland, University of Hamburg, Hamburg, Germany
S. Khan, DELTA, Dortmund, Germany
S. Ackermann, S. Bajt, H. Dachraoui, H. Delsim-Hashemi, S. Düsterer, B. Faatz, K. Honkavaara, T. Laarmann, M. Mittenzwey, H. Schlarb, S. Schreiber, L. Schroedter, M. Tischer, DESY, Hamburg, Germany
F. Curbis, MAX IV Laboratory, Lund University, Sweden
R. Ischebeck, Paul Scherrer Institut, Villigen, Switzerland

Abstract

The sFLASH project at DESY is an experiment to study direct seeding using a source based on the high-harmonic generation (HHG) process. In contrast to SASE, a seeded FEL exhibits greatly improved longitudinal coherence and higher shot-to-shot stability (both spectral and energetic). In addition, the output of the seeded FEL is intrinsically synchronized to the HHG drive laser, thus enabling pump-probe experiments with a resolution of the order of 10 fs. The installation and successful commissioning of the sFLASH components in 2010/2011 has been followed by a planned upgrade in autumn 2011. As a result of these improvements, in spring 2012 direct HHG seeding at 38 nm has been successfully demonstrated. In this contribution, we describe the experimental layout and announce the first seeding at 38 nm.

INTRODUCTION

The SASE start-up from noise has an impact on the properties of the emitted light pulses. To name but a few, spectrum and energy of the pulses are varying on a shot-to-shot basis, and multiple uncorrelated modes lead to reduced longitudinal coherence. One way to address these issues is to operate the FEL as an amplifier for externally generated radiation fields. A promising source for the external radiation field is the laser-driven high-harmonic generation (HHG) process. The HHG pulse is longitudinally coherent with stable spectrum and energy. When correctly brought into overlap with the electron bunch in the first undulator, amplification of the HHG pulse to the GW-level can be expected. To some extent, the timing of the FEL output signal is insensitive to the arrival time jitter of the electron bunch, since it is intrinsically synchronized to the HHG drive laser. This makes the HHG-seeded FEL an ideal source for pump-probe experiments.

sFLASH is a project to study the concept of direct HHG seeding. It is installed at FLASH [1], the free-electron laser user facility in Hamburg, delivering high-brilliance SASE FEL radiation in the XUV and soft X-ray wavelength ranges. The sFLASH experiment has been installed in a 40 m long part of the FLASH beamline upstream of the FLASH SASE undulators which has been rebuilt in 2010, compare Fig. 1. Upstream of the last dipole magnet of the FLASH energy collimator, the injection chamber is installed, at which the XUV seed pulses arriving from the laser laboratory adjacent to the tunnel are sent into the electron beamline. The injection chamber is followed by a section originally installed for the ORS experiment (optical-replica synthesizer [2]). This section, which has been used for beam diagnostics, comprises two undulators in a modulator-radiator arrangement. The sFLASH longitudinal overlap setup is located at the exit of the first ORS undulator. The light pulses can be sent either to the experimental hutch outside the tunnel or to the in-tunnel diagnostic devices. This diagnostic assembly features a high-resolution XUV spectrometer and several micro-channel plates (MCPs) used to measure the pulse energy. A dedicated beamline will provide the infrastructure for detailed temporal characterization of the XUV radiation pulses. For this experiment, an NIR beamline will be commissioned to transport light from the HHG drive laser (wavelength 800 nm) to the experimental station.

sFLASH aims at sub-40 nm seeded operation without disturbing parallel FLASH SASE delivery to the already existing user stations.

EXPERIMENTAL LAYOUT

In this section we describe the layout of the hardware used in the sFLASH experiment. For the following discussion we break the setup shown in Fig. 1 down into three parts: (i) injection of the XUV seed pulses, (ii) electron beamline (where the amplification process takes place), and (iii) extraction and photon diagnostics.

Electron Beamline

As apparent in Fig.1, the sFLASH electron beamline can be subdivided in two sections: The ORS section, which we use for the longitudinal overlap of electron bunches and XUV pulses as well as to match the electron optics to the

* Supported by the Federal Ministry of Education and Research of Germany under contract No. 05 K10 GU1 and the German Research Foundation programme graduate school 1355
† christoph.lechner@desy.de
‡ present address: Max-Planck-Institut für Physik, Munich, Germany

ISBN 978-3-95450-123-6

SPECTRAL CHARACTERIZATION OF THE FERMI PULSES IN THE PRESENCE OF ELECTRON-BEAM PHASE-SPACE MODULATIONS*

E. Allaria#, S. Di Mitri, W. M. Fawley, E. Ferrari, L. Froehlich, G. Penco, Spezzani, M. Trovo, Sincrotrone Trieste, Strada Statale 14 - km 163.5, 34149 Basovizza, Trieste, Italy

G. De Ninno, B. Mahieu, S. Spampinati, Sincrotrone Trieste, Strada Statale 14 - km 163.5, 34149 Basovizza, Trieste, Italy and University of Nova Gorica, Nova Gorica, Slovenia

L. Giannessi, Sincrotrone Trieste, Strada Statale 14 - km 163.5, 34149 Basovizza, Trieste, Italy and ENEA C.R. Frascati, Frascati (Roma), Italy

Abstract

As a seeded FEL based on a single stage HGHG configuration, FERMI's FEL-1 has produced very narrow bandwidth FEL pulses in the XUV wavelength region relative to those typical of SASE devices. This important feature of seeded FELs relies however upon the capability to produce high quality electron beams with clean longitudinal phase spaces. As has been predicted previously, the FEL output spectra can be modified from a simple, nearly transform-limited single spike by modulation and distortions of the longitudinal phase space of the electron beam. In this work we report a study of the FEL spectra recorded at FERMI for various situations showing the effects of phase-space modulation on the FEL properties.

INTRODUCTION

FERMI@Elettra [1] is a free electron laser user facility recently built in Trieste, Italy. Based on two FEL lines that uses the electron beam produced by a common accelerator, FERMI@Elettra covers the spectral range from ~80 nm down to 4 nm. Both FELs rely upon a seeding scheme that allows FERMI to improve the quality of the longitudinal coherence of FEL pulses with respect to existing SASE FELs covering the same spectral range. For both FELs the seeding is done with an external laser in the UV and harmonic conversion is used to reach the desired FEL wavelength. The first FEL (FEL-1), covering the spectral range from 80 to 20 nm, is based on the high gain harmonic generation (HGHG) [2] and has been already operated since end 2010 [3]. The second FEL (FEL-2) requires a two stage HGHG configuration to reach wavelengths as short as 4 nm. The first stage of FEL-2 has been already operated [4] while the second stage will be commissioned late this year.

The capability of seeded harmonic generation to produce highly coherent FEL pulses has been previously demonstrated [2,5]. However it is known that this desirable feature depends on the quality of the electron beam and that distortion of the phase space of the electron beam may lead to significant deterioration of the longitudinal coherence of the FEL pulses.

Over the past two years as we have operated FEL-1, several new accelerator components have become available that have allowed us to vary the FERMI electron beam parameters. In this work we report how various electron beam properties appear to affect the FEL spectra, in particular at 32-nm output wavelength (the 8th harmonic of the seed laser).

HGHG AT FERMI

An HGHG or a coherent harmonic generation (CHG) FEL can be divided into three parts, the modulator, the bunching section and the radiator (see Fig. 1).

In the modulator the electron beam is in resonance with the electromagnetic wave of the external seed laser. Due to the interaction with the seed laser the electron beam become energy modulated with a periodicity equal to the seed wavelength. At FERMI the magnetic period of the modulator is 100 mm and the seed laser is typically operated at 260 nm with a pulse length of about 150 fs (FWHM).

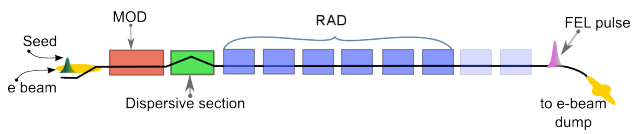

Figure 1: Layout of the undulator system of FERMI FEL-1 used for this work.

The energy modulation is then converted into density modulation when the electron beam passes through the dispersive section where higher-energy electrons follow a shorter path than lower energy electrons. Density modulation is created at the seed laser wavelength and also at higher harmonics. Typical values for the strength of the dispersive section correspond to an R56 in the range between 50 and 90 μm. In addition to producing bunching, if the electron beam has an energy chirp, the chicane acts also as a bunch compressor for the electron beam, as a result of the bunch compression also the wavelength periodicity is changed.

The magnetic strength of the final radiator is set so that the electron beam is at resonance with the desired harmonic of the seed laser. As a consequence of their

*Work partially supported by the Italian Ministry of University and Research under grants FIRB-RBAP045JF2 and FIRB-RBAP06AWK3
#enrico.allaria@elettra.trieste.it

ISBN 978-3-95450-123-6

COMPARISON OF HARD X-RAY SELF-SEEDING WITH SASE AFTER A MONOCHROMATOR AT LCLS*

J. Welch†, F.-J. Decker, J. Hastings, Z. Huang, A. Lutman, M. Messerschmidt, J. L. Turner
SLAC, Menlo Park, Ca. 94320, USA

Abstract

Self-seeding using hard x-rays was demonstrated at LCLS in January 2012 and produced a factor of 40-50 bandwidth reduction from normal SASE operation. For many hard x-ray users, the photon intensity after a monochromator is an important performance parameter, whether or not the beam is seeded or SASE. In this paper, we report results from a study of self-seeding performance using the Si (111) K- monochromator with a full bandwidth of 1.2 eV at 8.2 keV. These include a direct comparison of the average intensity of the monochromatized seeded beam with that of a monochromatized fully tuned-up SASE beam, in both cases using 150 pC bunch charge.

SEEDING AT LCLS

The main goal of the hard x-ray self-seeding project at LCLS is to increase the peak spectral brightness. Near-monochromatic beams of hard x-rays can be manipulated efficiently using bragg reflection, rather than low incidence angle x-ray mirrors and long drift spaces, and allow for complex beam manipulation such as split and delay [1] similar to what is done with conventional laser beams.

LCLS [2] was designed to operate in the SASE mode, where shot noise in the electron beam is amplified by the FEL process producing x-ray beams with RMS bandwidths that are typically of order the FEL ρ parameter [3, 4]. By seeding the FEL with near-monochromatic x-rays, the output bandwidth can be drastically reduced, provided the seed power is sufficient to overcome the relatively broad band power fluctuations due to shot noise.

In an upgrade to LCLS [5], originally proposed by Geloni, et. al. [6], a seed pulse is generated by sending the SASE output from the first $\sim$ 45 m of undulator, called 'U1', through a thin diamond crystal set at the bragg angle. The effect of the crystal is to generate a near-monochromatic 'ringing' in the transmitted x-ray beam which forms the x-ray seed. A short 4 m electron beam chicane diverts the electron beam around the crystal, smears out any micro-bunching from U1, and provides the proper time delay between the electron bunch and the seed x-rays. The downstream $\sim$ 68 m of undulator amplify the seed ultimately to reach saturation levels. An overview showing the seeding chicane and the LCLS undulator is given in Fig. 1.

Since the seeding chicane and crystal were installed in LCLS and commissioned [7] various configurations for seeding have been investigated. These include seeding with relatively long pulses, different crystal planes including 004, 220, 133, and 111; and simultaneous seeding from 004 and 220. All of these configurations have produced seeded beams.

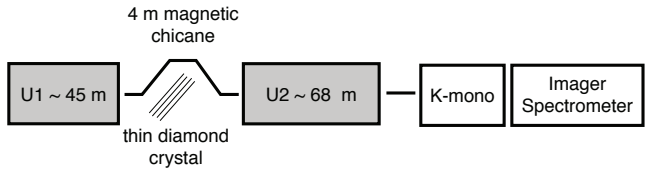

Figure 1: Schematic of hard x-ray seeding at LCLS.

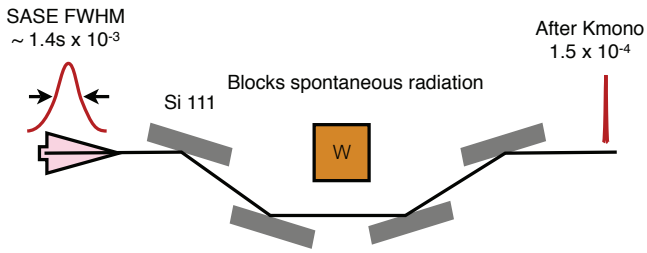

Figure 2: Functional schematic of the K-monochromator.

The K-monochromator (Kmono)

A single purpose monochromator was originally developed and installed in LCLS for precision measurement of undulator K-parameters [8]. It has found a new function as a tuning aid for self-seeding operation. The device, shown schematically in Fig. 2, is designed so that there are four bragg reflections of x-ray beam from Si 111 planes resulting in no net deflection of the beam. Because of the four bounce arrangement the device only transmits one energy (8194 eV) with a bandwidth of 1.2 eV and for one angle of incidence. It has a large acceptance area, no cooling, and is located about 90 meters from the end of the undulator

The Kmono transmits only about one-tenth of the output SASE spectrum, but essentially 100% of a seeded spectrum. Thus, when tuning on the intensity seen through the Kmono the SASE contribution to the overall transmitted intensity, which can otherwise dominate, is greatly reduced, and the peak spectral brightness is optimized rather than the overall pulse energy.

* Work supported in part by the DOE Contract DE-AC02-76SF00515.
† welch@slac.stanford.edu

ISBN 978-3-95450-123-6

SYSTEM DESIGN FOR SELF-SEEDING THE LCLS AT SOFT X-RAY ENERGIES*

Y. Feng#, J. Amann, D. Cocco, C. Field, J. Hastings, P. Heimann, Z. Huang, H. Loos, J. Welch, J. Wu, SLAC, Menlo Park CA 94025, U.S.A.
K. Chow, P. Emma, N. Rodes, R. Schoenlein, LBNL, Berkeley, CA 94720, U.S.A.

Abstract

The complete design for self-seeding the LCLS at soft X-ray energies from 500 to 1000 eV based on a grating monochromator is described. The X-ray optics system consists of a toroidal variable-line-space (VLS) grating and focusing mirrors for imaging the seed pulse onto the downstream seeding undulator. The system has a resolving power greater than 5000 creating a near-transform-limited seed pulse from the upstream SASE undulator for pulse durations up to 36 fs FWHM at 500 eV and 18 fs FWHM at 1000 eV. Diagnostics for ensuring overlap with the electron beam are included in the design. The optical system is sufficiently compact to fit within a single 3.9 m LCLS undulator segment. The electron chicane system which serves to delay the electron beam to match the less than 1 ps delay from the optical system is similar to the chicane used in the hard X-ray self-seeding at LCLS. The seeded FEL pulse is expected to be nearly transform-limited with a bandwidth in the 2×10^{-4} range, potentially increasing the low-charge FEL X-ray peak spectral brightness by 1 to 2 orders of magnitude.

INTRODUCTION

LCLS presently produces X-ray radiation that is transversely coherent but not longitudinally. The temporal profile is a spiky structure characteristic of the SASE process that starts from the shot noise in the electron beam. The spectral domain has a similar spiky profile [1] and has been observed experimentally for soft [2] and hard [3] X-rays. Seeding (overlapping) the electron beam with a monochromatic X-ray beam of sufficiently narrow bandwidth and sufficient power would force the FEL to produce nearly transform-limited pulses, minimal jitter in X-ray wavelength and potentially higher spectral brightness by 1 to 2 orders of magnitude if taken to full saturation. These enhanced beam qualities will benefit the users by not only improving the measurement efficiency and data analysis, but also enabling experimental studies in many areas of biology, materials, chemistry, and atomic, molecular, and optical sciences where high spectral brightness or high peak power is essential.

* Portions of this research were carried out at the Linac Coherent Light Source (LCLS) at the SLAC National Accelerator Laboratory. LCLS is an Office of Science User Facility operated for the U.S. Department of Energy Office of Science by Stanford University under Contract No. DE-ACO2-76SF00515. LBNL part of work is supported by the Director, Office of Science, of the U.S. Department of Energy under Contract No. DE-AC02-05CH11231
#yfeng@slac.stanford.edu

A possible concept for self-seeding, originally proposed by a DESY team [4], uses a grating monochromator between a SASE and seeding undulator to generate the soft X-ray seed. This principle was adopted for a conceptual design aimed at seeding the future LCLS-II soft X-ray undulator between 200 and 2000 eV with a minimum bandwidth of 5×10^{-5} [5]. A more compact X-ray optics design ensued for the current LCLS soft X-ray undulator in a limited energy range with a more modest bandwidth requirement of 2×10^{-4} [6]. Following the successful demonstration of the hard X-ray self-seeding (HXRSS) at LCLS using a thin diamond monochromator in transmission [7], there is a pressing need for a parallel implementation in the soft X-ray energies. To preserve the performance of the current LCLS FEL, it is necessary that the X-ray optics be designed such that the entire seeding system fit within a single 3.4 m LCLS undulator segment space in an arrangement similar to that of the HXRSS. This paper describes the overall design of the system for soft X-ray self-seeding (SXRSS) the LCLS.

SEEDING SYSTEM OVERVIEW

The SXRSS system, proposed to replace the existing U9 undulator segment, is shown schematically Figure 1. It consists of 3 major components: 1) a complete grating monochromator system with its vacuum vessel and internal motions, isolation valves, pumps, and gauges, and all necessary mechanical supports to the existing undulator girder; 2) A weak four-dipole magnetic chicane, five rack-mountable power supplies (1 main & 4 trims) and appropriate cables, chicane vacuum chamber, and all necessary mechanical supports to the existing U9 sliders; 3) Diagnostics to measure the overlap of the electron and seeding X-ray beams.

The system supports both the seeded and SASE mode. In the seeded mode, the magnetic chicane is powered, and the electron beam breaks from co-propagation with X-rays in the upstream SASE undulator U8 at the first dipole B1 of the chicane and is displaced with proper delay and then re-introduced into the downstream seeding undulator U10 after the fourth dipole B4. The SASE X-rays are monochromatized by the grating, the mirror M1 and the slit and imaged by the mirrors M2 and M3 onto the mid-section of the immediate downstream undulator U10 to merge with the electron beam to seed the FEL process. X-ray and electron diagnostics (not shown) are distributed strategically to ensure spatial and pointing overlap of the two beams.

ISBN 978-3-95450-123-6

USE OF THE PROJECTED TORUS KNOT LATTICE FOR A COMPACT STORAGE RING FEL

S. Sasaki#, A. Miyamoto, Hiroshima Synchrotron Radiation Center,
Hiroshima University, Higashi-Hiroshima, Japan

Abstract

We proposed a new scheme of lattice design for a compact storage ring in which a design orbit of electron beam closes after completing multiple turns. This new lattice can be made by placing necessary accelerator components at certain positions on a projected torus knot in the horizontal orbit plane. In this type of storage ring, the beam trajectory crosses in a bending magnet, i.e. each bending magnet accepts two beam orbits. For example, in the ring having the (11, 3) torus knot lattice with 11 bending magnets, a bunch goes through bending magnets 22-times to complete its 3-turn closed orbit. Since the maximum output laser power is proportional to the synchrotron radiation loss in the complete turn round a closed orbit starting from the optical resonator section, the maximum laser power from the projected torus knot storage ring FEL can be doubled for 2-turn lattice and tripled for 3-turn lattice compared with that from a conventional storage ring FEL. The new lattice scheme may contribute to more stable operation of a compact storage ring FEL.

INTRODUCTION

In general, the design orbit in a synchrotron accelerator or a storage ring closes in one turn around the ring, i.e. the length of closed orbit is equal to the circumference of the ring. On the other hand, a stellarator or a heliotron for a plasma confinement with magnetic fields has a donut (torus) shape with helically wound coils. Each coil winding does not close in one turn but closes after multiple turns around a torus. The shape of a coil winding on a torus is called torus knot. Similar to the coil winding of a stellarator, if the beam in an accelerator draws a torus knot trajectory, a design orbit closes after multiple turns.

The realistic multiple-turn lattice can be realized by placing conventional accelerator components on a projected torus knot in the horizontal plane [1]. The ring with this lattice may have larger maximum stored charge in multiple-bunch mode, and longer bunch-to-bunch interval in a single-bunch mode if compared with a conventional ring having the same footprint. Also, for an electron storage ring as the synchrotron light source or the ring FEL, a larger number of straight sections may accommodate with many insertion devices.

As a successive machine of current storage ring at Hiroshima Synchrotron Radiation Center, we have a plan to construct a third generation compact storage ring called HiSOR-II in order to serve brilliant synchrotron radiation (SR) from VUV to soft X-ray for SR users in the field of materials science, solid state physics, bio-molecular science, etc. Due to the requirement for the photon energy ranges from user community and the space limitation of construction area on the campus of Hiroshima University, the expected ring energy is 0.7 GeV and the ring diameter should be nearly equal to or smaller than 15 m. To meet all requirements including the oscillator FEL capability, construction of a compact storage ring with the lattice of torus knot architecture seems to be most plausible.

TORUS KNOT AND LATTECE

The Möbius strip is a one-sided nonorientable surface. It can be made from a band or a single strip by connecting both ends, so that one of the ends is half-twisted each other. As one can easily see by drawing a line on the surface of Möbius strip, the line closes after completing two turns (4π) around the ring. Analogically, if the top and bottom surfaces of a tall triangular prism are twisted $2\pi/3$ angle and then connected, the ridgeline closes after three turns (6π) [2]. These mathematical features are extended, generalized, and categorized as the group of torus knots [3]. Figure 1 shows an example of variations of (1,3) torus knot.

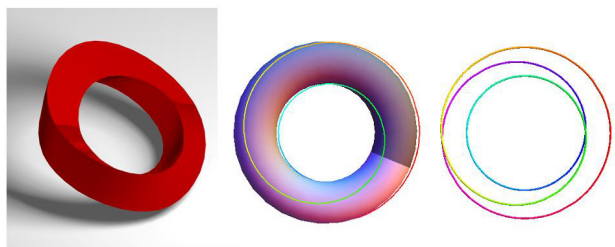

Figure 1: Left: Möbius triangular prizm, Middle: (1,3) torus knot wound around a torus, Right: (1,3) torus knot without torus.

Figure 2 shows some other torus knots.

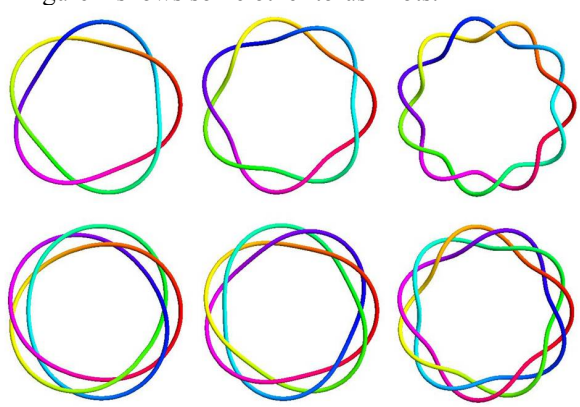

Figure 2: Examples of torus knots.

#sasakis@hiroshima-u.ac.jp

ISBN 978-3-95450-123-6

A NEW APPROACH TO IMPROVING THE EFFICIENCY OF FEL OSCILLATOR SIMULATIONS*

Michelle D. Shinn#, Stephen V. Benson, and Anne M. Watson
Jefferson Lab, 12000 Jefferson Ave, Newport News, VA, 23606 U.S.A.
Peter J. M. van der Slot
University of Twente, P.O. Box 217 7500 AE Enschede, the Netherlands and
Colorado State University, Dept. of Electrical and Computer Eng., Fort Collins, CO 80523 USA
Henry P. Freund and Dinh C. Nguyen
Los Alamos National Laboratory, Los Alamos, NM 87545 USA

Abstract

During the last year we have been benchmarking FEL oscillator simulation codes against the measured performance of the three Jefferson Lab oscillator FELs. While one might think that a full 4D simulation is *de facto* the best predictor of performance, the simulations are computationally intensive, even when analytical approximations to the electron bunch longitudinal distribution are used. In this presentation we compare the predictions of the 4D FEL interaction codes Genesis and Medusa, in combination with the optical code OPC, with those using a combination of the 2D & 3D versions of these codes, which can be run quickly on a single CPU core desktop computer.

INTRODUCTION

Since the initiation of the FEL program at Jefferson Lab (JLab) in 1995, three FELs have been designed and operating; the IR Demo [1], the IR Upgrade [2], and most recently the UV Demo [3,4]. All three FELs were designed using 1D models as discussed in Ref [5]. Clearly, use of these programs requires acceptance of a number of simplifications, such as the use of analytical (parabolic or Gaussian) electron beam distributions that interact with a low order TEM optical mode, or some superposition of modes that doesn't vary as the oscillator power saturates. Nevertheless, we found that these two FEL simulation tools reasonably (better than 30% difference) predicted the lasing efficiency of all 3 FELs the IR FELs. The gain predictions were also in reasonable agreement for the IR FELs, but low by about 50% for the UV Demo. This discrepancy has been studied using 3D and 4D FEL simulation codes [6].

While we believe that the use of a 4D code with a start-to-end (S2E) simulation of the electron bunch characteristics will yield the most accurate prediction, in our experience the creation of such a distribution takes weeks, and then a 4D FEL simulation takes about a week when performed on a parallelized cluster of computers comprising +40 cpus. This does not allow one to look at the performance of the FEL parametrically on a reasonable time scale. So we investigated whether we could use somewhat more sophisticated time dependent 2D FEL oscillator codes, with time independent 3D codes, that fully treat the spatial interaction of the electron and optical fields, as a good approximation to the full 4D codes. These lower dimensional codes can be run on dual core personal computers quickly, *i.e.*, in seconds to a couple of hours, To keep the computational times reasonable for the 4D simulations, all codes used parabolic longitudinal distributions. In this paper, we present preliminary results of our investigations to predict the measured performance of the 3 JLab FELs

THE FEL MODELS

Several performance parameters for the JLab FELs were used for benchmarking the codes. These parameters are 1) the lasing efficiency η, 2) the detuning length δl_c, and 3) the net gain g_{net}. Determining the lasing efficiency, equal to the average output power/electron beam power allows one to design an FEL to have considerable margin in this parameter, to ensure the end user's requirements are met. Knowing in advance the length of the detuning curve tells the FEL designer how insensitive the FEL parameters are to small cavity drifts. And the net gain tells the designer whether they are outcoupling the FEL efficiently. The measured values are given in Table I. Inputs for each of the FELs are given in Table 2. The 1D pulse propagation codes were discussed in the Introduction; we also used two 2D codes and 4D codes, and three 3D codes. In brief, the 2D codes are known as Pulsevnm, developed by the Naval Postgraduate School [7], and Medusa1D, developed by one of the co-authors [8]. The former code has been in use for some time, while the latter code has heretofore not been used for oscillator modelling. While both codes model the FEL interaction between an optical field and an electron bunch matched to the wiggler, there are differences. Pulsevnm averages the Lorentz force equations that describe the electron dynamics over a wiggler period. Medusa1D does

*Authored by Jefferson Science Associates, LLC and supported by the ONR, the Commonwealth of Virginia and U.S. DOE Contract No. DE-AC05-06OR23177. The U.S. government retains a non-exclusive, paid-up, irrevocable, world-wide license to reproduce this manuscript.
#shinn@jlab.org

ISBN 978-3-95450-123-6

PRELIMINARY FEL SIMULATION STUDY FOR PAL XFEL

Ilmoon Hwang*, Jang Hui Han, Yong Woon Parc,
Pohang Accelerator Laboratory, POSTECH, Pohang, Republic of Korea,
Jaeyu Lee,
Department of Physics , POSTECH, Pohang, Republic of Korea

Abstract

Pohang Accelerator Laboratory X-ray Free Electron Laser (PAL XFEL) will provide X-ray FEL radiation in a range of 0.1 and 10nm with five undulator beamlines. A undulator section for hard X-ray is designed for 0.1nm SASE FEL. We present FEL simulation study by using GENESIS.

INTRODUCTION

Pohang Accelerator Laboratory X-ray Free Electron Laser (PAL XFEL) will generate X-ray FEL radiation in a range of 0.1 and 10nm in five undulator beamlines [1]. It consists of a photocathode RF gun, a 10-GeV linac with S-band and undulators. A major goal is a hard X-ray with wavelength of 0.1nm by Self-Amplified Stimulated Emission (SASE). The lasing performance in the steady-state and the time-dependent model is investigated by tracking simulation, GENESIS [2]. Tapering is considered. The main parameters for a hard X-ray generation are listed in Table 1.

Table 1: PAL XFEL parameter for 0.1nm X-ray

Electron energy	10 GeV
Charge	200 pC
Peak current	3 kA
Emittance	0.5 umrad
Energy spread	10^{-4}
Undulator period	24.4 mm
Undulator parameter K	2.0683
Beta function	18 m

UNDULATOR LATTICE

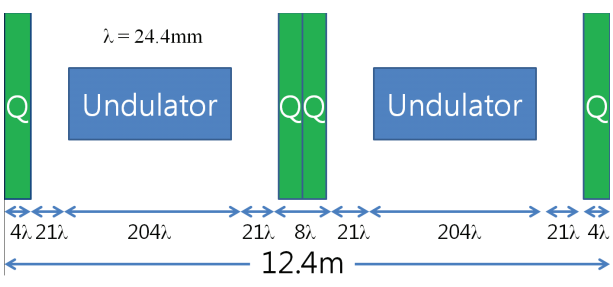

Figure 1: Schematic layout of undulator and FODO cell for simulation.

* imhwang@postech.ac.kr

The saturation power and length are affected by the averaged beta-function. A symmetric FODO configuration can be adopted in the undulator section. The length of half-cell is 6.2 m and the phase advance is 45 degrees. The beta functions at quadrupoles are 24.1m and 10.9m.

SASE SIMULATION

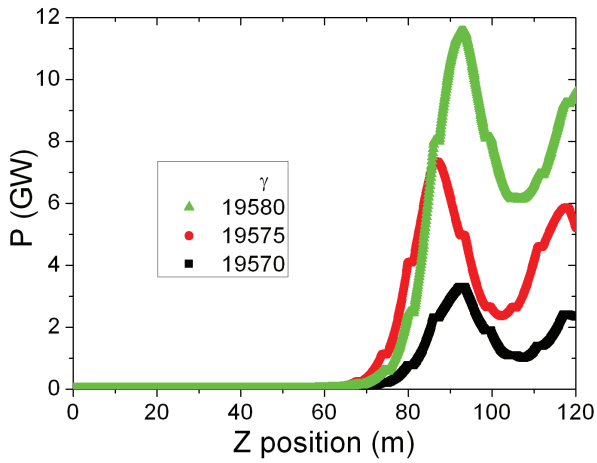

Figure 2: SASE lasing in steady-state with various energy.

The lasing performances are studied by code GENESIS. At first, the steady-state simulation was performed at 0.1 nm wavelength with the input condition of electron beam 10 GeV, charge 200 pC, normalized emittance 0.5 umrad and 3 kA beam current. The saturation power of 13.9 GW and length 53.7 m are expected by Ming Xie's formula.

Figure 2 shows the saturation power and length along the longitudinal coordinate. SASE radiation at 0.1 nm can be saturated at 75 m with 7.5 GW while12 GW power is obtained at 92 m with higher beam energy. These are longer length and weaker power due to space for quadrupoles and diagnositics.

Figure 3 shows slice properties of a beam profile for time dependent simulation. This beam profile satisfies the requirements except the beam current. Some required values are marked as red line. While the beam current is smaller than the target value 3kA in most parts, the normalized transverse emittances are slightly lower than the requirements and the energy spread is acceptable. The beam energy was selected by scan-test and one of the best cases is shown in Fig. 3. The energy of the center slice is higher than the theoretical value by 8 in gamma unit.

ISBN 978-3-95450-123-6

SENSITIVITIES OF FEL PARAMETERS IN LUNEX5 IN FRANCE BY GENESIS SIMULATION

T. Tanikawa, M.E. Couprie, M. Labat, A. Loulergue, Synchrotron SOLEIL, Saint-Aubin, France
S. Bielawski, C. Evain, C. Szwaj, PhLAM/CERLA, Villeneuve d'Ascq, France

Abstract

LUNEX5 (free-electron Laser (FEL) Using a New accelerator for the Exploitation of X-ray radiation of 5th generation) aims at producing short and intense laser pulses in the soft x-ray region. This FEL comports either a conventional linear accelerator or a laser wakefield accelerator, and includes an innovative schemes such an echo-enable harmonic generation and a higher-order-harmonics seeding generated in gases to obtain a high spatio-temporal coherent radiation. Sensitivities of FEL radiation property to the parameter such as the beam energy, the energy spread, the emittance, the peak current, the input seeding power, and the deflection parameter of undulators (radiators) have been studied by using GENESIS simulations.

INTRODUCTION

The recent developments of free-electron laser (FEL) based new generation synchrotron radiation sources in the x-ray domain enable to provide new insights on the matter investigations, thanks to the source properties. Indeed, new schemes such as the higher-harmonics seeding generated in the gases (HHG seeding) [1] and the echo-enable harmonic generation (EEHG) [2] provide a further control of the FEL pulse properties and access to short wavelength in a rather compact way. Another strategy to make the FEL sources be smaller is to replace a conventional linear accelerator (CLA) by a laser wake-field accelerator (LWFA) [3] (so-called 5th generation of synchrotron light sources), enabling to produce the electron beam of GeV regime in a plasma of cm length with the acceleration of GV/m and very short pulses of electron bunches [4].

The French project "LUNEX5" (free electron Laser Using a New accelerator for the Exploitation of X-ray radiation of 5th generation) aims at providing short and intense laser pulses in the soft x-ray region. This FEL comports either the CLA or the LWFA, and includes the HHG and EEHG options on the common FEL line. The FEL radiation covers the spectral range of 4 - 40 nm with the pulse duration of 20 fs.

LUNEX5 REFERENCE CASE

"LUNEX5" consists in the 400 MeV CLA with superconductive accelerator cavities or the 0.3 - 1 GeV LWFA, both providing short electron bunches to undulators. To achieve the soft x-ray especially with the advanced 4th generation light sources, the HHG and EEHG are adopted.

The CLA configures the superconductive L-band linac with a photo-cathode gun. It is designed for continuous-wave operation in the future. The LWFA will use the dedicated laser system of 200 TW with the laser power of either 10 PW from CILEX (Centre Interdisciplinaire de Lumière EXtrême) or 60 TW from LOA (Laboratoire d'Optique Appliquée). The FEL line comports in-vacuum undulators [5] with the magnetic fields of 1.5 T at the gap of 3 mm and the periodic length of 15 mm.

A Ti-Sapphire oscillator (the wavelength of 800 nm, the pulse duration of 30 fs), a regenerative and a multi-pass amplifier (the wavelength of 800nm, the pulse duration of 30 fs, the power of 10 mJ, the repetition of 50 Hz with the option of 1 kHz) will be used for the both seeding schemes. For the EEHG, the amplifier output is 3rd harmonic (the wavelength of 266 nm) and split in two parts, then injected. For the HHG, the amplifier output is injected directly to the gas cell. In the case of EEHG, the 266 nm seed laser is injected at the chicanes for EEHG, and the 20 - 40 nm HHG seed laser is injected at the entrance of the undulators in the case of HHG seeding (see Fig. 1 [5]).

These sensitivity studies to the parameters of FEL performance have been carried on a reference LUNEX5 case [6], developed for cascaded FEL of the wavelength of 20 nm with parameters given in Table 1 (the CLA case). The performances have been calculated by using

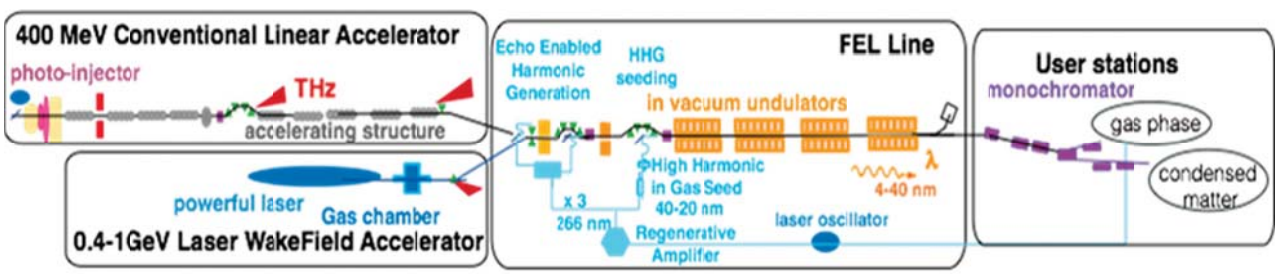

Figure 1: LUNEX5 scheme.

ISBN 978-3-95450-123-6

GENERATION OF LONGITUDINALLY COHERENT ULTRA HIGH POWER X-RAY FEL PULSES BY PHASE AND AMPLITUDE MIXING*

J. Wu#, SLAC, Menlo Park, CA 94025, USA
A. Marinelli, UCLA, Los Angeles, California 90095-1547, USA
C. Pellegrini, UCLA, Los Angeles, CA 90095-1547, USA, SLAC, Menlo Park, CA 94025, USA

Abstract

We study an improved SASE (iSASE) scheme to generate narrow bandwidth X- ray FEL pulses by introducing repeating delays of the electron beam respect to the radiation field, thus mixing the spikes phase and amplitude, increasing the cooperation length and generating a bandwidth much smaller than in the SASE case. The improved longitudinal coherence is used, in combination with a tapered undulator, to increase the efficiency of energy transfer to the radiation and generate ultra-high peak power. We report results of theoretical and simulations studies for a hard X-ray iSASE FEL at 0.15 nm, using an LCLS-II undulator to generate X-ray pulses with peak power between 0.1 and 1 TW. The analysis is carried out using a time dependent 1-dimensional model and with GENESIS numerical simulation including 3-dimensional effects.

INTRODUCTION

The Linac Coherent Light Source (LCLS), the most powerful operating source of transversely coherent, few to hundred femtosecond pulse duration, X ray Free Electron Laser (FEL) [1], offers novel ways to study the structure and dynamics of atomic and molecular system. LCLS could become even more useful by increasing its longitudinal coherence and peak power. Its line width, about 5×10^{-4}-10^{-3}, is determined by the temporal spikes [2] characteristic of the Self-Amplified Spontaneous Emission (SASE) process [3]. The peak power at saturation is limited to 30-50 GW.

Much attention has been given recently to overcome these limitations, by using seeding, self-seeding and tapered undulators [4-6]. In this paper we consider an alternative method, that we call improved SASE (iSASE), to achieve both objectives using phase and amplitude mixing between spikes.

The spiking and longitudinal coherence of an X-ray SASE FEL is limited by the radiation-electron slippage. Only electrons within one cooperation length interact through their emitted radiation field [2]. The cooperation length Lc, is related to the power gain length L_G by the relationship $Lc = 2L_G\ \lambda/\lambda u$, where λ and λu are the radiation wavelength and the undulator period. The length of each spike is of the order of Lc. An electron bunch shorter than the cooperation length generates a transform limited X-ray pulse [9]. The FEL bandwidth for a longer bunch is determined by the single spike length and is larger than the transform limit.

In this paper we study a method to effectively increase the cooperation length using an iSASE FEL. The concept is to introduce in the FEL undulator, divided in modules separated by a break, additional slippage (i.e. localized shifts of the electron bunch respect to the radiation field) by repeated delays of the electron beam respect to the radiation field. The shifts are introduced with small magnetic chicanes at the end of each module, as in Fig. 1.

A delay of the order of the cooperation length introduces a correlation between the electromagnetic field phases and amplitudes of the spikes, in effect increasing the slippage length and the longitudinal coherence. The most important parameters in the mixing process are the electron delay, δ, the cooperation length Lc, the number of delays introduced and the gain in each module. This concept has been studied before, in one case to increase the FEL power output [10], in another case to introduce mode locking in the radiation field [11] or improve its temporal coherence [12].

This paper extends the previous work to include 3-dimensional effects, a more general sequence of delays to minimize the line width, and using a tapered undulator to increase the peak power. We show that a choice of delays increasing geometrically along the undulator can yield a line width about ten times smaller than what can be achieved by the constant delay considered in Ref. [12]. When using a tapered undulator we compare iSASE with a SASE and a self-seeded FEL. Recent work on self-seeding [7] has demonstrated the feasibility but also the limitations of this method, including expected large intensity fluctuations associated with shot to shot changes in electron beam energy and current distribution [8]. We show in this paper that iSASE is not sensitive to electron beam energy fluctuations.

THE UNIVERSAL 1-D MODEL AND BANDWIDTH REDUCTION

We use a universal 1-D model to study the dependence of the line width on the choice of the delays and of the gain of each undulator module.

*Work supported by the U.S. Department of Energy under contract DE-AC02-76SF00515
#jhwu@SLAC.Stanford.EDU

ISBN 978-3-95450-123-6

TOLERANCES FOR A SEEDED FREE ELECTRON LASER*

J. Wu#, T. O. Raubenheimer, SLAC, Menlo Park, CA 94025, USA

Abstract

Tolerance and stability are important issues for designing and operating accelerator and FEL. Jitter can come from various sources. We identify and study well-known sources as well as some particular ones, important for a seeded tapered high power FEL. Seed laser phase error, electron bunch current profile, self-seeding residual density bunching and energy modulation after the chicane, and undulator wakefield are just a few important examples.

INTRODUCTION

The Linac Coherent Light Source (LCLS), the most powerful operating source of transversely coherent, few to hundred femtosecond pulse duration, X ray Free Electron Laser (FEL) [1], offers novel ways to study the structure and dynamics of atomic and molecular system. LCLS is becoming more attractive because of the recent upgrade to have self-seeding functionality [2]. Recent work has demonstrated narrow bandwidth source in such a self-seeding scheme, but also the limitations of this method, including expected large intensity fluctuations associated with shot-to-shot changes in electron beam energy and current distribution [3]. How to overcome these issues become critical. In fact, tolerance and stability are important in general for designing and operating accelerator and FEL due to various jitter sources in such complicated systems. Here we discuss well-known sources as well as some particular ones, important for a seeded tapered high power FEL.

For a Seeded FEL (SFEL), one has to study the imperfectness of the seed laser and how it affects the FEL performance. For this regard, we look at seed laser imperfection in its chirp, curvature, and modulation. In fact, the electron bunch can also have energy chirp, curvature, and modulation which are seen in start-to-end simulation. Due to the accelerator system jitter, *e.g.*, RF jitter and compressor jitter, the electron bunch properties will jitter in energy, the pulse duration, and current profile. Besides these bunch global properties, the electron bunch slice properties also varies from slice to slice, which will affect the phase coherence in a SFEL, and therefore, affect the SFEL intrinsic bandwidth. For a self-seeding FEL (SSFEL), some additional issues can be important, *e.g.*, the temporal and spatial overlap of the seed and the electron bunch at the beginning of the second undulator. Furthermore, the by-pass chicane can greatly smear out the density microbunching generated from the SASE process in the SASE FEL, yet, it normally does not smear out the residual energy modulation along the electron bunch. Such residual energy modulation will be further converted into density modulation due to the R_{56} in the by-pass chicane and the R_{56} in the SFEL undulator. These effects from the residual modulation call for a scheme to use a fresh bunch in the SFEL undulator. Using a dominant coherent seed with large signal-to-noise ratio, the SFEL undulator can be tapered after the exponential growth saturation point to further amplify the FEL to high power at the terawatts (TW)-level. However, such a high tapered undulator system requires a stable electron bunch both in the centroid energy and the current profile. Jitter in accelerating phase can largely affect the tapered FEL performance; hence tolerance on the jitter becomes very stringent.

*Work supported by the U.S. Department of Energy under contract DE-AC02-76SF00515

#jhwu@SLAC.Stanford.EDU

EFFECTS OF VARIOUS IMPERFECTNESS AND JITTER

In the following, we discuss more details, which should be studied to budget the tolerance of a SFEL. The simulation is done with three codes: *GENESIS* [4] for the FEL simulation, *IMPACT-T* [5] for the injector dynamics and *elegant* [6] for the LINAC beam dynamics.

Seed Laser Imperfectness

In a SFEL, the undulator strength jitter or the electron centroid energy jitter will translate into amplification efficiency of the seed, if the seed is perfect as shown in Fig. 1, where the undulator parameter variation is $\Delta a_w/a_w$ = ±5E-04. Thinking this as the variation in electron centroid energy, we are essentially seeing the well-known detuning theory.

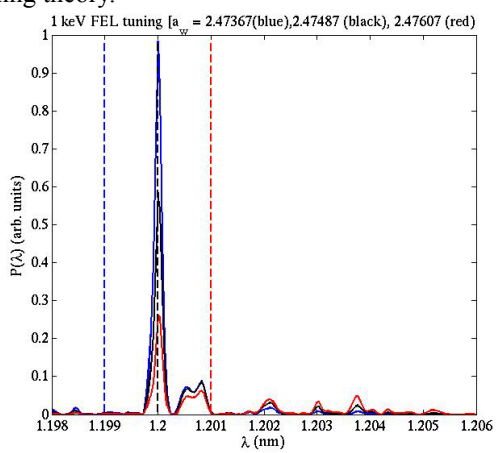

Figure 1: A SFEL subject to a variation of a_w: $\Delta a_w/a_w$ = 5E-04 (red), 0 (black), and -5E-04 (blue).

In contrast to a perfect seed with a bandwidth narrower than the FEL amplification bandwidth, if the seed has a chirp of 0.1 % over the seed duration, the effective bandwidth of the seed is now wide enough as compared with the FEL amplification bandwidth in our example. In this case, rather than what is predicted by the detuning theory, *i.e.*, the SFEL wavelength is fixed, the amplification frequency peak can be no longer at the seed

ISBN 978-3-95450-123-6

STATUS OF POLARIZATION CONTROL EXPERIMENT AT SHANGHAI DEEP ULTRAVIOLET FREE ELECTRON LASER*

Haixiao Deng#, Tong Zhang, Lie Feng, Bo Liu, Jianhui Chen, Zhimin Dai, Yong Fan, Chao Feng, Yongzhou He, Taihe Lan, Dong Wang, Xingtao Wang, Zhishan Wang, Jidong Zhang, Meng Zhang, Miao Zhang, Zhentang Zhao, SINAP, Shanghai 201204, China
Lin Song, BUAA, Beijing100191, China

Abstract

A polarization control experiment by utilizing a pair of crossed undulators has been proposed for the Shanghai deep ultraviolet free electron laser test facility. Numerical simulations indicate that, with the electromagnetic phase-shifter located between the two crossed planar undulators, fully coherent radiation with 100 nJ order pulse energy, 5 picoseconds pulse length and circular polarization degree above 90% could be generated. The physical design study and the preparation status of the experiment are presented in the paper.

INTRODUCTION

With the rapid development of accelerators and other related techniques, scientists now have the ability to investigate into realms with much smaller and faster scale, especially thanks to the great success of x-ray FEL light sources, LCLS [1] and SACLA [2]. On the other hand, in order to study the regime such as electron spins, bonding dynamics and the valence charge [3] etc., the light sources with controllable polarization is necessary. Taking the great advantages of FEL, scientists can obtain the light sources with both powerful and polarization controllable coherent radiations within the full spectral regime from far infrared to the hard x-ray. Conventionally, polarization controllable light can be directly made from the helical undulators, e.g. APPLE-type [4], at the 3rd synchrotron radiation light sources [5]. However, it is quite difficult to achieve fast helicity switching by the abovementioned approach.

One possible solution for fast helicity switching is the technique of crossed planar undulators [6]. The so called crossed planar undulators are a pair of planar undulators with the orthogonal magnetic orientation, thus providing a combined radiation with various polarization. The crossed undulators have been successfully utilized to generate the circularly polarized radiation at storage ring-based FELs [7, 8], and was proposed at high-gain FELs [9-14].

In the following sections, we report the recent progress of the polarization control FEL experiments proposed at Shanghai deep ultraviolet free electron laser (SDUV-FEL) test facility, both the physical designs and the hardware status will be covered.

PHYSICAL DESIGN AND SIMULATION

The SDUV-FEL is a versatile test bed, well suited for testing novel FEL principles [15]. Up to now, various great successes have been achieved on this machine experimentally, including SASE [16], HGHG saturation [17] and first lasing of EEHG [18]. In order to carrying out the FEL polarization control experiment, actually a proof-of-principle experiment for the future x-ray FEL, a few hardware modifications have to be performed.

The schematic layout of the FEL polarization control experiment at SDUV-FEL is shown in Figure 1 [19], from which, a pair of planar undulators with crossed magnetic orientation and phase-shifter between them can be found.

The three-dimensional start-to-end simulation has been accomplished with the codes ASTRA [20], ELEGANT [21] and GENESIS [22]. The electron beam with energy of ~136MeV interacts with the seed laser (1047 nm) in the modulator (EMU65), so as to form beam energy modulation. The dispersive Chicane-I is introduced to convert the energy modulation into longitudinal density modulation, so as to enhance the harmonic bunching (here is 523 nm, i.e. 2nd harmonic of the seed laser).

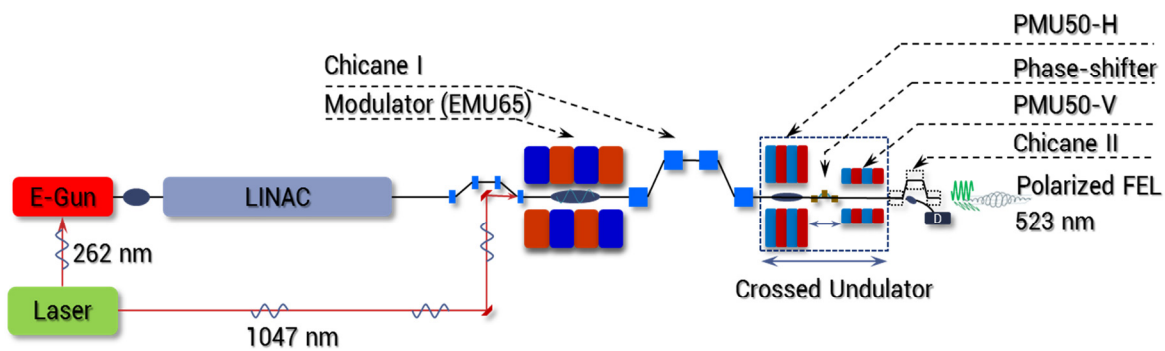

Figure 1: The schematic layout of polarization control FEL experiments at SDUV-FEL.

*Supported by NSFC (11175240) and 973 Program (2011CB808300).
#denghaixiao@sinap.ac.cn

ISBN 978-3-95450-123-6

OPTIMIZATION OF HHG SEEDING AT FLASH II

S. Ackermann*, B. Faatz, DESY, Hamburg, Germany
V. Miltchev, J. Rossbach, University of Hamburg, Hamburg, Germany

Abstract

FLASH, the **F**ree-Electron **Las**er in **H**amburg, generates coherent XUV radiation used in various research projects. In order to provide more beam time for the growing community of photon users, DESY in collaboration with HZB started the FLASH II project. FLASH II is an extension of FLASH consisting of a new undulator section (See Fig. 1) in a separate tunnel and a new experimental hall. The two FEL share the same super conducting linac. Due to the fixed gap undulators used in the present FLASH setup the FEL-wavelength can be changed only by changing the electron energy. FLASH II, in contrast, will benefit from variable gap undulators which will allow to have largely independent radiation wavelength.

In the range of 10 nm to 40 nm a direct HHG seeding option is foreseen to improve the FEL radiation quality. For experiments it is important to have the saturation point of the FEL radiation at a constant longitudinal position, close to the end of the undulator. On the other hand, one would like to keep the waist of the HHG seed at a fixed longitudinal position, too, for all wavelengths. In this paper, we present an optimized configuration of the undulator gaps, assuming fixed positions for both, the HHG seed waist and the FEL radiation saturation point.

INTRODUCTION

The free-electron laser FLASH [1],[2] consists of a photocathode RF gun followed by a superconducting linac, which delivers a maximum electron energy of 1.25 GeV. The linac is followed by 27 m of fixed-gap undulators. The FEL operates in the SASE mode, producing FEL radiation with a wavelength down to 4.12 nm, corresponding to the maximum electron energy. Since FLASH can only deliver SASE radiation to a single experiment at a time, DESY and HZB proposed the FLASH II project - a second undulator branch driven by the same superconducting accelerator modules (see Fig. 1) [3].

The FLASH II project

For FLASH1 and FLASH2 (the two beamlines of the FLASH II facility) two different photocathode lasers will be used to produce two bunch trains within the same RF pulse, which consist of two temporally separated flat tops, one for each bunch train. Therefore the bunch trains will experience different acceleration gradients and phases allowing to independently tune the charge, beam energy and compression for each bunch train. A set of kicker magnets combined with a septum, downstream the last acceleration module, will extract one of the bunch trains to FLASH2 [4]. After a matching section the electrons enter the FLASH2 undulator beam line, consisting of 12 variable gap undulators installed in a FODO lattice. The current status of the project will be presented in [5], additional information can be found in [6].

Seeding option

For wavelength range between 10 nm and 40 nm a direct high-harmonic generation (HHG) seeding option is foreseen. A novel gas jet target has been developed for the seed source [7]. Alternatively, for the longer wavelengths, a target similar to the one of the sFLASH experiment (where seeding at 38.1 nm has already been demonstrated [8]) can be used. In order to reduce the overall number of mirrors and therefore the technical complexity of the HHG seed injection beam line, it is desirable to keep the seed waist position fixed. According to zemax calculations for the HHG setup at FLASH2, this point is inside the third undulator.

Photon user requirements

The photon users have to image the saturation point of the radiation to the respective target. The position of the saturation point depends among others on the FEL gain length and wavelength. The required effective undulator length increases with the decreasing wavelength. For SASE one can open undulators upstream such that the required saturation length is achieved. If the position of the source point (the onset of the FEL saturation) is kept at a fixed position, then from the users side focus adjustments will not be needed.

NUMERICAL SIMULATIONS

Goal

The goal of the numerical studies is to determine the optimal undulator configuration (gaps closed or opened), while keeping the HHG seed waist and FEL saturation point position fixed.

Undulator and simulation setup

The individual simulations were performed using the full 3D FEL simulation code `GENESIS 1.3` [9]. The FLASH2 undulator section consists of 12 variable gap undulators. The undulator parameters are given in Table 1. For seeding, only the undulator modules #3 through #12 are used. The position of the waist of the HHG beam is located inside undulator module #3. It is assumed that the gap of this undulator is always closed as the interaction of the seed and the electron beam takes place here. It has been also assumed that undulator gap #12 is always closed since the saturation

* sven.ackermann@desy.de

ISBN 978-3-95450-123-6

EXTENSION OF SELF-SEEDING TO HARD X-RAYS > 10 keV AS A WAY TO INCREASE USER ACCESS AT THE EUROPEAN XFEL

G. Geloni, European XFEL GmbH, Hamburg, Germany
V. Kocharyan, E. Saldin, DESY, Hamburg, Germany

Abstract

We propose to use a self-seeding scheme with single crystal monochromator at the European X-ray FEL to produce monochromatic, high-power radiation at 16 keV. The FEL power of the transform-limited pulses can reach about 100 GW by exploiting tapering in the tunable-gap baseline undulator. The combination of high photon energy, high peak power, and very narrow bandwidth opens a new range of applications, and allows to increase the user capacity and exploit the high repetition rate of the European XFEL. Dealing with monochromatic hard X-ray radiation one may use crystals as deflectors with minimum beam loss. To this end, a photon beam distribution system based on the use of crystals in the Bragg reflection geometry is proposed for future study and possible extension of the baseline facility. They can be repeated a number of times to form an almost complete (one meter scale) ring with an angle of 20 degrees between two neighboring lines. The reflectivity of crystal deflectors can be switched fast enough by flipping the crystals with piezo-electric devices. It is then possible to distribute monochromatic hard X-rays among 10 independent instruments. More details can be found in [1].

INTRODUCTION

Radiation from SASE XFEL consists of many independent spikes in both the temporal and spectral domains. Self-seeding is a promising approach to significantly narrow the SASE bandwidth to produce nearly transform-limited pulses [2]-[16]. We discussed the implementation of a single-crystal self-seeding scheme in the hard X-ray lines of European XFEL in [17, 18]. For this facility, transform-limited pulses are particularly valuable, since they naturally support the extraction of more FEL power than at saturation by exploiting tapering in the tunable-gap baseline undulators [19]-[26]. Tapering is implemented as a stepwise change of the undulator gap from segment to segment. Simulation results presented in [17, 18] show that the FEL power of the transform-limited X-ray pulses may be increased up to 0.4 TW by operating with the tapered baseline undulator SASE1 (or SASE2). In particular, it is possible to create a source capable of delivering fully-coherent, 7 fs (FWHM)-long X-ray pulses with $2 \cdot 10^{12}$ photons per pulse at a wavelength of 0.15 nm, Fig. 1.

We can apply the same scheme to harder X-rays, and obtain 100 GW fully-coherent X-ray pulses at a wavelength of 0.075 nm. In this paper we propose to perform monochromatization at 0.15 nm with the help of self-seeding, and amplify the seed in a first part of the output undulator. The amplification process can be stopped at some position well before the FEL reaches saturation, where the electron beam gets considerable bunching at the 2nd harmonic of the coherent radiation. A second part of the output undulator tuned to the 2nd harmonic frequency, follows beginning at that position, and is used to obtain 2nd harmonic radiation at saturation. One can prolong the exchange of energy to the advantage of the photon beam by tapering the last part of the output undulator on a segment by segment basis. Fig. 2 shows the design principle of our self-seeding setup for harder photon energy mode of operation. Two self-seeding cascades, identical to those considered in [17, 18] (see Fig. 1), are followed by the same output undulator with changed gap configuration, compared to Fig. 1.

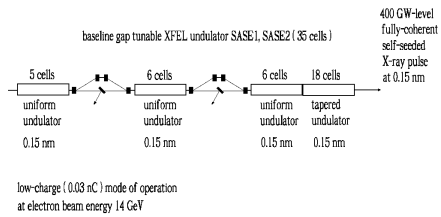

Figure 1: Sketch of an undulator system for high power mode of operation at a photon energy of 8 keV.

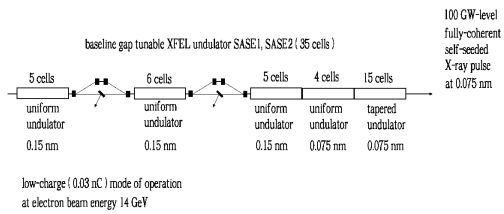

Figure 2: Generating high power, highly monochromatic hard X-ray beam at a photon energy of 16 keV.

An advantage of the proposed scheme is the possibility to increase user capacity. In this paper we describe a photon beam distribution system, which may allow to switch the hard X-ray beam quickly among many experiments in order to make a more effective use of the facility. Monochromaticity is the key for implementing multi-user operation in the hard X-ray range, which can be granted by using crystal deflectors and small absorption of the radiation in crystals at photon energies larger than 15 keV. In contrast

ISBN 978-3-95450-123-6

PROGRESS TOWARDS HGHG AND EEHG SEEDING AT FLASH

Kirsten Hacker, Robert Molo, Shaukat Khan, Technische Universitaet Dortmund, Germany
Christopher Behrens, Holger Schlarb, DESY Hamburg, Germany
Peter Van der Meulen, Peter Salen, Stockholm University, Sweden
Joern Boedewadt, Armin Azima, University of Hamburg, Germany
Gergana Angelova Hamberg, Volker Ziemann, Uppsala University, Sweden

Abstract

Using the undulators and chicanes developed for an Optical Replica Synthesizer (ORS) experiment together with the sFLASH 800 nm seed laser, undulators and diagnostics, a High Gain Harmonic Generation (HGHG) seeding experiment will be conducted at the Free-Electron LASer in Hamburg (FLASH) starting in September 2012. For this experiment, a 30 mJ 160 fs FWHM 800 nm laser pulse has been transported with a new, evacuated laser transport line. On an in-vacuum optical breadboard, the laser frequency was tripled through second and third harmonic generation in beta-BBO crystals. Longitudinal and transverse overlap with the electron beam has been achieved through streak camera and Ce-YAG screen diagnostics. Once the HGHG seeding has been established, a shutdown period in early 2013 will be used to add a UV-TG FROG diagnostic for seed laser characterization. An additional alpha BBO crystal will be installed in order to split the 270 nm beam longitudinally into two pulses with orthogonal polarization states corresponding to the orthogonal orientations of the ORS undulators, setting the stage for Echo-Enabled Harmonic Generation (EEHG) seeding experiments in 2013.

INTRODUCTION

High Gain Harmonic Generation (HGHG) seeding has been successfully demonstrated by several facilities [1-3] and has been used to deliver fully coherent FEL pulses with wavelengths ranging from 20-50 nm to users at the ELLETRA facility in Trieste since 2010 [4]. At FLASH, a new 270 nm laser transport line has recently been added to the existing sFLASH seeding infrastructure [5-9] in order enable similar HGHG seeding experiments in the sFLASH section.

First overlap between seed and electron bunch was achieved in June 2012 and first seeding is expected during shifts scheduled for September-November 2012. After learning from the sensitivity of HGHG seeding to laser and chicane parameters, we plan to upgrade the laser setup during a shutdown in early 2013 to begin Echo-Enabled Harmonic Generation (EEHG) seeding experiments at 14 nm. This constitutes an attempt at external seeding in a wavelength range which is shorter than what has been achieved by any facility to date.

EEHG is a technique which was proposed in 2008 [10, 11] that calls for the co-propagation of an electron bunch and laser pulse through a series of three undulators and two chicanes (Fig. 1). Through interaction with a seed laser, the electron beam develops an energy modulation in the first undulator which is then over-compressed in the first chicane. The electron bunch is then modulated again in the second undulator by another laser pulse and compressed in the second chicane, resulting in vertical stripes of charge in longitudinal phase space with a periodicity of a mixture of seed laser harmonics.

EEHG schemes have been proposed for several seeded FELs [12-14] and two experiments have been able to generate low harmonics of the seed laser wavelength [15,16]. These EEHG schemes all call for a large R_{56} (1-10 mm) in the first chicane. With the first Optical Replica Synthesizer (ORS) chicane at FLASH [17], one can achieve a maximum R_{56} of 0.7 mm and while this is somewhat small compared to other proposed schemes [12-14], the amount of laser power available in this section is large, enabling EEHG for seeding wavelengths between 10 and 30 nm.

If seeding at 14 nm is successful, using the beam to seed at the 3rd harmonic in the subsequent SASE undulator section would be a natural next step. This would potentially produce fully coherent 4.7 nm radiation for users (Fig. 1).

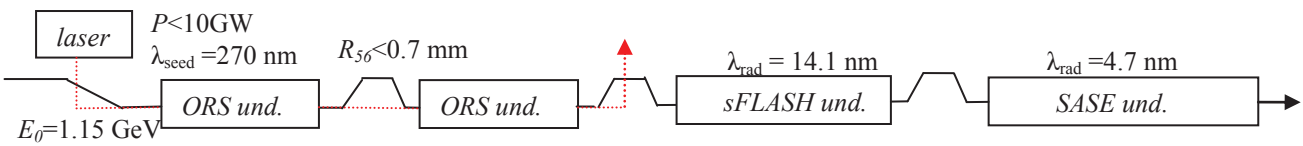

Figure 1: The FLASH I ORS section is located directly prior to the sFLASH undulators. The sFLASH undulators are followed by a small chicane and the "SASE" undulators. Using EEHG to seed the sFLASH undulator section with 14 nm could enable an HGHG scheme at 1.15 GeV to seed the SASE undulator section with 4.7 nm. The laser, diagnostics, chicanes, and undulators are already commissioned.

ISBN 978-3-95450-123-6

OPTICAL REPLICA SYNTHESIZER TO BE RECOMMISSIONED WITH 270 nm SEED AT FLASH

Kirsten Hacker*, Robert Molo, Shaukat Khan, Technische Universitaet Dortmund, Germany
Peter Salen, Peter Van der Meulen, Stockholm University, Sweden
Gergana Angelova Hamberg, Volker Ziemann, Uppsala University, Sweden

Abstract

An Optical Replica Synthesizer (ORS) was commissioned at the Free Electron LASer in Hamburg, FLASH, in 2008 using an 800 nm seed. The experiment was affected by radiation from unwanted microbunches which were generated upstream of the experiment. Given new, 270 nm seeding infrastructure and the understanding that microbunches with separations smaller than 600 nm can effectively be smeared out in the dogleg of the machine, the experiment will be attempted again with this new wavelength. The new, 270 nm laser has been successfully overlapped with the electron beam in July 2012 and a measurement of the pulse energy which can be radiated in an optical replica will follow. The UV-TG-FROG diagnostic which will be used to measure the longitudinal profile of the optical replica has been delivered and is undergoing tests in a laser lab. Following these tests, it will be installed in the FLASH tunnel for the ORS experiments in 2013.

INTRODUCTION

Characterization of the relativistic and ultra-short electron bunches of a linac-based free electron laser (FEL) is important for machine operation. This need has triggered the development of several successful methods for measuring the longitudinal profile of the electron bunch, including the transverse deflecting cavity [1], electro-optical sampling [2], and single-shot THz spectrometer [3]. A different method for electron bunch characterization, called Optical Replica Synthesizer (ORS), was proposed in 2005 [4] and first attempted at the Free Electron LASer in Hamburg, FLASH, in 2008 [5].

The ORS technique, depicted in Fig. 1, uses an external laser to produce seed pulses which interact with the electrons in an undulator, thereby modulating the energy of the electrons in a sinusoidal fashion. The energy modulation is transformed into a density modulation of the electrons in the following chicane. When the beam then traverses the undulator located downstream of this chicane, it radiates coherently and the emitted light pulse will have the same longitudinal profile as the electron beam; it is called the optical replica. The replica pulse and seed pulse are then extracted from the vacuum pipe by a mirror and directed onto an optical table where a polarizer can be used to separate the seed from the replica. This is facilitated by making the first planar undulator orthogonal to the second. The spectrum and spectral phase of the replica pulse can then be measured by a FROG (Frequency Resolved Optical Gating) device. This measurement directly gives the longitudinal profile of the electron bunch with a resolution that is ultimately limited by the slippage of the laser over the electron bunch as they co-propagate through a 5 period undulator with a period length of 20 cm. For our seed wavelength of 270 nm, this resolution limitation is around 5 fs, but practical considerations related to measuring extremely short laser pulses would likely limit the resolution of the measurement before the slippage plays a role.

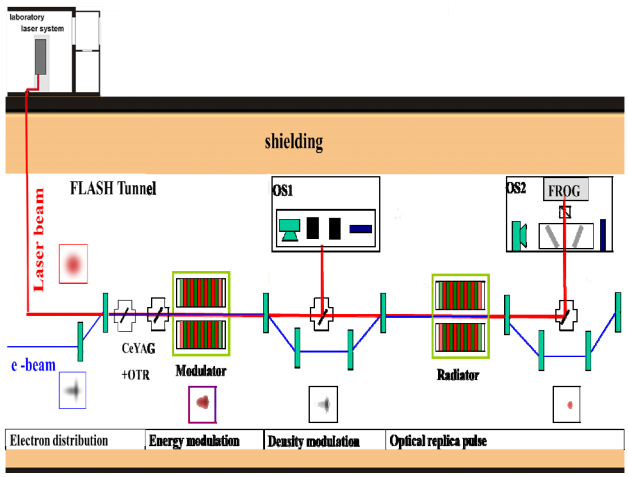

Figure 1: ORS infrastructure. The beam energy is modulated by a laser pulse in the first undulator, bunched in the first chicane, and the optical replica is radiated in the second undulator with a polarization which is orthogonal to the seed laser pulse. The replica and the seed laser are then outcoupled in the second chicane and separated with a polarizer. The spectrum and spectral phase of the replica are measured with a FROG, thereby giving a measurement of the longitudinal profile of the electron beam.

The first attempt at demonstration of the ORS technique was conducted at FLASH in 2008 with an 800 nm seed [5] and for fully compressed bunches with several kA of peak current. It was affected by unwanted radiation from microbunches which were not generated through the interaction with the laser seed. This radiation produced a background to the optical replica signal and was not easy to filter out. These undesired microbunches have a broadband spectrum and are created/amplified by coherent synchrotron radiation in the upstream bunch

*kirsten.hacker@desy.de

ISBN 978-3-95450-123-6

SEEDED COHERENT HARMONIC GENERATION WITH IN-LINE GAS TARGET

F. Curbis*, N. Cutic, O. Karlberg, F. Lindau, E. Mansten, S. Thorin, S. Werin,
MAX IV laboratory, Lund University, Sweden
F. Brizuela, B. Kim, D. Kroon, A. L'Huillier, Lund University, Division of Atomic Physics
M. Gisselbrecht, Lund University, Div. of Synchrotron Radiation Research Department of Physics

Abstract

The test-FEL at MAX-lab already demonstrated seeded coherent harmonic generation down to 40 nm [1]. As a step further in the development of our seeding techniques, we plan to use a gas target to generate harmonics of the drive laser and seed the electron beam with them. In order to optimize the injection process, our aim is to place the gas target for harmonic generation as close as possible to the first undulator. In order to minimize the losses the transport of the drive laser is done with a minimal number of mirrors and there are neither focusing nor filtering elements between the harmonic chamber and the first undulator. The goal is to test whether the harmonic intensity in the undulator is high enough to induce full energy modulation of the electron beam. The wavelength range of the harmonics that will be used as seed is around 100 nm and we plan to detect the coherent harmonic signal of the second harmonic generated in the radiator. The flexibility of the setup will allow us to drive the harmonic generation process with the fundamental wavelength of the laser or the second harmonic or the combination of them. Adding the second harmonic will lead to the generation of even harmonics, thus increasing the range of seeding wavelength.

INTRODUCTION

Due to the increasing interest in seeding at short wavelengths and in the optimization of the injection process, we plan to implement a new configuration for seeding with harmonics generated in a gas target. The basic setup is borrowed from the test-FEL at MAX-lab, which already demonstrated seeded coherent harmonic generation (CHG) and variable polarization down to 40 nm [1]. Since our aim is to minimize the losses in the transport and focusing, the gas target for high-order harmonic generation (HHG) will be placed directly in front of the first undulator. Preliminary analytical estimations indicate that the co-propagation of the electrons with the drive laser and the harmonics should not degrade the quality of the electron beam. We expect to imprint full energy modulation to the electron beam which will lead to produce bunching at the fundamental wavelength and its higher harmonics. This can be demonstrated detecting the coherent harmonic signal of the second harmonic generated in the radiator. The whole setup is very flexible and it makes possible to drive the HHG process also with a combination of the fundamental wavelength and second harmonic, which opens to a better wavelength tunability.

* francesca.curbis@maxlab.lu.se

EXPERIMENTAL SETUP

The Test-FEL at MAX-lab

The test-FEL utilizes the injector for the MAX-lab rings and consists of two linac structures plus a recirculator that allows to reach almost 400 MeV after the second passage of the electron beam through the linacs (see Fig. 1). The thermionic gun is used as photocathode gun [3], with the heating almost turned off and the BaO cathode is illuminated by the second harmonic of a Ti:Sa laser. The bunch can be compressed mainly in the extraction chicane after the second passage through the linacs. Then a dog-leg lifts up the beam to the level where the undulators are placed.

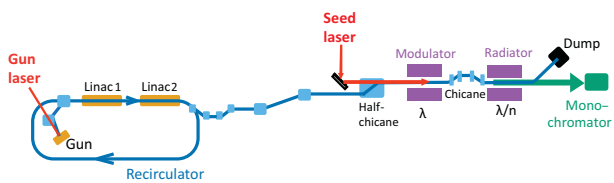

Figure 1: Layout of the experimental setup.

Before the first undulator (modulator) a half-chicane allows to insert an external laser for seeding. The second undulator (radiator) has different period length. In between the undulators a small chicane is used both for producing some bunching and for stopping the seed laser (if needed). After the second undulator the electron beam is bent to the beam dump while the radiation produced is detected by a spectrometer. More details about the setup and the undulator parameters can be found in [1, 2].

The typical parameters of the electron beam for the test-FEL operations are shown in Tab. 1.

Table 1: Electron Beam Parameters

Energy	375 MeV
Charge	40 pC
Bunch length	1 ps
Energy spread	$0.5 \cdot 10^{-3}$

ISBN 978-3-95450-123-6

SEEDING OF SPARC-FEL WITH A TUNABLE FIBRE-BASED SOURCE

N.Y. Joly, University of Erlangen-Nuremberg, Erlangen-Nuremberg, Germany
G. De Ninno, B. Mahieu, ELETTRA, Basovizza, Italy
F. Ciocci, L. Giannessi, A. Petralia, M. Quattromini, ENEA C.R. Frascati, Frascati (Roma), Italy
G. Gatti, INFN/LNF, Frascati (Roma), Italy
J.V. Rau, ISM-CNR, Rome, Italy
V. Petrillo, Istituto Nazionale di Fisica Nucleare, Milano, Italy
W. Chang, P. Hölzer, K. Mak, P. Russell, F. Tani, J.C. Travers, MPI for the Science of Light, Erlangen, Germany
S. Bielawski, PhLAM/CERCLA, Villeneuve d'Ascq Cedex, France
M.-E. Couprie, M. Labat, T. Tanikawa, SOLEIL, Gif-sur-Yvette, France

Abstract

Instead of seeding a free electron laser in the UV-VUV with a frequency doubled or tripled laser or high order harmonics, here we investigate and present the first results on seeding the SPARC-FEL with a fibre-based tunable ultraviolet source. The seed generation system consists of a kagome hollow-core photonic crystal fibre (HC-PCF) filled with noble gas. Diffraction-limited DUV pulses of > 50 nJ and fs-duration which are continuously tunable from below 200 nm to above 300 nm are generated. The process is based on soliton-effect self-compression of the pump pulse down to a few optical cycles, accompanied by the emission of a resonant dispersive wave in the DUV spectral region. The quality of the compression highly depends strongly on the pump pulse duration, and ideally, pulses < 60 fs should be used. Our experimental set-up and associated GENESIS simulations enable us to study the utility of the seed tunability, and the influence of the seed quality, on the performance of the SPARC-FEL in the 200-300 nm range.

Single-pass free-electron lasers (FELs) can be used to generate powerful short pulses at very short wavelengths. Moreover, when seeded with an appropriate pulse, the overall properties of the FEL are greatly enhanced because the temporal coherence of the seed is transferred onto the FEL output wavelength [1,2]. Pulse-to-pulse fluctuations usually present when the FEL runs in the self-amplification spontaneous-emission (SASE) regime are also reduced. In addition, in a seeded configuration, the required length of the undulator is shorter than a SASE configuration. This is an advantage when striving for a more compact source. For short wavelength FELs, seeding sources include harmonics in gas [3] or harmonics of a mode-locked Ti:sapphire (Ti:Sa) laser [4]. Here we propose a recently developed ultra-compact deep-UV laser source. This tunable source consists of a HC-PCF filled with Argon, and pumped with fs-pulses. For the conversion from the pump to the UV to be efficient, the input pulse duration should not be too long (typically < 40 fs) and for this reason it is important to adapt our device to seed the SPARC-FEL [5]. Calculations using GENESIS show possible amplification.

In HC-PCFs, light propagates in an effectively diffraction-free manner, and can then interact efficiently with any material filling the core region. Furthermore, the very broad transmission window and the ultra-low dispersion of a kagome-lattice HC-PCf make it a unique tool for controlling nonlinear effects and especially spectral broadening [6,7]. Under appropriate conditions, an input pulse can experience soliton effects and be self-compress down to a few cycles, at which point it emits a resonant dispersive wave at a phase-matched wavelength in the UV spectral range [7,8]. The ultra-low dispersion of the fibre can be tuned through the gas pressure. Varying the filling pressure allows the tuning of the phase-matching conditions [9], and therefore the wavelength of the generated band. Tunability from < 200 nm to 320 nm with argon-filled fibre is possible (Fig.1d). More important, the UV band emerges in a single-lobed mode. To generated UV-light efficiently, we used ~20 cm of kagome HC-PCF sealed between two gas-cells (Fig.1). The fibre has a ~28 µm core diameter and low transmission loss (~1.1 dB/m at 800 nm) from 700 nm to 1.2 µm and the pressure of argon can be continuously adjusted up to 20 bar. Pumped with a 30 fs long pulse from an amplified Ti:Sa laser system, we measured a conversion efficiency of more than 8% from the pump wavelength to the UV [7].

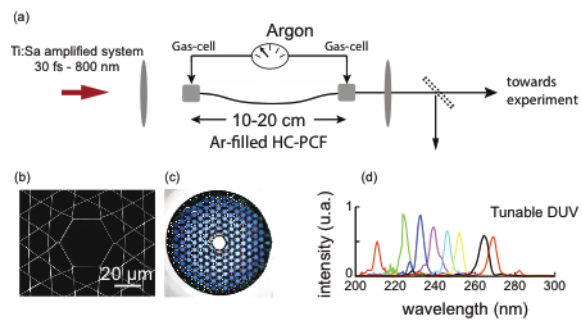

Figure 1: (a) Experimental set-up for the generation of tunable UV light. (b) A scanning electron micrograph and (c) an optical microscograph of the kagomé-fibre. (d) Tunable UV generated with various combinations of pressure/input power. Each colour corresponds to a different spectrum.

ISBN 978-3-95450-123-6

THE RADIATOR-FIRST HGHG MULTI-MHz X-RAY FEL CONCEPT

M. Reinsch*, G. Penn, LBNL, Berkeley, CA 94720, USA
P. Gandhi, J. Wurtele†, University of California, Berkeley, CA 94720, USA

Abstract

A novel configuration for a high repetition rate X-ray FEL is investigated. In this scheme longitudinally coherent FEL pulses are obtained using a high gain harmonic generation (HGHG) system in which the seed power is generated in an FEL oscillator downstream of the HGHG section. The oscillator is powered by the spent beams that leave the HGHG radiator. Radiation from the oscillator is sent to the modulator of the HGHG section. The dynamics and stability of the radiator-first scheme is explored analytically and numerically. A single-pass map is derived using a semi-analytic model for FEL gain and saturation. Iteration of the map is shown to be in good agreement with simulations. A numerical example is presented for a soft X-ray FEL in which the oscillator operates at 13.4 nm and HGHG radiation is generated at 1.34 nm. This radiator-first configuration potentially solves (i) the challenge of finding sources to seed future FELs driven by multi-MHz superconducting RF linacs and (ii) the difficulty of producing X-ray radiation with a bunch that exits an oscillator in the more "natural" configuration in which the oscillator precedes the radiator.

INTRODUCTION

Superconducting linear accelerators (sc linacs) operating in continuous wave (cw) mode have the ability to produce high quality electron beams with bunch repetition rates of MHz and above [1]. There is a strong interest in X-ray beamlines that can deliver pulses with a high average flux at a non-destructive peak flux. FEL oscillators can meet these goals and provide longitudinal coherence, but tunability and availability at specific wavelengths are limited by mirror technologies. In the soft x-ray regime, the state of the art multilayer mirrors can only be made to reflect at certain wavelengths. Many seeding schemes have also been proposed to provide longitudinal coherence and allow for tunability, but rely on high power external lasers [2] that would limit the repetition rate at which they can operate.

Wurtele, *et al.*, [3] have proposed various schemes for producing longitudinally coherent light at high repetition rates by modifying these seeding schemes to remove the need for external lasers. The underlying idea is to use the electron beam to generate the required radiation instead of using a laser. The "radiator first" scheme makes further use of the electron beam after the target radiation has been generated in order to produce the seed radiation for a harmonic generation scheme [4, 5]. Wurtele et al originally proposed this in conjuction with echo-enabled harmonic generation (EEHG) [6]; here we consider a high gain harmonic generation (HGHG) [7] scheme. The current configuration is less technically challenging in terms of hardware and requirements. It also allows for a straightforward analysis which yields useful expressions for quickly finding workable parameters, and provides insight into the operation of coupled radiator-oscillator FEL systems.

In this paper, we first provide a description of the HGHG radiator-first scheme, and then give examples of a simplified pass-to-pass map which models the evolution of this system. The dynamics predicted from this map are compared to time-independent, one-dimensional simulations for a soft x-ray case.

A MODIFIED HGHG LAYOUT

The major motivation for considering the type of scheme diagrammed in Fig. 1, as was mentioned in the introduction, is that it eliminates the need for an external seed laser. Since the electrons are doing all the work of generating the seed and target radiation, the limiting factor on the repetition rate is now the electron source and accelerator. The HGHG section is laid out as in the conventional scheme, but it is surrounded by a system for the production and transport of the modulating laser pulse, based on the electron beam after passing through the radiator. While the radiator delivers a stream of radiation pulses to the user, the electron beam coming out of the radiator is also used to drive an oscillator which is tuned to the same wavelength as the modulator. Each seed pulse has been outcoupled and transported from this oscillator during the previous pass or passes. The longitudinal coherence of the oscillator pulse should lead to longitudinal coherence of the pulse delivered to users.

Others have considered similar schemes in which the oscillator is used in place of the modulator, but only with the oscillator placed before the radiator [8, 9, 10]. This may seem like the simplest option since the combined modulator/oscillator produces its own field, but the oscillator tends to induce a large energy spread that significantly degrades the performance of the radiator. It is also difficult to prevent the beam from becoming overbunched out of the modulator at saturation. While using a transverse optical klystron configuration has been shown in simulations to help control

* mwreinsch@lbl.gov
† also at LBNL, Berkeley, CA 94720, USA

ISBN 978-3-95450-123-6

SOFT X-RAY SASE AND SELF-SEEDING STUDIES FOR A NEXT-GENERATION LIGHT SOURCE

G. Penn*, P.J. Emma, D. Prosnitz, J. Qiang, M. Reinsch, LBNL, Berkeley, CA 94720, USA

Abstract

In the self-seeding scheme, the longitudinal coherence and spectral density of an unseeded FEL can be improved by placing a monochromator at a location before the radiation reaches saturation levels, followed by a second stage of amplification. The final output pulse properties are determined by a complex combination of the monochromator properties, undulator settings, variations in the electron beam, and wakefields. We perform simulations for the output of SASE and self-seeded configurations for a soft x-ray FEL using both idealized beams and realistic beams from start-to-end simulations.

INTRODUCTION

The longitudinal coherence and spectral density of a SASE FEL can be improved without using an external seed by introducing a monochromator in the middle of the undulator beamline [1]. The narrow bandwidth selected by the monochromator will act as a seed in the following undulators, leading to a final bandwidth that can be much narrower than the original SASE bandwidth. A hard X-ray version of such a device [2] has been implemented and tested at LCLS [3]. A soft X-ray self-seeding beamline is currently under development for implementation at LCLS as well [4]. Here, simulations of a soft x-ray self-seeded beamline are presented using a beam tracked from an RF injector through a superconducting (SC) linac.

SELF-SEEDING SCHEME

The self-seeding scheme, shown in Fig. 1, breaks the SASE configuration into two parts, with a monochromator and chicane in between. The noisy SASE bunching is eliminated by the chicane, and the monochromator selects a narrow bandwidth to seed the second stage. The monochromator should be roughly in the middle of the undulator length, constrained to be far enough downstream so that enough power gets through the monochromator to overcome shot noise, but not too far that the increased energy spread of the beam entering the second stage seriously degrades the FEL performance. To reach saturation, the total undulator length must be increased from that of a SASE beamline by enough to compensate for the following effects: the reduction in radiation power due to both the narrower bandwidth; losses or mismatch in the radiation transport; an effective loss in power by a factor of roughly 9 as some of the radiation field couples to FEL modes which do not get amplified; and the increased gain length in the second stage due to the increase in energy spread. For a monochromator with a bandwidth selection of around 20 meV, for a relative bandwidth of a few times 10^{-5}, and a 10% transport efficiency in this bandwidth, an extra 5 undulator sections (16 m of undulator) are required. Overall, there is a factor of almost 10^4 in power amplification, which corresponds to around 9 gain lengths, that must be added to the FEL beamline.

Only planar undulators are considered; polarization control can be obtained through the use of cross-planar undulators at the very end of the beamline [5]. The current design places two such undulator sections at the end of the beamline for maximum flexibility. The possibility of additional undulators are added to the beginning and end of the beamline to account for expected imperfections, such as undulator field errors and steering errors which are allowed a budget of a 10% increase in gain length, and unknown effects which may degrade the electron beam quality or the efficiency of the monochromator.

BEAMLINE PARAMETERS

The nominal parameters and those obtain in full start-to-end (S2E) simulations starting from the injector [6] and passing through a SC linac [7] are shown in Table 1. However, the beamlines are designed to be able to handle a worse beam emittance, of up to 0.9 μm, as well as an energy spread of 150 keV. The energy spread is adjustable by the use of a laser heater [8], to damp out microbunching instabilities.

Table 1: Electron beam parameters, both original nominal parameters and results from S2E simulations. Except for bunch charge, parameters correspond to typical values in the core region of the bunch.

	Nominal	S2E core
Bunch charge	300 pC	300 pC
Electron energy	2.4 GeV	2.4 GeV
Slice energy spread	100 keV	90 keV
Slice transverse emittance	0.60 μm	0.75 μm
Peak current	600 A	450 A

The beamline is designed to cover the range in photon energies from 270 eV (just below the Carbon K-edge) up to 1.24 keV. We focus on undulators using superconducting (SC) technology with relatively short undulator period, to provide the full tuning range with reasonably large (not much smaller than unity) dimensionless undulator parameter at the highest photon energy. SC undulators have the advantage of being able to produce higher magnetic fields for a larger gap, especially for undulator periods shorter

* gepenn@lbl.gov

ISBN 978-3-95450-123-6

SELF-SEEDING DESIGN FOR SwissFEL

E. Prat, S. Reiche, PSI, Villigen, Switzerland
D.J. Dunning, ASTeC, STFC Daresbury Laboratory, United Kingdom

Abstract

The SwissFEL facility, planned at the Paul Scherrer Institute, is based on the SASE operation of a hard (1-7 Å) and soft (7-70 Å) X-ray FEL beamline. In addition, seeding is foreseen for the soft X-ray beamline (down to a wavelength of 10 Å), and it is currently also under consideration for the hard X-ray beamline. We have investigated two methods, Echo-Enabled Harmonic Generation (EEHG) and self-seeding for each of the two FEL beamlines. Presently we consider self-seeding the most robust and lowest risk strategy for both lines. The paper discusses our considerations and presents the design of self-seeding implementation for the soft and the hard X-ray beamlines including the layout and simulation results.

INTRODUCTION

Seeding for FELs has several advantages in comparison to SASE radiation: the longitudinal coherence is increased and therefore the FEL brilliance is improved, the pulse to pulse spectral stability is increased, the temporal pulse shape is improved, etc. Operation of a seeded soft X-ray beamline is planned at SwissFEL for 2018 down to a wavelength of 1 nm [1], and it is presently also under investigation for the hard X-ray beamline.

Echo-Enabled Harmonic Generation (EEHG) [2] has been considered until recently the first choice for seeding at the soft X-ray beamline of SwissFEL, based on successful demonstration for wavelengths of hundred nanometers [3, 4] and the potential to produce high bunching directly at 1 nm. A design of seeding based on EEHG for the soft X-ray beamline of SwissFEL was presented one year ago at this conference [5]. We considered some effects like ISR/CSR that limit the EEHG performance at short wavelengths (i.e. below 5 nm). However, other effects such as the transport of the fine EEHG structures through the magnetic lattice or intra-beam scattering [6] limit even more the EEHG performance and make it very difficult and risky to work at 1 nm.

Self-seeding [7] is currently the only seeding scheme that does not exhibit stringent "short wavelength" limitations, like all the other "laser-based" approaches do, therefore being the most robust and lowest risk strategy to seed a soft X-ray [8]. The classical self-seeding proposals had a long monochromator section (of about 20-25 m) and a complicated electron beam line with many quadrupoles and sextupole magnets. Recently a compact design with reduced resolution within less than 4 m has been proposed [9], making this option much more feasible and realistic. As a consequence we consider self-seeding as the first option for seeding the soft X-ray beamline of SwissFEL.

Self-seeding is also a strategy, so far the only one, which allows to seed a hard X-ray FEL [10, 11]. A proof-of-principle experiment of the self-seeding scheme based on the proposal of Geloni et al [11] was successfully carried out at LCLS for hard X-rays at the beginning of this year [12]. Therefore we are also considering implementing the self-seeding scheme in the hard X-ray beamline of SwissFEL.

Self-seeding uses the SASE-FEL radiation output to provide an at-wavelength seed signal within the FEL beamline. Figure 1 shows a generic layout of the self-seeding scheme for soft and hard X-rays. The first undulator stage generates normal SASE-FEL radiation. After that the FEL radiation goes through a monochromator, while the electron beam travels through a magnetic chicane. Finally in the second undulator stage the transmitted "short-bandwidth" radiation overlaps with the electron beam to produce seeded-FEL radiation. Apart from separating the electron beam from the radiation, the chicane delays the electron to allow the longitudinal overlap between the electrons and the photons, and smears out the electron bunching created at the first undulator section to eliminate the SASE information imprinted in the electron bunch. The first undulator stage works in the exponential regime before saturation to avoid a blow-up of the energy spread of the electron beam that would prevent the beam to amplify the FEL signal in the second stage. At the same time it has to provide enough radiation so that at the second undulator stage the seed power is well above the shot-noise level.

The difference between the hard and the soft X-ray is the monochromator. For soft X-rays a grating monochromator can be used, while for hard X-rays a crystal (e.g. diamond crystal) is used. For both cases the intersection with the monochromator (grating or crystal) and the chicane can be placed in a section of about 4 m, i.e. roughly the space occupied by a typical undulator module.

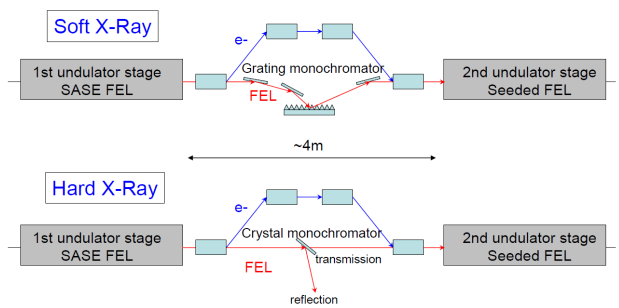

Figure 1: Generic layout of the self-seeding scheme for soft and hard X-rays.

ISBN 978-3-95450-123-6

GENERATING MULTIPLE SUPERRADIANCE PULSES IN A SLIPPAGE-DOMINANT FREE-ELECTRON LASER AMPLIFIER

X. Yang, Y. Shen,
National Synchrotron Light Source, Brookhaven National Laboratory, Upton, NY 11973, USA

Abstract

We report the first numerical demonstration of the generation of multiple superradiance pulses in a slippage-dominant free-electron laser amplifier. In this simulation, the 1st and 2nd multiple radiation-pulses are created from the deformation of the longitudinal phase space. Our simulation confirmed controllability over the temporal profile of these pulses, and paves the way for applying this technique, such as generating multiple pulses for slippage-dominant laser-seeded FELs.

INTRODUCTION

The free-electron laser (FEL) is a tunable source of coherent radiation, ranging from terahertz (THz) waves to hard X-rays, with the capability for femtosecond time-resolution. Progress was made recently in single-pass FELs in moving toward the X-ray region of the spectrum, such as the self-amplified spontaneous emission (SASE) FEL that successfully lased from soft X-rays down to 1.5Å [1,2], the laser-seeded FEL amplifier [3], and the high-gain harmonic generation (HGHG) FEL [4] that emitted radiation in the deep ultraviolet (DUV), i.e., below 300nm. One of the main advantages of the HGHG and laser-seeded FEL over the SASE FEL is that they produce temporally as well as transversely coherent pulses. In contrast, SASE radiation starts from the initial shot-noise of the electron beam, so that the resulting radiation exhibits excellent spatial but a rather poor temporal coherence.

In this report, we present numerical evidence for a new slippage-dominant superradiance FEL interaction regime, wherein the emitted FEL pulse is followed by multiple pulses, which we dubbed a "multi-pulse regime". This dynamic behavior occurs in seeded FELs where the duration of the seed pulse is short; it may be important for next-generation short-wavelength-seeded FELs, such as FERMI [5], and LCLS-II [6]. Understanding control of these regimes is essential for optimizing the power and quality of the FEL sources, features demanded by the user communities. Using the Perseo simulation [7], we investigated the behavior of the seeded FEL, and obtained new insights on multiple-pulse generation that we interpreted in terms of the deformation of the longitudinal phase space (LPS) and the formation of new buckets. Here, the term "bucket" denotes the electric field of an optical pulse that assures longitudinal focusing, thereby constraining the electron's motion to a stable region in the LPS.

The mechanism of FEL amplification commonly is analyzed in three steps [8]: (i) energy modulation [9], (ii) exponential growth, and (iii) saturation. In the first evolutionary step, energy is exchanged between the electrons and the radiation, leading to an energy modulation, and further, to a density modulation (microbunching) of the electrons at the resonant wavelength $\lambda_r = \lambda_w(1+K^2/2) / (2\gamma_r^2)$, determined by the electron beam's energy $E_r=mc^2\gamma_r$. $K = eB_w/mck_w$ is the dimensionless undulator parameter, and λ_w, k_w, and B_w are, respectively, the undulator's wavelength, wave number, and magnetic field [11]. Using a coherent seed to initiate the FEL process enables us to lock in the phase of the microbunches and to achieve much better temporal coherence. Afterwards, the FEL enters the second evolutionary step in which the radiated power increases exponentially to the detriment of the electron beam's kinetic energy. The strong energy losses, corresponding to a redshift of λ_r, thereafter disable interaction between the electron and the radiation field. In steady state, the FEL reaches a maximum power and saturates. Its final characteristics (power, duration, spectral width) depend only on the parameters of the undulator and electron beam. Taking time-dependence into account, the optical pulse slips forward with respect to the electron beam by one wavelength λ per undulator period, resulting in the so-called slippage regime characterized by the slippage length $\delta_s = N_w\lambda$. δ_s is the displacement of the optical pulse with respect to the electron beam at the end of the N_w periods of the undulator. The slippage-dominant superradiance regime [12] is characterized by the propagation of a solitary wavelike pulse where the power of the optical pulse (main pulse) grows quadratically with time and its pulse length decreases [13,14,15], resulting in a decrease in the interaction length where the electrons overlap with the main pulse and thereby limiting the output power. However, the interaction length can be extended *via* generating multiple pulses. Here, the multi-pulse regime covers the entire slippage distance along the electron bunch except the part overlapping the seed- and main- radiation pulses [Fig. 1]. Numerical studies reveal that LPS fragmentation and the formation of new buckets are core ingredients of the multi-pulse dynamics. In these circumstances, an ultra-short seed-pulse induces microbunching only when it slips over the electrons at $v_g \sim c$ [12]. Microbunching induces coherent emission from the electrons, forming the main radiation pulse and leaving behind those electrons with a large energy spread. Afterwards, they shear in phase due to intrinsic dispersion [9,10]. The low-energy part ($p < 0$) having more electrons [≥70%, obtained by counting the number of particles in the low-energy part *vs*. the total number of particles distributed within (-π, π)] and, accordingly, a larger bunching coefficient than the high-energy part, emits

ISBN 978-3-95450-123-6

FAST BEAM-BASED BPM CALIBRATION*

K. Bertsche#, H. Loos, H.-D. Nuhn, F. Peters,
SLAC, Menlo Park, CA 94025, U.S.A.

Abstract

The Alignment Diagnostic System (ADS) of the LCLS undulator system indicates that the 33 undulator quadrupoles have extremely high position stability over many weeks. However, beam trajectory straightness and lasing efficiency degrade more quickly than this. A lengthy Beam Based Alignment (BBA) procedure must be executed every two to four weeks to re-optimize the X-ray beam parameters.

The undulator system includes RF cavity Beam Position Monitors (RFBPMs), several of which are utilized by an automatic feedback system to align the incoming electron-beam trajectory to the undulator axis. The beam trajectory straightness degradation has been traced to electronic drifts of the gain and offset of the BPMs used in the beam feedback system. To quickly recover the trajectory straightness, we have developed a fast beam-based procedure to recalibrate the BPMs. This procedure takes advantage of the high-precision monitoring capability of the ADS, which allows highly repeatable positioning of undulator quadrupoles.

This report describes the ADS, the position stability of the LCLS undulator quadrupoles, and some results of the new recovery procedure.

ADS SYSTEM

The ADS system has two major components, a wire position monitor (WPM) system, and a hydrostatic leveling system (HLS). [1]

The WPM [2] consists of two stretched wires running parallel to the beam, each 140 m in length. Wire position monitors attached to the undulator girders sense the girder position with respect to the wires. This allows better than 1 μm position determination in x (the transverse direction). Position in y (vertical) is nearly as well determined, in spite of the sag of the wire.

The HLS consists of a system of water pipes running parallel to the beam, extending for 140 m. Capacitive and ultrasonic sensors on the girders sense the water level. This provides an independent measurement of the vertical position of the girders, which is not subject to wire sag.

The ADS system has shown that quadrupole positions are quite stable long-term. Early characterizations showed stability to within about 2 μm over a 2-3 day period [3,4]. More recent measurements over a period of 19 days in August 2011 have showed quadrupole positions to be stable to better than 2 μm RMS [Fig. 1].

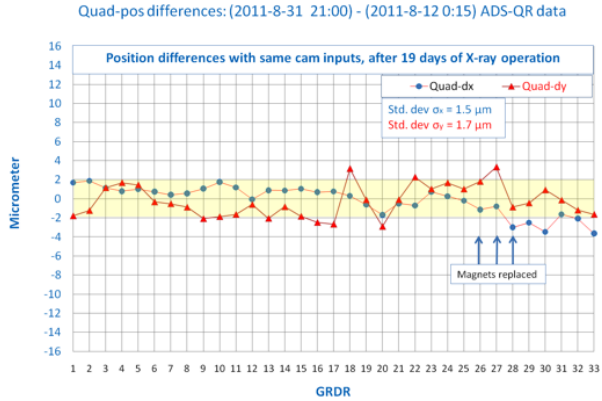

Figure 1: Quadrupole position stability over a 19-day period.

BEAM BASED ALIGNMENT (BBA)

Although the mechanical positions of the quadrupoles are quite stable over many weeks, the straightness of the electron beam trajectory and the FEL lasing efficiency degrade more quickly than this. A BBA procedure must be executed every two to four weeks to straighten the trajectory. This entails operating the linac at four different energies and fitting the trajectories for betatron oscillations, initial beam position and angle, and quadrupole and BPM offsets. Quadrupole magnets are moved to eliminate first and second magnetic field integrals between magnets, and BPM offsets are changed in software to reflect their true positions. This procedure is frequently repeated two or three times to ensure convergence. A full BBA typically takes three to four hours; much of this time involves re-establishing linac configurations for the four energies. [3,5]

BPM DRIFT

The RFBPMs used in the undulator provide high precision beam position measurements. However, they are subject to long-term electronic drift of both their gain and offset. Gain calibrations are typically done at the beginning of each BBA. (This accounts for about 30 minutes of the BBA time.) Over a period of a few weeks, the BPM gain change is on the order of 1%. Long-term BPM offset stability appears to be similar.

Changes in BPM offset do not directly affect the *actual* electron beam position in the undulators. But they directly affect the *apparent* beam position. These apparent beam positions indirectly affect the actual beam positions through a launch feedback system. This launch feedback system attempts to straighten the beam as much as possible, by looking at the apparent beam position as

*Work supported by the U.S. Department of Energy under contract number DE-AC02-76SF00515.
#bertsche@slac.stanford.edu

ISBN 978-3-95450-123-6

BEAM BASED ALIGNMENT OF AN X-FEL UNDULATOR SECTION UTILIZING THE CORRECTOR PATTERN

M. Aiba and M. Böge, PSI, Villigen, Switzerland

Abstract

Beam based alignment of the undulator section is one of the delicate issues in beam commissioning and regular beam tuning of X-FEL facilities since the tolerance on the electron beam orbit straightness is tight, typically a few μm rms. A new approach to align beam position monitors based on dipole corrector strengths is under investigation for the PSI future X-FEL facility, SwissFEL. The methodology and simulations applied to the SwissFEL undulator section are presented in this paper.

INTRODUCTION

Beam based alignment (BBA) of the undulator section is one of the delicate issues in beam commissioning and regular beam tuning of X-FEL facilities since the tolerance on the orbit straightness is tight, typically a few μm rms.

A BBA method which identifies position misalignments of beam position monitors (BPMs) and quadrupoles [1] has been established at the LCLS and was successful in achieving lasing. A misalignment of a BPM changes its reading and a shift is independent of the beam momentum. In contrast, a quadrupole misalignment, which introduces a feed-down dipole component, varies the downstream beam orbit depending on the beam momentum. Therefore the beam orbit measurements for various beam momenta allow one to find these misalignments.

The procedure, however, is rather complicated. In order to find the avobe misalignments precisely, a wide variation of beam momentum is required, where one must ensure the beam transmission to the beam dump. Although an orbit measurement for two different beam momenta is minimal, one or two more measurements are performed to increase accuracy. According to the operation experiences at the LCLS, the entire procedure is usually completed within a few hours [2].

A new approach is under investigation for the PSI future X-FEL facility, SwissFEL, motivated by possible simplification of beam commissioning and machine tuning. The hard X-ray undulator section of SwissFEL is described with technical details in [3]. The BPM and quadrupole are paired on common motorized support (BPM-Quad unit). It is noted that the undulator is to be situated on an independent girder at SwissFEL while all three components are on the same girder at the LCLS. The dipole corrector is integrated into the quadrupole as additional winding coils.

The BBA procedure in this layout consists essentially of two steps: 1) aligning the BPM-Quad units onto a line as straight as possible and 2) aligning the undulators with respect to the electron beam orbit determined by the aligned BPMs. The proposed BBA algorithm, in order to find misalignments of the BPM-Quad units, requires only measuring the corrector strengths needed to steer the electron beam to the BPM centers (for the nominal beam momentum). With an orbit feedback in operation, these are available immediately, and thus the first step can be performed in a few minutes. The second step, once done, may not be always necessary since the alignment tolerance for the undulator is an order of magnitude looser than that of the BPM-Quad unit.

The methodology and simulations applied to the SwissFEL undulator section are presented in this paper.

BBA ALGORITHM

The BBA algorithm utilizes information contained in the dipole corrector strengths needed to steer the electron beam to the BPM centers. These are determined by two contributions, that is, dipolar error fields and BPM misalignments. The first contribution may contain undulator error field, stray field and feed-down dipole component from quadrupoles. The undulator error field must not be significant by definition to realize lasing. Typically the electron beam orbit through an undulator is controlled within the 1 μm level. The stray field must be also negligible or enough suppressed/shielded, and furthermore the BBA algorithm is able to filter out the influence of periodic and uniform stray field. The feed-down dipole component can be avoided by aligning quadrupoles with respect to the pair BPMs based on beam measurements. Therefore the second contribution, i.e. the BPM misalignments, mainly determines the corrector strengths and can be identified.

The BBA is performed by moving the BPM-Quad units so as to minimize the deviation of corrector strengths. By minimizing the deviation with respect to the average strength, periodic and uniform error field can be excluded as long as the initial BPM misalignments are random. Figure 1 illustrates an ideal BPM alignment under uniform dipole field.

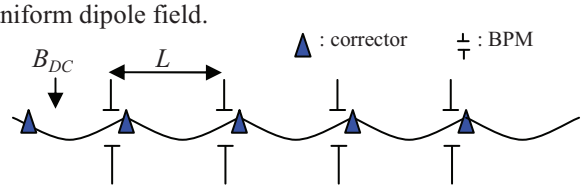

Figure 1: BPMs are ideally aligned on a straight line by minimizing the deviation of corrector strengths under uniform dipole field, B_{DC}. The layout is periodic as in a general undulator section. The corrector strength in units of radian is constant, $B_{DC}L/B\rho$, where L is the unit length and $B\rho$ is the magnetic rigidity of the electron beam, and thereby the deviation is zero.

ISBN 978-3-95450-123-6

BUNCH COMPRESSION LAYOUT AND LONGITUDINAL OPERATION MODES FOR THE SwissFEL ARAMIS LINE

Bolko Beutner*, Paul Scherrer Institute, 5232 Villigen PSI, Switzerland

Abstract

The SwissFEL Aramis Undulator line will produce SASE photon pulses covering a wavelength range from 0.07 nm to 0.7 nm. The facility will consists of an S-band RF-gun and booster, an X-band lineariser, and a C-band main linac, which accelerates the beam up to 5.8 GeV. Two compression chicanes at about 330 MeV and 2.1 GeV will provide a nominal peak current up to 3 kA. It is foreseen to deliver electron pulses between 3 and 19 fs length to the undulator. This is done by adjusting the charge between 10 and 200 pC. Longitudinal wakes in the C-band linac are used to remove the chirp to deliver small bandwidth radiation. A special mode uses these wakes to increase the energy chirp to deliver a photon bandwidth on the percent level for special applications like single shot spectroscopy. In addition a fully compressed 10 pC beam is used as a source of sub femto-second pulses. An iterative semi-analytic procedure was used to setup and optimise the setup efficiently. In this paper these optimised operation modes are presented and discussed.

OVERVIEW

The setup of a global compression scenario for the SwissFEL [1][2] hard-x-ray line has to fulfil certain boundary conditions. Besides a sufficiently high peak current with tolerable low slice emittance, the shape of the current profile, namely the homogeneity of compression, and the overall robustness against parameter jitter are important.

A manual design of such a system is challenging. However, recent work by Zagorodnov and Dohlus [3] offers the possibility for systematic studies and optimisation of longitudinal dynamics setup in a multi-stage bunch compression linac. Their semi-analytic setup algorithm is implemented and applied for the SwissFEL facility design.

SEMI-ANALYTIC LONGITUDINAL SETUP ALGORITHM

The correlation between longitudinal positions of each particle upstream and downstream of compression chicanes is a convenient method to describe the longitudinal dynamics. These correlation function contains not only information on the compression factor but gives insights on the final bunch shape. Let us write the correlation function as

$$Z_i = \frac{\partial s_i}{\partial s_0} \tag{1}$$

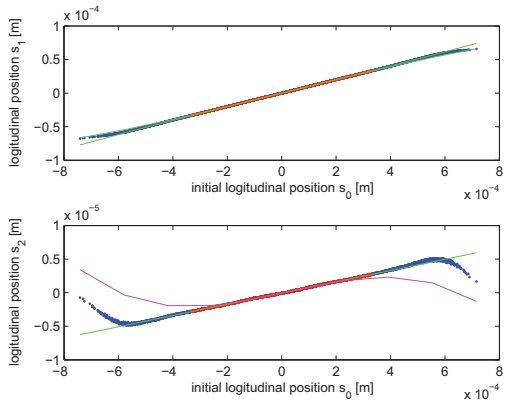

Figure 1: Longitudinal position of each particle are plotted vs. their initial positions for the two compression stages. The compression factor is the inverse of the slope in the central part of the bunch. A polynomial fit is used to quantify this value. Typically a one sigma region in the centre of the bunch (red particles) is considered to avoid complications from the tails.

with i being the number of the compression stage and s the set of longitudinal particle positions- The compression factor is then $C_i = 1/Z_i$. While the value of Z_i corresponds to the compression factor, higher derivatives of Z_i contain information about the general longitudinal shape and the homogeneity of the compression. These parameters Z_i, Z_i', Z_i'' are numerically be calculated by a polynomial fit to the particle distribution (see an example in Fig. 1). In general Z_1' corresponds to the position of the current "peak" along the bunch, while Z_i'' is the overall flatness of the current profile. It can i.e. be increased to suppress "spikes" in the tail regions of the bunch.

A straightforward calculation of the longitudinal dynamics to first order is symbolically summarised as $\mathbf{A_0}$. Assuming a set of RF parameters (phase and amplitude) denoted by $\mathbf{x_0}$ we can write the beam parameters $\mathbf{f_0}$, consisting of energies E_i and Z_i, Z_i', and Z_i'', as

$$\mathbf{A_0}(\mathbf{x_0}) = \mathbf{f_0} \tag{2}$$

with $\mathbf{f_0} = (\mathbf{E_i}, \mathbf{Z_i}, \mathbf{Z_i'}, \mathbf{Z_i''})$. A symbolic inversion of $\mathbf{A_0}$ is possible and explicitly calculated for linear beam transport in [3], such that

$$\mathbf{x_0} = \mathbf{A_0^{-1}}(\mathbf{f_0}). \tag{3}$$

This makes it possible to determine the required RF setup $\mathbf{x_0}$ to achieve the required parameters $\mathbf{f_0}$.

In order to include nonlinear effects an expansion of this method is required. Let us denote a nonlinear particle transport (i.e. particle tracking codes like elegant [4]) with the

* bolko.beutner@psi.ch

ISBN 978-3-95450-123-6

SIMULTANEOUS OPERATION OF A MULTI BEAMLINE FEL FACILITY

S. Ackermann, V. Ayvazyan, W. Decking, B. Faatz*, C. Gruen, E. Hass,
K. Klose, F. Obier, S. Pfeiffer, M. Scholz, J. Wortmann, DESY, Hamburg, Germany

Abstract

The FLASH II project will add an undulator beamline and a new experimental Hall to the existing FLASH Facility. In addition to improving the radiation properties of the FEL by using seeding, one of the main goals is to double the beamtime of the facility for users. At the moment, we deliver photon pulses in 10 Hz bursts with up to 800 bunches within each RF pulse. In order not to limit parameter ranges, we will have to give those same tuning possibilities within an RF pulse for each of the users independently.

For this purpose, several tests have been performed to determine the limits of the difference in beam parameters which can be delivered. We will show to what extend we can switch fast between two beamlines, how we can change photon pulse length by allowing different charges, have different energy in the two beamlines simultaneously to allow for wavelength scans for the fixed-gap undulator presently built in FLASH, while not interfering with user operation of the new beamline.

INTRODUCTION

FLASH [1–4], the free-electron laser (FEL) user facility at DESY, delivers high brilliance XUV and soft x-ray FEL radiation for photon experiments since summer 2005. In order to provide more beam time for experiments and to improve the properties of the delivered FEL radiation, an extension of the FLASH facility - FLASH II Project [6] - was proposed in 2008 by DESY in collaboration with Helmholtz Zentrum Berlin (HZB). The project has been approved in 2010 and the civil construction started in 2011. The first beam of the extended facility is foreseen in late summer 2013.

Because the user time is overbooked by approximately a factor of four, one of the main goals is to extend the capacity of FLASH. Important in this respect is that a doubling of the capacity should not be at the expense of flexibility. This means that we need to be able to deliver all parameters requested by users independently to both beamlines.

LAYOUT

The present FLASH facility consists of an injector with a laser driven RF-gun to produce high quality electron bunches, a superconducting linac with TESLA type accelerator modules to accelerate the electron beam up to 1.25 GeV, and an undulator section with fixed gap undulators to produce SASE (Self Amplified Spontaneous Emission) FEL radiation in the wavelength range from 4.1 nm - 45 nm. More details of FLASH and its parameters are, for example, in [2, 3].

The aim of the FLASH II project is to extend FLASH with a second undulator beamline to allow a more flexible operation and more beam time for photon experiments with improved photon beam properties. The FLASH linac drives the both undulator lines: the present fixed gap undulator (referred here as FLASH1) and the new variable gap undulator (referred here as FLASH2). The separation between the two is downstream of the last accelerating module. Figure 1 shows the layout of the extended FLASH facility. Details of the FLASH II project and its parameters are discussed in Ref. [5]. More details on the extraction can be found in [7].

In order to actually achieve a doubling of beamtime for users, a number of conditions have to be fullfilled. The minimum requirement is that both users get the 10 Hz rep. rate that present FLASH users have. In order to achieve this, a faster kicker-septum system is needed to disxctribute the beam beatween the two undulators. Because both users need to have the long bunch trains, the kicker needs to have, in addition to stability, also a flatness over the bunch trains of 800 μs to achieve equal lasing for all bunches.

The fast switching (and the independent wavelength tunability) does not give us the flexibility needed to organize experiemnts independently. Users will request different bunch patterns, different photon pulse lengths and for FLASH II the possibility to seed with HHG. In order to meet with this lagre variety of conditions, FLASH I and FLASH II will use two different injector laser systems which are shifted in time by a few tens to a few 100 μs, depending on required bunch number and rep. rates for each of the users. This way we can independently set charge and rep.rate for both users. In addition, we need to be able to change compression settings, e.g. RF-parameters, depoending on bunch charge.

In the next section, we will first show results on the stratus of the fast kicker system. Then, we will show the progress on the RF-system to allow for changes in RF phase and gradient within an RF-pulse. This is compared to the parameters which have been experimentally determined as sufficient to obtain lasing over a large range of charges. Finally, we will look at the steps still needed for a full test.

FAST SWITCHING

Figure 2 shows the switching scheme as it is foreseen for FLASH. Each RF pulse with a flat-top of 800 μs has to be distributed between FLASH1 and FLASH2 users. The

* bart.faatz@desy.de

ISBN 978-3-95450-123-6

EXTRACTION ARC FOR FLASH II

M. Scholz*, W. Decking, B. Faatz, T. Limberg, DESY, Hamburg, Germany

Abstract

FLASH II is an extension of FLASH, an FEL user facility at DESY, Hamburg. It uses the same linear accelerator. Fast kickers and a septum will be installed behind the last superconducting acceleration module of the FLASH linac, providing the possibility to distribute beam to the FLASH undulator beamline and through the new extraction arc. It is foreseen that at the end of the extraction arc for FLASH II the beam can be split again into two separate beamlines: The main beamline hosting undulators for SASE and space for HHG seeding, the other beamline might serve later a plasma wakefield experiment or an additional long wavelength SASE source. The extraction arc was designed to mitigate the effects from coherent synchrotron radiation (CSR) like emittance and energy spread growth. The extraction arc for FLASH II places also demands on the existing FLASH beamline which are taken into account. The lattice optimization of the arc was done using the program ELEGANT. Start to end simulations for different bunch charges including FEL simulations with GENESIS were carried out to show the feasibility of the lattice design for the extraction arc.

INTRODUCTION

The existing single-pass high-gain SASE FEL FLASH (Free-electron LASer in Hamburg) at DESY, Hamburg [1] delivers photons in the wavelength range from 4.1 nm to 44 nm. The photons generated by six fixed-gap SASE-undulators can be delivered to five experimental stations in the FLASH experimental hall. FLASH II was planed and is now under construction to increase the beam time for users [2]. Three fast kickers and a DC Lambertson-Septum to be installed behind the FLASH linac give the possibility to distribute the beam either to the existing beam line or to the new extraction arc. At the end of the arc there will be a pulsed bend which allows to steer the beam away from the main beam line, which hosts variable gab undulators for SASE and space for HHG seeding, or to a 3rd beamline serving a proposed plasma wake field experiment.

The variable cap undulators in the new beamline will have a segment length of 2.5 m and a period of 31.4 mm. The total number of segments is 12. The proposed wavelength range for this undulator beamline is 4 nm - 80 nm for SASE and 10 nm - 40 nm for HHG seeding.

SPECIFIC REQUIREMENTS TO THE BEAM TRANSPORT

The challenge for the extraction arc is to fulfill several conditions given by the building environment and by the beam optics. Besides of little free space for additional elements in the existing FLASH installation, the new photon beamline downstream the undulators has to cross PETRA3, a brilliant storage-ring-based X-ray radiation source [3], at a dedicated place which fixes the extraction angle at 12 degree. In addition, the maximum length of the new tunnel is also limited by the PETRA3 accelerator.

In order to mitigate CSR-effects, the beta functions have to be small in all strong horizontal bends [4] [5]. Further requirements on the beam optics are a closed dispersions in both planes and zero momentum compaction.

LATTICE OPTIMIZATION

In an earlier solution for this extraction arc realized with bending magnets of 7, 1.5 and 3.5 degree and a negative dispersion in the second bend to archive zero momentum compaction [2], the impact of the beam transport on the beam quality was too strong and not suitable for the new beamlines. It was necessary to reduce the strength of the quadrupole magnets between septum and the next bending magnet to improve the beam quality. However these strong quadrupole magnets were necessary to get the negative dispersion in the second bend. The idea for the new extraction arc presented in this paper was to implement a weak reverse bend downstream the septum at a location with positive dispersion which allows to archive zero momentum compaction.

The final solution for the extraction has now deflection angles of 6.5, -0.9, 3.2 and 3.2 degree. A top view of all magnet positions can be found in Fig. 1. The program used for all optimizations and for particle tracking was ELEGANT [6].

The new optics design shows small beam waist in all strong horizontal bends as necessary to mitigate the coherent synchrotron radiation effects. The required vertical offset for the Lambertson-septum is achieved with 3 kickers upstream of the septum. The kick is increased by two out of the three quadruples between kickers an septum which are passed with a vertical offset. The third quadrupole magnet deflects the beam back to straight trajectory. These quads provide the beam waist in the septum. The vertical dispersion caused by the kickers is closed with two vertical bends at the end of the extraction arc. In horizontal plane, closed dispersion is achieved. Three sextupole magnets in the extraction arc are required to close the second order vertical dispersion.

Zero R56 is obtained by use of the reverse bend and proper characteristics of the dispersion function. Plots of the betatron functions, the dispersion functions, the momentum compaction function as well as for the vertical beam center position are presented in Fig. 2.

* matthias.scholz@desy.de

ISBN 978-3-95450-123-6

BEAM OPTICS DESIGN FOR PAL-XFEL*

H. S. Kang†, J.-H. Han, T. H. Kang, I. S. Ko,
Pohang Accelerator Laboratory, POSTECH, Pohang 790-784, Korea

Abstract

The PAL-XFEL lattice is designed to generate a 0.1 nm hard X-ray FEL using a 10 GeV electron linac with a switch line at 3 GeV point for 1-3 nm soft X-ray FEL. The beam optics is designed so as to have robustness in matching at the sections of Injector, Linac section (L1, L2, L3, L4), bunch compressors (BC1, BC2, BC3), soft X-ray switch line, dechirper and deflector, emittance measurement unit (EMU), dogleg line, Undulator, and beam dump. The optics design also includes geometric and energy collimators to protect undulator magnets, whose performance is confirmed by the particle tracking simulation.

OUTLINE OF PAL-XFEL

The PAL-XFEL is designed to generate a 0.1 nm hard X-ray FEL using a 10 GeV electron linac with a switch line at 3 GeV point for soft X-ray FEL. The target slice emittance is 0.4 mm-mrad at 0.2 nC and the acceptable emittance is set at 0.6, which is used in the undulator design to have a reasonable margin of error [1].

Figure 1 depicts the layout of the PAL-XFEL. It consists of a 139-MeV injector, four acceleration sections (L1, L2, L3, and L4), three bunch compressors (BC1, BC2, BC3), and a dogleg transport line to undulators. The injector uses an S-band photo-cathode RF-gun to make the slice emittance smaller than 0.3 mm-mrad at 0.2 nC [2]. A laser heater, which placed right after the injector, is to mitigate micro-bunching instability by increasing the uncorrelated energy spread to Landau damp the instability. An X-band cavity placed after L1 is to linearize the non-linear energy-to-time correlation growing at the injector and L1 where the electron beam bunch is so long that non-linear time-varying RF field increases the non-linearity. A deflector, which is an RF cavity resonant at TM110 mode, is to measure the temporal profile of the electron beam and able to measure the energy-time correlation by incorporating with a following energy spectrometer. Emittance measurement unit (EMU) utilizes a FODO lattice with wire scanners placed between quads with a fixed betatron phase difference. A de-chirper located right after BC3-S in the soft X-ray FEL beamline is a corrugated pipe to actively use the resistive longitudinal wake field induced from the head of the bunch to decrease the energy of the tail. The energy chirp, time-correlated energy difference in the bunch, required in the bunch compression process is well compensated in the hard x-ray FEL beamline due to the long acceleration section L4, while it is not available in the soft X-ray FEL beamline because there is no wake structure after the last bunch compressor (BC3-S). A 20-m long de-chirper is used in the soft X-ray FEL beamline while a short (6 m long) de-chirper will be used at the hard X-ray FEL beamline to have a possibility of increasing energy chirp, therefore, reducing R56, which means it allows us to reduce the amplitude of parameters affecting microbunching instability such as R56, chicane bend angle, and the distance between the first and the 2-nd dipole of chicane.

Figure 2 shows the layout of hard X-ray and soft X-ray FEL beamlines. Two FEL beamlines, one soft X-ray (SX1) and one hard X-ray (HX1), which will be prepared in the first phase, are to provide the FEL beam in the range of 0.56 to 0.1 nm and 4.5 to 1 nm, respectively. To have a capability of full polarization control in the soft x-ray FEL, APPLE-II type undulators are used for saturation at the last section of undulators before which planar-type undulators are used for full development of microbunching before saturation. The shortest wavelength of HX1 beamline is extendable to 0.06 nm by changing the undulator gap. The SX1 undulator line is nominally to deliver the FEL radiation from 3 nm to 1 nm, while it should be able to deliver a 4.5 nm FEL beam by reducing the beam energy from 3.15 to 2.6 GeV.

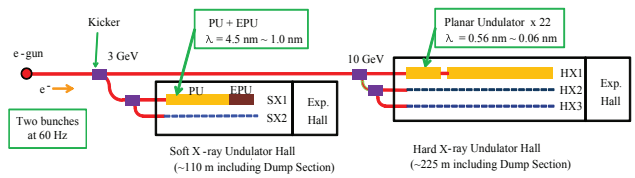

Figure 2: Layout of hard X-ray and soft X-ray FEL beamlines.

OPTICS DESIGN FOR HARD X-RAY FEL BEAMLINE

Hard X-ray FEL beamline

Figure 3 shows the lattice of the hard X-ray FEL beamline. Four acceleration sections (L1, L2, L3, and L4) have different FODO lattice with different betatron phases. The length of the S-band accelerating structure (A/C) is 3.0 meters. At L1, one quad per one A/C is selected to make betatron function smaller than 15 meters, and At L2 and L3, one quad per two A/Cs is selected to make betatron function smaller than 25 meters for L2 and 35 meters for L3. At L4, one quad per four A/Cs is selected because of small emittance of the electron beam.

* Work supported by Korean Ministry of Science and Technology
† hskang@postech.ac.kr

ISBN 978-3-95450-123-6

FEMTOSECOND LEVEL SYNCHRONIZATION OF A LINAC BASED SUPER-RADIANT THz FACILITY

M. Kuntzsch#, F. Röser, U. Lehnert, M. Gensch#, HZDR, Dresden, Germany
M. Bousonville, H. Schlarb, N. Stojanovic, S. Vilcins-Czvitkovits, DESY, Hamburg, Germany

Abstract

The superconducting radiofrequency (SRF) electron accelerator ELBE at Helmholtz-Zentrum Dresden-Rossendorf (HZDR) is currently upgraded. A SRF Gun and a femtosecond (fs) electron beamline will enable quasi continuous wave (cw) operation with bunch charges of up to 1 nC and bunch durations down to 150 fs (FWHM). The new femtosecond electron beamline will be used to drive one super-radiant THz test facility and one X-ray source based on Thomson scattering. Both of these facilities will at some stage rely on synchronization of external laser systems to the accelerator on the sub 100 fs timescale. In the next few years one focus of the accelerator research activities at HZDR will lie in the development of suitable techniques to timing and synchronizing the accelerator. Our approach is based on an optical synchronization system, adapted from a similar system installed at FLASH [1]. This system is installed and tested in a close cooperation between DESY and HZDR.

CONCEPT

Overview

The femtosecond synchronization system at ELBE is using single-mode optical fibers to distribute stable laser pulses to several remote stations. The laser light is partially used for an optical phase detection scheme to monitor and compensate for jitter and drifts [1]. The master laser oscillator (MLO), operating at 78 MHz, is locked to the master radio frequency (RF) oscillator, which defines the long term stability.

The link stabilizers are adapted from the units installed at FLASH and have been setup at ELBE in collaboration with DESY, Hamburg. In spring 2012 the first prototype link stabilizer has been commissioned at HZDR and showed promising performance [2].

The layout of the synchronization system is shown in Figure 1.

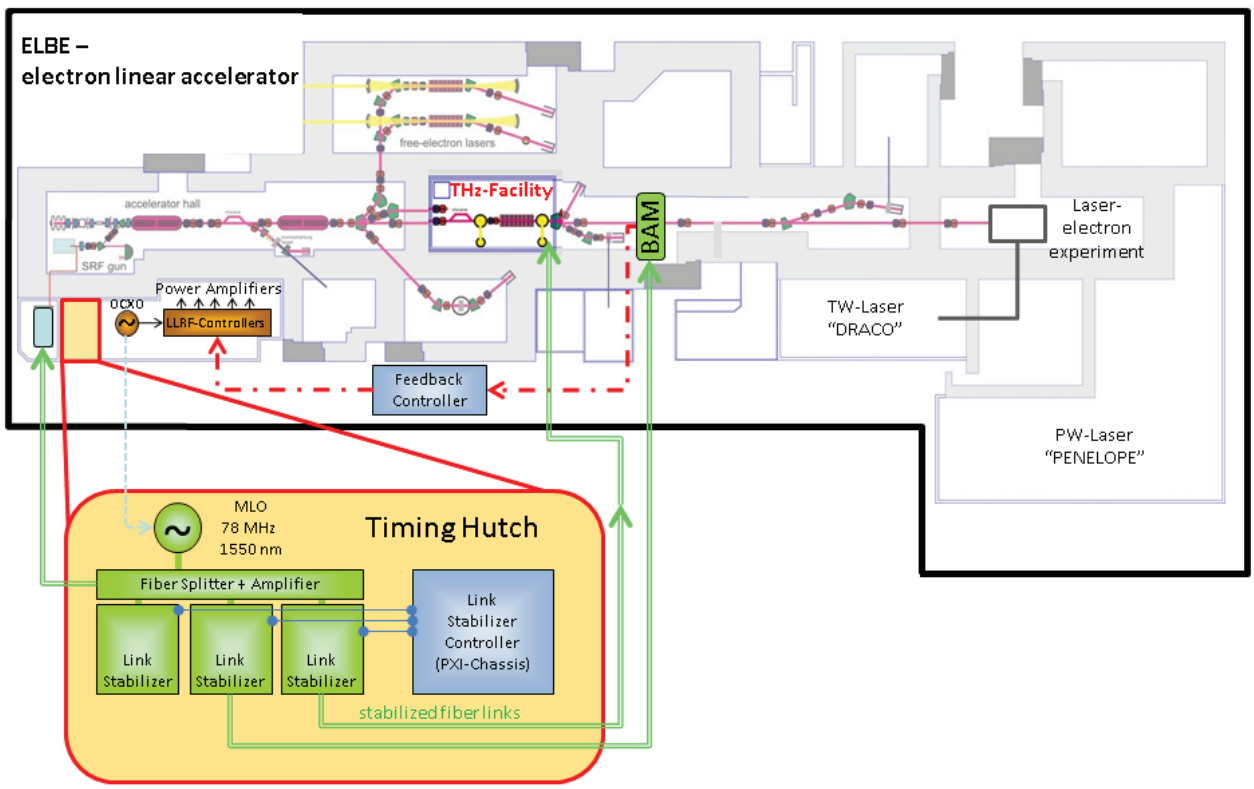

Figure 1: ELBE layout with synchronization system for THz facility.

#corresponding author, email: m.kuntzsch@hzdr.de;
m.gensch@hzdr.de

ISBN 978-3-95450-123-6

VARIATION OF BEAM ARRIVAL TIMING AT SACLA

Takashi Ohshima#, Hirokazu Maesaka, Yuji Otake,
RIKEN, 1-1-1, Kouto, Sayo, Hyogo, 679-5148, Japan
Shin-ichi Matsubara, JASRI, 1-1-1, Kouto, Sayo, Hyogo, 679-5198, Japan

Abstract

SPring-8 Angstrom Compact Laser (SACLA) is a XFEL facility which provides intense pulsed X-ray laser to various scientific fields. It is a key issue to deliver stable timing signals to the accelerator components, the beam monitor units and apparatus of XFEL users with a precision of less than 100 fs RMS. Since the arrival timing of the X-ray at an experimental station depends on that of the electron beam, we measured the arrival timing of the electron beam by comparing a reference rf signal and a beam induced signal from an rf beam position monitor (RF BPM). A jitter of the arrival timing monitor was 41 fs in RMS calculated from a correlation plot of two adjacent BPMs data. To evaluate the stability of the timing monitor, we measured the difference of the arrival timings between two BPMs located at the entrance and the exit of the BL3 section. The difference of the arrival timings was about 180 fs pk-pk for 2 days measurement, which is the present accuracy of our beam arrival timing monitor.

INTRODUCTION

SACLA is a XFEL facility at SPring-8 [1]. For the accelerator of this facility, it is important to stabilize the phases of the accelerating cavities around the injector and bunch compression process of SACLA within 100 fs RMS to keep the stable laser oscillation. For this purpose a transmission system to deliver reference rf signals though optical fibers was installed [2]. One method to evaluate the stability of the transmission system is to measure the difference between two beam arrival timings along a straight beam-drift section. The high energy electron beam reaches almost the speed of light and hence, the difference of the beam arrival timings measured at two points along the straight beam-drift section is constant. If the optical path length is changed in the transmission system, the change also appears in the difference between the beam arrival timings. We have a beam position monitor which can measure the phase as beam arrival timing between the beam induced signal and the reference rf signal [3, 4]. Its temporal resolution was evaluated at the SCSS test accelerator and was measured to be 25 fs in RMS [5]. We measured again this temporal resolution at SACLA by using two adjacent BPMs. Then we measured the difference of the beam arrival timing between two BPMs located at the entrance and the exit of a BL3 undulator straight section. The measurement results of the arrival timing and the stability of the reference signal transmission system are reported in this paper.

BPM SYSTEM AND TRANSMISSION SYSTEM OF REFERENCE RF SIGNALS

To attain the submicron position measurement resolution, a cavity type BPM is used at SACLA [3, 4]. It consists of two cavities; one is a TM110 dipole mode cavity in order to measure the beam position, and the other is a TM010 monopole mode cavity to measure a beam charge amount and a reference beam phase for normalization. The resonant frequencies of the cavities are 4760 MHz. The BPM electronic circuit consists of an In-phase Quadrature (IQ) demodulator in order to detect the amplitude and the phase of the signal. The detected

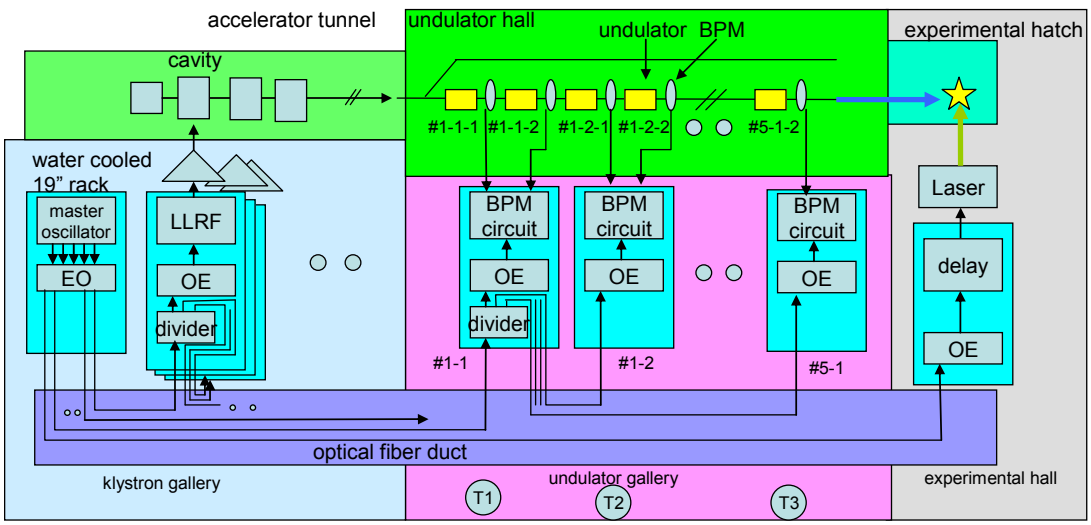

Figure 1: Schematic view of the BPM system and the transmission system of the reference rf signals.

#ohshima@spring8.or.jp

ISBN 978-3-95450-123-6

UPGRADE OF A PRECISE TEMPERATURE REGULATION SYSTEM FOR THE INJECTOR AT SACLA

Teruaki Hasegawa#, Takao Asaka, Hirokazu Maesaka, Takahiro Inagaki,
Kazuaki Togawa, Yuji Otake
RIKEN SPring-8 Center, 1-1-1 Kouto, Sayo-cho, Sayo-gun, Hyogo 679-5148, Japan
Sunao Takahashi, Toru Fukui
JASRI, 1-1-1 Kouto, Sayo-cho, Sayo-gun, Hyogo 679-5198, Japan

Abstract

A precise temperature regulation system for an injector at SACLA is being upgraded. Although an existing temperature control system has been able to regulate an RF cavity temperature within 0.08 K, it has become clear that even a tiny fluctuation in a cooling water temperature, such as 0.1 K, for the RF cavities of an injector significantly influenced lasing stability. This temperature stability is limited by a PLC temperature measurement module, which has non-negligible temperature drift. In addition, it has been found that an ON-OFF alternatively heating method with a pulse width modulation signal generated a laser intensity variation having a high correlation with this modulation frequency. This variation is considered to be caused by a tiny-pulsed temperature variation due to the heater power switching, or small magnetic field leakage from heater current. Therefore, the temperature controller module was replaced by a more precise one with an extremely high temperature resolution of 0.001 K and an excellent stability of 0.01 K. We will also apply continuous level control of a heater with a DC power supply. Prior to full-scale introduction of this new scheme to the injector, we have introduced only a new temperature measurement and control module to the RF cavities in the injector, as a preliminary test, and estimated performance. As a result, the cavity temperature fluctuation could be drastically improved to 0.01 K (p-p).

INTRODUCTION

Following about one year of beam commissioning, public use at SACLA (SPring-8 Angstrom Compact Free Electron Laser) finally started on March 7th, 2012. To realize stable user operation, it is necessary to keep laser intensity and position as stable as possible over long periods. In particular, as extremely high stability of accelerator components is indispensable in the injector section [1], a low level RF (LLRF) feedback control over RF phase and RF amplitude is applied to pickup signal from RF cavities. We also established a precise temperature regulation system (PTRS) that is able to regulate a temperature within 0.08 K at each RF cavity. [2] [3]

However, during the beam commissioning, it has become clear that even a tiny fluctuation in cooling water temperature, such as 0.1 K, for the RF cavities of the injector significantly influenced the stability of laser intensity. [4] [5] This temperature stability is limited by a PLC temperature measurement module, which has non-negligible temperature drift. In addition, it was found that a frequency of an ON-OFF alternatively heating method with a pulse width modulation (PWM) signal had a high correlation with that of a position variation in an electron beam synchronized with a laser intensity variation. This is probably due to a tiny-pulsed temperature variation by the heater power switching, or small magnetic field leakage from heater current. Therefore, the present temperature measurement module was replaced with a more precise one having an extremely high temperature resolution, which is mentioned in the succeeding sections. In addition, continuous level control of a heater with a DC power supply, which we also argue in the next, is employed.

PRECISE TEMPERATURE-REGULATION SYSTEM

Technical Issues of the Existing System

Figure 1 shows a schematic layout of the injector at SACLA. At first, an electron beam emitted from a 500 keV thermionic gun is sliced to be 1 ns/1 A by a chopper. After the bunch compression (by velocity bunching) and beam acceleration with 238MHz/Sub-harmonic buncher (SHB), 476MHz/Booster and two L-band (1428MHz) alternating-periodic accelerating structures (APS), and a bunch compressor chicane, an 30 MeV electron beam with a bunch length of 3 ps is generated. L-band and C-band (5712MHz) correction cavities are installed in order to linearize the curvature of an energy chirp.

A cooling water system, which comprises a primary chilled water system of 12 °C supplied by a turbo refrigerator and a secondary circulating pure water system

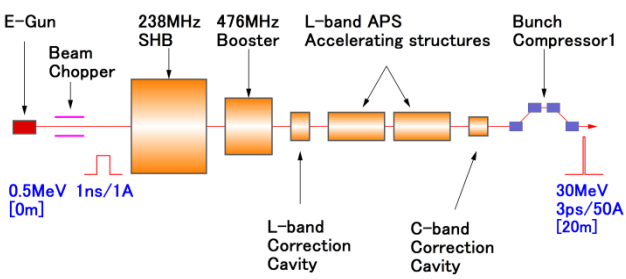

Figure 1: Schematic layout of an injector at SACLA.

hasegawa@spring8.or.jp

ISBN 978-3-95450-123-6

STABILITY IMPROVEMENTS OF SACLA

Hirokazu Maesaka#, Takao Asaka, Toru Hara, Teruaki Hasegawa, Takahiro Inagaki,
Takashi Ohshima, Kazuaki Togawa, Hitoshi Tanaka, Yuji Otake,
RIKEN SPring-8 Center, Sayo-cho, Sayo-gun, Hyogo, Japan
Shin-ichi Matsubara, JASRI , Sayo-cho, Sayo-gun, Hyogo, Japan
Taichi Hasegawa, Yutaka Kano, Takuya Morinaga, Yasuyuki Tajiri, Shin-ichiro Tanaka,
Ryo Yamamoto, SPring-8 Service Co., Ltd., Shingu-cho, Tatsuno-shi Hyogo, Japan

Abstract

For stable user operation of SACLA, an XFEL intensity is demanded to be sufficiently stable within 10% level for a long-term drift. In the early period of XFEL lasing at SACLA, however, the XFEL intensity significantly decreased in a few hours, if we did not adjust the accelerator condition. We found that the rf phase of an injector part had significant fluctuation, which could be a major source of the XFEL intensity degradation. Therefore, we improved the temperature stability of the acceleration cavity in the injector from 0.08 K pk-pk to less than 0.01 K pk-pk by using a further precise temperature regulation system. As a result, the long term XFEL intensity drift was reduced to 10% pk-pk level, if operators sometimes finely adjusted rf parameters of the injector. At this moment, some more improvements for the XFEL intensity stabilization, such as the reduction of the temperature coefficient of low-level rf electronics, the construction of the fiber length control system for a reference rf transmission system etc. are ongoing. After these improvements, the XFEL intensity is expected to be sufficiently stable without any adjustments by operators.

INTRODUCTION

In order to utilize an x-ray free electron laser (XFEL) for physics experiments and biological sciences, the stability of XFEL intensity is important. For the effective use of XFEL, a long-term intensity drift of less than 10% pk-pk and a short-term jitter of less than 10% rms are demanded. In the early period of the commissioning of SACLA [1,2], however, the stability of the XFEL intensity was not sufficiently stable for user experiments. The XFEL intensity was degraded within a few hours if we did not tune the injector part of the accelerator, as shown in Fig. 1. In addition, a short-term jitter was more than 10% rms, which was larger than the intrinsic fluctuation of a SASE-FEL (a little less than 10% rms).

One of the causes of XFEL intensity variation is the peak-current fluctuation of an electron beam. In SACLA, we use velocity bunching in the injector part and three bunch compressors (BC) in the upstream part of the accelerator, as illustrated in Fig. 2, in order to obtain a required peak current of 3 kA. If a bunch compression ratio at each compression stage is changed, the peak current of the electron beam is degraded and the XFEL intensity is also decreased. In the bunch compression stage, an electron beam is accelerated at an off-crest phase of an acceleration rf field. Therefore, the small rf phase drift of the accelerator can affect the bunch compression ratio and the XFEL intensity can be degraded. The requirements for the rf phase stability in SACLA are 50 fs rms short-term jitter and a few 100 fs pk-pk long-term drift in the time-equivalent value of the rf phase [3].

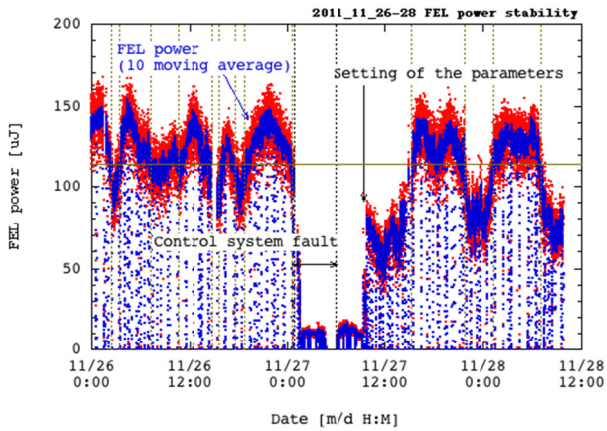

Figure 1: XFEL power trend graph in the early period of x-ray lasing at SACLA. Red points are shot-by-shot intensities and blue ones are 10-shot moving average. Although there was no FEL output in the middle of the measurement, this was not the stability issue but a machine trouble. In this data acquisition period, only the feedback control of each rf phase and the beam orbit in the undulator were performed.

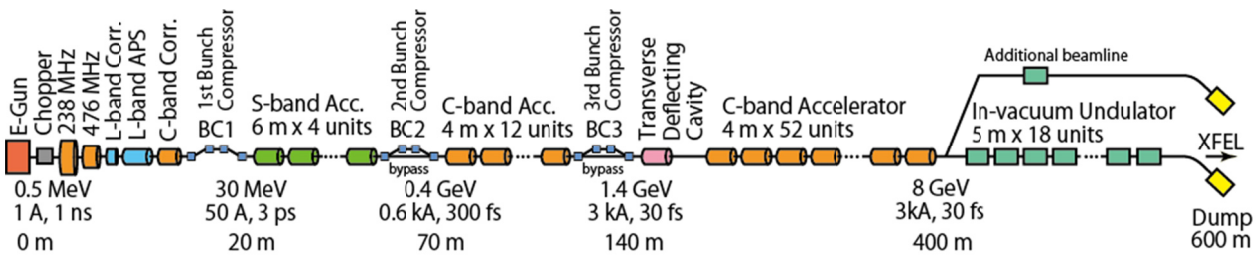

Figure 2: Schematic layout of SACLA.

maesaka@spring8.or.jp

ISBN 978-3-95450-123-6

EFFECT OF ACTIVE FIBRE STABILIZATION ON GROUP AND PHASE DELAY

T. T. Thakker, S. P. Jamison, STFC, Sci-Tech Daresbury, UK

Abstract

Many current optical timing schemes use detection of the pulse group or phase delay through an optical fibre to allow them to stabilize propagation through the fibre to the fs or sub-fs scale. However, it is recognised that stabilizing one leaves a residual drift in the other.

We have contructed a phase delay detector to investigate the phase-group delay walk-off (PGW) in fibre distribution systems. The phase monitor uses polarisation rotation associated with sub-wavelength delays in the fibre to detect changes in the carrier phase of ultrashort pulses. Used in conjunction with a group delay monitor, we can measure the PGW in actively stabilized fibre links and its implications on the feasibility of stabilizing both carrier and envelope phase in pulsed synchronisation systems. The ability to stabilize both the carrier and envelope phase in these systems could give the higher resolution of interferometric based stabilization systems while continuing to deliver ultrashort pulses for use at delivery sites.

INTRODUCTION

An optical clock distribution system is being developed on the ALICE accelerator at Daresbury Laboratory. The system is based on a mode-locked laser fibre stabilization scheme which delivers the clock signal with ultrashort optical pulses over an actively stabilized optical fibre. Such systems have been shown to deliver clock stability with rms jitter as low as 5 fs [1].

In contrast to short pulse synchronisation schemes, inteferometric timing schemes can offer link stabilities to the 800 as level by utilizing the finer scale carrier oscillations [2]. However, while RF modulation on the carrier can be used to deliver a clock signal to remote sites, these systems require a secondary laser at the remote site to synchronize with if short short pulses are required locally. Furthermore, the difference in phase and group velocity in the fibre means that any RF modulation imposed onto the optical signal is not fully stabilised by stabilisation of the phase transit time. This is due to the phase velocity being proportional to the refractive index of the medium and the group velocity being proportional to its derivative as given by

$$v_\phi = \frac{\omega_0}{\beta_0}\left(\frac{d\beta}{d\omega}\right)_{\omega=\omega_0} v_g \,. \qquad (1)$$

Interferometric schemes can instead employ a scaling factor to account for the differences in phase and group delay in their fibre [2]. While this is a good approximation for static fibre it is not evident that stresses and geometry changes to fibre when stretched at high frequencies can be accounted for with a fixed calibration factor. Thus, to effectively compensate for both the phase and group delay changes in a link it is necessary to simultaneously monitor both of these changes in real time.

In looking at the effect of fibre stretching on changes to the group and phase velocity of distributed signals, we aim to gain an understanding of the level and characteristic of residual phase jitter on a group delay stabilized link. This will enable us to assess the feasibility and methods for simultaneous stabilization of both group and phase delay in our system.

DETECTION SCHEMES

To monitor both the phase and group delay in the fibre link, we used a configuration as shown in Fig. 1. Short 65 fs pulses from a mode-locked Erbium fibre ring laser are

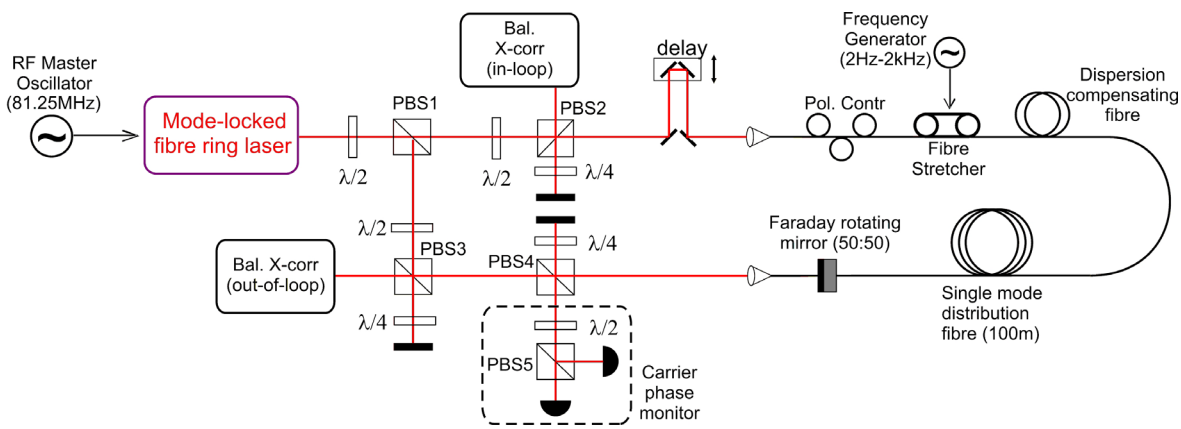

Figure 1: Layout of monitoring system to simultaneously measure the phase and group delay of pulses through the fibre link.

ISBN 978-3-95450-123-6

PRACTICAL DESIGN OF RESONANCE FREQUENCY TUNING SYSTEM FOR COAXIAL RF CAVITY FOR THERMIONIC TRIODE RF GUN

K. Torgasin*, H. Imon, M. Takasaki, R. Kinjo, Y.W. Choi, M. Omer, K. Yoshida, H. Negm,
K. Shimahashi, M. Shibata, K. Okumura, H. Zen, T. Kii, K. Masuda, K. Nagasaki and H. Ohgaki
Institute of Advanced Energy, Kyoto University, Gokasho Uji, Kyoto 611-0011, Japan

Abstract

A prototype of coaxial rf cavity for thermionic triode rf gun has been fabricated and tested at low power.

The low power test reveals the dependency of cavity resonance frequency on cavity and cathode temperature. Another critical point for resonance frequency is the cavity length. Inaccuracies in machining or simulation of cavity length cause errors in resonance frequency of manufactured cavity. In order to compensate for undesired resonance changes a tuning mechanism has been installed for the prototype of coaxial rf cavity.

In this paper we present the capability of the stub tuning system and propose a modified coaxial rf cavity design.

INTRODUCTION

A FEL (free electron laser) facility require low emittance and high peak current electron beams[1].
Thermionic rf electron guns are often used for generation of high quality electron beams, which are used for generation of FEL. The conventional thermionic rf guns suffer from electron back- bombardment effect, which causes large energy spread of generated electron beams[2]. In order to mitigate the amount of back streaming electrons our group has developed a new triode type thermionic rf gun[3-4]. The triode design consist of an additional coaxial rf cavity with a thermionic cathode on its inner rode. This cavity can be integrated into the main body of a rf gun[3].

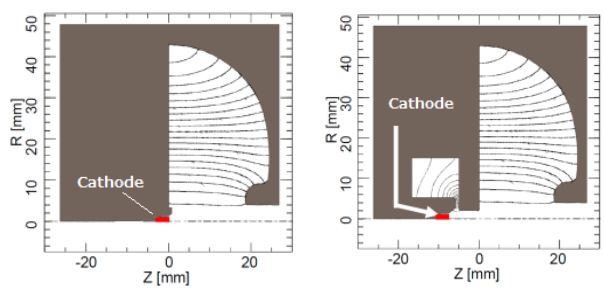

(a) Conventional (b) Triode type

Figure 1: Electric field distribution in cross section of conventional and triode coaxial rf cavity.

*Contact: konstant@iae.kyoto-u.ac.jp

Figure 1 shows the comparison between the 1st cell of thermionic rf gun body in conventional and triode type design in cross section. The triode thermionic rf gun has an additional coaxial rf cavity, later referred as triode cavity. This cavity is supplied by an electric field which is independent from that of the first cell of the gun body. By adjusting the phase and amplitude of the electric field in the triode cavity the extraction of thermionic electrons from the cathode can be synchronized with the accelerating rf phase of 1st cell of the main accelerating cavity. By this means the amount of back streaming electrons can be reduced and as the consequence the energy spread of electron beam mitigated[3].

The efficiency of the triode approach shall be proved for the KU-FEL(Kyoto University Free Electron Laser) facility[5]. The facility uses 4.5 cell thermionic rf gun[3] for electron beam generation. This rf gun is intended to be modified to triode type in order to mitigate the back-bombardment effect[6]. A corresponded prototype of triode cavity for thermionic rf gun has been fabricated.

The resonance frequency of triode cavity must correspond to that of the main accelerating cavities of the gun. The test of fabricated triode cavity prototype reveals the resonance deviation of 462 MHz from expected value[4]. For reasons of refinement of resonance frequency we have implemented a stub based frequency tuning system. This mechanism allows the frequency tuning up to 102 MHz at the present experimental setup. Further frequency tuning can be achieved by changing of triode cavity length.

FREQUENCY TUNING SYSTEM

Figure 2 shows a schematic cross-sectional view of the triode cavity and the fabricated prototype with cavity length of L=19.2 mm.

A thermionic cathode is set on the inner rod of the coaxial cavity. The cathode is heated in order to ensure emission of electrons. Since the cavity length L is sensitive to the temperature, the resonance frequency is changed according to cathode heating conditions.

Figure 3 shows the measured correlation of cavity resonance frequency and cathode temperature. The increase in temperature causes resonance shift of max. 10 MHz towards lower frequency at operational conditions (1290 K-1570 K). In order to correct for temperature rise

ISBN 978-3-95450-123-6

MACHINE PROTECTION FOR SINGLE-PASS FELS

L. Fröhlich*, Sincrotrone Trieste, Basovizza, Italy

Abstract

The linacs driving modern single-pass FELs carry electron beams of unprecedented brightness with average powers ranging from few watts to hundreds of kilowatts. The article discusses the scope of machine protection for these accelerators, reviews the parameters of existing and planned facilities, and gives an overview about typical hazards and damage scenarios. As a common problem faced by all single-pass FELs, the effect of radiation-induced demagnetization of permanent magnet undulators is discussed.

INTRODUCTION

The linacs used to drive modern single-pass FELs carry electron beams of unprecedented brightness. These machines are also equipped with unusual amounts of instrumentation that needs to be protected from beam losses. The FEL process itself depends crucially on the precision of the magnetic field inside undulator structures that are prone to demagnetization under radiation exposure. This combination makes machine protection for single-pass FELs much more challenging than for traditional electron linacs.

After introducing the broad scope of the term *machine protection*, this paper reviews the parameters and damage potentials of existing and future FEL facilities. The various hazards connected with electron beam losses are summarized and the effect of radiation-induced demagnetization on the phase error of an FEL undulator is discussed.

SCOPE

The term *machine protection* is often understood as a mere synonym for a system of protective interlocks and beam loss diagnostics. While such active systems play an important role, an effective protection from damage involves many fields of accelerator engineering and physics. To attempt a definition, we may state that *machine protection is the sum of all measures that protect an accelerator and its infrastructure from the beam.* Traditionally, the focus is on the charged particle beam, but the generated photon beam needs to be considered as well, especially due to the unprecedented peak power of X-ray FELs.

From the above definition, we can identify a number of fields connected with machine protection:

Machine protection system: The MPS implements interlocks on components that may interfere with a safe beam transport (e.g. magnets, screens). It monitors the beam with instrumentation that may be generic (BPMs, current monitors) or specifically designed for protection purposes (beam loss monitors, dosimetry systems). When excessive beam losses or other problems are detected, the MPS intervenes according to a mitigation strategy—it might simply inform the operator, reduce the repetition rate, or stop the beam production.

Collimators: Collimators and scrapers are used to limit the extent of the electron bunch (and of possible dark currents) in phase space. In case of trajectory or focusing problems, they should intercept the electron beam before it reaches sensitive components. The electromagnetic cascades originating from the interaction of high energy electrons beams with matter are not easy to contain, so care must be taken to place suitable absorbers.

Shielding: The loss of a small fraction of an electron beam at the GeV level releases a dangerous amount of spontaneous radiation. Even if the average power of the beam is as low as few watts, the radiation can quickly cause temporary or permanent damage to electronics in the vicinity of the beamline. Sustained exposure causes various types of radiation damage like the darkening of optical components. Beam loss can also release sizable quantities of neutrons and activate materials in the process. Depending on the beam power, shielding may therefore be necessary against both electromagnetic dose and neutrons.

Beam physics: A loss-free transport of charge from the injector to the dump requires a good understanding of the optics and of the whole acceleration process. The higher the beam power, the more important it is to have good control over the optics matching and over collective effects that create emittance blowups, tails, or halos.

Robust systems: Every system or software that has a direct or indirect influence on the beam contributes to the protection of the machine by providing a certain level of robustness. Cardinal examples are beam-based feedback systems, low-level radiofrequency (LLRF) systems, or even high-level physics tools for the optimization of the FEL output.

Procedures: Well-defined procedures for typical linac operations like switch-on, change of energy, or ramp to full power contribute to safety and make the machine state more reproducible. Automatization of these procedures can further help to avoid errors.

* lars.froehlich@elettra.trieste.it

ISBN 978-3-95450-123-6

TIME-RESOLVED IMAGES OF COHERENT SYNCHROTRON RADIATION EFFECTS IN THE LCLS FIRST BUNCH COMPRESSOR

P. Emma, F. Zhou, Z. Huang, SLAC, Stanford, CA 94309, USA
C. Behrens, DESY, 22607 Hamburg, Germany

Abstract

The Linac Coherent Light Source (*LCLS*) is an x-ray Free-Electron Laser (FEL) facility now in operation at SLAC. One of the limiting effects on electron beam brightness is the coherent synchrotron radiation (CSR) generated in the bunch compressor chicanes, which can significantly dilute the bend-plane (horizontal) emittance. Since simple emittance measurements [1] do not tell the full story, we would like to see the time-dependent CSR-kicks along the length of the bunch. We present measured images and simulations of the effects of CSR seen on an intercepting beam screen just downstream of the *LCLS* BC1 chicane while powering a skew quadrupole magnet near the center of the chicane [2]. The skew quadrupole maps the time coordinate of the pre-BC1 bunch onto the vertical axis of the screen, allowing the time-dependent CSR-induced horizontal kicks to become clearly visible.

INTRODUCTION

The effects of CSR can degrade the brightness of an electron bunch, especially as it is being compressed in a magnetic chicane and begins to radiate coherently at wavelengths which are long compared with the shrinking bunch length. The CSR wake tends to kick the head and tail of the bunch in different bend-plane directions due to the CSR-altered head and tail energies which arise during passage of the bunch through the chicane bends. The net effect is typically an increased bend-plane emittance, usually characterized by the spot size projection onto an intercepting screen. In fact, it will also be very useful to time-resolve these kicks along the length of the bunch.

With this goal in mind we have installed a skew quadrupole magnet [2] (rotated by 45° wrt a standard quadrupole magnet) near the center of the BC1 chicane, which couples the x-position of an electron at chicane center to a y-position after the chicane. The *LCLS* BC1 layout [3] is shown in Figure 1 with parameters in Table 1.

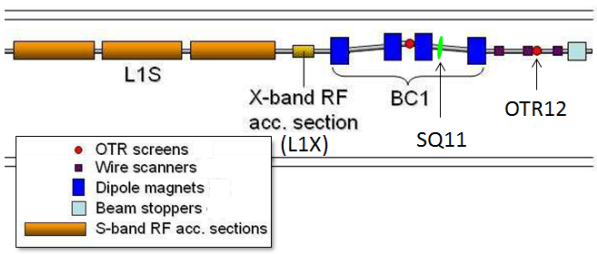

Figure 1: Layout of *LCLS* injector in the BC1 area. The 9-m long S-band linac section (L1S) is followed by a 60-cm long X-band RF section (L1X) feeding the BC1 chicane at 220 MeV. The "SQ11" skew quad and "OTR12" screen are also shown.

Table 1: LCLS Injector and BC1 Parameters

Parameter	sym.	Value	Unit
Bunch charge	Q	0.25	nC
BC1 Momentum Compaction	$\lvert R_{56}\rvert$	45.5	mm
Electron energy at BC1	E	220	MeV
Pre-BC1 bunch length (rms)	σ_z	0.62	mm
Focal length of skew quad	f	14	m

In order to compress the bunch length in BC1, the bunch must be energy chirped (linearly correlated energy along bunch length) by operating the L1S RF (nominally accelerates from 135 MeV to 239 MeV) off its accelerating crest phase by –25 degrees (sets head of bunch at lower energy than tail). The chicane then delays the low-energy bunch head ($\gamma >> 1$) and advances the high-energy bunch tail, compressing the bunch.

Since the accelerating RF wave is sinusoidal and the pre-compressed bunch length (~0.6 mm rms) is not insignificant compared to the S-band (2.856 GHz) RF wavelength (105 mm), there is also a significant 2nd-order chirp on the bunch induced by the RF. If not corrected, this 2nd-order chirp can generate a sharp temporal spike on the bunch if enough compression is applied. This very short, intense spike generates even more CSR power and can amplify the emittance growth.

To remove this 2nd-order chirp, and also to compensate the slight 2nd-order compression effect of the chicane, a short harmonic RF section [4,5] is installed just before the chicane and operated at the *decelerating* crest phase (decelerates from 239 MeV to 220 MeV at –180° here). At *LCLS* this is a 4th harmonic RF section (wavelength of ~26 mm) at X-band frequencies (11.424 GHz). When the X-band peak RF voltage, V_{L1X}, is set properly (typically about 19 MV at *LCLS*), the bunch compression process is quite linear, producing an unchanged temporal distribution, except shorter (*i.e.*, no temporal spikes develop). If the X-band voltage is set too low, the 2nd-order chirp will persist (negative 2nd derivative of energy with time) and a spike will first begin to develop at the *head* of the bunch as the compression is further increased (by setting the L1S phase to more negative values). If the X-band voltage is set too high, the 2nd-order chirp will flip sign (positive 2nd derivative) and a spike will begin to develop, first at the *tail* of the bunch. If the L1X voltage is set at the ideal voltage, no spikes will develop.

In order to see the effects these spikes have on the CSR-induced kicks as a function of the compression level and in a time-resolved way, we have carried out an experiment using the 'SQ11' skew quad and the 'OTR12' screen (see Figure 1), where the L1X voltage is varied

ISBN 978-3-95450-123-6

APEX INITIAL COMMISSIONING RESULTS*

D. Filippetto†, B. Bailey, K. Baptiste, J. Corlett, C. Cork, S. De Santis, S. Dimaggio, L. Doolittle, J. Doyle, G. Huang, H. Huang, T. Kramasz, S. Kwiatkowski, R. Lellinger, V. Moroz, W.E. Norum, C. Pappas, C.F. Papadopoulos, G. Portmann, C. Pogue, F. Sannibale, J. Staples, M. Vinco, R. Wells, M. Zolotorev, F. Zucca, LBNL, Berkeley, CA94720, U.S.A.

Abstract

APEX, the Advanced Photo-injector Experiment at the Lawrence Berkeley National Laboratory, is devoted to the development of a MHz-class repetition rate high-brightness electron injector for X-ray FEL applications. The injector is based on a new concept photocathode gun utilizing a room-temperature 186 MHz RF cavity operating in CW mode in conjunction with high quantum efficiency semiconductor photocathodes capable of delivering the required charge at repetition rates consistent with commercially available laser technology. APEX is organized in three main phases. Phase 0 demonstrates several important milestones for the project: gun cavity conditioning to full RF power in CW mode to demonstrate the required field at the cathode; the gun vacuum performance impacting the lifetime of photo-cathodes; and tests of several different photocathodes at full repetition rate at the nominal gun energy of 750 keV. Phase I, continues cathode studies with a new suite of beam diagnostics added to characterize the electron beam at the gun energy and at full repetition rate. In Phase II, a pulsed linac will be added for accelerating the beam to several tens of MeV to reduce space charge effects and measure the high-brightness performance of the gun when integrated in an injector scheme. Phase 0 is presently under commissioning, and the first experimental results from this phase are presented.

INTRODUCTION

The construction of several linac based MHz repetiton rate facilities serving multiple independent FELs has recently been proposed [1, 2, 3, 4], supported by a strong demand from FEL users [5], to be able to extend FEL performance to MHz and beyond, allowing for experiments where large statistical samples are required, and dramatically decreasing the time required to perform experiments.

The APEX project is aiming to the construction and test of an high repetition rate (MHz) high brightness photogun capable of producing bunches with brightness high enough to drive an X-ray FEL, but with an average current 10^4 times higher than the present rf guns. The successful normal-conducting (NC) high-frequency (greater than 1 GHz) high-brightness technology used in present low repetition rates X-ray FEL RF guns [6] can indeed not be scaled to repetition rates beyond $\sim$ 10 kHz because the heat load due to Omhic losses in the gun cavity becomes too large for being dissipated by the cooling system [7]. Many alternative electron gun schemes and technologies are being pursued around the world in order to achieve the required brightness at high repetition rates [8] but at the present time none have demonstrated the necessary set of requirements [9].

The Advanced Photo-injector EXperiment (APEX) [10] is designed to fill that gap by developing a gun and an injector capable of the required performance. The gun, based on a novel concept [11, 12], has been fabricated and recently completed the first phase of its commissioning. All the performance milestones included in this part of the project were successfully achieved and this paper reports the results of the related tests.

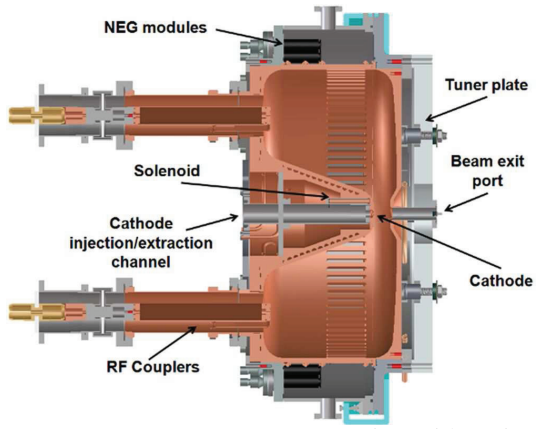

Figure 1: APEX VHF Gun cross section with main components.

APEX, THE ADVANCED PHOTO-INJECTOR EXPERIMENT

APEX is an electron injector built around a RF photogun based on reliable and mature mechanical and RF technologies. The core of the gun is a NC copper RF cavity operating in continuous wave (CW) mode in the VHF band at 186 MHz. The frequency value is chosen to be close to either the 7^{th} sub-harmonic of 1.3 GHz or the 8^{th} subharmonic of 1.5 GHz, making the gun operation compatible with both of the main super-conducting electron linac technologies presently available [13, 14].

Figure 1 shows a CAD cross section of the cavity with its main components, and Table 1 contains the VHF gun main design parameters selected to satisfy the requirements set in reference [9]. The resonant copper structure is sur-

* Work supported by the Director of the Office of Science of the US Department of Energy under Contract No. DEAC02-05CH11231

† Dfilippetto@lbl.gov

ISBN 978-3-95450-123-6

OPTICAL DIFFRACTION RADIATION INTERFERENCE AS A NON-INTERCEPTING EMITTANCE MEASUREMENT FOR HIGH BRIGHTNESS AND HIGH REPETITION RATE ELECTRON BEAM

A. Cianchi*, University of Rome "Tor Vergata" and INFN, V. R. Scientifica 1, 00133 Rome, Italy
M. Castellano, E. Chiadroni, LNF-INFN, V. E. Fermi 40, 00044 Frascati (Rome), Italy
L. Catani, INFN- Roma Tor Vergata, V. R. Scientifica 1, 00133 Rome, Italy
V. Balandin, N. Golubeva, K. Honkavaara, G. Kube, DESY, Notkestrasse 85, 22607 Hamburg, Germany
M. Migliorati, Dept. SBAI, Sapienza University of Rome ,Via A. Scarpa 16, 00161 Roma, Italy

Abstract

Conventional intercepting transverse electron beam diagnostics, as the one based on Optical Transition Radiation (OTR), cannot tolerate high power beams without significant mechanical damages of the diagnostics device. Optical Diffraction Radiation (ODR), instead, is an excellent candidate for the measurements of the transverse phase space parameters in a non-intercepting way. One of the main limitations of this method is the low signal to noise ratio, mainly due to the synchrotron radiation background. This problem can be overcome by using ODRI (ODR Interference). In this case the beam goes through slits opened in two metallic foils placed at a distance shorter than the radiation formation zone. Due to the shielding effect of the first screen a nearly background-free ODR interference pattern can be measured allowing the determination of the beam size and the angular divergence. We report here the result of the first measurements of the beam emittance using ODRI carried out at FLASH (DESY). Our result demonstrates the potential of this technique suitable to be used as non-intercepting diagnostic for accelerators operated with high brightness and high repetition rate electron beams.

INTRODUCTION

High brightness or high repetition rate beams can deposit a large amount of energy in the intercepting diagnostic devices, enough to destroy them. Non-intercepting devices are needed in order to avoid such a problem. The laser wire [1] is an attractive option, facing however tight mechanical and optical requirements. The angular distribution of far field Optical Diffraction Radiation (ODR) has been proposed several years ago [2] as non-intercepting device to measure the beam size, which is the fundamental parameter in order to determine the emittance value. In ODR based measurements, the beam goes through a hole in a metallic screen. When the radial extension of the electromagnetic field (in the order of $\gamma\lambda$, being γ the relativistic factor and λ the observed wavelength) is larger than the hole size, it interacts with the screen resulting in the emission of ODR.

The first measurement of the beam size ever using ODR has been realized at KEK [3], showing both the large potential of this technique as well as some unexpected problems. The Synchrotron Radiation (SR) background, produced by magnetic elements upstream the diagnostic station and scattered around the beam pipe, can hide or confuse the signal from ODR. Therefore, in order to avoid a systematic error in beam size measurements [2], ODR based technique requires a complementary diagnostic device to align the beam into the center of the slit.

* cianchi@roma2.infn.it

ODRI

A detailed description of the ODRI physics, as well as the used formulas and approximations, can be found in [4]. Here we just emphasize the principal features.

We considered the realization of an apparatus that can measure electron beam sizes down to ten of microns at an energy of about 1 GeV using DR emitted at optical wavelengths. All the dimensions in the following description can be rescaled in order to fit different scenarios. To shield the SR we have placed a second metallic screen with an aperture in front of the slit at a distance of a couple of centimeters. A schematic sketch of the layout is shown in Fig. 1.

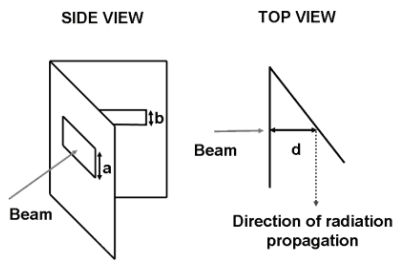

Figure 1: Sketch of the two-slits setup.

At GeV range energy the radiation formation length ($L \approx \gamma^2\lambda$) in the optical wavelength range is of the order of few meters. A metallic screen with 1 mm slit is placed normal to the beam axis. A second 0.5 mm wide slit, opened by means of lithographic technique on a silicon aluminized wafer, is placed at 45 degrees with respect to the beam axis. The distance between the centers of the two apertures is about 2 cm.

When a charge passes through the first aperture forward diffraction radiation (FDR) is emitted. It interferes with the backward diffraction radiation (BDR), produced by the interaction of the EM field with the second screen. The first screen acts also as a mask for the SR background. Although the best choice for SR masking would be the use of two identical slit apertures, the two DR fields would cancel,

ISBN 978-3-95450-123-6

FIRST OBSERVATION OF OPTICAL CURRENT NOISE SUPPRESSION BELOW THE SHOT-NOISE LIMIT

A. Gover, A. Nause, E. Dyunin, Tel Aviv University, Israel

Abstract

In this paper we present experimental results that demonstrate noise suppression in the optical regime, for a relativistic e-beam, below the well-known classical shot-noise limit. Shot-noise amplitude is linear to the e-beam current due to the random nature of particles emission (Poisson statistics) from the cathode. Plasma oscillations driven by collective Coulomb interaction during beam drift between the electrons of a cold intense beam are the source of this phenomenon [1]. The effect was experimentally demonstrated by measuring Optical Transition Radiation (OTR) power per unit e-beam pulse charge. The noise suppression effect implies beam charge homogenization (sub-Poissonian particle number distribution) and therefore the spontaneous radiation emission from such a beam would also be suppressed (Dicke's subradiance [2]). This can be utilized to suppress SASE radiation emission in FEL [3],[4]) and enhance the coherence [5] of seed-injected FELs [6] beyond the classical coherence limits.

MAIN

Current shot-noise suppression in an electron beam in the optical frequency regime is an effect of particle self-ordering and charge homogenization on the scale of optical wavelengths [7], which statistically corresponds to the exhibition of sub-Poissonian electron number statistics (similarly to photons in squeezed light [8]). A dispute over the feasibility of this effect is resolved in the experiment reported here [9]. We have evidence for e-beam noise suppression from measurement of the Optical Transition Radiation (OTR) power emitted by a beam upon incidence on a metal screen. The OTR emission is proportional to the current shot noise of the incident beam.

In a randomly distributed stream of particles that satisfies Poison statistics, the variance of the number of particles that pass through any cross section at any time period T is equal to the number of particles N_T that pass this cross section during the same time T, averaged over different times of measurements. Consequently, the current fluctuation is $I = e\sqrt{N_T}/T = e\sqrt{I_b T e}/T = \sqrt{eI_b T}$. When formally calculated, the average beam shot-noise spectral power $(-\infty < \omega < \infty)$ is:

$$\overline{|\breve{I}(\omega)|^2} = eI_b \qquad (1)$$

here $I(t)$ is the beam current modulation, and the Fourier Transform is defined as $\breve{I}(\omega) = \int_{-\infty}^{\infty} e^{i\omega t} I(t) dt$.

In RF accelerators it is usually assumed that collective inter-particle interaction is negligible during beam acceleration and transport, and the shot-noise limit 1 applies. However, with recent technological advances in RF accelerators, and in particular the development of photocathode guns [10], high quality cold and intense RF- LINAC-accelerated electron beams are available, and the neglect of collective micro-dynamic interaction effects in the transport of such electron beams is no longer justified. Effects of coherent OTR emission and super-linear scaling with I_b of the OTR emission intensity were observed in SLAC 's LCLS injector [11] and other labs [12]. These effects, originally referred to as "unexplained physics" [13], are now clearly recognized as the result of collective Coulomb micro-dynamic interaction and establishment of phase correlation between the electrons in the beam. In these cases, however, the collective interaction led to shot-noise and OTR power enhancement (gain), and not to suppression. Collective effects were shown to be responsible also for beam instabilities (micro-bunching instability) which were observed in dispersive e-beam transport elements [14],[15] Recently Musumeci et al demonstrated in Pegasus collective microdynamic evolution of 1THz coherent single-frequency current modulation [16], but no stochastic optical noise suppression effect could be observed.

While noise gain due to collective interaction has been demonstrated in numerous labs, the notion of beam noise suppression at optical frequencies1 has been controversial (though analogous effects were known in non-relativistic microwave tubes [17]). To explain the physics of the noise suppression, we point out that in the e-beam frame of reference the effect of noise suppression comes into expression as charge homogenization. A simple argument shows that the space-charge force, which is directed to expand higher density charge bunches, has a dominant effect over the randomly directed Coulomb repulsion force between the particles (see Fig. 1).

Assume that in some regions of the beam, there is higher particle-density bunching. Encompassing such a bunch within a sphere of diameter d'. The excess charge in this sphere is $e\Delta N'$, and the potential energy of an electron on the surface of the sphere is $\epsilon_{sc} = e^2\Delta N'/(2\pi\epsilon_0 d'$. This potential energy turns in time into kinetic energy of electrons, accelerated in the direction of bunch expansion (homogenization). At the same time, the electron also possesses an average potential energy due to the Coulomb interaction with neighbor electrons at an average distance ${n'_0}^{-1/3}$ (n'_0 is the average density in the beam frame). This potential energy $\epsilon_{Coul} = e^2(4\pi\epsilon_0 {n'_0}^{-1/3}$ turns into kinetic energy of electrons that are accelerated in random directions. In a randomly distributed electron beam that satisfies

ISBN 978-3-95450-123-6

THE NOVOSIBIRSK TERAHERTZ FEL FACILITY – CURRENT STATUS AND FUTURE PROSPECTS*

O.A.Shevchenko#, V.S.Arbuzov, K.N.Chernov, E.N.Dementyev, B.A.Dovzhenko, Ya.V.Getmanov, E.I.Gorniker, B.A.Knyazev, E.I.Kolobanov, A.A.Kondakov, V.R.Kozak, E.V.Kozyrev, V.V.Kubarev, G.N.Kulipanov, E.A.Kuper, I.V.Kuptsov, G.Ya.Kurkin, L.E.Medvedev, L.A.Mironenko, V.K.Ovchar, B.Z.Persov, A.M.Pilan, V.M.Popik, V.V.Repkov, T.V.Salikova, M.A.Scheglov, I.K.Sedlyarov, G.V.Serdobintsev, S.S.Serednyakov, A.N.Skrinsky, S.V.Tararyshkin, V.G.Tcheskidov, N.A.Vinokurov, M.G.Vlasenko, P.D.Vobly, V.N.Volkov, BINP, Novosibirsk, Russia

Abstract

The Novosibirsk terahertz FEL facility is based on the normal conducting CW energy recovery linac (ERL) with rather complicated lattice. This is the only multiorbit ERL in the world. It can operate in three different modes providing electron beam for three different FELs.

The first FEL works for users since 2003. This FEL radiation is used by several groups of scientists which include biologists, chemists and physicists. Its maximum average and peak powers are 500 W and 1MW and wavelength can be tuned from 110 up to 240 microns. The high peak and average powers are used in experiments on material ablation and biological objects modification. The second FEL is installed on the second orbit. The first lasing of this FEL was achieved in 2009. Its radiation has almost the same average and peak powers and is delivered to the same user stations as the first FEL one, but its tunability range lies between 35 and 80 microns. The third FEL will be installed on the fourth orbit.

In this paper we report the latest results obtained from the operating FELs as well as our progress with the commissioning of the two remaining ERL orbits. We also discuss possible options for the future upgrade.

ACCELERATOR DESIGN

The Novosibirsk FEL facility is based on the multiturn energy recovery linac (ERL) which scheme is shown in Fig. 1. In this scheme the beam goes through the linac several times before it enters undulator. As the result one can increase the final electron energy.

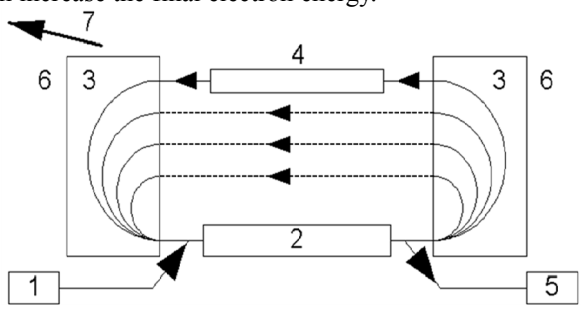

Figure 1: Simplest multiturn ERL scheme: 1 – injector, 2 – linac, 3 – bending magnets, 4 – undulator, 5 – dump.

Multiturn ERLs look very promising for making ERLs less expensive and more flexible, but they have some serious intrinsic problems. Particularly in the simplest scheme shown in Fig.1 one has to use the same tracks for accelerating and decelerating beams which essentially complicates adjustment of the magnetic system. This problem can be solved by using more sophisticated scheme based on two linacs [1].

At present the Novosibirsk ERL is the only one multiturn ERL in the world. It has rather complicated lattice as it can be seen from Fig. 2. The ERL can operate in three modes providing electron beam for three different FELs. The whole facility can be treated as three different ERLs (one-turn, two-turn and four-turn) which use the same injector and the same linac. The one-turn ERL is placed in vertical plane. It works for the THz FEL which undulators are installed at the floor. This part of the facility is called the first stage. It was commissioned in 2003 [2].

The other two ERL beamlines are placed in horizontal plane at the ceiling. At the common track there are two round magnets. By switching these magnets on and off one can direct the beam either to horizontal or to vertical beamlines. The 180-degree bending arcs also include small bending magnets with parallel edges and quadrupoles. To reduce sensitivity to the power supply ripples, all magnets on each side are connected in series. The quadrupole gradients are chosen so that all bends are achromatic. The vacuum chambers are made from aluminium. They have water-cooling channels inside.

The second horizontal track has bypass with the second FEL undulator. The bypass provides about 0.7 m lengthening of the second orbit. Therefore when the beam goes through the bypass it returns back to the linac in decelerating phase and after two decelerations it finaly comes to the dump. This part (the second stage) was commissioned in 2009. The final third stage will include full-scale four-turn ERL and FEL installed on the last track.

The basic beam and linac parameters common for all three ERLs are listed in Table 1.

*Work supported by the Ministry of Education and Science of the Russian Federation; RFBR grant 11-02-91320
#O.A.Shevchenko@inp.nsk.su

ISBN 978-3-95450-123-6

ACCELERATOR BEAMLINE PERFORMANCE FOR THE IR FEL AT THE FRITZ-HABER-INSTITUT, BERLIN

H. P. Bluem#, D. Dowell*, H. Loos*, J. Park, A. M. M. Todd and L. M. Young*
Advanced Energy Systems, Medford, NY, USA.
S. Gewinner and W. Schöllkopf
Fritz-Haber-Institut der Max-Planck-Gesellschaft, Berlin, Germany.

Abstract

An electron accelerator and beamline for an IR and THz FEL with a design wavelength range from 4 to 500 μm has been commissioned by Advanced Energy Systems at the Fritz-Haber-Institut (FHI) [1] in Berlin, Germany, for applications in molecular and cluster spectroscopy as well as surface science. The linac comprises two S-band standing-wave copper structures and was designed to meet challenging specifications, including a final energy adjustable in the range of 15 to 50 MeV, low longitudinal emittance (< 50 keV-psec) and transverse emittance (< 20 π mm-mrad), at more than 200 pC bunch charge with a micro pulse repetition rate of 1 GHz. First lasing was achieved February 2012.

INTRODUCTION

The FHI FEL shown in Figure 1 will be utilized for research in gas-phase spectroscopy of (bio-)molecules, clusters, and nano-particles, as well as in surface science. Advanced Energy Systems (AES) has designed and installed the accelerator and electron beam transport system. STI Optronics fabricated the 40 mm-period MIR undulator [2] with Bestec GmbH delivering the MIR oscillator mirror optical equipment [3]. The FIR beamline has not yet been installed. We describe the achievement of first light at 16 microns and present the performance milestones achieved.

SYSTEM DESCRIPTION

The design, fabrication and installation of the FEL has been described previously [4,5,6]. The accelerator system is comprised of a gridded gun followed by a 1 GHz sub-harmonic buncher and two 3 GHz, pi/2 copper linac structures. A chicane between the linacs affords bunch length control of the 20 MeV beam out of linac-1. Linac-2 can then be operated in accel or decel mode to provide beams at 15 to 50 MeV to isochronous bends directing beam to the undulators or to a diagnostic station.

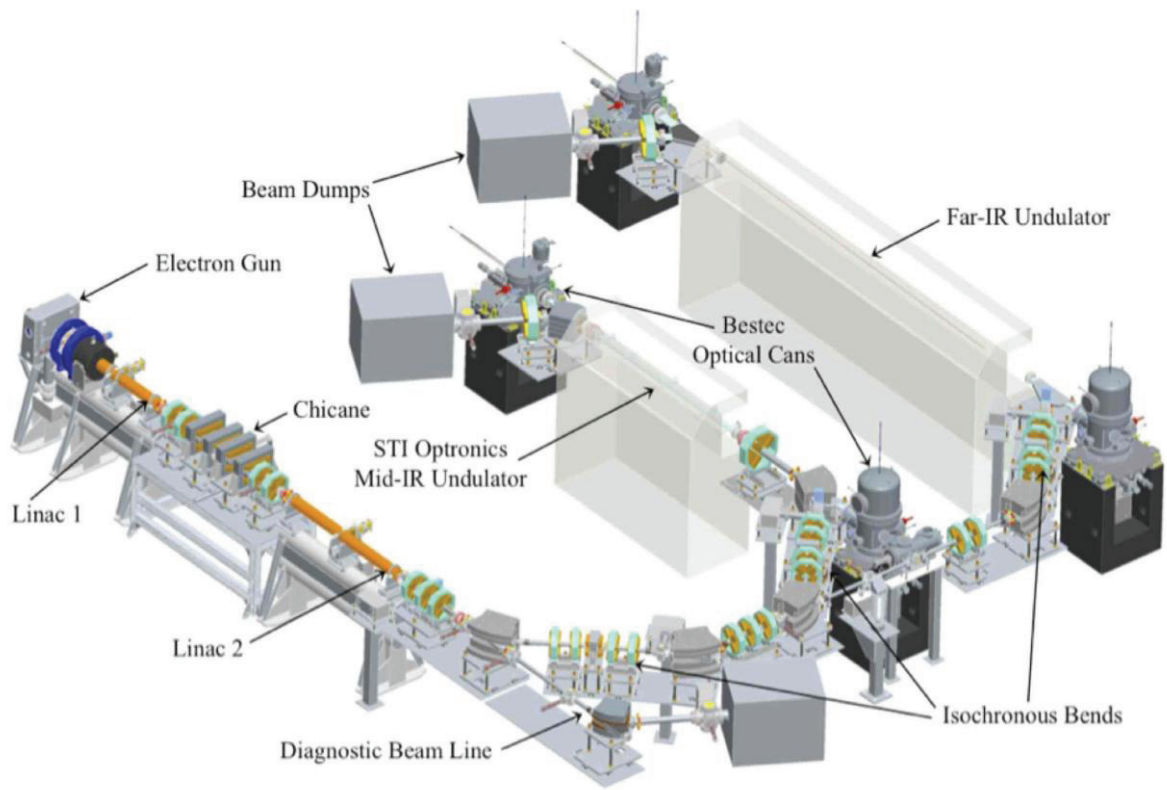

Figure 1: Schematic diagram of the Fritz Haber Institute FEL showing key components.

hans_bluem@mail.aesys.net
* Consultants to AES

ISBN 978-3-95450-123-6

FREE ELECTRON LASERS IN 2012

J. Blau#, K. Cohn, W. B. Colson, A. Laney and J. Wilcox
Physics Department, Naval Postgraduate School, Monterey CA 93943 USA

Abstract

Thirty-six years after the first operation of the free electron laser (FEL) at Stanford University, there continue to be many important experiments, proposed experiments, and user facilities around the world. Properties of FELs operating in the infrared, visible, UV, and X-ray wavelength regimes are tabulated and discussed.

The following tables list existing (Table 1) and proposed (Tables 2, 3) relativistic free electron lasers (FELs) in 2012. The 1st column lists a location or institution, and the FEL's name in parentheses. References are listed in Tables 4 and 5; another useful reference is http://sbfel3.ucsb.edu/www/vl_fel.html.

The 2nd column of each table lists the operating wavelength λ, or wavelength range. The longer wavelength FELs are listed at the top and the shorter wavelength FELs at the bottom of each table. The large range of operating wavelengths, seven orders of magnitude, indicates the flexible design characteristics of the FEL mechanism.

In the 3rd column, t_b is the electron bunch duration (FWHM) at the beginning of the undulator, and ranges from almost CW to short sub-picosecond time scales. The expected optical pulse length in an FEL oscillator can be several times shorter or longer than the electron bunch depending on the optical cavity Q, the FEL desynchronism and gain. The optical pulse can be many times shorter in a high-gain FEL amplifier. Also, if the FEL is in an electron storage-ring, the optical pulse is typically much shorter than the electron bunch. Most FEL oscillators produce an optical spectrum that is Fourier transform limited by the optical pulse length.

The electron beam kinetic energy E and peak current I are listed in the 4th and 5th columns, respectively. The next three columns list the number of undulator periods N, the undulator wavelength λ_0, and the rms undulator parameter $K=eB\lambda_0/2\pi mc^2$ (cgs units), where e is the electron charge magnitude, B is the rms undulator field strength, m is the electron mass, and c is the speed of light. For an FEL klystron undulator, there are multiple undulator sections as listed in the N-column; for example 2x7. Some undulators used for harmonic generation have multiple sections with varying N, λ_0, and K values as shown. Some FELs operate at a range of wavelengths by varying the undulator gap as indicated in the table by a range of values for K. The FEL resonance condition, $\lambda = \lambda_0(1+K^2)/2\gamma^2$, relates the fundamental wavelength λ to K, λ_0, and the electron beam energy $E=(\gamma-1)mc^2$, where γ is the relativistic Lorentz factor. Some FELs achieve shorter wavelengths by using coherent harmonic generation (CHG), high-gain harmonic generation (HGHG), or echo-enabled harmonic generation (EEHG).

The last column lists the accelerator types and FEL types, using the abbreviations listed after Table 3.

The FEL optical power is determined by the fraction of the electron beam energy extracted and the pulse repetition frequency. For the conventional oscillator in steady-state, the extraction can be estimated by 1/(2N); for the high-gain FEL amplifier, the extraction at saturation can be substantially greater. In a storage ring FEL, the extraction at saturation is substantially less than this estimate and depends on ring properties.

In the FEL oscillator, the optical mode that best couples to the electron beam in an undulator of length $L=N\lambda_0$ has a Rayleigh length $z_0 \approx L/12^{1/2}$ and has a fundamental mode waist radius $w_0 \approx (z_0\lambda/\pi)^{1/2}$. The FEL typically has more than 90% of the power in the fundamental mode.

At the 2012 FEL Conference, there were three new lasings reported worldwide: a mid-IR FEL at the Fritz-Haber-Institut (FHI) in Berlin, a THz FEL (FLARE) at Radboud University in Nijmegen, and a direct seeded VUV FEL (sFLASH) at DESY in Hamburg. Progress continues on many other existing and proposed FELs, including several large X-ray FEL facilities around the world.

ACKNOWLEDGMENTS

The authors are grateful for support from ONR.

#blau@nps.edu

ISBN 978-3-95450-123-6

THE CSU ACCELERATOR AND FEL FACILITY*

S. Milton, S. Biedron, T. Burleson, C. Carrico, J. Edelen, C. Hall, K. Horovitz, A. Morin, L. Rand, N. Sipahi, T. Sipahi, CSU, Fort Collins, Colorado, USA
P. van der Slot, Mesa+, Enschede, NL and CSU, Fort Collins, Colorado, USA
H. Yehudah, Morgan Park Academy, Chicago, Illinois, USA
A. Dong, University of Illinois, Urbana, Illinois, USA

Abstract

The Colorado State University (CSU) Accelerator Facility will include a 6-MeV L-Band electron linear accelerator (linac) with a free-electron laser (FEL) system capable of producing Terahertz (THz) radiation, a laser laboratory, a microwave test stand, and a magnetic test stand. The photocathode drive linac will be used in conjunction with a hybrid undulator capable of producing THz radiation. Details of the systems used in CSU Accelerator Facility are discussed.

FACILITY GOALS

There is an expanding demand across a wide variety of discipline in academia, laboratories, and industry for particle accelerators [1,2]. The growing demand of trained accelerator experts continues to motivate the expansion of facilities in a university setting dedicated to training engineers and physicists in accelerator technology. Part of the goal of the CSU Accelerator Facility is to provide a place where both accelerator research and training of high-school through post-doctoral students can flourish. The CSU Accelerator Facility will initially focus on generating long-wavelength free-electron lasers, electron-beam components, and peripherals for free-electron lasers and other light sources. It will also serve as a test bed for particle and laser beam research and development.

FACILITY OVERVIEW

There are four major systems to the CSU Accelerator Facility: an accelerator and FEL system, a laser laboratory, a microwave test stand, and a magnetic test stand. A diagram of the setup of the major accelerator and FEL components is shown in Figure 1. Overviews of the accelerator, undulator, the laser laboratory, the microwave test stand, and the magnetic test stand are given in the following sections.

The Accelerator

The linac to be used was constructed by the Los Alamos National Laboratory for the University of Twente. The University of Twente has generously donated the entire system for use at CSU and their team will remain in close collaboration with CSU.

The accelerator is a five and a half cell copper structure operating at an RF frequency of 1.3 GHz. The accelerator will operate at a 10-Hz repetition rate and a micropulse repetition rate of 81.25 MHz (the 16th subharmonic of 1.3 GHz). Additional specifications are given in Table 1.

Table 1: Linear Accelerator Characteristics

Energy	6 MeV
Number of Cells	5 ½
RF Frequency	1.3 GHz
Unloaded Q	18,000
Axial Electric Field	
Cell no. 1	26 MV/m
Cell No. 2	14.4 MV/m
Cell No. 3 - 6	10.6 MV/m
Peak Solenoid Field	1,200 G

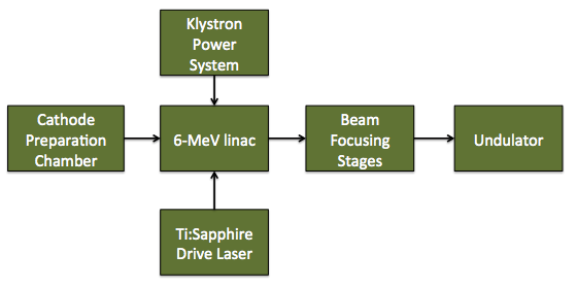

Figure 1: Schematic of the accelerator and FEL.

Initial characterization of a single linac cell was performed using SUPERFISH (Figure 2) [3]. This included an assessment of the variation in resonant frequency due to thermal expansion. Thermal expansion calculations showed a possible shift of about 200 kHz/°C that is acceptable for resonant tuning via water temperature control.

Work is currently being done to build a total cavity model combined with solenoid and beamline models to establish the initial setup requirements for operation.

The cathode preparation chamber for the accelerator can support a variety of cathode types, including those previously used: CsK_2Sb, K_3Sb, and copper. In the high vacuum of the preparation chamber (~$4x10^{-10}$ Torr), it has been demonstrated that acceptable cathode lifetimes can be on the order of days.

* Work supported by Colorado State University, the Office of Naval Research, and the High-Energy Laser Joint Technology Office.
Corresponding author: Milton@engr.colostate.edu

ISBN 978-3-95450-123-6

STATUS OF THE SOLEIL FEMTOSECOND X-RAY SOURCE

O. Marcouille*, L. Cassinari, M.-E. Couprie, P. Hollander, C. Herbeaux, M. Labat, C. Laulhe, J. Luning, V. Leroux, L. Manceron, J.-L. Marlats, T. Moreno, P. Morin, A. Nadji, P. Prigent, J-B. Pruvost, S. Ravy, P. Roy, M. Silly, F. Sirotti, K. Tavakoli, D. Zerbib, J. Zhang.

Synchrotron SOLEIL, L'Orme des Merisiers, Saint-Aubin, BP 48, 91192 Gif-sur-Yvette Cedex, FRANCE.

Abstract

An electron bunch slicing setup is presently under construction on the SOLEIL storage ring for delivering 100 fs (rms) long photon pulses to two undulator-based beamlines providing soft (TEMPO) and hard X-rays (CRISTAL). Thanks to the non-zero dispersion function present in all straight sections of the storage ring, the sliced bunches can be easily separated from the core bunches. The modulator is a wiggler composed of 20 periods of 164.4 mm. It produces a magnetic field of 1.8 T at a minimum gap of 14.5 mm. To modulate the kinetic energy of the electrons in the wiggler, a Ti:Sa laser will be used, which produces 50 fs pulses at 800 nm with a repetition rate of 2.5 kHz. The laser beam is splitted into two branches in order to provide 2 mJ to the modulator and 0.5 mJ as pump pulse for the CRISTAL and TEMPO end stations. Focusing optics and beam path, from the laser hutch to the inside of the storage ring tunnel are presently under finalization. In this paper, we will report on the specificities of the SOLEIL setup, the status of its installation and the expected performances.

INTRODUCTION

SOLEIL is a third generation synchrotron radiation light source operating at 2.75 GeV. The facility produces routinely photon beams of high brightness from infrared (IR) to hard X-Rays with short pulses (20 ps FWHM) whose duration is determined by the electron bunch structure. Going down to the pico or sub-picosecond range is of great interest for studies of the dynamics of the chemical reactions, phase transitions and rapid structural changes in crystals, but is hardly achievable with the usual optics of storage ring [1]. A Slicing-based facility [2] is presently under construction at SOLEIL. The concept is based on the interaction between a short (50 fs) laser pulse operating at 800 nm and electrons oscillating in a wiggler, called "modulator". The exchange of energy between electrons and the laser pulses is driven by the analytical expression:

$$\frac{d\gamma}{dt} = \frac{-e}{m_0 c}\vec{E}.\vec{\beta} \quad (1)$$

Where γ, e and m_0 are respectively the relativistic factor, the charge and rest mass of the electrons, c the light celerity, $\vec{E}$ and $\vec{\beta}$ the electric field of the laser and the normalized speed of the electrons in the modulator. Considering a planar wiggler generating a vertical magnetic field as a modulator, the exchange differs from 0 if laser is horizontally polarized and if the fundamental wavelength λ_{RS} of the modulator equals the laser wavelength λ_L:

$$\lambda_L = \lambda_{RS} = \frac{\lambda_w}{2\gamma^2}\left[1 + \frac{K^2}{2}\right] \quad (2)$$

where λ_w is the modulator period and K the deflection parameter defined as:

$$K = 0.934\, B_0[T]\, \lambda_w[cm] \quad (3)$$

where B_0 is the peak magnetic field. The interaction between laser pulses and electrons results in a modulation in energy of the electron bunches which is converted into spatial (longitudinal) modulation inside the electron bunches. Assuming the use of a modulator generating a vertical magnetic field and a horizontal polarized laser, the maximum energy modulation $\Delta\gamma_{max}$ is given by [3]:

$$\Delta\gamma_{max} \approx \frac{2}{m_0 c^2}.\sqrt{5.A_L.\alpha.h.\frac{c}{\lambda}}\left\{J_0\left[\frac{K^2}{2}(2+K^2)\right] - J_1\left[\frac{K^2}{2}(2+K^2)\right]\right\} \quad (4)$$

where A_L is the laser pulse energy, α the fine structure constant, h the Planck constant, J_0 and J_1 the Bessel function of order 0 and 1.

Slicing was demonstrated experimentally at ALS [4] and is now used routinely at BESSY II [5], SLS [6] and ALS upgrade [7] and new setup with 2 stages of energy modulation have been proposed [8] . The slicing setup of SOLEIL presents some particularities. Firstly, several beamlines are able to use the ultra-short pulses simultaneously such as CRISTAL and TEMPO operating respectively in the 4 keV-30 keV range and 50 eV-1.5 keV range. Second, the spatial separation between the core beam and the sliced beam is performed without using any additional magnetic elements since all straight sections (SS) have a non-zero horizontal dispersion. Third, the radiation produced by the modulator will be routinely used as a source for the PUMA beam line, dedicated for the study of ancient materials [9].

This paper presents the progress of the construction of the femtosecond X-ray source: the modulator, the laser system and the diagnostics of the slicing effect.

LASER SYSTEM

The laser characteristics are presented in Table 1. The laser is already installed in the CRISTAL beamline. It serves in particular for IR pump-X ray probe experiment

* corresponding author: marcouille@synchrotron-soleil.fr

ISBN 978-3-95450-123-6

STATUS OF THE FLASH II PROJECT

K. Honkavaara,* S. Ackermann, V. Ayvazyan, N. Baboi, V. Balandin, W. Decking, S. Düsterer, H.-J. Eckoldt, B. Faatz, M. Felber, J. Feldhaus, N. Golubeva, M. Körfer, M. Kuhlmann, T. Laarmann, A. Leuschner, L. Lilje, T. Limberg, N. Mildner, D. Nölle, F. Obier, A. Petrov, E. Plönjes, K. Rehlich, H. Remde, H. Schlarb, B. Schmidt, M. Schmitz, M. Scholz, S. Schreiber, H. Schulte-Schrepping, J. Spengler, M. Staack, N. Stojanovic, K. Tiedtke, M. Tischer, R. Treusch, M. Vogt, H.C. Weddig, T. Wohlenberg
Deutsches Elektronen-Synchrotron (DESY), Hamburg, Germany
M. Drescher, A. Hage, V. Miltchev, R. Riedel, J. Rönsch-Schulenburg, J. Rossbach, M. Schulz, A. Willner
University of Hamburg, Hamburg, Germany
F. Tavella
Helmholtz-Institute Jena, Jena, Germany

Abstract

The extension of the FLASH facility at DESY (Hamburg, Germany) – FLASH II Project – is under way. The extension includes a second undulator line with variable gap undulators to allow a more flexible operation, and a new experimental hall for photon experiments. The present FLASH linac will drive the both undulator beamlines. Civil construction of the new buildings has been started in autumn 2011 continuing in several steps until spring 2013. The design of the new electron beamline including the extraction from the FLASH linac and the undulator section is mostly finished, and the manufacturing of the components is under way. Design of the photon beamline and layout of the experimental hall is in an advanced stage. The beamline mounting starts end of 2012, and the commissioning with beam is scheduled for the second half of 2013.

INTRODUCTION

FLASH [1–4], the free-electron laser (FEL) user facility at DESY, delivers high brilliance XUV and soft x-ray FEL radiation for photon experiments since summer 2005. In order to provide more beam time for user experiments and to improve the properties of the delivered FEL radiation, an extension of the FLASH facility – the FLASH II Project [5, 6] – was proposed in 2008 by DESY in collaboration with Helmholtz Zentrum Berlin (HZB). The project has been approved in 2010 and the civil construction started in 2011. The first beam of the extended facility is foreseen in late summer 2013.

LAYOUT

The present FLASH facility consists of an injector with a laser driven RF-gun to produce high quality electron bunches, a superconducting linac with TESLA type accelerator modules to accelerate the electron beam up to 1.25 GeV, and an undulator section with fixed gap undulators to produce SASE (Self Amplified Spontaneous Emission) FEL radiation. The total length of the facility including the experimental hall is about 315 meters. More details of FLASH and its parameters are, for example, in [2, 3].

The aim of the FLASH II project is to extend FLASH with a second undulator line to allow a more flexible operation and more beam time for photon experiments with improved photon beam properties. The FLASH linac drives both undulator lines: the present fixed gap undulator line (referred here as FLASH1) and the new variable gap undulator line (referred here as FLASH2). The separation between the two beamlines is downstream of the last accelerating module. Figure 1 shows the layout of the extended FLASH facility; the location of the HHG (High Harmonic Generation) seeding experiment sFLASH [7, 8] is indicated as well.

The FLASH2 undulator beamline will be placed in a new building separated from the existing FLASH tunnel. It provides enough space for future upgrades, like a third undulator line. The FLASH2 photon beamlines and experiments are located in a new experimental hall. Since most of civil construction and installation work in the new beamline building and experimental hall can take place while FLASH accelerator is in operation, the interruptions of FLASH operation could be limited to two short periods: the first one (3.5 months) has already taken place in autumn 2011, and the second one (4 months) is scheduled for spring 2013.

The extraction of the electron beam is realized by a kicker-septum system. The superconducting accelerating modules have a long RF-pulse allowing operation with up to 800 μs long electron bunch trains. The repetition rate is 10 Hz. The bunch train can be divided between the two undulator lines by using a flat-top kicker with a fast rise (or fall) time less than 50 μs. The extraction angle between FLASH1 and FLASH2 is large (12 deg). Therefore the

* katja.honkavaara@desy.de

ISBN 978-3-95450-123-6

UPGRADES OF THE PHOTOINJECTOR LASER SYSTEM AT FLASH

S. Schreiber*, M. Gross, C. Grün, O. Hensler, G. Klemz, K. Klose, G. Koss, S. Schulz, T. Schulz, M. Staack, DESY, Hamburg and Zeuthen, Germany
I. Will, I.H. Templin, H. Willert, MBI, Berlin, Germany

Abstract

The photoinjector of FLASH uses an RF gun equipped with cesium telluride photocathodes illuminated by appropriate UV laser pulses as a source of ultra-bright electron beams. The superconducting accelerator of FLASH is able to accelerate 800 µs long trains of thousands of electron bunches in a burst mode. This puts special demands on the design of the laser system, since it has to produce flat pulse trains with a flexible pattern. The construction of a second undulator beamline FLASH2 has started. The pulse train will be divided into two parts to serve both beamlines simultaneously. Since experiments with the FLASH soft X-ray beam need flexibility, we plan to use two laser systems each serving one beamline. This makes it possible to deliver two trains with different properties in charge, number of bunches, and bunch spacing in the same RF pulse. This also required an upgrade of the laser beamline design. Moreover, we report on recent improvements in arrival time stabilization.

INTRODUCTION

Since 2005, the free-electron laser FLASH at DESY, Germany operates as a user facility providing laser-like radiation pulses from the XUV to the soft X-ray wavelength regime with durations down to a few ten femtoseconds.[1] FLASH uses L-band superconducting TESLA-type accelerating technology. The acceleration is driven by long RF pulses with a length of 1.5 ms, and a usable flat part for acceleration of 0.8 ms. The repetition rate is 10 Hz, the RF frequency 1.3 GHz. With seven accelerating modules installed, the beam energy of FLASH reaches 1.25 GeV.

The high duty cycle is efficiently used by accelerating bursts (or trains) of electron bunches. The standard operation mode is 800 bunches spaced by 1 µs (1 MHz) in a pulse train.

THE ELECTRON SOURCE

The electron source is based on a normal conducting RF-gun operated with a 10 MW, 1.3 GHz klystron at a repetition rate of 10 Hz. The RF pulse length is up to 850 µs, sufficient for generation of the required bunch trains of 800 µs duration.

In order to keep the average power of the laser system reasonably small, a photocathode with a high quantum efficiency is used. Cesium telluride has been proven to be a reliable and stable cathode material with a quantum efficiency above 5 % for a wavelength around 260 nm for a long time of more than 170 days of continuous operation [2, 3]. The bunch charge required for FLASH is up to 1 nC, some experiments require up to 3 nC per bunch. Assuming a very conservative quantum efficiency of the cathode of 0.5 %, a laser pulse energy of not more then 3 µJ on the cathode is sufficient to produce a 3 nC electron bunch. For 800 bunches in 800 µs long trains, this corresponds to a reasonable intra train power of 3 W in the UV (average power 24 mW for 10 Hz).

A challenge for the laser system is, that it has to provide the same flat burst structure in the UV as required for the electron beam. In addition, the picosecond long pulses must be synchronized to the RF of the accelerator to substantially better than 1 ps.

THE LASER SYSTEM

The laser systems [4] described in this report have been installed in 2010 [5] and 2012, and are a substantial upgrade compared to the previous lasers in operation at FLASH and the former TESLA Test facility [6, 7]. The lasers have been developed in the Max Born Institute, tested at DESY (PITZ) and finally installed at FLASH.

Recently, a second laser system has been installed, almost identical to the one in operation, The laser system design is described in detail in [4]. Both systems consist of a pulsed laser oscillator with subsequent amplification stages. Figure 1 shows a schematic overview of the laser. The laser material chosen is Nd:YLF, lasing at a wavelength of 1047 nm. The material has together with a high gain, a long upper-state lifetime of 480 µs, and exhibits only a weak thermal lensing. This makes it suitable to produce pulse trains with milliseconds duration. After amplification, the wavelength is converted in two steps using an LBO and BBO to the UV wavelength of 262 nm. Figure 2 shows examples of pulse trains measured with photodiodes.

The pulse energy is adjusted by two remote controlled attenuators. One attenuator is used by a feedback system to compensate for slow drifts in pulse energy, the other by the operators of FLASH. The laser beam is expanded and collimated to overfill a set of remotely controlled hard edge apertures of various sizes. The chosen aperture corresponding to the required transverse size is imaged onto the cathode of the RF-gun. The nominal laser pulse diameter is 1.2 mm flat-hat.

The laser is equipped with a pulse picker which is used by the operator to chose the number of laser pulses,

* siegfried.schreiber@desy.de

ISBN 978-3-95450-123-6

SCHEME FOR GENERATING AND TRANSPORTING THZ RADIATION TO THE X-RAY EXPERIMENTAL HALL AT THE EUROPEAN XFEL

W. Decking, V. Kocharyan, E. Saldin and I. Zagorodnov, DESY, Hamburg, Germany
G. Geloni, European XFEL GmbH, Hamburg, Germany

Abstract

We consider generation of THz radiation from the spent electron beam downstream of the SASE2 undulator in the electron beam dump area. The THz output must propagate at least for 250 meters through the photon beam tunnel to the experimental hall to reach the SASE2 X-ray hutches. We propose to use an open beam waveguide such as an iris guide as transmission line. In order to efficiently couple radiation into the iris transmission line, generation of the THz radiation pulse can be performed directly within the iris guide. The line transporting the THz radiation to the SASE2 X-ray hutches introduces a path delay of about 20 m. Since THz pump/X-ray probe experiments should be enabled, we propose to exploit the European XFEL baseline multi-bunch mode of operation, with 222 ns electron bunch separation, in order to cope with the delay between THz and X-ray pulses. We present start-to-end simulations for 1 nC bunch operation-parameters, optimized for THz pump/X-ray probe experiments. Detailed characterization of the THz and SASE X-ray radiation pulses is performed. Highly focused THz beams will approach the high field limit of 1 V/atomic size.

INTRODUCTION

The exploitation of a high power coherent THz source as a part of the LCLS-II user facility has been proposed in the LCLS-II CDR [1]. THz radiation pulses can be generated by the spent electron beam downstream of the X-ray undulator. In this way, intrinsic synchronization with the X-ray pulses can be achieved. A first, natural application of this kind of photon beams is for the pump-probe experiments. Through the combination of THz pump and X-ray probe, XFELs would offer unique opportunities for studies of ultrafast surface chemistry and catalysis [1]. Also, the LCLS team started an $R\&D$ project on THz radiation production from the spent electron beam downstream of the LCLS baseline undulator [2]-[4]. In that case, THz pulses are generated by inserting a thin Beryllium foil into the electron beam. In this paper we describe a scheme for integrating such kind of radiation source at the European XFEL facility [5].

We begin our considerations with the generation of THz radiation from the spent electron beam downstream of the SASE2 undulator in the electron beam-dump area. We then move to consider the transport of THz radiation pulses from the XFEL beam dump-area to the experimental hall. This constitutes a challenge, because the THz output must propagate at least 250 meters in the photon beam tunnel and in the experimental hall to reach the SASE2 X-ray hutches. Since THz beams are prone to significant diffraction, a suitable beam transport system must be provided to guide the beam along large distances maintaining it, at the same time, within a reasonable size. Moreover, the THz beamline should be designed to obtain a large transmission efficiency for the radiation over a wide wavelength range. Transmission of the THz beam can only be accomplished with quasi-optical techniques. In this paper, similarly as in [6], which focused on the LCLS baseline, we propose to use an open beam waveguide such as an iris guide, that is made of periodically spaced metallic screens with holes, for transporting the THz beam at the European XFEL. The eigenmodes of the iris guide have been calculated numerically for the first time by Fox and Li [7] and later obtained analytically by Vainstein [8, 9]. In [6] we already presented a complete iris guide theory. In particular, the requirements on the accuracy of the iris alignment were studied. In order to efficiently couple radiation into the transmission line, it is desirable to match the spatial pattern of the source radiation to the mode of the transmission line. To this end, it is advisable to generate radiation from the spent electron beam directly in the iris line with the same parameters used in transmission line. In this way, the source generates THz radiation pulses with a transverse mode that automatically matches the mode of the transmission line. The theory described in [6] supports this choice of THz source.

In the present work we present a conceptual design for a THz edge radiation source at the European XFEL. It includes an 80 m-long electron beam vacuum chamber equipped with an iris line, and a 250 m-long transmission line with the same parameters. The transmission line, which develops through the XTD7 distribution tunnel and field 5 of the experimental hall, includes at least ten 90-degrees turns with plane mirrors at 45 degrees as functional components. It is possible to match incident and outgoing radiation without extra losses in these irregularities. The transport line introduces a path delay of about 20 m between THz and X-ray pulses generated from the same electron bunch. Since THz pump/X-ray probe experiments should be enabled, in order to cope with this delay we propose to exploit the unique bunch structure foreseen as baseline mode of operation at the European XFEL, with 222 ns electron bunch separation, together with an additional delay line in experimental hall. More details can be found in [10].

ISBN 978-3-95450-123-6

CONCEPTUAL DESIGN OF AN UNDULATOR SYSTEM FOR A DEDICATED BIO-IMAGING BEAMLINE AT THE EUROPEAN X-RAY FEL

G. Geloni, European XFEL GmbH, Hamburg, Germany
V. Kocharyan and E. Saldin, DESY, Hamburg, Germany

Abstract

We describe a future possible upgrade of the European XFEL consisting of a new undulator beamline dedicated to coherent diffraction imaging of complex molecules. Crucial parameters are photon energy range, peak power, and pulse duration. The peak power is maximized in the photon energy range between 3 keV and 12 keV by the use of a very efficient combination of self-seeding, fresh bunch and tapered undulator techniques. The unique combination of ultra-high peak power of 1 TW in the entire energy range, and ultrashort pulse duration tunable from 2 fs to 10 fs, would allow for single shot coherent imaging of protein molecules with size larger than 10 nm. Also, the new beamline would enable ima ing of large biological structures in the water window, between 0.3 and 0.4 keV. In order to make use of standardized components, at present we favor the use of SASE3-type undulator segments. The number segments, 40, is determined by the tapered length for the design output power of 1 TW. The present plan assumes the use of a nominal electron bunch with charge of 0.1 nC. Experiments would be performed without interference with the other three undulator beamlines.

INTRODUCTION

Structural biology aims at understanding biological functions of proteins by studying their three-dimensional structures. The main technique for elucidating three-dimensional structures of macromolecules is X-ray crystallography (see references in [1]). One of the requirements of X-ray crystallography of biological molecules is that they form crystalline samples large enough for crystallographic study. This requirement severely limits the number of biological molecules that can be studied as many fail to form crystals. The development of XFELs promises to open up new areas in life science by allowing structure determination without the need for crystallization. In fact, as suggested in (see references in[1]), sufficiently short and intense pulses from X-ray lasers may allow for the imaging of single protein molecules.

This article describes a possible future upgrade of the European XFEL. We present a study for a dedicated beamline for single-biomolecular imaging. The main idea is to use one of the free undulator tunnels of the European XFEL for providing the user community with the three SASE1, SASE2 and SASE3 lines, with the addition of a fourth beamline where the combination of 1 TW peak power in the energy range between 3 keV and 13 keV, and tunability of the pulse duration from 2 fs to 10 fs will provide significantly better conditions for single shot coherent imaging of protein molecules than at other XFEL facilities.

The European XFEL equipped with a dedicated bio-imaging beamline represents a development half way in between a proof-of-principle and a fully dedicated bio-imaging XFEL facility with high-rate of protein structure determination. The main advantage of the new beamline is the operation point at 1 TW with 2 fs-5 fs long pulses in the particular energy range between 3 keV and 5 keV, where the diffraction signal is strong. Operation at 1 TW in this peculiar energy range will not be accessible to other XFEL facilities at least until the end of the next decade. These characteristics would enable new exciting possibilities for coherent imaging of protein molecules with size larger than 10 nm.

BASIC CONCEPT OF THE BIO-IMAGING BEAMLINE

For the realization of the bio-imaging beamline we propose to use the same undulator technology optimized for the generation of soft X-rays at the European XFEL. The installation and commissioning of the new beamline can take place gradually. In the beginning, the new beamline would just extend the soft X-ray (SASE3) beamline and take advantage of the long XTD4 tunnel. An additional undulator composed by 19 cells would be added into the 300 m-long XTD4 tunnel. This undulator would extend the existing SASE3 line, composed by 21 cells, and have the same period of SASE3, in order to obtain a total cell number of 40. With this, SASE3 would be de facto converted into a bio-imaging beamline. Then, a new soft X-ray beamline, identical to the SASE3 baseline, could be installed in the free 150 m-long XTD3 tunnel.

Setup Description

The proposed setup is composed of four undulators separated by three magnetic chicanes as shown in Fig. 1. These undulators consist of 4, 3, 4 and 29 undulator cells, respectively. Each magnetic chicane is compact enough to fit one undulator segment. The installation of chicanes does not perturb the undulator focusing system. The implementation of the self-seeding scheme for soft X-ray and hard X-ray would exploit the first and the third magnetic chicane, respectively. Both self-seeding setups should be compact enough to fit one undulator module.

A retractable grating monochromator based on a recent SLAC design (see references in [1]) will be introduced in the space created by the first chicane to enable soft X-ray

ISBN 978-3-95450-123-6

DEPENDENCE OF FEL INTENSITY ON THE AVAILABLE NUMBER OF UNDULATORS FOR FERMI FEL-1*

E. Allaria#, Sincrotrone Trieste, Strada Statale 14 - km 163.5, 34149 Basovizza, Trieste ITALY

Abstract

FERMI@Elettra [1] is a free electron laser user facility based in Trieste Italy. The first FEL line (FEL-1), based on the high gain harmonic generation scheme, covers the spectral range from about 80nm down to 20nm with high quality FEL pulses and started producing FEL light for user operations in 2011. FERMI FEL-1 radiator is composed by six undulators 2.4 meter long with the available space for additional two undulators. In this work we investigate the impact of additional undulators on the FEL performance in the case of FERMI FEL-1. We finally extend the work studying the dependence of the FEL power as a function of the length of the radiator for FELs based on the high gain harmonic generation scheme showing that for typical parameters there is a linear dependence.

INTRODUCTION

The use of harmonic generation to produce FEL pulses at short wavelength starting from an external seed laser at long wavelength has been applied to high gain single pass FELs to generate VUV coherent emission [2]. In the last decade HGHG has been demonstrated and studied in few FEL test facilities [3] and all experiments have shown the capability of HGHG to produce FEL pulses with a well-controlled and narrow bandwidth. Due to the quality of available electron beam parameters and the length of undulators some of these experiments does not necessary implies a strong exponential growth of the power along the undulator that in some cases is just few meter long. In those cases, the FEL power only has coherent emission in the radiator without exponential gain and the process is generally called coherent harmonic generation (CHG) while HGHG should be associated to cases with an exponential growth of the power in the radiator that generally is much longer.

In this work we focus on the impact of the length for the final radiator in the case of a HGHG FEL using the parameters of FERMI as a case study.

As it will be shown the results for HGHG are different from what occurs for a simple FEL amplifier that starts from a week signal. In FEL amplifiers the input signal can be provided by an external source or by the spontaneous emission as in self-amplified spontaneous emission (SASE) [4] and the output power drastically depends on the length of the radiator. Indeed, the power that a FEL amplifier can produce increases exponentially with the length of the available radiator till saturation is reached.

*Work partially supported by the Italian Ministry of University and Research under grants FIRB-RBAP045JF2 and FIRB-RBAP06AWK3
#enrico.allaria@elettra.trieste.it

HGHG AT FERMI

An HGHG or a coherent harmonic generation (CHG) FEL can be divided into three parts, the modulator, the bunching section and the radiator.

In the modulator the electron beam is in resonance with the electromagnetic wave of the external seed laser. Due to the interaction with the seed laser the electron beam become energy modulated with a periodicity equal to the seed wavelength.

The energy modulation is then converted into density modulation when the electron beam is passing through the dispersive section where high-energy electrons perform a path shorter than low energy electrons. Density modulation is created at the seed laser wavelength and its harmonics

The final radiator is set so that the electron beam is at resonance with the desired harmonic of the seed laser. As a consequence of the bunching, electrons will immediately emit coherently and this emission is generally several orders of magnitude larger than the spontaneous emission. In HGHG the further interaction of the electron beam with the produced coherent radiation lead to an increase of the bunching and a rapid increase of the produced FEL radiation.

In a simple view the first part, where only coherent emission is generated, power increases quadratically with the undulator length while an exponential growth of the power along the undulator characterize the second part. In this final part the bunching increase is associated with the self induced effect that characterized high gain FELs

FERMI Parameterts

FERMI uses electron beams accelerated by a normal conducting linear accelerator with electron beam energy in the range between 0.9 and 1.5GeV. Electron bunches with a charge of few hundreds of pC are generated in a high brightness RF photocathode gun. The accelerator has two bunch compressors and has been designed to preserve the high quality and brightness of the beam up to the entrance of the undulator. The design value for the normalized emittance of the electron beam at the undulator entrance is of the order of 1 mm mrad and the energy spread of the order of 100keV. A more detailed description of the accelerator design and configuration is reported in [1].

FEL studies at FERMI started in 2011 demonstrating the capability to generate high quality FEL pulses in the 30 nm spectral range starting from an UV seed laser at about 260nm [5]. Due to incomplete installation of all accelerator components, the electron beam used in the first period of FERMI has not been the final one. In particular the electron beam peak current used during first

ISBN 978-3-95450-123-6

STATUS OF THE DELTA SHORT-PULSE FACILITY*

H. Huck†,
M. Bakr, M. Höner, S. Khan, R. Molo, A. Nowaczyk, A. Schick, P. Ungelenk, M. Zeinalzadeh,
Center for Synchrotron Radiation (DELTA), TU Dortmund University, 44221 Dortmund, Germany

Abstract

Since 2011, a new Coherent Harmonic Generation (CHG) source is under commissioning at the 1.5-GeV storage ring DELTA. Following first experiments using the fundamental wavelength of a Ti:sapphire laser to modulate the electron energy in a small slice of the electron bunches, 400 nm pulses from a second-harmonic conversion unit are used since early 2012. With the radiator tuned to the second harmonic thereof, 200 nm CHG pulses are routinely observed. In order to detect higher harmonics and to proceed to a seed wavelength of 266 nm, an evacuated diagnostics beamline is under construction. Additionally, an existing VUV beamline is being upgraded to allow for the detection of the CHG pulses and their utilization in pump-probe experiments. Furthermore, a dedicated THz beamline provides valuable information about the laser-induced energy modulation of the electrons. In this paper, the status of the project and technical details will be presented.

INTRODUCTION

At free-electron lasers (FELs) based on linear accelerators, good progress is being made in generating ultrashort radiation pulses in the VUV and X-ray regime in order to investigate atomic phenomena on the femtosecond timescale. The large fluctuations of arrival time and spectra of the pulses generated by SASE FELs can be effectively alleviated by seeding the FEL process with external laser pulses, or, most recently, with pulses generated by an upstream undulator [1]. It is nevertheless worthwhile to develop methods to generate ultrashort pulses at conventional synchrotron radiation sources, given the large number of existing facilities and their well-established user communities. One method is Coherent Harmonic Generation (CHG) [2, 3, 4].

The principle of CHG is illustrated in Fig. 1. The interaction between the electrons and a co-propagating laser pulse in a first undulator (the "modulator") causes a periodic energy modulation within a small slice (typically 50 fs long) of the bunch. Tilting the phase-space distribution by means of a dispersive chicane results in microbunches, which radiate coherently at harmonics of the laser wavelength in a second undulator, the "radiator". Typically, the radiator can be tuned to provide ultrashort pulses with reasonable intensity up to the 5th harmonic. Doubling or tripling the frequency of the external laser pulse through nonlinear crystals, as well as the extension of the scheme to so-called Echo-Enabled Harmonic Generation (EEHG) [5], allows for even shorter wavelengths.

At the storage ring DELTA operated by the TU Dortmund University, a new CHG source with focus on user availability is under commissioning since 2011 [6, 7]. The goal is to provide ultrashort pulses at 23 eV (53 nm, the 5th harmonic of 265 nm) for future pump-probe experiments in standard routine operation.

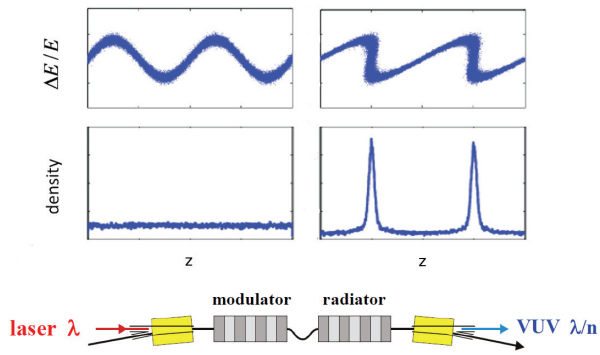

Figure 1: Principle of Coherent Harmonic Generation. In the modulator, a laser pulse imprints an energy modulation onto a short slice of the electron bunch. This slice is micro-bunched in a dispersive chicane, and the micro-bunched electrons then radiate coherently at harmonics of the laser wavelength.

SETUP AND IMPROVEMENTS

DELTA is a 1.5-GeV synchrotron light source with a circumference of 115.2 m (Fig. 2). Located in the northern straight section, the electromagnetic undulator U250 consists of 19 periods of 25 cm each, and was in the past used as optical klystron for storage-ring FEL studies. New power supplies allow separate tuning of the first and last part up to a wavelength of $\lambda = 1$ µm (undulator parameter $K = 12$), while the three central periods serve as a dispersive chicane with magnetic fields up to 0.76 T.

Seed Beamline

A Ti:sapphire laser system (Tab. 1) sends pulses of 35 fs duration through beamline BL3 into the U250 undulator (Fig. 2). The position and size of the laser waist can be changed by remote-controlled mirrors and lenses. A second/third harmonic generation unit (SHG/THG) is located between the laser amplifier and the telescope.

* Work supported by DFG (INST 212/236-1 FUGG), BMBF (05K10PE1, 05K10PEB), and the Federal State NRW
† holger.huck@tu-dortmund.de

ISBN 978-3-95450-123-6

BEAM DYNAMICS DESIGN OF THE CLARA FEL TEST ACCELERATOR

J. W. McKenzie* & P. H. Williams
STFC Daresbury Laboratory, ASTeC & Cockcroft Institute, UK

Abstract

CLARA (Compact Linear Advanced Research Accelerator) is a proposed FEL test facility at Daresbury Laboratory in the UK. This is proposed to be a 250 MeV normal-conducting linac capable of producing short, high brightness electron bunches which can be synchronised with an external source. CLARA will build upon the EBTF photoinjector under construction at Daresbury, utilising the S-band RF electron gun. Bunch compression will be achieved via two methods: a variable magnetic chicane with fourth harmonic cavity, or velocity bunching in the low energy regime. CLARA will be capable of providing beams for various novel FEL schemes.

INTRODUCTION

CLARA is proposed to be the UK's national FEL test facility. The design approach adopted is to build flexibility in both operation and layout, enabling as wide an exploration of FEL schemes as possible. For a full overview of the aims of the project and details of FEL schemes under consideration see [1]. The accelerator design is aimed at being flexible, allowing for various modes of operation at different energies and ultilising different compression methods.

CLARA will be based on normal conducting S-band RF linac structures, with a maximum energy of 250 MeV. Four linac structures will be used. The first one a short 2 m long section, and the next three either 4 or 5 m in length. A schematic is shown in Fig. 1.

There will be two modes of bunch compression in CLARA: the first uses velocity bunching in the first 2 m linac section, and the second uses a magnetic chicane at around 70 MeV. Two modes are proposed for the velocity bunching scheme, one pushing high peak current for single-spike SASE FEL operation, and the other a more generic bunch with around 300 A peak current.

For the seeded FEL schemes, a bunch with a flat current profile over 300 fs is desirable. The long flat-top will help reduce any effects of jitter between the electron bunch and seed laser. Simulations suggest such a bunch cannot be produced by velocity bunching so compression by a magnetic chicane was also investigated. However, a long, flat-top longitudinal profile cannot be produced if the bunch entering the magnetic chicane has curvature in longitudinal phasespace. As such, various options were investigated for correcting this curvature, including introducing non-linear elements, such as sextupoles, into the chicane. It was found that the best solution was to use a higher harmonic cavity before the chicane.

MODES OF OPERATION

Five different FEL modes have currently been identified: long pulse for the seeded FEL experiments, short pulse for SASE, ultra-short pulse for single spike SASE, multibunch mode for an oscillator FEL and a high repetition rate mode. The high repetition rate mode will be a technology demonstrator to push normal conducting linac technology, with the aim being 400 Hz. It is envisaged that to reach this repetition rate, the gradient in the cavities might need to be reduced, so the final electron beam energy could be lower. Bunch charges of up to 250 pC have been investigated, with 100 pC nominal for the velocity bunched schemes and 200 pC for the magnetic compression. For the oscillator FEL, 20 bunches at a spacing of 200 ns will be required. The RF pulse width will need to be able to accommodate this.

PHOTOINJECTOR

The photoinjector for CLARA will be based around that of the Electron Beam Test Facility (EBTF), currently under construction at Daresbury Laboratory [2]. The electron gun in the first stage will be a 2.5 cell normal conducting S-band RF gun, as shown in Fig. 2. This was originally intended for use on the ALPHA-X laser wakefield project [3]. A solenoid surrounds the gun cavity with a bucking coil to zero the magnetic field on the cathode plane. The design gradient is 100 MV/m.

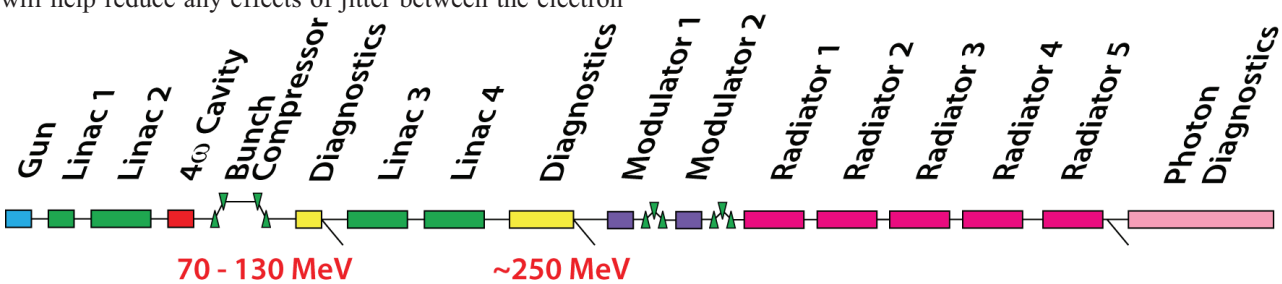

Figure 1: CLARA Schematic.

*julian.mckenzie@stfc.ac.uk

ISBN 978-3-95450-123-6

POTENTIAL FOR LASER-INDUCED MICROBUNCHING STUDIES WITH THE 3-MHz-RATE ELECTRON BEAMS AT ASTA*

A.H. Lumpkin#, J. Ruan, Fermi National Accelerator Laboratory, Batavia, IL 60510, USA
J.M. Byrd, R.B. Wilcox, Lawrence Berkeley National Laboratory, Berkeley, CA 94720, USA

Abstract

Investigations of the laser-induced microbunching as it is related to time-sliced electron-beam diagnostics and high-gain-harmonic generation (HGHG) free-electron lasers using bright electron beams are proposed for the ASTA facility. Initial tests at 40-50 MeV with an amplified 800-nm seed laser beam co-propagating with the electron beam through a short undulator (or modulator) tuned for the resonance condition followed by transport through a subsequent chicane will result in energy modulation and z-density modulation (microbunching), respectively. The latter microbunching will result in generation of coherent optical or UV transition radiation (COTR, CUVTR) at a metal converter screen which can reveal slice beam size, centroid, and energy spread. Additionally, direct assessment of the microbunching factors related to HGHG by measurement of the COTR intensity and harmonic content after the chicane as a function of seed laser power and beam parameters will be done. These experiments will be performed using the ASTA 3-MHz-rate micropulse train for up to 1ms which is unique to test facilities in the USA.

INTRODUCTION

We have identified critical aspects of laser-induced microbunching (LIM) to be explored at the Advanced Superconducting Test Accelerator (ASTA) which relate directly to time-sliced electron-beam diagnostics and seeded free-electron laser (FEL) issues. In the first category the capability of evaluating the electron beam parameters such as beam size, centroid, and energy spread as well as the microbunching factors in sub-ps time slices should be possible by imaging the LIM coherent optical and UV transition radiation (COTR, CUVTR). In the second category, enhanced performance in gain length, spectral bandwidth, central wavelength stability, etc. of free-electron lasers (FELs) can be obtained by seeding the FEL either with electron beam microbunching at the resonant wavelength as in the case of high gain harmonic generation (HGHG), cascaded HGHG, and echo-enhanced harmonic generation (EEHG) [1-3] or by generating a photon beam at short wavelengths such as from a plasma as in high harmonic generation (HHG) [4]. These seeding processes are initiated by co-propagating a laser beam with the electron beam through a short undulator (modulator) tuned to the seed wavelength to generate an energy modulation which is then converted to a z density modulation (microbunching) in a dispersive section such as a chicane. It has been found that the electron beam is also microbunched at the harmonics of the laser fundamental after the chicane, and the radiator undulator is tuned to one of them for the FEL [1]. Yu et al. have reported lasing on the 3rd harmonic of the laser fundamental of 800 nm, and FERMI@Elettra staff have reported recent HGHG results out to the 13th harmonic of 266 nm [5]. The direct measurement of the microbunching by looking at the coherent optical and UV transition radiation (COTR) was first done in a SASE FEL [6], but microbunching generated by LIM has rarely been measured [7]. Moreover, high harmonic content has not been directly observed, but it has been deduced from the HGHG radiator results [8]. Direct microbunching measurements have been proposed on the SDUV FEL in Shanghai [9], and discussions are underway with FERMI@elettra staff for VUV tests on their HGHG FEL. Elucidating the harmonic content, optimizing it, and benchmarking codes would be critical to present and future short wavelength (VUV-soft x-ray) FEL projects based on HGHG or EEHG. Only ASTA has the high-micropulse-repetition rate (3 MHz for 1 ms) beam such as proposed for the next generation of FELs [10], albeit with higher duty factor for the latter.

Our emphasis in this paper is on the use of COTR (ultimately CVUVTR) as a direct microbunching diagnostic with the potential for time–resolved electron beam diagnostics and for benchmarking relevant FEL codes. As context, we point out that there are at least three mechanisms for generating optical-regime microbunching (which can be extended to the VUV) in an electron beam:

1. Longitudinal-space-charge-induced microbunching (LSCIM): This mechanism has been suggested by Saldin et al. [11] to contribute more in the visible wavelength regime than coherent synchrotron radiation (CSR) or wakefields. This effect can be considered as starting from shot noise in the charge distribution that couples through the longitudinal impedance of the transport line and linac into an energy modulation. This energy modulation will become a z-density modulation, or microbunching, after bunch compression in a chicane (or other R_{56} lattice point) [12]. It is generally a broadband effect in wavelength, and most of the gain is in the FIR (>10-μm regime). However, we have the LCLS/SLAC [13], APS/ANL [14], FLASH/DESY [15], and FERMI@Elettra [16] results on COTR in the OTR images and even scintillator screens. Spatially localized enhancements of 10-10,000 at visible wavelengths have been reported which prevent using the

lumpkin@fnal.gov
*Work supported under Contract No. DE-AC02-07CH11359 with the United States Department of Energy.

ISBN 978-3-95450-123-6

DESIGN OF A PROOF-OF-PRINCIPLE EXPERIMENT TOWARD THE GENERATION OF COHERENT OPTICAL RADIATION USING A 4-MeV ELECTRON BEAM*

Y.-E Sun, P. Piot, Fermi National Accelerator Laboratory, Batavia, IL 60510, USA
D. Mihalcea, H. Panuganti, P. Piot
Department of Physics, Northern Illinois University, DeKalb, IL 60115, USA
W.S. Graves, Massachusetts Institute of Technology, Cambridge, MA 02139, USA

Abstract

Transverse-to-longitudinal phase-space-exchange techniques have opened new possibilities towards shaping the temporal distribution of electron beams. Sub-ps bunch trains have been experimentally realized at the A0 photoinjector at Fermilab. Recently, the combination of such emittance-exchange methods with nanocathode arrays was suggested as the backbone of compact coherent short-wavelength sources. In this paper, we discuss a possible proof-of-principle experiment to produce coherent optical transition radiation using a ~ 4 MeV electron bunch. The optically-modulated bunch is produced from a structured cathode combined with a transverse-to-longitudinal phase space exchanger.

INTRODUCTION

It is well known that radiation produced by a bunch of charged particles is greatly enhanced when observed at wavelengths of the order or shorter than the bunch length. In general, the spectral angular fluence emitted by a bunch of $N \gg 1$ electrons from any electromagnetic process is related to the single-electron spectral fluence, $\frac{d^2W}{d\omega d\Omega}\big|_1$, via

$$\frac{d^2W}{d\omega d\Omega}\Big|_N \simeq \frac{d^2W}{d\Omega d\omega}\Big|_1 [N + N^2|S(\omega)|^2$$

where $\omega \equiv 2\pi f$ (f is the frequency) and $S(\omega)$, the bunch form factor (BFF), is the intensity-normalized Fourier transform of the normalized charge distribution $S(t)$ [1]. The former equation assumes the bunch can be approximated as a line charge distribution. Considering a series of N_b identical bunches with normalized distribution $\Lambda(t)$ we have $S(t) = N_b^{-1} \sum_{n=1}^{N_b} \Lambda(t + nT)$ (where T is the period between the bunches) giving $|S(\omega)|^2 = \xi|\Lambda(\omega)|^2$ where $\Lambda(\omega)$ is the Fourier transform of $\Lambda(t)$ and the intra-bunch coherence factor $\xi \equiv N_b^{-2} \sin^2(\omega N_b T/2)/[\sin^2(\omega T/2)]$ describes the enhancement of radiation emission at the resonant frequencies $\omega_n = 2\pi n/T$.

Therefore, coherent optical radiation can be produced by a train of electron bunches with sub-micron separation. The recent experimental demonstration of sub-picosecond electron bunch train generation using an emittance exchange (EEX) technique [2] and its use to produce narrow-band Terahertz transition radiation [3] has open new possibilities.

Recently, it was proposed to adapt this method to generate vacuum-ultraviolet and possibly x-ray coherent radiation using inverse Compton scattering of a pre-bunched beam [4]. Downscaling the pre-bunching wavelength by emittance-exchanging a transversely-segmented beam obtained via interception of the beam with a multi-slit mask is challenging. Instead, Ref. [4] proposes to produce the needed transversely-segmented beam using a patterned cathode such as a field emitter array (FEA). Experimentally validating such a concept is of importance: as the bunch spacing becomes shorter, deleterious effects (such as, e.g., thick-lens effects associated to the deflecting cavity) are more prominent and can significantly impact the EEX process. Therefore, we are exploring such an experiment using the EEX beamline readily available at Fermilab in combination with a FEA cathode to be installed in the available L-band rf gun. This paper describes our plans and provides some numerical simulations supporting the possible generation of optically-modulated beams.

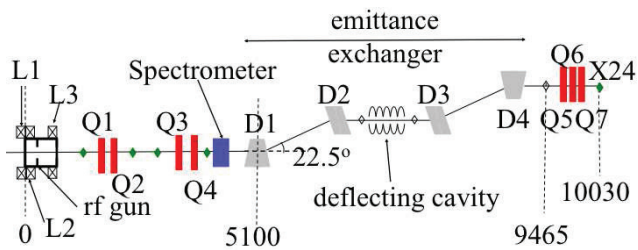

Figure 1: Schematic drawing of the HBESL beamline. A set of four quadrupoles (Q1-Q4) are used to tune the beam transverse phase space parameters at the entrance of the EEX beamline, which includes the four dipole magnets (D1-D4) and the deflecting cavity.

* Work supported by DOE under contract No. DE-AC02-07CH11359 with the Fermi Research Alliance, LLC and by DARPA under grant No. N66001-11-1-4192 with MIT.

ISBN 978-3-95450-123-6

TIME-SLICED EMITTANCE AND ENERGY SPREAD MEASUREMENTS AT FERMI@ELETTRA*

G. Penco†, E. Allaria, P. Craievich‡, G. De Ninno, S. Di Mitri, W. B. Fawley, E. Ferrari,
L. Giannessi, C. Spezzani, M. Trovò, Sincrotrone Trieste, Italy
S. Spampinati, SLAC, Menlo Park, California, USA

Abstract

FERMI@Elettra is a single pass seeded FEL based on the high gain harmonic generation scheme, producing intense photon pulses at short wavelengths. For that, a high-brightness electron beam is required, with a small uncorrelated energy spread. In this paper, we present a detailed campaign of measurements aimed at characterizing the electron-beam time-sliced emittance and energy spread, both after the first magnetic compressor and at the end of the linac.

INTRODUCTION

The FERMI@Elettra free electron laser (FEL) at the Elettra Laboratory of Sincrotrone Trieste [1] is a major European FEL project. FERMI is a single-pass, S-band linac-based externally seeded FEL implementing high gain harmonic generation in the 80-4 nm fundamental output wavelength range [2]. The commissioning of the first stage, named FEL-1, has been completed, providing intense photon beams (few hundreds of micro Joules) ranging from 80nm to 20nm [3] to the beam-lines for first preliminary experiments. A high brightness electron beam with small energy spread was required to guarantee the high quality performance of the FEL and a strong effort was spent to preserve the beam transverse emittance after the longitudinal compression. Nevertheless, the transverse emittance and the uncorrelated energy spread may strongly vary along the bunch due to collective effects, as space-charge forces and coherent synchrotron radiation, which have an important role especially when the charge density increased during the longitudinal compression. Since only a fraction of the electron bunch is interested in the interaction with the seed laser to carry on the FEL process, it is crucial to measure and to control the time-sliced emittance and energy spread. The layout of the FERMI linac includes two magnetic chicanes to longitudinally compress the electron bunch, located respectively at about 320MeV and at about 670MeV. Two RF deflecting cavities were installed respectively after the first magnetic chicane (low energy RF deflector, LERFD) and at the end of the linac (high energy RF deflector, HERFD), to measure the horizontal time-sliced emittance and, by sending the electrons in the close spectrometer, to measure the time-sliced energy spread. A third RF deflecting cavity is going to be installed at the end of the linac to horizontally "stretch" the beam and investigate the vertical time-sliced emittance.

TIME SLICED EMITTANCE

The design goal illustrated in the CDR [4] is sending into the undulators beam-lines a 750A-600fs (full width in the core) electron bunch with a slice emittance below 1.5 μm. At the present, the FERMI photoinjector has been providing a 500pC bunch, 2.8 ps long (rms) which is longitudinal compressed by about a factor 10 in the first bunch compressor. As already mentioned, the low energy RF deflecting cavity (LERFD) is located just after the first magnetic chicane (BC1), allowing measuring the slice parameters of the beam after the longitudinal compression [5]. The LERFD cavity is a five cell standing wave structure, sharing the same klystron of the electron gun. An attenuator and a phase shifter allow to independently modulate the input power. The required deflecting voltage $V_t = 3MV$ can be reached with an input power $P_{in} = 1.9MW$ and a maximum electric peak of $E_p = 48MV/m$. After the LERFD cavity, four quadrupoles and three multi-screens stations are placed for measuring the beam optics parameters and matching them after the longitudinal compression (see the layout in figure 1).

The Twiss function and the emittance measurements have been performed by implementing the well known quadrupole scan technique [6], by using the fourth quadrupole and the second screen, placed in correspondence of the beam waist, at about 9 meters from the LERFD cavity. The multi-screen stations are equipped with Optical Transition Radiation (OTR) and Yttrium Aluminum Garnet (YAG) targets. For improving the emittance measurement accuracy we have used the OTR targets, that could provide a beam spot size estimation with $20\mu m$ resolution. Nevertheless for high compression factor, the OTR targets suffer from coherent optical transition radiation that corrupts the beam spot image. This effect has been mitigated by the implementation of the X-band cavity that linearizes the longitudinal phase space and flats the beam current profile, and by the activation of the Laser Heater [7]. Figure 2 shows the comparison between the OTR image of the same beam spot (a compressed beam ($\sigma_t \approx 1ps$ at 300MeV) with and without the laser heater working. The signal intensity drops sensitively when activating the laser heater and this indicates that microbunching structures along the bunch are present already at moderate compression factor. Thus in order to have a reliable measurement of the beam spot size with OTR screens, it is necessary to switch on the

* This work was supported in part by the Italian Ministry of University and Research under grants FIRB-RBAP045JF2 and FIRB-RBAP-6AWK3
† giuseppe.penco@elettra.trieste.it
‡ now working at Paul Scherrer Institute

ISBN 978-3-95450-123-6

COLLECTIVE AND INDIVIDUAL ASPECTS OF FLUCTUATIONS IN RELATIVISTIC ELECTRON BEAMS FOR FREE-ELECTRON LASERS*

R.R. Lindberg† and K.-J. Kim, ANL, Argonne, IL 60439, USA

Abstract

Fluctuations in relativistic electron beams for free-electron lasers (FELs) exhibit both collective and individual particle aspects, similar to that seen in non-relativistic plasmas. We show that the density fluctuations are described by a linear combination of the collective plasma oscillation and the random individual motion of Debye-screened dressed particles. The relative importance of the individual to the collective motion is determined by comparing the fluctuation length scale divided by two pi with the relativistic beam Debye length. Taking into account the fact that the velocity spread is caused by both the energy spread and the angular divergence, we derive a simple formula for the minimum value of the Debye length using a solvable 1-D model. For electron beams used for x-ray self-amplified spontaneous emission (SASE) we find that the Debye length is comparable to the radiation wavelength, and that therefore the collective motion is not relevant..

INTRODUCTION

Shot noise in relativistic electron beams has its origins in the discrete nature of the electron: over sufficiently small time and length scales the current will fluctuate due to variations in the number of electrons measured. However, the term "shot noise" has a more precise definition with more restrictive properties than being merely the fluctuations associated with discrete particles. Specifically, shot noise is connected with a Poisson process; in an electron beam this means that while the average flow is given by the current, the arrival time of any particular electron is independent of the arrival times of all other electrons, and the characteristic fluctuations in number N scales as $\delta N/N \sim 1/\sqrt{N}$. To be more explicit, we define the time of the j^{th} electron in the bunch as $\zeta_j(z) \equiv z - c\beta_0 t_j$, where z and t_j are the longitudinal coordinate and particle time, respectively, while β_0 is the reference velocity scaled by the speed of light c. If we consider the spectral content of the density fluctuations or bunching given by

$$b_k(z) \equiv \frac{1}{N}\sum_{j=1}^{N} e^{-ik\zeta_j(z)}, \qquad (1)$$

than the ensemble average $\langle b_k(z)\rangle = 0$, while the average value of $\langle |b_k(z)|^2\rangle = 1/N$ for a beam that is characterized by shot noise.

The equilibrium fluctuations of an ideal gas are those of shot noise. Additionally, the emission processes of excited atoms, diodes, and cathodes is typically assumed to be Poisson, so that laser light, electric currents, and particle beams are produced with shot-noise type fluctuations. However, inter-particle forces can induce correlations that can change the fluctuation statistics from that of shot noise. For example, the ponderomotive force in an undulator tends to increase any density fluctuations near the resonant wavelength, which is the origin of the free-electron laser (FEL) instability and self-amplified spontaneous emission (SASE). On the other hand, electrostatic repulsion tends to smooth out density fluctuations. This physical effect has been given the name "shot noise suppression" in the FEL literature [1, 2, 3].

Due to the long-range electrostatic force, the equlibrium density fluctuations in a plasma are quite different than those of shot noise. We can understand this by considering a plasma of density n_0, whose natural plasma frequency is $\omega_p \equiv \sqrt{e^2 n_0/\epsilon_0 m}$, where e is the magnitude of the electron charge, m is its mass, and ϵ_0 is the vacuum dielectric constant. If we assume that the rms thermal spread is σ_v, we can define the Debye length $\lambda_D \equiv \sigma_v/\omega_p$ which is the distance a particle moves due to its thermal motion during one plasma oscillation. For distances less than $2\pi\lambda_D$, the particle is not aware of the plasma, and individual particle interactions dominate the dynamics. Conversely, the plasma can organize itself so as to screen any individual test particle over length-scales much longer than $2\pi\lambda_D$, so that the long-scale physics is characterized by collective motion of the particles [the plasma (or Langmuir) oscillation]. To be more quantitative, Rostoker has shown in an elegant calculation that in a Maxwellian plasma the ensemble averaged bunching squared is given by [4]

$$\left\langle |b_k|^2 \right\rangle = \frac{1}{N}\frac{(k\lambda_D)^2}{1+(k\lambda_D)^2}. \qquad (2)$$

In the limit $k\lambda_D \ll 1$, $\langle |b_k|^2\rangle \to (k\lambda_D)^2/N$, and we see that the correlations have reduced the density fluctuations far below that of shot noise. The electrostatic energy associated with these density fluctuations can be shown to be $k_B\sigma_v^2/2$ per mode as one would expect from equipartition (k_B is Boltzmann's constant). In the other limit, when $k\lambda_D \gtrsim 1$ the fluctuations in the bunching approach that of shot noise, $\langle |b_k|^2\rangle \approx 1$.

In the following we review a simple non-equilibrium model for the electron beam developed in [5, 6] which shares certain characteristics with classical plasmas. We compute the fluctuation characteristics and compare these to simple simulation results. We then compute the relevant Debye length, and show that collective oscillations are not relevant for electron beams suitable for x-ray generation.

* Work supported by U.S. Dept. of Energy Office of Sciences under Contract No. DE-AC02-06CH11357

† lindberg@aps.anl.gov

ISBN 978-3-95450-123-6

ELECTRON OPTICS AND MAGNETIC CHICANE FOR MATCHING AN XFEL-OSCILLATOR CAVITY INTO A BEAMLINE AT THE EUROPEAN XFEL LABORATORY

C. Maag, DESY, Hamburg, Germany
J. Zemella, J. Rossbach, University of Hamburg, Germany

Abstract

At DESY the European XFEL (X-Ray Free-Electron Laser) laboratory is currently under construction. Due to the time structure of its electron bunch trains it is in principle possible to run a FELO (Free-Electron Laser Oscillator) at the European XFEL. The major elements of a FELO are the cavity and the undulator. To couple the electron beam with the required beta functions into the cavity, a magnetic chicane and an appropriate focusing structure are considered. In this paper we discuss the lattice design of the magnetic chicane and the focusing section. We also present the results of the beam dynamics simulations performed.

INTRODUCTION

The XFELO concepts as described in [1] and [2] is predicted to offer performance complementary to a SASE (self-amplified spontaneous emission) based FEL. The described XFELO is based on an ERL (energy-recovery linac) and uses a crystal cavity to provide narrow band feedback of the undulator-radiation. The cavity consists of Bragg crystal mirrors which reflect only a narrow bandwidth of the x-rays in the desired direction and grazing incidence mirrors or compound refractive lenses (CRL) to control the modes inside the cavity. Since the European XFEL will be able to generate long bunch trains with a high repetition rate of the bunches it might be possible to adopt this concept for the European XFEL [3]. Compared to a SASE FEL the spectral bandwidth of the radiation of a XFELO is narrower by two to four orders of magnitudes and the longitudinal coherence of the radiation along the photon pulse is significantly larger. In order to bypass the mirrors with the electron beam and match it with the x-ray beam a magnetic chicane or the like and a focusing section are required. Since at DESY a XFELO concept is under consideration there is a need for a corresponding chicane and focusing section.

LAYOUT

The layout of the chicane and the focusing section is mainly determined by the required offset of the electron beam and by the desired twiss parameters inside the undulator. The offset has to be sufficient for the electrons to pass by the mirrors of the FELO cavity. Due to the relatively small diameters of the x-ray and electron beam, both in the range of tens of µm and the arrangement of the x-ray optics, an offset of 10 mm is sufficient. That allowed to design a chicane of 21 m length with a deflection angle of 0.1° without any focusing elements in between. Because of the symmetry of the chicane the dispersion is compensated automatically. In order to overlap the Gaussian x-ray and the electron beam inside the undulator properly a round electron beam with the waist in the middle of the undulator is required. In addition it is desired to keep the beta functions small to reduce beam distortions due to field errors of the magnets. It was investigated if these requirements are met by the scheme shown in Fig. 1. The focusing into the undulator is performed by quadrupoles before and after the chicane. With the deflection angle of 0.1° compression effects of the bunches are negligible.

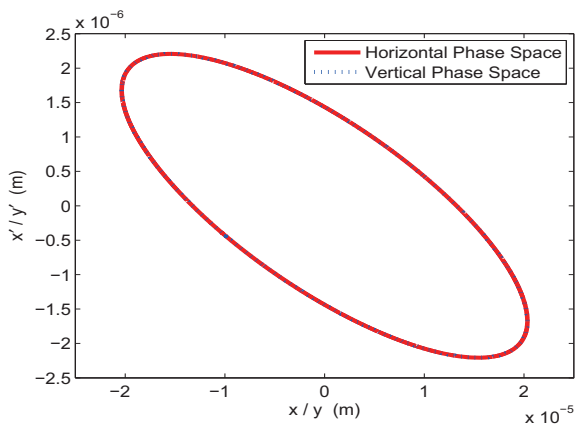

Figure 2: One-σ phase space ellipses in the transversal phase space at the entrance of the undulator. The two ellipses overlap.

Table 1: Beam Parameters

Parameter	Value
Electron energy	17.5 GeV
Bunch charge	1 nC
Bunch length (FWHM)	178 fs
Slice emittance (normalized)	1 µm
Slice energy spread	0.45 MeV

SIMULATIONS

The calculation of the electron optics were performed by using the code elegant [4]. The underlying beam parameters are shown in table 1. The initial α- and β-values

ISBN 978-3-95450-123-6

NUMERICAL SIMULATIONS OF AN XFELO FOR THE EUROPEAN XFEL DRIVEN BY A SPENT BEAM

J. Zemella*, J. Rossbach, University of Hamburg, Germany
C. P. Maag, DESY and University of Hamburg, Germany
H. Sinn European XFEL GmbH, Hamburg, Germany, M. Tolkiehn, DESY, Hamburg, Germany

Abstract

The European XFEL will be an X-ray free electron laser laboratory at DESY in Hamburg Germany. In the baseline design the light pulses will be generated in long undulators via the SASE process. The wavelengths of the light pulses will be between 5 nm and 0.05 nm. Since SASE pulses have a poor longitudinal coherence a lot of research is ongoing to overcome the statistical fluctuations of the SASE pulses. Some years ago Kim et al. proposed an FEL oscillator for light sources based on energy-recovery linacs (ERL), using Diamond Bragg crystals to build up a high reflective cavity in the X-ray regime (XFELO). Since the European XFEL will be based on superconducting accelerator structures it will deliver a long train of electron bunches which might be suitable to support an XFELO arrangement as well. In particular, the spent beam at the exit of a SASE FEL might be still qualified to drive an XFELO. Theoretical simulations of an oscillator based on Diamond crystals for the European XFEL will be presented using electron bunches of a spent beam.

INTRODUCTION

The beam parameters of the European XFEL allow to operate high-gain free electron lasers (FEL) [1]. Sufficient gain levels for multi pass approaches with significantly shorter undulators can be reached. For an XFELO for the European XFEL the undulator length is assumed to be less than 15 m instead of the SASE undulators which need to be at least 60 m for wavelengths of 1.5 Å and even longer for two-stage approaches [2, 3, 4]. The bandwidth of the radiation of a self-seeded XFEL or XFELO is more narrow than for SASE-FELs ($\Delta\nu/\nu \sim 10^{-3}$) and will be in the order of $\Delta\nu/\nu \approx 10^{-5} - 10^{-7}$. The pulses will have a significantly larger longitudinal coherence up to full longitudinal coherence along the photon pulse.

A cavity scheme to feed back X-ray pulses to the entrance of the undulator has been proposed for ERLs some years ago [7]. The cavity is based on Bragg deflecting crystals. Some studies have been done on cavities using Diamond crystals due to their high reflectivity and heat conduction and low thermal expansion [8, 9, 10, 11].

A numerical simulation is presented using a spent beam after a SASE undulator to generate an X-ray pulse using an XFELO. The spent beam has a significantly larger energy spread due to the emitted radiation in the SASE undulator which reduces the FEL gain [12]. The induced energy spread is approximately 10 MeV [1]. Since multi pass approaches offer a longer effective undulator length than a single pass approach it is possible to get into saturation during one pulse train containing 2600 bunches. For numerical simulation the FEL-code Ginger is used. This code offers the possibility to include the reflection characteristics of Bragg deflection crystal by an extra data file [13, 14].

Secondly, the temperature evolution of Diamond crystal absorbing XFELO like pulses considering ballistic heat transport effects is presented [18]. At cryogenic temperatures Diamond offers a high heat conduction. This is necessary to have a small temperature rise when the following pulse is absorbed. Also the free mean path increases with lower temperature [19]. At the highest thermal diffusivity at about 50 K the mean free path is about hundreds of micrometers and even at 100 K it is about tens of mircometers. If the mean free path is comparable to the thickness of the crystal, ballistic heat transfer has to be taken into account. A radial simulation code calculating the thermal evolution is modified by using an effective thermal conductivity which is valid in both regimes, diffusive resp. ballistic [18].

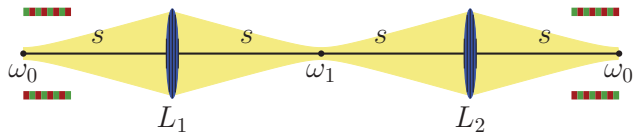

Figure 1: Schematic of one periode of the simulated unfolded crystal cavity using the Ginger FEL code. ω_0 and ω_1 referred to the waist of the photon beam in the middle of the undulator. L_1 and L_2 represents the curved Bragg deflecting crystals and s denotes the distance between the waist and the curved Bragg deflecting crystals. The green red bars refer to the undulator.

NUMERICAL SIMULATION

Ginger simulates a cavity with two curved mirrors in a certain distance (see fig. 1) and filters the radiation using the wavelengths dependent complex reflectivity of a Bragg deflection crystal, fig. 2 using the dynamical theory of X-ray diffraction from [16]. To couple out a fraction of the pulses, one crystal is thinner to transmit a part of the photon pulses. For this simulations the fraction to couple out is about 4 %. The added length to the cavity length due

* e-mail: Johann.Zemella@desy.de

ISBN 978-3-95450-123-6

SIMULATIONS OF XFELO FOR THE KEK ERL

R. Hajima#, N. Nishimori, JAEA, Tokai, Ibaraki, 319-1195, Japan
N. Sei, AIST, Tsukuba, Ibaraki, 305-8568, Japan
M. Shimada, N. Nakamura, KEK, Tsukuba, Ibaraki, 305-0801, Japan

Abstract

Following the recent development of high-brightness electron guns and high-reflectivity X-ray crystal optics, an FEL oscillator operated in a hard X-ray wavelength region (XFELO) has been considered as a possible extension of the 3-GeV ERL light source proposed at KEK. In order to deliver a 6-GeV electron beam to the XFELO, the ERL is operated at the energy-doubling mode with a low average current. In this paper, we present results of electron beam simulations and FEL simulations for the XFELO proposed at KEK.

INTRODUCTION

Energy-recovery linac (ERL) to produce an electron beam of small emittance and high-average current is a promising technology for future light sources such as synchrotron radiation facility for coherent X-rays and laser Compton scattered γ-ray sources [1]. A collaborative project for the next-generation light sources based on energy-recovery linac has been established in Japan [2]. Critical components such as photocathode DC gun [3] and superconducting cavities [4] have been developed in JAEA and KEK. A test facility, the Compact ERL, is under construction to demonstrate the generation and acceleration of "ERL quality" electron beams. The first beam at the Compact ERL is scheduled in March 2013 [2].

One of the future ERL light sources under proposal in Japan is a synchrotron X-ray light source based on a 3-GeV ERL to be a successor of Photon Factory at KEK [5]. The 3-GeV ERL will offer far higher performance than the existing storage ring. The high repetition rate, short pulse, high spatial coherence and high brightness of ERL will drive forward a distinct paradigm shift in X-ray science from "static and homogenous" systems to "dynamic and heterogeneous" systems, in other words, from "time- and space-averaged" analysis to "time- and space-resolved" analysis.

In addition, an X-ray FEL oscillator (XFELO) is proposed as a part of the ERL facility. The XFELO is driven by 6-GeV beam obtained from double-pass acceleration by main linac of the ERL as shown in Fig.1. The XFELO is operated at low repetition with small average current, thus, the energy recovery is not necessary. The XFELO to produce X-rays with full transverse and temporal coherence will be complementary to the undulator X-rays at the ERL [6].

In this paper, we describe design parameters of XFELO at the KEK ERL, results of electron beam degradation evaluation and XFELO simulations.

XFELO PARAMETERS AND GAIN

Bragg mirrors such as perfect crystals of diamond are used for the XFELO. Recently, Bragg mirrors having reflectivity more than 99% are becoming available at hard X-ray wavelengths [7]. We have, therefore, chosen FEL parameters to obtain small signal FEL gain larger than 30% to compensate the mirror loss and the extraction from the oscillator. Table 1 shows the parameters of electron beam, undulator and FEL gain for the XFELO, where the FEL wavelength is fixed at 1 Å as a representative example. Two sets of parameters are case (A) for typical electron beam parameters to obtain high-brilliant undulator radiation at the ERL, case (B) for shorter electron bunches with velocity bunching at the ERL main linac [8]. The case (B) with a smaller bunch charge is preferable for reducing thermal heat load on the Bragg mirrors. We plan to carry out beam dynamics studies specific to the XFELO such as small charge operation, velocity bunching in the Compact ERL.

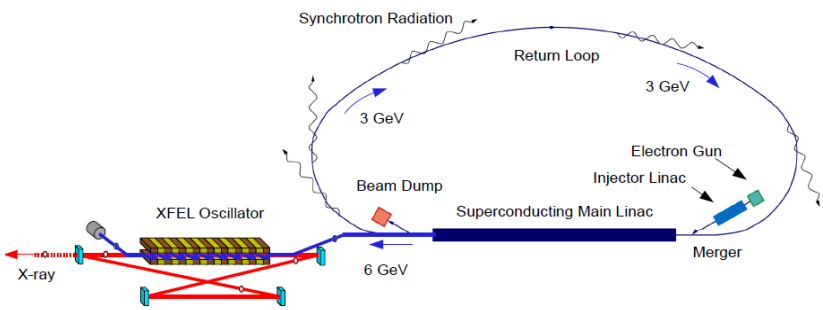

Figure 1: Conceptual layout of the 3-GeV ERL integrated with XFELO at KEK.

hajima.ryoichi@jaea.go.jp

ISBN 978-3-95450-123-6

SUB-ÅNGSTRÖM STABILIZATION OF AN X-RAY FREE ELECTRON LASER OSCILLATOR AND NUCLEAR RESONANCE METROLOGY*

B.W. Adams†, K.J. Kim‡, ANL, Argonne, IL 60439, USA

Abstract

A scheme is described to length-stabilize the cavity of an x-ray free-electron-laser oscillator (XFELO) by locking one of its longitudinal modes to the narrow nuclear resonance line of ^{57}Fe at 14.4 keV. With a cavity thus stabilized, a standing-wave pattern can be maintained over hours, to be probed by another sample of ^{57}Fe in a meter-long scan to compare the nuclear-resonant wavelength with a known optical standard. This will improve by at least four orders of magnitude the accuracy at which the ^{57}Fe resonance wavelength can be measured. The technique can be refined for other, narrower resonances such as ^{181}Ta (6.2 keV, 75 peV), opening up precision x-ray metrology for technological applications and fundamental physics, such as, e.g., experimental quantum gravity.

INTRODUCTION

Metrology is at the core of modern physics and technology, both for fundamental studies, and practical applications. A striking example for the latter is the global positioning system (GPS), which relies on the accuracy of atomic clocks and shows the relevance of general-relativistic corrections for the Earth's gravitational field. Atomic clocks can measure time - and thus also length - to an accuracy of a few times 10^{-16}. Following current trends [1], this figure will probably improve incrementally over the next few years. Progress is made through careful control of environmental perturbations and ensemble averaging for good signal statistics of the clock phase. Efforts are underway to replace the current, microwave-based clocks with optical ones. These are less susceptible to stray fields, and tick at a higher rate for faster phase accumulation. The next natural step in this progression is to use x-ray nuclear resonances for their even higher frequencies and the high degree of isolation of nuclei within their host electronic shells. For nuclear-resonant length and time standards to be useful, one has to be able to relate them to the existing optical ones. This would require means of optical coupling the two. Unlike in the optical regime, where lasers provide intense coherent light, and nonlinear optics can couple modes, x-ray optics has to date been mainly restricted to low-coherence and linear-optical cases. The reasons for this are mainly the lack of intense, coherent, and stable x-ray sources, and the weakness of nonlinear-optical effects at x-ray frequencies. The former of these can now be addressed with the recently studied x-ray free-electron oscillator (XFELO) [2, 3, 4], which can provide x-ray beams of high coherence and high intensity (measured in terms of the number of photons per mode). The present proposal has two part to it - the first showing a way to further improve the coherence characteristics of an XFELO through cavity stabilization, and the other proposing a way of relating x-ray to optical wavelengths without the use of nonlinear optics. Although the high intensity of an XFELO beam could presumably lead to nonlinear-optical effects, this is currently too much an uncharted territory to be the basis of a proposal. Instead, the identities of well-defined pieces of matter in an interferometer are exploited for their interactions with visible light and with x-rays.

* This work was supported by the U.S. Department of Energy, Office of Basic Energy Sciences, under Contract No. DE-AC02-06CH11357.

† adams@aps.anl.gov

‡ kwangje@aps.anl.gov

XFELO

An XFELO combines an x-ray optical cavity made of near-backscattering Bragg crystals with an x-ray free-electron laser to produce a constant stream of intense, coherent, and wavelength-tunable pulses. The XFELO pulses are copies of the same pulse circulating in the cavity. Thus, if the pulse spacings can be stabilized to much better than the wavelength, then the XFELO output will be a frequency comb similar to that in mode-locked optical lasers. Unlike in the optical case, the x-ray comb does not cover a full octave in frequency, and thus cannot be used in self-referencing schemes. As a specific example optimized for the present proposal, an XFELO with the following parameters will be considered: The cavity is tuned to the 14.4-keV nuclear resonance of ^{57}Fe, and is formed by four diamond crystals oriented to the (337) reflection ($2\Theta = 162°$). It has a round-trip length of L=90 m, corresponding to a pulse spacing of $T = L/c = 0.3\mu$s, and a longitudinal-mode spacing of 3 MHz in the frequency comb, i.e., 14 neV on the energy scale. Electrons of 7 GeV in bunches of 25 pC in an rms length of 0.5 ps will be used for for the FEL. The intracavity peak power of this XFELO is 35 MW, and the output has $3 \cdot 10^8$ photons in a 3-meV bandwidth. This amounts to about 1000 photons per mode and pulse. The small-signal gain is 0.5, and the round-trip loss (including outcoupling) is 26%. [1].

The linewidth of the modes in the frequency comb is given by fluctuations in the cavity length, spontaneous undulator emission, and by noise in the FEL gain process. The former are caused by seismic ground motion and vibrations due to local machinery. These, and ways to mitigate them, have been studied extensively by the gravitational-wave-detector community, and their experience is used here. Spontaneous undulator emission into the FEL lasing mode has a power of about 10^{-8} of the intracavity radiation. This leads to a random phase jump of about 10^{-4}

[1] We thank R.R. Lindberg for these parameters

ISBN 978-3-95450-123-6

INJECTOR SYSTEM FOR LINAC-BASED INFRARED FREE-ELECTRON LASER IN THAILAND

S. Rimjaem*, P. Boonpornprasert, J. Saisut, S. Suphakul, C. Thongbai, Department of Physics and Materials Science, Faculty of Science, Chiang Mai University, Chiang Mai, 50200, Thailand
S. Chunjarean, Thailand Center of Excellence in Physics, CHE, Bangkok 10400, Thailand

Abstract

A possibility to develop a compact linac-based Infrared free-electron laser (IR FEL) facility has been studied at Chiang Mai University (CMU) in Thailand. Characteristics of the emitted FEL light and reliability in operation of the FEL system are determined by the properties of the electron injector, the undulator, and the optical cavity. The proposed injector system for the future IR FEL is based on the electron linear accelerator system at the Plasma and Beam Physics Research Facility at CMU (PBP-CMU). Numerical and experimental studies to adjust the existing system to be able to drive the IR FEL have been performed. The results of preliminary studies and the proposed parameters for the injector and the FEL system are concluded in this contribution.

INTRODUCTION

Linac-based free-electron lasers (FELs) have recently gain interest worldwide in the accelerator and particle beam community as the new generation light source, which can be utilized in numerous applications. Characteristics of the output FEL radiation are determined by the properties of the electron beam and the undulator, where the light is emitted. Since the FEL light sources require electron beams of high quality, the development and optimization of the injector system are important.

Electromagnetic radiation in the infrared wavelength regime, especially the far-infrared (FIR) or THz radiation, is of a great interest source for applications in various fields [1-4]. A possibility to develop an infrared free-electron laser (IR FEL) is studied at the Plasma and Beam Physics Research Facility, Chiang Mai University (PBP-CMU). At this initial stage, we concentrate on the development of an FEL covering the THz radiation wavelength around 50-200 μm. Study of the FEL radiation in the mid-infrared (MIR) and near-infrared (NIR) regime will be considered in the future.

In order to develop the FEL system, optimization of both injector and FEL system is ongoing. In this paper, we concentrate on an overview of the project and preliminary optimization of a thermionic based electron radiofrequency (RF) injector to produce electron beams with properties yielding the requirements for an IR FEL.

PROPOSED IR FEL FACILITY

Generally, an IR FEL facility consists of an injector system for generating and accelerating electron beam, an undulator magnet for FEL lasing and an optical cavity for amplifying the FEL radiation output power. For the considered injector system of the proposed IR FEL at CMU, we plan to make use of the existing linac system as much as possible while maintaining its functionality as the femtosecond electron and photon pulse facility.

The proposed IR FEL system shown in Fig. 1 consists of an injector system, an accelerating structure, a 180° achromat section, an undulator magnet and an optical cavity. The injector system combines a thermionic cathode RF-gun and an alpha magnet as a magnetic bunch compressor. The accelerating structure is an S-band travelling wave SLAC-type linac, which can be used to accelerate an electron beam to reach a maximum energy of about 30 MeV. The injector system, the linac structure, beam steering and focusing elements as well as beam diagnostic instruments upstream the achromat section will be modified from the existing PBP-CMU linac system [5]. The undulator magnet is a planar type with a length of 1.67 m. The optical cavity composes of two symmetric spherical mirrors with a coupling hole on one of the mirrors. Some parameters of the undulator and the optical cavity used in preliminary FEL optimization are listed in Table 1.

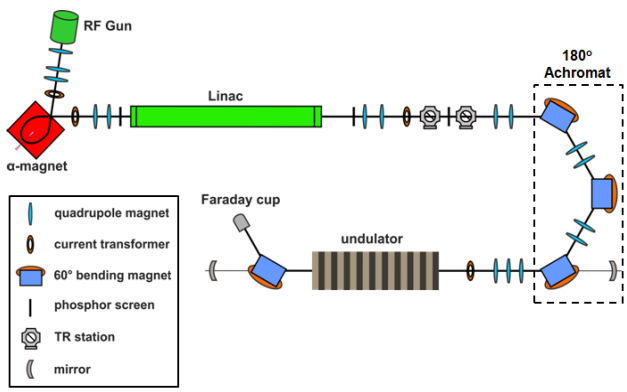

Figure 1: Schematic layout of the possible IR/THz FEL system at Chiang Mai University, Thailand.

In electron beam and FEL optimizations, we consider two scenarios. The first one is studying the FEL radiation in the case of the electron beam whose bunch length is longer than the radiation wavelength. The other one is for the case of the electron beam whose bunch length is shorter than the radiation wavelength.

*sakhorn.rimjaem@cmu.ac.th

ISBN 978-3-95450-123-6

BEAM DYNAMICS SIMULATION AND OPTIMIZATION OF ELECTRON BEAM PROPERTIES FOR IR FEL AT CHIANG MAI UNIVERSITY

S. Suphakul*, S. Rimjaem, C. Thongbai, Department of Physics and
Materials Science, Faculty of Science, Chiang Mai University, Chiang Mai 50200, Thailand
Thailand Center of Excellence in Physics, CHE, Bangkok 10400, Thailand

Abstract

The linear accelerator system at the Plasma and Beam Physics Research Facility (PBP), Chiang Mai University (CMU), Thailand, is planned to be upgraded to be an injector system for the Infrared Free-electron Lasers (IR FEL). The PBP linac system consists of an S-band thermionic cathode RF-gun, a bunch compressor in a form of alpha-magnet and a 3-m SLAC-type linear accelerator. The current system will be modified to generate the electron beam with properties suitable for the IR FEL. Numerical simulations have been performed to investigate and optimize the electron beam parameters. The planned modification of the system and optimization of the electron beam parameters are presented in this contribution.

INTRODUCTION

The Infrared Free-electron Lasers (IR FEL) facility at Chiang Mai University has been developed under the plan of a new research facility establishment of the Thailand Center of Excellence in Physics. The facility focuses on the production and utilization of the mid- and far-infrared radiation (MIR and FIR) based on femto-second electron pulses and free-electron lasers technology [1]. As shown in Fig. 1, the facility considered in this paper consists of a thermionic cathode RF-gun as an electron source [2], a magnetic bunch compressor in a form of an alpha-magnet [3], a 3-m SLAC-type S-band linear accelerator (linac), a 180° achromat section, a planar type undulator and an optical resonator.

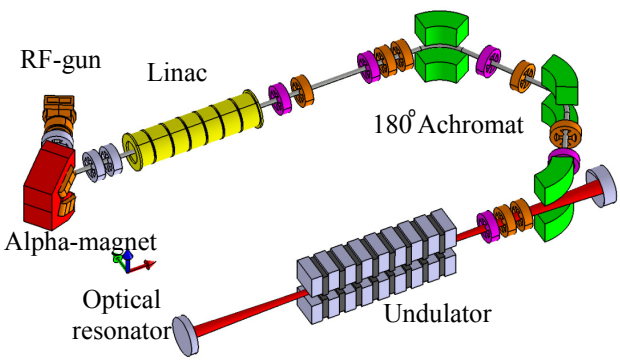

Figure 1: Schematic view of planned IR-FEL at CMU.

The first three components of the existing PBP-CMU linac system are planned for both coherent THz transition radiation from femto-second electron pulses and free-electron lasers. Details of the current PBP-CMU linac system were reported in [4]. The 180° achromat section is a new component which is under detailed consideration. Therefore, we adopt the magnet lattice of the Kyoto University Free-Electron Lasers (KU-FEL) for initial optimization in this study. The achromat section consists of three 60° deflecting angle dipole magnets and two sets of doublet quadrupole magnets. Details of KU-FEL achromat system have been described in [5]. Through the achromat, the electron bunch length shortens and the peak current becomes higher for a given bunch charge.

This study investigates and optimizes the electron beam parameters suitable for the IR FEL project at CMU by modifying the PBP-CMU linac driving condition and considering the bunch compression in the 180° achromat. To investigate the beam dynamics, the computer code PARMELA [6] or the "Phase And Radial Motion in Electron Linear Accelerator" code has been used for simulations of multi-particle beam dynamics from the RF-gun to undulator and optimization of the electron beam lattice parameters.

ELECTRON BEAM OPTIMIZATION

Generally, electron beams for FELs must have high peak current, small emittance, and low energy spread in order to generate intense coherent FEL light in an undulator. For the IR FEL at CMU, some electron beam requirements have been proposed and are shown in Table. 1. In this study, we focus on optimization of longitudinal electron beam dynamics by adjusting the parameters of three main components; the RF-gun, the linac and the 180° achromat. For the simulation of multi-particle beam dynamics, 30,000 particles per 2856 MHz are assumed to be emitted uniformly from the cathode with current of 2.9 A. One particle represents a charge of 33.85 fC equivalent to 2.12×10^5 electrons .

*sikharin.sup@gmail.com

ISBN 978-3-95450-123-6

IMPROVEMENT OF KU-FEL PERFORMANCE BY REPLACING UNDULATOR AND OPTICAL CAVITY

H. Zen#, K. Okumura, K. Shimahashi, M. Shibata, H. Imon, T. Konstantin, H. Negm, M. Omer, K. Yoshida, Y.W. Choi, R. Kinjo, M. A. Bakr, T. Kii, K. Masuda, H. Ohgaki
Institute of Advanced Energy, Kyoto University, Gokasho, Uji, Kyoto, Japan

Abstract

An upgrade project of the MIR-FEL facility developed in the Institute of Advanced Energy, Kyoto University has been in progress since 2010. The project consists of two topics; one is replacement of undulator and the other is replacement of the optical cavity mirrors. Those replacements were accomplished in January 2012. After the upgrade, we have so far succeeded in FEL lasing from 5 to 14.5 μm. Details of upgrade project and design work on a new optical cavity is reported in this paper. In addition, the results of the commissioning of a newly installed undulator and optical cavity is reported.

INTRODUCTION

An oscillator type Mid-Infrared Free Electron Laser (MIR-FEL) named the KU-FEL has been developed in Institute of Advanced Energy, Kyoto University, for aiding energy related sciences [1]. A 4.5-cell thermionic RF gun is employed as the electron source. After introduction of some cures of back-bombardment effects in the gun [2, 3, 4, 5], we have achieved first lasing [6], and laser saturation in 2008 [7]. However, a trade off relationship, caused by back-bombardment effects, between the bunch charge and the macro-pulse duration, limited the tunable range of the FEL to only 10 to 14 μm. An upgrade project for extending the tunable range of the FEL was started in 2010. The project consists of two topics. One is replacement of undulator and the other is replacement of optical cavity mirrors, which were newly designed in this work. In January 2012, those replacements were accomplished. After the upgrade, the tunable range of the FEL was extended to 5 – 14.5 μm.

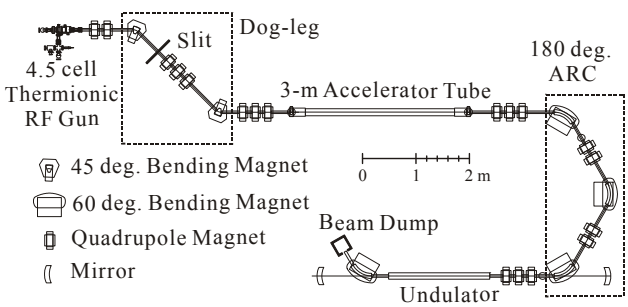

Figure 1: Schematic diagram of KU-FEL accelerator.

#zen@iae.kyoto-u.ac.jp

KU-FEL DEVICE

Figure 1 shows a schematic diagram of the KU-FEL device, consisting of a 4.5-cell thermionic RF gun, a dog-leg section for energy filtering, a 3-m accelerator tube, a 180-degree arc section for a bunch compression, an undulator and an optical cavity. Parameters of the undulator (undulator #1) and the optical cavity before upgrade are shown in Table 1.

Table 1: Parameters of Undulator and Optical Cavity Before the Upgrade

Undulator #1 (until Dec. 2011)		
Structure		Halbach
Period length		40 mm
Number of periods		40
Maximum K-value		0.99
Optical cavity (upstream mirror has out-coupling hole)		
Mirror curvature	Upstream	3.03 m
	Downstream	1.87 m
Diameter of out-coupling hole		2 mm
Cavity length		4.513 m
Reflectivity		99.04%

UPGRADE PROJECT

An upgrade project was started in 2010. The objective of this upgrade was an extension of the wavelength range of the FEL. The project consists of two topics. One is replacement of undulator and the other is replacement of optical cavity mirrors.

Replacement of Undulator

The operation of the ERL-FEL developed in JAEA [8] was terminated in 2009. We were able to obtain the undulator (undulator #2) used for the ERL-FEL and install it into KU-FEL. Parameters of the undulator are listed in Table 2.

The undulator #2 has a shorter period length, larger number of periods and almost the same maximum K-value compared with undulator #1. The larger number of periods contributes to enhanced FEL gain for the same wavelength.

Results of magnetic field measurements of undulator #2 were reported in FEL 2011 [9]. Large amplitude fields errors (± 3.5%) were observed in the measurements and

ISBN 978-3-95450-123-6

STATUS OF IR-FEL AT TOKYO UNIVERSITY OF SCIENCE

T. Imai#, T. Kawasaki, J. Fujioka, M. Matsubara, K. Komiya, K. Tsukiyama, IR-FEL Research Center of Tokyo University of Science, Noda, Chiba, Japan
T. Morotomi, K.Hisazumi, Mitsubishi Electric System & Service Co., Ltd., Tsukuba, Ibaraki, Japan
T. Shidara, M. Yoshida, KEK, Tsukuba, Ibaraki, Japan

Abstract

IR-FEL research center of Tokyo University of Science (FEL-TUS) is a facility for aiming at development of the high performance FEL device and promotion of photo-sciences using it. The main part of FEL-TUS involves a mid-infrared FEL (MIR-FEL) which provides continuously tunable radiation in the range of 5 -14 μm and a variety of experiments by the use of this photon energy corresponding to the various vibrational modes of molecules are now underway. We are also making effort to develop a far-infrared FEL (FIR-FEL) in order to realize FEL lasing in the THz region. This paper will describe the status of research activities at FEL-TUS.

INTRODUCTION

The Infra-red free electron laser research center of Tokyo University of Science (FEL-TUS) [1] was established in 1999 as a user facility dedicated for the application of infra-red free electron laser.

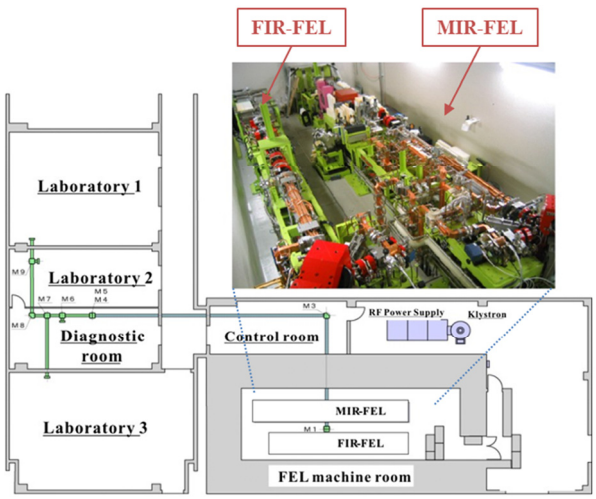

Figure 1: Layout of FEL-TUS.

The main device of FEL-TUS is a mid-infrared FEL (MIR-FEL) which covers the wavelength region of 5-14 μm, which corresponds to the absorption frequencies for vibrational modes of molecules. A variety of experiments utilizing special characteristics of MIR-FEL are now underway. Another FEL device is a far-infrared FEL (FIR-FEL), which is expected to cover the wavelength region of 300-1000 μm. Figure 1 shows the top-view of the facility with a picture of two FEL devices.

FEL-TUS is open to researchers of not only Tokyo University of Science but also other universities, institutes and companies and has been supported by Open Advanced Research Facilities Initiative from the Ministry of Education, Culture, Sports, Science and Technology of Japan since 2007 fiscal year.

FEL DEVICE

Both MIR-FEL and FIR-FEL adopt a similar structure which consists of S-band linac with a thermionic cathode RF-gun and an alpha magnet, and an undulator combined with an optical resonance cavity.

The essential difference between the two FEL devices is the structure of optical resonator cavity. In the longer wavelength region, the large slippage effect may lead to the FEL gain reduction. In order to suppress the reduction, a hybrid resonator which consists of a rectangular waveguide and cylindrical mirrors is adopted for FIR-FEL.

Figures 2 and 3 illustrate the schematic layout and photo of MIR-FEL and FIR-FEL, respectively. The comparison of parameters of two FEL devices is listed in Table 1.

Table 1: Comparison of MIR-FEL and FIR-FEL

	MIR-FEL	FIR-FEL	
Wavelength	5-14	300-1000	μm
e^- beam energy	40	10	MeV
RF Gun Cavity	On-axis coupled structure	Disk and Washer	
Length of Acc. tube	3	1.5	m
Undulator			
Period	32	70	
No. of periods	43	25	
Optical Resonator	Fabry-Perot	Hybrid*	
Mirror Size	43	4.1 x 65	mm
Cavity length	3.36	2.5	m
Status	User Operation	Commissioning in progress	

* a rectangular waveguide and cylindrical mirrors

#timai@rs.noda.tus.ac.jp

ISBN 978-3-95450-123-6

HOLE-COUPLING IN IR FELS: AN EXPERIMENTAL STUDY

A.F.G. van der Meer, FELIX facility, FOM-Institute Rijnhuizen, Nieuwegein, The Netherlands
and Radboud University, IMM, Nijmegen, The Netherlands

Abstract

Even though hole-coupling has been used for many years at several IR FEL facilities, its usefulness as out-coupling scheme has recently been questioned[1]. Also, it has been suggested that the output beam profile will inevitably show strong asymmetries at the short-wavelength end of the tuning curve[2]. In this contribution, experimental results for the dependence of cavity loss, energy extraction from the electron beam, output power and optical beam profile on the size of the hole in relation to the wavelength are presented.

INTRODUCTION

In IR FELs, on-axis hole-coupling is a common method for coupling out part of the circulating optical power in the resonator, primarily for lack of transparent materials that could be used as substrate for the mirrors. Many years ago, when this scheme was proposed in the context of FELs, it was already mentioned that in an empty cavity that supports a large number of transverse modes, an optical mode with a null at the position of the hole will naturally develop as this would be the mode having the lowest roundtrip loss. Recently, this point was raised again as a serious problem of hole-coupling[1]. Moreover, significant distortions of measured beam profiles of the out-coupled radiation at the CLIO facility were reported and it was argued that this was an inevitable effect at the short-wavelength end of the tuning curve of a mirror with a hole[2]. As hole-coupling has been used at the FELIX facility for over 20 years now without apparent problems, it seemed appropriate to investigate its performance in greater detail.

EXPERIMENT

In particular, we measured the out-coupled macropulse energy, the decay of the output after turn-off of the electron beam, the profile of the out-coupled radiation and the energy extracted from the electron beam for a number of hole sizes and wavelengths. All these measurements were done for the short-wavelength free-electron laser (FELIX FEL2) at a fixed beam energy of 44 MeV. Undulator gap-tuning was used to vary the wavelength. The parameters of the resonator of FEL2 are given in table 1.

Table 1: Resonator Parameters

Tuning range:	fundamental	5 - 45 μm
	3rd harmonic	2.7 - 5.0 μm
Resonator length:		6 m
OFHC copper mirrors:		
	diameter	50 mm
	ROC upstream	4 m
	ROC downstream	2.75 m
Rayleigh range:		1.03 m
Out-coupling via on-axis hole in upstream mirror		
Hole sizes: 0.9, 1.4, 2.2 or 3.0 mm diameter		

EFFICIENCY

After reflection from the mirror with the hole, the optical mode will have zero intensity at the position of the hole. This 'hole' in the intensity profile will lead to enhanced diffraction and hence the development of radial 'tails' that are likely to be clipped by apertures such as the vacuum chamber inside the undulator. When the hole size becomes smaller, the extent of the tails grows and therefore the likelihood of clipping these. As the reflected beam can be thought of as the interference of two beams, an undisturbed reflected beam and the reflection of the out-coupled beam shifted in phase by π, the potential diffraction loss equals the energy coupled out through the hole. This means that the intrinsic efficiency of small holes is only 50%. In fig. 1, the measured ring-down of the power coupled out through the hole after the electron beam is turned off (α = decay per roundtrip) is compared to the computed out-coupling fraction for the lowest-order resonator mode (α_0). For each of the hole sizes we find an almost linear relationship between α and α_0 for the wavelengths used (7, 9, 12, 15 and 19 μm). However, the

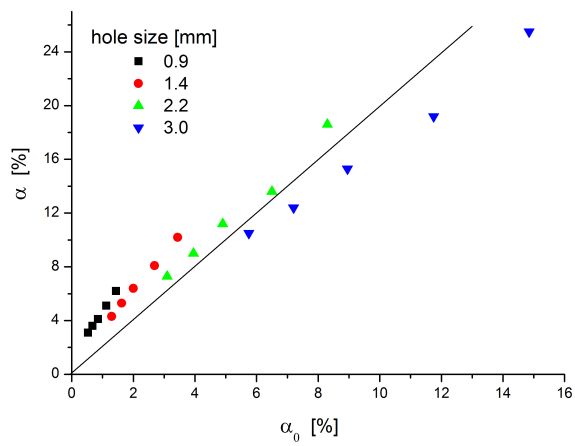

Figure 1: Roundtrip loss versus computed out-coupling. The drawn line has a slope of 2.

slope increases with decreasing hole size, and therefore the intrinsic efficiency seems to drop to only 25% for the 0.9 mm case. A disturbing finding that even led us to re-measure the hole sizes. Shortly after this measurement campaign was finished, the machine was being dismantled for the relocation to the university of Nijmegen and the downstream mirror was found to be

ISBN 978-3-95450-123-6

CONSTRUCTION AND COMMISSIONING OF COHERENT LIGHT SOURCE EXPERIMENT STATION AT UVSOR

Sei-ichi Tanaka#, Masahiro Adachi, Kenji Hayashi, Masahiro Katoh, Shin-ichi Kimura, Eiken Nakamura, Jun-ichiro Yamazaki, UVSOR, Institute for Molecular Science Myodaiji-cho, Okazaki, 444-8585, Japan
Masahito Hosaka, Yoshifumi Takashima, Yoshitaka Taira, Naoto Yamamoto, Synchrotron Radiation Research Center, Nagoya University Furo-cho, Chikusa-ku, Nagoya, 464-8603, Japan
Toshiharu Takahash, KURRI, Kyoto University Kumatori-cho, Sennan-gun, Osaka, 590-0494, Japan
Heishun Zen, IAE, Kyoto University Gokasho, Uji-shi, Kyoto, 611-0011, Japan

Abstract

At UVSOR, coherent light source technologies, such as resonator free electron laser, coherent harmonic generation and coherent synchrotron radiation via laser modulation, had been developed by parasitically using an undulator and a beam-line normally used for photo-electron spectroscopy. Under Quantum Beam Technology Program of MEXT in Japan, we started constructing a new experiment station dedicated for the source developments. We created a new straight section by moving the beam injection line. An optical klystron was constructed and installed there. Two beam-lines, BL1U and BL1B, were constructed, the former of which is for free electron laser and coherent harmonic generation and the later for the coherent synchrotron radiation in the terahertz range. The seed laser system was reinforced and a new laser transport line was constructed. Generation of coherent synchrotron radiation by laser modulation was successfully demonstrated at the new station.

INTRODUCTION

At UVSOR, coherent light source technologies, such as resonator free electron laser, coherent harmonic generation and coherent synchrotron radiation via laser modulation, had been developed by parasitically using an undulator and a beam-line normally used for photo-electron spectroscopy [1-7]. Under Quantum Beam Technology Program of MEXT in Japan, we started constructing a new experiment station dedicated for the coherent light source developments. FY2010, we created a new straight section by moving the injection line. FY2011, a new optical klystron was constructed and installed. FY2009-2010, the seed laser system was moved and upgraded. FY2011, two beam-lines dedicated for coherent light source development were constructed. We describe the present status of the new coherent light source experiment station at UVSOR.

CONSTRUCTION OF COHERENT LIGHT SOURCE EXPERIMENTAL STATION

The new experiment station of coherent light source is comprised of an optical klystron, a seed laser system and beam-lines.

Construction of Optical Klystron

FY2009-2010, the beam injection line was extended by adding three bending magnets and four quadrupole magnets, and the injection septum was relocated to a short straight section. The new straight section of 4 m became available for coherent light source development [8]. An optical klystron was constructed and installed in the new straight section. Previously, a conventional, optical klystron had been used for many years, in which the radiator, the modulator and the buncher were integrated in one undulator [9]. The new optical klystron consists of separated undulators, a modulator and a

Table 1: Optical Klystron Parameters

Magnetic configuration	Apple-II
Number of Periods	10 + 10
Period length	84 mm
Max. R_{56} of buncher (600 MeV)	67 μm
Overall length of buncher	442 mm

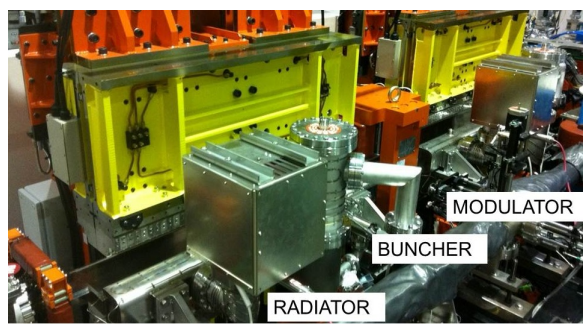

Fig. 1 : Optical klystron.

stanaka@ims.ac.jp

ISBN 978-3-95450-123-6

ELECTRON BEAM DYNAMICS IN THE ALICE IR-FEL FACILITY

F. Jackson, D. Angal-Kalinin, J. W. McKenzie, Y. M. Saveliev, T. Thakker, N. Thompson,
P. H. Williams, STFC Daresbury Laboratory, ASTeC & Cockcroft Institute, UK.
A. Wolski, University of Liverpool, UK.

Abstract

The ALICE facility at Daresbury Laboratory is an energy recovery test accelerator which includes an infra-red oscillator-type free electron laser (IR-FEL). The longitudinal phase space of the electron bunches and the longitudinal transport functions in the ALICE accelerator are studied in this paper.

INTRODUCTION

The ALICE (Accelerators and Lasers in Combined Experiments) facility is an energy recovery test accelerator [1][2] operated at Daresbury Laboratory since 2006 [3].

The accelerator consists of: a photoinjector with DC gun (up to 350 keV), buncher and superconducting booster (typically 6.5 MeV beam energy); a main energy-recovery loop (typically 26 MeV beam energy) containing a superconducting linac module, a bunch compression chicane, and an undulator.

ALICE is a test facility which has pursued several different goals and applications including an infra-red free-electron laser (IR-FEL) of the cavity oscillator type, and a terahertz (THz) research programme. In addition, ALICE serves as the injector to EMMA, the non-scaling FFAG (fixed field alternating gradient) demonstration machine [4]. Historically, the first application of ALICE was a demonstration of Compton backscattered x-rays [5].

The main demands on the ALICE beam dynamics and beam quality comes from the IR-FEL [6] which requires small energy spread (roughly 0.5%) and a small compressed bunch length (roughly 1 ps).

Throughout the operation of ALICE, beam delivery to the various applications has taken priority over fine measurement of beam dynamics or detailed machine characterisation. The machine design, especially beam transport and optics, has proved reasonably robust; pragmatic optimisation of machine performance has usually been sufficient for successful operation of the different applications. More recently, with greater reliability in application delivery, efforts to investigate the beam dynamics in a more systematic way have begun [7][8].

The first attempts to achieve IR-FEL operation were unsuccessful until the average beam current was reduced by reducing the bunch repetition frequency from its design value of 81.25 MHz, strongly implying beam loading effects causing energy droop over the bunch trains. The normal bunch repetition rate for the IR-FEL is currently 16.25 MHz.

The main beam dynamics factors relevant to the IR-FEL include the following: transverse steering and focussing of the beam in the FEL cavity; optimisation of the ALICE injector dynamics; and finally optimisation of the longitudinal beam transport in the main energy recovery loop including the arcs and bunch compressor.

The steering and focussing in the undulator is determined by intra-undulator beryllium alignment wedges which provide both optical alignment of the cavity mirrors and steering of the electron beam. The use of the wedges is usually sufficient to provide alignment of the electron beam with the undulator and oscillator cavity, and beam position monitors (BPMs) in the undulator section of the beamline are not usually required.

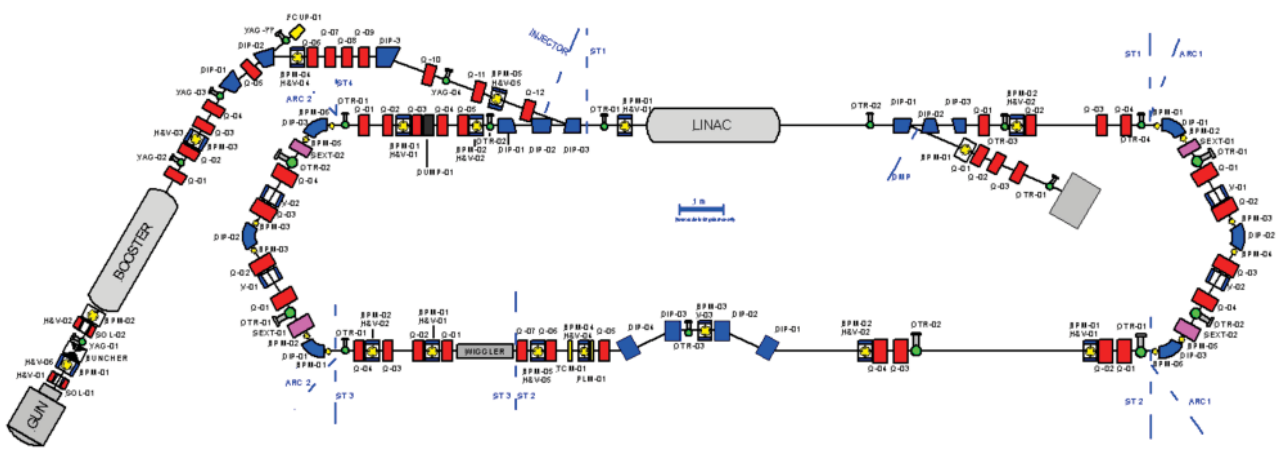

Figure 1: Layout of the ALICE accelerator.

ISBN 978-3-95450-123-6

FEL RESEARCH AND DEVELOPMENT AT STFC DARESBURY LABORATORY

N.R. Thompson[1,3], J. A. Clarke[1], D. J. Dunning[1,3], G. M. Holder[2], S. Jamison[1], B. W. J. M[c]Neil[3], M. D. Roper[1], M. R. F. Siggel-King[2,4], A. D. Smith[2], M. Surman[1], P. Weightman[2] and A. Wolski[2,4]
[1]Accelerator Science and Technology Centre (ASTeC), STFC Daresbury Laboratory, UK
[2]The University of Liverpool, Liverpool, UK
[3]University of Strathclyde (SUPA), Glasgow G4 0NG, UK
[4]Cockcroft Institute, Warrington, UK

Abstract

In this paper we present an overview of current and proposed FEL developments at STFC Daresbury Laboratory in the UK. We discuss progress on the ALICE IR-FEL since first lasing in October 2010, covering the optimisation of the FEL performance, progress on the demonstration of a single shot cross correlation experiment and the results obtained so far with a Scanning Near-Field Optical Microscopy beamline. We discuss a proposal for a 250 MeV single pass FEL test facility named CLARA to be built at Daresbury and dedicated to research for future light source applications. Finally we present a brief overview of other recent research highlights.

INTRODUCTION

In this paper we report on the progress in FEL research and development at STFC Daresbury Laboratory in the United Kingdom. We discuss progress on an operating IR-FEL which is part of the ALICE test facility, we report on design work for a proposed 250 MeV single-pass FEL test facility named CLARA (Compact Linear Accelerator for Research and Applications), and we summarise recent developments in theoretical work on novel FEL concepts.

ALICE

The ALICE facility at Daresbury Laboratory [1] has evolved from an ERL prototype for the 4GLS project [2] to a multi-functional facility hosting projects including the world's first non-scaling FFAG, EMMA [3], THz generation for use in a tissue culture facility and the UK's first FEL [4]. The FEL is an infra-red oscillator lasing over ∼5.5–9 μm. It is used for: developing experimental FEL expertise; benchmarking modelling; accelerator physics studies; a source for user experiments.

Figure 1 shows the ALICE layout including a view of the FEL line. A DC photoelectron gun (recently upgraded to a larger diameter gun ceramic to increase the operating voltage from 230 kV to 325 kV) with GaAs photocathode injects into the first superconducting module which accelerates to 6.5 MeV. For FEL operation the main linac operates in energy recovery mode and accelerates to typically 26 MeV. The nominal bunch charge is 60 pC, with bunches delivered at 16.25 MHz in trains of up to 100 μs with train repetition frequency up to 10 Hz. The variable gap undulator has 40 periods of length 2.7 cm. The optical cavity comprises two spherical gold-coated copper mirrors with hole-outcoupling in the downstream mirror. The FEL output is transported in-vacuo to a diagnostics room by a multi-optics beamline with a transmission efficiency of typically 35% for detailed characterisation and experimental use. The FEL delivers ∼3 μJ energy per micro-pulse, corresponding to ∼4 mJ per macro-pulse. Further details of the FEL operating parameters and performance are given in [4].

Calculations of the gain, from the exponential rise at the start of the train, have previously been made using a Mercury Cadmium Telluride (MCT) detector. The MCT detector does not fully resolve individual FEL pulses but exhibits a small modulation of the signal corresponding to the pulse train structure. Single-pass gain values of up to ∼25% have been measured using the MCT. Pre-amplification of the MCT signal slows the response, introducing an artificial limit to gain measurements. A new photoelectromagnetic IR detector, with sufficiently fast response to resolve individual FEL pulses, has recently been added. New software has been developed to continuously monitor the gain by fitting to the envelope of the exponential rise. This is proving valuable for more rapid optimisation.

The FEL pulse duration has thus far been inferred both from measurement of the output power and spectrum, and from direct measurements of the electron bunch length. Work has been done towards capturing the longitudinal profile of the FEL pulse in a single shot. This involves cross-correlating the FEL pulse and an external laser via co-propagation in a non-linear crystal. Preliminary experiments have demonstrated both spatial and temporal overlap in a co-linear arrangement and the next step is to move to a non-co-linear alignment to allow extraction of the FEL pulse profile.

The FEL output has also been integrated with a Scanning Near-field Optical Microscope (SNOM) [5] as part of a collaboration with the Universities of Liverpool and Rome. The motivation is sub-diffraction biochemical imaging of human tissue. The research programme aims to develop diagnostics and understand the mechanism and drug action in oesophageal cancer. The FEL tuning range of 5.5 – 9 μm is well matched to the molecular fingerprint region.

ISBN 978-3-95450-123-6

PULSE STRUCTURE MEASUREMENT OF NEAR-INFRARED FEL IN BURST-MODE OPERATION OF LEBRA LINAC

K. Nakao*, K.Hayakawa, Y. Hayakawa, M. Inagaki, K. Nogami, T. Sakai, T. Tanaka,
Laboratory for Electron Beam Research and Application (LEBRA), Nihon University, Chiba, Japan
H. Zen, Kyoto University Institute for Advanced Energy, Kyoto, Japan

Abstract

The near-infrared free electron laser (FEL) at the Laboratory for Electron Beam Research and Application (LEBRA) in Nihon University has been provided for scientific studies in various fields since 2003. Improvement in the electron beam injector system for the LEBRA 125MeV electron linac made possible to accelerate the electron beam in three different modes, full-bunch mode, superimpose mode and burst mode. FEL lasing in the second and the third modes was achieved in 2011. In these three modes, the pulse length of the FEL of wavelength 1600 nm was measured by using the autocorrelation trace obtained from the Michelson interferometer.

LEBRA 125MEV LINAC

The LEBRA has supplied the infrared free electron laser (FEL) and parametric X-ray (PXR) for various user experiments since 2004 [1].

Table 1 lists the parameters of the LEBRA 125MeV linac. The linac uses the conventional 100kV DC electron triode gun. The grid of this DC gun is fed pulse from two grid pulsars, the conventional macro grid pulsar and the high-speed grid pulsar. The emitted electron beam is accelerated to maximum 125MeV in three 4m accelerator tubes. Two klystrons, PV-3040 and PV-3040N manufactured by Mitsubishi Electric amplify to approximately 20MW each. RF is generated from the master oscillator and fed to each klystron. The amplified RF is fed to the pre-buncher, the buncher and three accelerator tubes. The accelerated beam is transported to the FEL undulator line by two 45-degree bending magnets. Table 2 lists the specification of the undulator. The round trip time of the undurator is 44.8ns.

Table 1: Specification of the LEBRA 125MeV Linac

Accelerating RF Frequency	2856 MHz
Klystron peak output power	30 MW
Number of klystron	2
Electron beam energy	30-125 MeV
Energy spread	0.5 $\sim$ 1 %
Macro pulse beam current	200 mA
Macro pulse duration	20 μs
Maximum Repetition Rate	12.5Hz

The output of the high-speed grid pulsar is superimposed on the output of the macro grid pulsar by the grid pulse coupler, and fed to the grid of the electron gun. Thus, there are three beam modes, the full bunch mode, the burst mode and the superimpose mode, as illustrated in Figure 1.

Table 2: Specification of the LEBRA Undurator

Resonator length	6720 mm
Undurator length	2.4 m
Undurator of period	48 mm
Number of periods	50
Maximum K value	1.36 rms

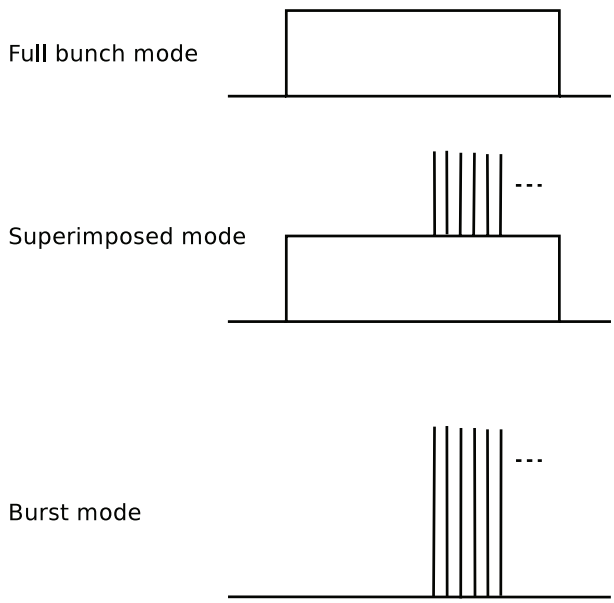

Figure 1: Illustration of pulse structure in full bunch Mode, Superimpose Mode and Burst Mode.

BURST MODE AND SUPERIMPOSE MODE BEAM

RF generated from the master oscillator is fed to the frequency divider. The high-speed grid pulser is driven by the 89.25MHz sine wave output from the frequency divider as a master clock input. The clock input is divided internally by 2 or 4. The gated output of the pulsar is a train of short pulses with a period of 22.4ns or 44.8ns and a pulse width of 600ps FWHM.

In the full-bunch mode, only the macro grid pulsar is used. When the superimpose mode is selected, both of grid

* nakao@lebra.nihon-u.ac.jp

ISBN 978-3-95450-123-6

DEVELOPMENT OF FREE-ELECTRON LASERS USING TWO "HIGHER ORDERS" WITH THE STORAGE RING NIJI-IV

N. Sei#, H. Ogawa, K. Yamada,
Research Institute of Instrumentation Frontier, National Institute of Advanced Industrial Science and Technology, 1-1-1 Umezono, Tsukuba, Ibaraki 305-8568, Japan

Abstract

We developed higher-harmonic free-electron laser (FEL) oscillations with the storage ring NIJI-IV from the visible to near-infrared region. Using another "higher order", that is, higher-diffraction order of the target wavelength of dielectric multilayer mirrors, we realized a lasing on the highest order in the harmonic FELs. Moreover, the FEL wavelength was shortened to the visible region in the NIJI-IV infrared FEL system. We demonstrated that wavelength regions of FEL oscillations could be selected by changing a condition of the optical cavity in the same conditions of the electron beam and insertion device. Our experimental results will give clues to realize a resonator-type FEL in the extreme ultraviolet and X-ray regions.

INTRODUCTION

A resonator-type free-electron laser (FEL) is superior for its highly coherence and stable lasing wavelength. Because it is necessary for the resonator-type FEL to use an optical cavity, it is thought that a lasing wavelength region of the resonator-type FEL is limited. However, a low-emittance and short-pulse electron beam is designed for an energy-recovery linac recently, so that FEL oscillations will be able to realize with a resonator in the extreme ultraviolet and X-ray regions. Utilization of higher harmonics of a spontaneous emission generated by an insertion device is effective for the resonator-type FEL to enhance a lasing wavelength region. Then, we developed the higher-harmonic FEL oscillations with using an infrared (IR) FEL system in the storage ring NIJI-IV [1]. It was clarified that there were differences between the fundamental harmonic and the higher harmonic FELs in their linewidths and pulse widths. Moreover, we achieved for the first time FEL oscillations with a higher-diffraction order of optical cavity mirrors [2]. Using the two 'higher orders' in the NIJI-IV IR-FEL system, we realized a lasing on the seventh harmonic [3], which was the highest order in the higher-harmonic FELs. In this article, we reported detailed characteristics of the higher-harmonic FEL oscillations with the higher-diffraction orders of the optical cavity mirrors.

NIJI-IV IR-FEL SYSTEM

The storage ring NIJI-IV has two 7.25 m straight sections in a circumference of 29.6 m. Short-wavelength FELs were developed with an optical klystron ETLOK-II installed in one of the straight sections in a wavelength region of 595–198 nm [4], which ranges from the visible to the vacuum ultraviolet. A planar optical klystron ETLOK-III, dedicated to development for IR FELs, was installed in another straight section [5]. It has two 1.4 m undulator sections comprised of seven periods and a 72 cm dispersive section. The maximum K value of the ETLOK-III is estimated to be 10.4 at the minimum undulator gap of 36 mm. IR FEL experiments were conducted with electron-beam energy of 310 MeV. Because the RF cavity voltage was low, approximately 20 kV, a natural bunch length was long, 90 ps, and the electron-beam current was less than 6 mA in a single-bunch operation. The relative energy spread of the electron bunch was 4.0×10^{-4} in the FEL experiments. The lasing wavelength region was reported to be from 838 to 1551 nm in the last FEL conference [6].

HIGHER-DIFFRACTION ORDER OF OPTICAL CAVITY MIRRORS

We used dielectric multilayer mirrors in the IR-FEL experiments as optical cavity mirrors. High reflectivity of the dielectric multilayer mirrors arises from constructive interference of lights reflected at consecutive interfaces of a multilayer structure. The designed high-reflectivity wavelength, or target wavelength, is four times the optical thickness of the layers [7]. If the absorptions of the two alternating dielectric materials are negligibly small, the high-reflectivity wavelengths are expected to appear at higher-diffraction orders having a positive odd number. However, the absorption of the dielectric multilayer mirrors at higher-diffraction orders is too large to oscillate storage ring FELs because the conventional target wavelengths are in the visible and ultraviolet regions. Therefore, to develop storage ring FEL oscillations in the middle-IR (MIR) region for the first time, we used niobium pentoxide (Nb_2O_5) and silicon dioxide (SiO_2) dielectric multilayer mirrors (radius of curvature, 8 m) manufactured by LAYERTEC (Germany) [8]. Figure 1 shows a cross-sectional image of the Nb_2O_5/SiO_2 dielectric multilayer mirror observed by field emission scanning electron microscopy (FE-SEM). It has 12 layers of Nb_2O_5 and 11 layers of SiO_2 stacked alternately on a 8.7 mm thick SiO_2 substrate. The thickness of a pair of the Nb_2O_5 and SiO_2 layers was uniform. The measured thickness was 0.75 μm, and the ratio of the thicknesses of the Nb_2O_5 and SiO_2 layers was 2:3. Because the target wavelength of the dielectric multilayer mirror was designed to be 2.56 μm, the refractive indices of Nb_2O_5 and SiO_2 were estimated to be 2.13 and 1.43, respectively, at this wavelength.

#sei.n@aist.go.jp

ISBN 978-3-95450-123-6

DEVELOPMENT OF INTENSE TERAHERTZ–WAVE COHERENT SYNCHROTRON RADIATIONS AT LEBRA

N Sei# , H. Ogawa, Research Institute of Instrumentation Frontier, National Institute of Advanced Industrial Science and Technology, 1-1-1 Umezono, Tsukuba, Ibaraki 305-8568, Japan

K. Hayakawa, T. Tanaka, Y. Hayakawa, K. Nakao, K. Nogami, M. Inagaki, Laboratory for Electron Beam Research and Application, Nihon University, 7-24-1 Narashinodai, Funabashi, 274-8501, Japan

Abstract

To obtain an intense light source in the terahertz region, we developed coherent synchrotron radiation (CSR) using an S-band linac at Laboratory for Electron Beam Research and Application in Nihon University. Intense radiation was observed in the D-band region and it was confirmed to be the CSR. The two-dimensional distribution of the CSR was measured, and the CSR reflected in the vacuum chamber of the bending magnet was found to be emitted through the quartz window for a few tens of picoseconds.

INTRODUCTION

Nihon University and National Institute of Advanced Industrial Science and Technology have jointly developed intense terahertz-wave coherent synchrotron radiation (CSR) at Laboratory for Electron Beam Research and Application (LEBRA) in Nihon University. Because the electron beam of a linac used in an FEL facility must have a short bunch length and a high charge in order to saturate the FEL power, it is suitable for generating intense coherent radiation [1]. We measured an intense terahertz (THz) wave from LEBRA and confirmed it to be the CSR [2]. In this article, we report the characteristics of the observed CSR.

S-BAND LINAC AT LEBRA

The S-band linac at LEBRA consists of a 100 keV DC electron gun, prebuncher, buncher, and three 4 m long traveling wave accelerator tubes [3]. The electron beam accelerated by the linac is guided to an FEL undulator line by two 45-degree bending magnets. Energy of the electron beam can be adjusted from 30 to 125 MeV, and the charge in a micropulse is approximately 30 pC in full-bunch mode, where the electron beam is bunched in 350-ps intervals [3, 4]. The macropulse duration determined by the flat-top pulse width of the 20 MW klystron output power is approximately 20μs. The insertion device is a 2.4-m planar undulator with a maximum K value of 1.9. The length of the undulator period and number of the periods are 48 mm and 50, respectively. The electron beam in the undulator is removed from the FEL undulator line by a 45-degree bending magnet and loses its energy in a beam dump. Mirror chambers, each containing a metal mirror, are set at the ends of the FEL undulator line; the mirrors are 6.72 m apart. Fundamental FELs oscillate

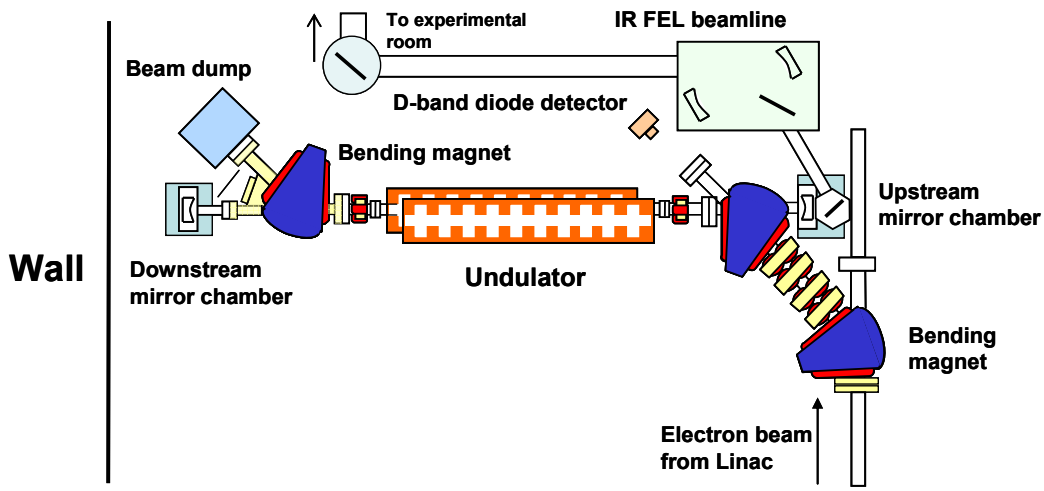

Figure 1: Outline of the CSR observation experiment at LEBRA.

*#sei.n@aist.go.jp

ISBN 978-3-95450-123-6

THE TERAHERTZ FEL FACILITY PROJECT AT CAEP

X. Yang, M. Li, Z. Xu, Institute of Applied Electronics, CAEP, China
X. Shu,Y. Dou, Institute of Applied Physics and Computation Mathematics, China
X. Lu, Peking University, China
W. Huang, Tsinghua University, China

Abstract

To meet the requirement of material and biomedicine study, a Terahertz FEL user facility project was proposed by China Academy of Engineering Physics(CAEP). At present the project has been approved and the facility will be constructed within 5years. The facility will operate in the quasi CW mode and the average power is about 10W . The wavelength of the light can be adjusted between 100μm/3THz to 300μm/1THz according to the user needed by changing the electron energy and the magnetic field of the wiggler. The facility mainly consists of the electron source, the main accelerating structure, the hybrid wiggler, the optical oscillator cavity, the THz-ray transmission system and the detector. In order to achieve the high brightness beam, the photocathode DC gun will be used as the electron source. The electron will obtain the energy by passing through a superconducting accelerator, the electron energy after the accelerator is about 8MeV, which is suitable to obtain the terahertz light. The facility will be a useful tool to the science.

INTRODUCTION

FEL-THz is one important kind of THz source which has the merits of high power, wide tunable spectral region[1,2,3]. The goal of the THz radiation frequency spans 1THz to 3THz which is absence of source and other kind of THz sources are not good at at the same time. The use of superconductive rf-linac cavities enables quasi-cw operation with the associated higher average THz radiation power level of ten Watt. The facility will operate at up to 8 MeV and with up to 5 mA average current at a 54.16 MHz pulse repetition rate. The length of the resonator is 2.769m, and the THz ray will output through the downstream mirror with an outcoupling hole in the center. A waveguide will be installed to fit the optical resonator mode into the wiggler gap. The cross section of the waveguide is rectangular with 30mmx14mm. The waveguide spans from the upstream mirror to the downstream mirror. The sketch map is showed in Fig. 1. The people from the Institute of Applied Physics and Computation Mathematics, Peking University, Tsinghua University and Institute of Applied Electronics will take part in the project.

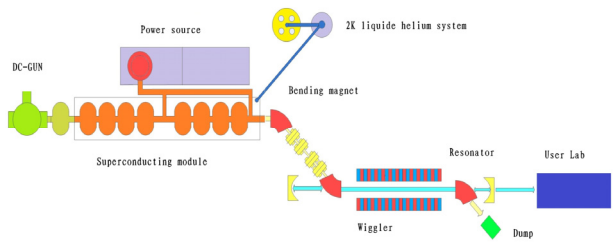

Figure 1: Layout of the FEL-THz facility.

THE SIMULATION OF THE OSCILLATOR

The normal parameters of the facility are listed in Table 1 which is used as the input parameters for the simulation.

Table 1: Parameters used for the Simulations

ELECTRON BEAM	
Energy	7.5MeV
Peak current	10A
Micro bunch	10ps
Normalized Emittance	10πmm mrad
Energy Spread (FWHM)	0.75%
Repetition rate	54.17MHz
WIGGLER	
Amplitude	3300Gs
Period	38mm
Length	42 periods/1.6 m
Optical	
Wavelength	160.3μm
Cavity length	2.769m
Mirror curvature	1.85m
wave-guide Cross-section	30mm×14mm

The simulation of oscillator cavity was done by a three dimension code[4], it includes the gain according the current, the energy spread and the emittance, the light power rising progress in the cavity, the optical loss, the coupling efficiency, the detuning, the sensitivity to vibration and misalignment etc. The simulation results are shown in Figs. 2~3. The calculated THz radiation power according different frequency is listed in Table 2.

ISBN 978-3-95450-123-6

THE PARAMETER STUDY OF TERAHERTZ FREE-ELECTRON LASER OSCILLATOR BASED ON ELECTROSTATIC ACCELERATOR*

Ailin Wu#, Qika Jia, USTC/NSRL, Hefei, China
Faya Wang, Juhao Wu, SLAC, Menlo Park, CA, USA.

Abstract

Free-Electron Laser Oscillator based on Electrostatic Accelerator (EA-FELO) is one of the best methods to realize the powerful terahertz source, which can not only produce high power, but also obtain coherent and tunable wavelength. In this paper, we investigate the effects of the main parameters in this scheme, including the initial electron-beam energy spread, emittance and beam current. Besides, the influence of the radius of the mirrors and the position of the undulator on FEL performance is also studied. The numerical results from 1D FEL Oscillator simulation code FELO are presented, and show that this compact device could achieve the terahertz light with the peak output power is about 5.3kW.

INTRODUCTION

Since the terahertz sources provide wide applications in medical science, material science and industry, a compact, wavelength tunable and high-power THz source attracted much attention in many laboratories [1]. It is noteworthy that EA-FELO could achieve high average power generation, high energy conversion efficiency and high spectral purity, because of its CW operation. Such devices have been developed and operated successfully, such as University of California Santa Barbara FEL (UCSB- FEL) employed a 6MeV Pelletron accelerator and obtained 2.5 mm to 30 μm FEL [2], Israel FEL based on a 6 MeV EN tandem acceleration can produce average power of 1kW in the range of 70-130 GHz [3]. Recently, we also have made some primary research and analysis on it [4-5].

On the basis of the research on FEL Oscillator's basic principle, a conceptual design and parameters study of a compact EA-FEL is proposed in this paper. The numerical modeling has been carried out by using 1D FEL stimulation code FELO [6].

BRIEF REVIEW OF THE EA-FEL OSCILLATOR SCHEME

In this scheme, electrostatic accelerator generates continuous beams of very high quality electrons and small energy spread. The resonator is of a symmetric near-concentric design and a collector collects the decelerated electrons. The schematic of this EA-FEL Oscillator is provided in Figure 1.

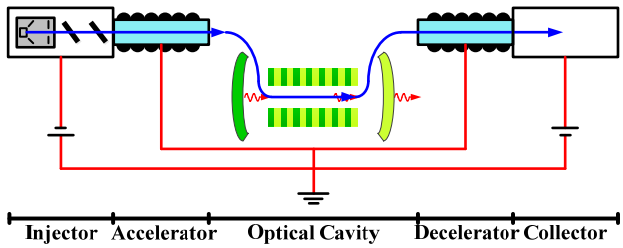

Figure 1: Conceptual design of the EA-FEL Oscillator.

Reference to the electron beam parameters of normal electrostatic accelerator and the present technology, we use a 3MeV beam to limit the size of EA tank and apply other electron parameter as in UCSB-FEL. According to the equation of maximum gain of FEL Oscillator, the small signal gain is proportional to the number of periods and on-axis field strength, so we must strike a balance between achieving larger output power and satisfying device miniaturization. The main design parameters for the simulations are listed in Table 1.

Table 1: The Main Parameters for EA-FEL Oscillator

Electron Beam	
Beam energy	3 MeV
Current	2 A
Energy spread	0.01%
Emittance	10 π mm-mrad
Undulator	
K	0.3
Period length	2 cm
Number of periods	50
Optical Cavity	
Radius of curvature of mirrors	1.08 m
Radiation wavelength	303 μm
Distance from upstream mirror to undulator centre	1m
Optical cavity length	2m

* Work supported by the Major State Basic Research Development Programme of China under Grant No. 2011CB808301 and the National Nature Science Foundation of China under Grant No. 10975137
# wuailing@mail.ustc.edu.cn

ISBN 978-3-95450-123-6

THz RADIATION SOURCES BASED ON RF-LINAC AT CHIANG MAI UNIVERSITY

C. Thongbai#, P. Boonpornprasert, S. Chunjarean, K. kusoljariyakul,
S. Rimjaem, J. Saisut, S. Supakul
Chiang Mai University, Chiangmai, 50200, Thailand
Thailand Center of Excellence in Physics, Bangkok 10400, Thailand

Abstract

A THz radiation source in a form of coherent radiation from short electron bunches has been constructed at the Plasma and Beam Physics (PBP) research facility, Chiang Mai University. The accelerator system consists of an RF-gun with a thermionic cathode, an alpha-magnet as a magnetic bunch compressor, and a SLAC-type linear accelerator. Coherent transition radiation emitted from short electron bunches passing through an Al-vacuum interface was used as the THz radiation source. This THz radiation can be used as a source of the THz imaging system and THz spectroscopy. Details of the accelerator system and THz radiation production will be presented. A plan for extension to accommodate Free Electron Lasers (FEL) optimized for mid-infrared and far-infrared/THz radiation will also be discussed.

INTRODUCTION

THz radiation is electromagnetic radiation spectrum which has wavelength of 1000μm to 100 μm (300 GHz - 3 THz) and lies in gap between Microwave and Infrared. In the past, this gap is unexplored region but nowadays technologiesand applications of THz radiation were developed rapidly and were reviewed in [1-4]. A THz facility based on femtosecond electron bunches has been established at the Plasma and Beam Physics research facility (PBP), formerly the Fast Neutron Research Facility (FNRF), Chiang Mai University. Figure 1 shows a schematic layout of the system.The main components of the system are a thermionic cathode RF-gun, an alpha-magnet as a magnetic bunch compressor, a SLAC-type linear accelerator (linac), beam steering and focusing elements, and beam diagnostic instruments.

The 1-1/2 cell S-band RF-gun was designed and optimized [5] for bunch compression such that the first electron is accelerated and reaches the end of the half-cell just before the field becomes decelerating. It is then further accelerated through the full-cell to reach maximum kinetic energy of 2.0-2.5 MeV at the gun-exit depending on accelerating field gradients. Later electrons feel some decelerating fields and gain less and less overall energyresulting in a well-defined correlation between energy and time for bunch compression. Electron bunches of 20-30 ps from the RF-gun are then compressed in an α-magnet, where the particle path length increases with energy. This allows the lower energy particles, emitted later in each bunch, to catch up with the front for effective bunch compression. The optimized and compressed part of the electron bunch is filtered by energy slits located in the alpha-magnet vacuum chamber and then transported through the linac and the beam transport line to experimental stations. At the experimental station, the bunches are compressed to less than 1 ps [6]. These short electron pulses can be used to produce high intensity THz radiation in the form of coherent transition radiation. Typical operating parameters and electron beam characteristics are shown in Table 1.

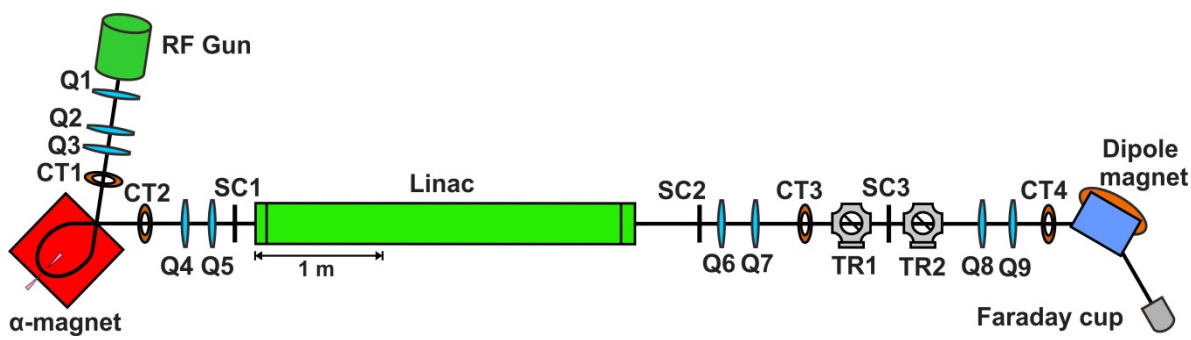

Figure 1: Schematic diagram of the accelerator system at Chiang Mai University for generation of short electron bunches and THz radiation [Q:quadrupole magnet, CT:current monitor, SC:screen, TR: transition radiation].

#chlada@yahoo.com

ISBN 978-3-95450-123-6

LINAC-BASED THZ IMAGING AT CHIANG MAI UNIVERSITY

J. Saisut#, P. Boonpornprasert, K. Kusoljariyakul, S. Rimjaem, C. Thongbai, Department of Physics and Materials Science, Chiang Mai University, Chiang Mai 50200, Thailand
M.W. Rhodes , P. Tamboon, STRI, Chiang Mai University, Chiangmai 50200, Thailand

Abstract

At the Plasma and Beam Physics Research Facility (PBP), Chiang Mai University, intense THz radiation is generated in a form of coherent transition radiation from femtosecond electron bunches. The THz radiation is used as a source of THz imaging system which was successfully setup and tested. The radiation is focused onto a sample which will be scanned using an xy-translation stage. The transmission or reflection at different points of the sample are recorded to construct a THz image. Details of the setup and the experimental results from the system will be presented. The THz imaging to accommodate a future IR-THz Free Electron Laser (FEL) will also be discussed.

INTRODUCTION

A THz facility based on femtosecond electron bunches has been established at the Plasma and Beam Physics Research Facility (PBP), Chiang Mai University. Femtosecond electron bunches are generated from a system consisting of an RF-gun with a thermionic cathode, an alpha-magnet as a magnetic bunch compressor and a linear accelerator as a post acceleration section. At the experimental station, the bunches are compressed to less than 1 ps. The experimental results reported in [1] show that electron bunches as short as σ_z =200 fs can be generated from the system. Typical operating parameters and electron beam characteristics of the facility are complied in Table 1.

The femtosecond electron bunches can be used to produce high intensity THz radiation in the form of coherent transition radiation by placing an aluminium foil (Al-foil) 45° in the electron path, representing a transition between vacuum and conductor [2]. The backward transition radiation is emitted perpendicular to the beam axis as shown in Fig. 1. The radiation is collimated by a 1-inch 90º parabolic mirror and transmits through a high density polyethylene (HDPE) window of 1.25-mm-thick and 32-mm diameter. The available THz radiation covers wavenumbers from 5 cm^{-1} to around 80 cm^{-1} which corresponding to a frequency range from 0.3 THz to 2.4 THz. This THz radiation is used as a source of the THz imaging system.

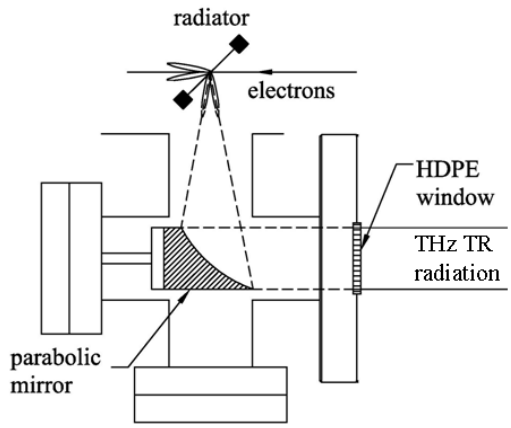

Figure 1: Setup to generate THz Transition radiation.

THZ IMAGING SYSTEM

A schematic diagram of the THz imaging system (transmission measurement) at the Plasma and Beam Physics Research Facility (PBP), Chiang Mai University is illustrated in Fig. 2 for transmission or reflection measurement. THz radiation is focused on a sample which will be scanned using an xy- translation stage

Table 1: Operating and beam parameters

Parameters	RF-gun	Linac
Maximum beam energy (MeV)	2.0-2.5	6 - 12
Macropulse peak current (mA)	700-1000	5-150
RF-pulse length (μs)	2.8	8
Repetition rate (Hz)	10	10
Beam-pulse length (μs)	2	0.8
Number of microbunches per macropulse	5700	2300
Number of electrons per microbunch	1.4×10^9	1.4×10^8

#jatuporn.saisut@cmu.ac.th

ISBN 978-3-95450-123-6

CHARACTERIZATION OF SINGLE-CYCLE THz PULSES AT THE CTR SOURCE AT FLASH

S. Wunderlich*, S. Schefer, B. Schmidt, S. Schulz, S. Wesch, DESY, 22603 Hamburg, Germany
M.C. Hoffmann, SLAC, Menlo Park, CA, 94025, USA

Abstract

At the coherent transition radiation (CTR) source at the Free-Electron Laser in Hamburg (FLASH) at DESY, single-cycle THz pulses with MV/cm electric field strengths are generated. We present the temporal and spatial characterization of this source with the technique of electro-optic sampling using a laser system synchronized with the accelerator to better than 100 fs. This method offers a quantitative detection of the electric field of the THz pulses in the time domain. Compared to other electron accelerator driven sources like undulator radiation, the transition radiation source provides pulses with a high bandwidth and durations shorter than one picosecond. This enables time-resolving and non-destructive experiments with radiation in the THz regime including THz pump / THz probe experiments. Broadband and intense THz pulses are expected to be valuable tools for the study of dynamics of excitation of complex materials in transient electric and magnetic fields.

INTRODUCTION

Far-infrared (FIR) radiation with wavelengths from 3 µm to 3 mm or frequencies in the terahertz (THz) regime offers the possibility for the non-destructive investigation of nonlinear effects in various materials [1, 2, 3].

In addition to laser-driven sources [4], electron accelerator-based sources, i.e. undulator radiation, light generated in the free-electron laser (FEL) process and transition radiation offer single- or few-cycle THz pulses of microjoule pulse energy and MV/cm electric field strengths [5].

Free-electron lasers require a peak current of several kiloamperes for lasing [6] which enables in parallel coherent transition radiation sources for THz generation.

When a charged particle passes the boundary of two media with different dielectric constants, transition radiation is emitted [7]. For a bunch of charged particles, a coherent superposition occurs for wavelengths longer than the bunch length. The spectral intensity distribution $dU/d\lambda$ now depends on the number of particles in the bunch N squared and on the 3-dimensional form factor F [8].

$$\frac{dU}{d\lambda} = \left(\frac{dU}{d\lambda}\right)_{\text{one particle}} \cdot \left(N + N(N-1)\cdot|F(\lambda)|^2\right)$$

A well established method for detection of THz radiation is the electro-optic sampling using a scanning delay (EOS) [9]. The *electro-optic* or *Pockels* effect is the induced change in birefringence of a medium by external electric fields and can be probed by laser pulses. In the electro-optic crystal, the incident linear polarization of the laser is transformed into an elliptical polarization state depending linearly on the electric field strength applied on the crystal. Using an analyzer consisting of a retarder and a Wollaston beam splitter, two orthogonal polarization components are separated and detected by two photo detectors in a balanced detection scheme. Without the THz field, the analyzer is set for equal intensities I_1 and I_2. In the presence of the electric field, the photo detector intensities are modulated and the electric field strength E can be deduced following

$$\begin{aligned}\Gamma(\alpha) &= \frac{\pi\, d}{\lambda}\, n_0^3\, t\, E\, r_{41}\, \sqrt{1+3\cos^2(\alpha)} \\ &= \sin^{-1}\left(\frac{I_1 - I_2}{I_1 + I_2}\right)\end{aligned}$$

with the laser wavelength λ, the crystal refractive index n_0 and thickness d, the Fresnel coefficient for reflective losses t and the angle α between the optically active crystal axis X and the THz field E [10]. The Pockels coefficient r_{41} is the response of the crystal in phase retardation.

The temporal resolution of EOS is restricted by the temporal laser pulse width as well as the phase matching bandwidth in $\langle 110\rangle$ cut gallium phosphide (GaP) which is limited to frequencies smaller than 8 THz by a phonon resonance. Furthermore, the temporal jitter between the laser and the CTR pulses leads to temporal averaging and thus, to a reduction in peak field strength detected by EOS.

EXPERIMENT

The CTR source at FLASH is located behind the last accelerating module providing electron energies up to 1.2 GeV. The screen made of silicon of 380 µm thickness and coated with aluminum is placed in the electron beam pipe at an *off-axis* position horizontally shifted from the standard electron trajectory. A kicker magnet enables a complementary operation to the FEL by deflecting one electron bunch onto the screen out of a pulse train in 10 Hz repetition rate.

After passing through a wedge-shaped diamond window, the radiation is guided into an external laboratory by a transfer line of approx. 21 m length. An optical system of seven gold-coated toroidal and plane mirrors images the radiation source into the setup described below. The

* steffen.wunderlich@desy.de

ISBN 978-3-95450-123-6

TUNABLE IR/THZ SOURCE FOR PUMP PROBE EXPERIMENTS AT THE EUROPEAN XFEL

E.A. Schneidmiller, M.V. Yurkov, DESY, Hamburg, Germany
M. Krasilnikov, F. Stephan, DESY, Zeuthen, Germany

Abstract

We present a concept of an accelerator based source of powerful, coherent IR/THz radiation for pump-probe experiments at the European XFEL. The electron accelerator is similar to that operating at the PITZ facility. It consists of an rf gun and a warm accelerating section (energy up to 30 MeV). The radiation is generated in an APPLE-II type undulator, thus providing polarization control. Radiation with wavelength below 200 micrometers is generated using the mechanism of SASE FEL. Powerful coherent radiation with wavelength above 200 micrometers is generated in the undulator by a tailored (compressed) electron beam. Properties of the radiation are: wavelength range is 10 to 1000 micrometers (30 THz - 0.3 THz), radiation pulse energy is up to a few hundred microjoule, peak power is 10 to 100 MW, spectrum bandwidth is 2 - 3 %. Pump-probe experiments involving ultrashort electron pulses can be realized as well. The time structure of the THz source and x-ray FEL are perfectly matched since the THz source is based on the same technology as the injector of the European XFEL. A similar scheme can also be realized at LCLS, SACLA, or SWISS FEL with S-band rf accelerator technology.

INTRODUCTION

Infrared and THz radiation is of high importance for applications in a wide variety of scientific fields like:

- study of quantum matter (strongly interacting quantum systems).
- magnetism and correlated states (High-Tc superconductivity, quantum Hall effect, Bose-Einstein condensation).
- complex fluids, petroleum, bio-fluids.
- study of structures and dynamics exploiting nuclear and electron magnetic resonance.
- condensed matter physics (nanoscale structure and determining phase diagrams).
- membrane proteins, bio-molecules (e.g. dynamics and function of metal ions in bio-systems).
- materials chemistry (element specific nuclear and electron spins, including quadrupolar nuclei).
- condensed matter technologies (glasses, ceramics, catalysts, zeolytes, batteries and fuel cells), etc.

Combination of IR/THz and x-ray pulses in pump-probe experiments at x-ray FEL facilities opens a new dimension to study the evolution of the above mentioned systems on atomic and molecular time scales [1–4].

An IR/THz source for pump-probe experiments at x-ray FELs should meet many requirements like tunability in a wide range (ideally from a fraction of micrometer up to a few millimeters), spectral and temporal properties, peak power, polarization, and the possibility for a precise synchronization with the x-ray pulse. For the moment, traditional techniques of IR/THz generation do not provide an universal solution for pump-probe experiments at x-ray FELs. Some part of the IR spectrum will be covered by quantum lasers. There are also developments of THz sources for pump-probe experiments. Each of such techniques may look to be a technically simple (table-top) solution, but an attempt to combine several devices in one place may lead to a complicated and expensive system.

Electron beams allow generating electromagnetic radiation in a wide wavelength range. Free electron lasers cover the full IR range [5–9]. Coherent radiation sources in a THz wavelength range operate in many location as well [10, 11]. Using the same electron beam to generate two colors for pump-probe experiments with a soft x-ray FEL has been implemented at FLASH [12–14]. The electron beam first generates the x-ray pulse in an x-ray undulator, and then passes a long period undulator and produces powerful, coherent undulator radiation at longer wavelengths down to the shortest scale of the electron bunch shape features. It has been shown experimentally that both pulses can be synchronized with femtosecond accuracy [15]. LCLS exploits the mechanism of coherent transition radiation (CTR) to generate THz radiation in a 2 μm thick Be foil placed after the x-ray undulator. A technical complication of such an approach is the necessity to transport the IR/THz radiation over long distances [13, 16, 17], but it is partially compensated by the good intrinsic synchronization of the IR/THz and x-ray pulses since they are generated by the same electron bunch. However, there exists a serious problem - nearly all application require the pump IR/THz pulse to come first. While there is no problem to delay the IR/THz radiation, it is an evident problem for x-rays. A solution of the problem can be to accelerate two closely spaced electron bunches such that the first bunch generates a IR/THz pulse with suppressed x-ray radiation [18, 19]. However, the first bunch always produces background radiation (spontaneous emission) which may be unacceptable for some experiments. To avoid this unwanted effect LCLS researches consider the option to bypass the x-ray undulator by the first bunch.

ISBN 978-3-95450-123-6

EMISSION OF COHERENT T-RAYS FROM TRAINS OF ULTRASHORT ELECTRON PULSES IN A PULSED HELICAL UNDULATOR

W.K. Lau, A.P. Lee, M.C. Chou, J.Y. Hwang, NSRRC, Hsinchu 30076, Taiwan.
N.Y. Huang, Institute of Photonics Technologies, NTHU, Hsinchu, Taiwan

Abstract

GHz-repetition-rate relativistic electron pulses with duration shorter than 100 fs can be produced from the thermionic rf gun injector system which is now under construction at NSRRC. Experiments for production of coherent sub-THz or THz radiations by passing this prebunched electron beam through an 8 cm period bifilar helical undulator are suggested. The undulator will be powered by a 200 μs current pulser at 10 Hz repetition frequency. Conditions for obtaining coherent emission and expected properties of the radiations are discussed.

INTRODUCTION

Relativistic ultrashort electron pulses at GHz-repetition-rate can be generated from a thermionic cathode rf gun injector system. In such system, A linearly energy chirped electron is produced from the gun with an optimum accelerating field profile. An alpha magnet is installed to provide the dispersion required for bunch compression [1, 2]. Alternatively, one can performs bunch compression by velocity bunching in the rf linac structure during the early stage of beam acceleration [3-5].

It is well known that the emission of coherent radiations from a bunch with N electrons is possible as long as its bunch length is much shorter than the radiation wavelengths [6-8]. The power of the coherent radiation will be $\sim N^2$ times higher than that of the spontaneous radiation from a single electron depending on the bunch form factor. Furthermore, as pointed out by Gover and Dyunin [7], the bandwidth of the coherent radiation from an undulator by a periodic train of electron bunches is inversely proportional to the number of bunches in the train. Since the thermionic rf gun injectors has the capability to produce long trains of periodic ultrashort bunches, they are very well suited for the generation of narrow-band coherent radiations. Generation of coherent transition radiations (CTR) in the THz range with the thermionic rf gun injectors of SUNSHINE and SURIYA facilities by hitting beams on metallic foils are good examples of pre-bunched electron beam coherent radiations [1, 9].

In this report, we describe the activities in NSRRC to construct a few tens MeV thermionic rf gun injector system for generation of high brightness ultrashort electron pulses. We plan to use a bifilar undulator to demonstrate the capability of this injector system for the production of coherent THz radiations. This undulator will be powered by a current pulser. Conditions for obtaining coherent emission and expected properties of the radiations are discussed.

GENERATION OF GHZ-REP-RATE ULTRASHORT ELECTRON PULSES

A 30 MeV, 2998 MHz thermionic rf gun injector is designed for light source R&D at NSRRC. This injector is able to deliver thousands of sub-100 fs electron pulses of few tens pC bunch charge in each macropulse. Each macropulse has pulse duration of ~1 μs at 10 Hz repetition frequency. Bunch compression scheme employed in this system rely mainly on velocity bunching. Experimental studies of inverse Compton scattering ultrafast x-ray and intense coherent THz radiation sources are planned.

The thermionic rf gun is designed to operate at accelerating field gradient of 25 MV/m and 50 MV/m in its half-cell and full-cell respectively. Since the electron at head of a bunch from the rf gun has higher kinetic energy than those at its tail, the bunch tends to decompress in drift sections. The alpha magnet helps to rotate the particle distribution in longitudinal phase space clockwise and the collimator installed in the vacuum chamber of the magnet can be used to select electrons in the desired range of momentum. In ideal situations that space charge effects are negligible, it may be feasible to compress the bunch to extremely short duration. However, as space charge effects become significant, bunch compression with alpha magnet at low beam energy becomes very ineffective. In this case, further bunch compression in the rf linac during beam acceleration by velocity bunching is indispensable. For velocity bunching, rf phase at beam injection has to be optimized for efficient compression. A high power phase shift will be installed for linac phase adjustment.

Expected Performances

Beam dynamics in the NSRRC thermionic rf gun injector has been studied extensively by computer simulation under various operation conditions with the effects of space charge included. Typical beam parameters near the entrance are listed in Table 1.

Table 1: Typical Beam Parameters at the Entrance of the rf Linac

Energy [MeV]	3.0
Bunch charge [pC]	30
Minimum bunch length [μm]	300 RMS
Peak current [A]	30
Normalized emittance [mm-mrad]	3.3
Energy spread [%]	0.28
Alpha magnet gradient [gauss/cm]	400

ISBN 978-3-95450-123-6

FLUTE, A COMPACT ACCELERATOR-BASED SOURCE FOR COHERENT THZ RADIATION

S. Naknaimueang*, E. Huttel, A.-S. Müller, M. J. Nasse,
R. Rossmanith, M. Schuh, M. Schwarz, P. Wesolowski, KIT, Germany
M. Schmelling, MPIK, Heidelberg, Germany

Abstract

In this paper beam dynamics simulations of the Linac-based THz source FLUTE (Ferninfrarot Linac- Und Test-Experiment) are presented. The optimization of various machine parameters such as laser spot size, laser pulse length, and lengths of the chicane magnets are discussed. Spectra of the generated coherent THz radiation, which depend on the compressed bunch length and charge, are shown.

INTRODUCTION

FLUTE is designed to be a test bench to answer various accelerator physics questions for future compact broadband accelerator-based THz sources. For example, effective bunch compression as well as THz generation schemes, such as coherent synchrotron, transition, and edge radiation (CSR, CTR, CER), will be implemented and compared, and corresponding diagnostic instrumentation will be studied. Furthermore, experiments using the strong THz pulses will be carried out.

The FLUTE design is a collaboration between PSI and KIT. The installation of FLUTE on the KIT campus is planned to start in 2013. The machine layout is shown in Fig. 1. The main components are a photo rf gun, a 50 MeV linac, a bunch compressor, and finally a beam dump. The pulse repetition rate is 10 Hz. FLUTE is designed to cover a large bunch charge range from 100 pC to 3 nC. The THz spectral range and intensity can be adjusted according to the experimental requirements by modifying both the electron bunch charge and length.

BEAM DYNAMICS SIMULATIONS

For the beam dynamics simulations we used both ASTRA [1] for calculating space charge effects for the entire machine, and CSRtrack [2] for calculating coherent synchrotron as well as space charge effects in the chicane.

Space Charge Effects in the Gun and Linac

We plan to use a Ti:Sa laser system together with a $2\frac{1}{2}$ cell photo-injector gun [3] to produce single electron bunches with an energy of 7 MeV. After this, the bunch is further accelerated by a 3 GHz linac with a maximum energy of 50 MeV.

The transverse beam size throughout the machine is determined by space charge effects in the gun. As shown in Fig. 2 for a bunch charge of 3 nC, the transverse electron beam size is minimal for a certain laser spot size. For smaller laser spot sizes the electron beam size is dominated by space charge effects, whereas for larger laser spots, the beam size is dominated by the laser spot size. The optimum laser spot size for various bunch charges and laser pulse lengths can be found in Table. 1.

Table 1: Optimum laser pulse and spot size for various bunch charges calculated with 3D CSRtrack for chicane magnet length of 30 cm. L_{rms} is RMS bunch length.

Charge	Laser spot	Laser pulse	L_{rms}
3 nC	2.25 mm	4 ps	287 fs
2 nC	1.5 mm	4 ps	235 fs
1 nC	1.5 mm	3 ps	199 fs
0.1 nC	0.5 mm	2 ps	70 fs

Fig. 3 shows the transverse beam size tracked through the machine for the 3 nC case with optimum laser spot size and pulse length (in this plot we have switched the chicane off to verify that the beam remains focused throughout the entire bunch compressor). The largest beam size occurs right after the gun due to the space charge effects and the relatively low energy at this point. The solenoid therefore has to be installed as close as possible to the gun to focus the beam through the linac. A quadrupole doublet after the linac is used to focus the beam through the bunch compressor. A solenoid is used in the first case because it focuses the beam symmetrically, while in the second case the quadrupole doublet allows the independent adjustment of the focusing in both transverse directions. This equips the machine with an additional knob for better beam tuning in and after the chicane.

Table 2: Compressed bunch vs chicane magnet lengths (L_b) for 3 nC calculated with CSRtrack (R_{56} is the momentum compaction, α is the bending angle of the chicane magnets and L_{rms} is RMS bunch length).

L_b	R_{56}	α	L_{rms} (1D)	3D
0.5 m	-36.1 mm	8.35°	184 fs	312 fs
0.3 m	-36.1 mm	9.08°	183 fs	287 fs
0.2 m	-36.1 mm	9.54°	183 fs	274 fs

* somprasong.naknaimueang@kit.edu

ISBN 978-3-95450-123-6

FEL GAIN MEASUREMENT WITH A NOVEL METHOD

Masaki Fujimoto#, Ryukou Kato, Keigo Kawase, Akinori Irizawa, Fumiyoshi Kamitsukasa,
Hiroki Ohsumi, Masaki Yaguchi, Goro Isoyama,
Institute of Scientific and Industrial Research, Osaka University, Osaka, Japan
Shigeru Kashiwagi,
Research Center for Electron Photon Science, Tohoku University, Miyagi, Japan
Shigeru Yamamoto,
Institute of Materials Structure Science, KEK, Ibaraki, Japan

Abstract

A novel method to measure temporal development of the FEL power has been developed using a silicon bolometer, which response linearly to input over a wide range[1]. The Si bolometer has the time resolution of ~1 ms, which is much longer than the FEL macropulse of a few μs, so that it measures energy in the macropulse. The number of amplifications is changed by varying the pulse length of electrons from the gun of the linac and energy in the FEL macropulse is measured at a wavelength ~100 μm with the detector and appropriate Teflon absorbers. The energy development of the FEL macropulse is measured over eight orders of magnitude from a very low power level close to the incoherent radiation up to the FEL power saturation. The temporal development of the FEL power is derived from the energy development as a function of the number of amplifications. Then the FEL gain is derived from the power development. We measured energy development in the macropulse and derived the FEL gain at some cavity lengths. The maximum FEL gain thus evaluated is about 56 percent, which agrees with calculation by the Super-Mode theory.

INTRODUCTION

We are conducting experiments on free-electron laser (FEL) physics using the THz-FEL based on the L-band electron linac at the Institute of Scientific and Industrial Research, Osaka University.

The gain of FEL is one of the most principal parameters of FEL and can be derived from the temporal development of the power in the FEL macropulse which is composed of many micropulses. The FEL gain was ever evaluated from a single saturated macropulse, but the macropulse was measured in a narrow range, which is limited by the dynamic range or the sensitivity of the detector. Therefore we insist that such the measured FEL gain concerned the power saturation and evaluated lower.

We measured some terahertz FEL macropulses with a germanium-gallium semiconductor detector, which has fast, ~10 ns, response, and derived the temporal development of the FEL power in a wide range with the macropulses overlapped. But we confirmed that the detector did not response to input power linearly. The gain evaluation needs a precise measurement of the variation of the FEL power and we concluded that the detector was not appropriate for the gain evaluation.

Therefore we have adopted a silicon bolometer as the detector which responses to input linearly over a wide range, ~5 decades. The detector measures energy of the FEL macropulse because of its slower response, ~1 ms, than the length of FEL macropulse. We measure the energy of macropulse with varying the number of FEL amplifications. The amplification can be varied by a control of the number of electron bunches or the beam length. The FEL power development is derived from the difference of the energy. We report the novel method for FEL gain measurement.

BACKGROUND OF EXPERIMENT

Figure 1 shows L-band linac and THz-FEL of ISIR, Osaka University. On the FEL experiment, we generate an electron beam of which the length is 8 μs from the electron gun, bunch the beam to a bunch array of which the interval is 9.2 ns with the subharmonic bunchers drived on 108 MHz and the 216 MHz and accelerate the beam to 12~18 MeV. The accelerated beam is led into THz-FEL, which is composed of a wiggler of which the magnetic period is 6 cm and the number of periods 32 and an optical resonator of which the cavity length is 5.531 m, then radiates FEL on 2~3 THz (25~150 μm).

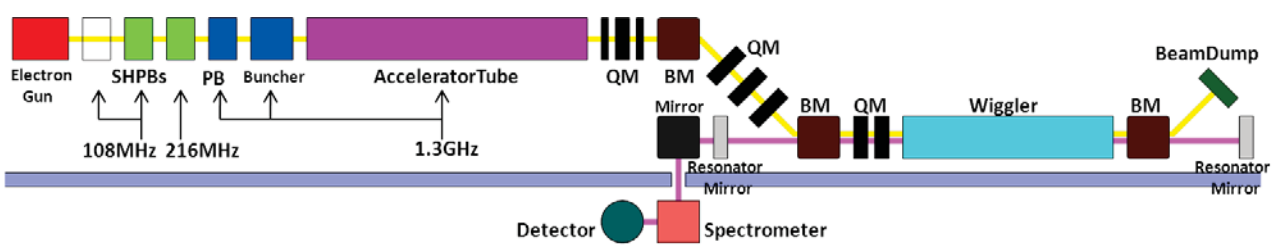

Figure 1: Diagram of L-band linac and THz-FEL.

mfmoto25@sanken.osaka-u.ac.jp

ISBN 978-3-95450-123-6

DESIGN AND NUMERICAL SIMULATION OF THz-FEL AMPLIFIER IN KYOTO UNIVERSITY

Mahmoud Bakr[1, 2], K. Shimahashi[1], K. Yoshida[1], H. Negm[1, 2], M. Omer[1, 2], R. Kinjo[1], Y.W. Choi[1], H. Zen[1], T. Kii[1], K. Masuda[1], and H.Ohgaki[1]
[1]Institute of Advanced Energy, Kyoto University, Uji 611-0011, Kyoto Japan.
[2] Physics Department, Faculty of Science Assiut University Assiut 71516, Egypt.

Abstract

We have designed a relatively simple, compact and powerful THz-FEL (terahertz free electron laser) amplifier in Kyoto University. The target wavelength range of the amplifier is 150–340 μm, corresponding to 0.5-1.1 THz. The system consists of 1.6 cell photocathode radio frequency (RF) gun, THz wave parametric generator, focusing solenoid, transport line, and 120 cm long undulator with 30 periods. A start-to-end simulation in the institute of advanced energy Kyoto University has been conducted to estimate the performance of the designed system. Tracking of the electron beam from the photocathode RF gun up to the undulator entrance has been done using Parmela code while Genesis 1.3 code has been used to estimate the FEL interaction in the undulator. For feasibility study the FEL temporal distribution at resonance wavelength 186 μm was determined. The results show that 1250% amplification could be achieved in the resonance wavelength in the present design compared with the seed THz power. Details of the design and calculation conditions together with the performance test are presented in this paper.

INTRODUCTION

Terahertz free electron laser (THz-FEL) has futures of high peak power, a narrow spectrum bandwidth, and a high coherency compared with coherent synchrotron radiation THz sources [1]. Therefore, over the last two decades, there has been a significant interest in using THz technology as strong tool in different research and application fields. THz has attracted attention in the industrial applications because it can penetrate fabrics and plastics. In the security imaging, THz radiation can detect concealed weapons since many non-metallic and non-polar materials are transparent to THz radiation. THz spectra can be used to identify the compounds of explosives and illicit drugs as well. In the medical field, THz radiation can be used in diagnosis as it has make no damage on tissue or DNA and no health risk for scanning [2].

The principle of THz-FEL operation can be simply explained as a relativistic electron beam with optimum properties travelling through a transverse magnetic field in an undulator associated with an electric field from THz seed light. At a resonance condition, the passing electron beam transfer energy to the optical field and generate FEL light. The matching between the electron beam energy and the undulator parameters to generate FEL with specific wavelength can be determined from Eq. 1.

$$\lambda_r = \frac{\lambda_u}{2\gamma^2}\left(1+\frac{K^2}{2}\right). \quad (1)$$

$$K = \frac{eB_u\lambda_u}{2\pi mc}. \quad (2)$$

where λ_r is the FEL wavelength, λ_u is the undulator period, γ is the electron Lorentz factor, e is the charge of the electron, B_u is the peak magnetic filed in the undulator, m is the electron mass, and c is the speed of light. The target THz range in the present proposal is 0.5-1.1 THz tuned only by changing the electron beam energy

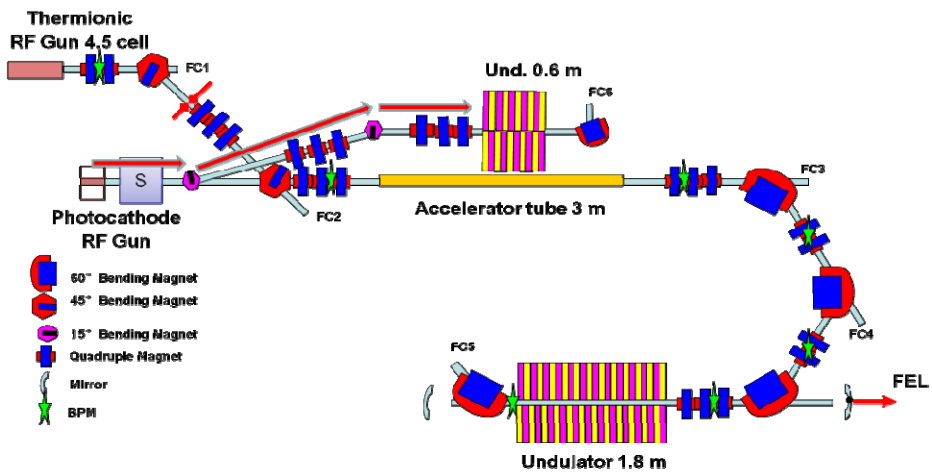

Figure 1: Schematic view of the KU-FEL facility configurations including the THz amplifier design.

#m-a-bakr@iae.kyoto-u.ac.jp

ISBN 978-3-95450-123-6

PHASE SPACE MANIPULATION WITH LASER-GENERATED TERAHERTZ PULSES

S.P. Jamison, T. Thakker, B. Muratori, Y.M. Saveliev, R.J. Smith,
Accelerator Science and Technology Centre, STFC Daresbury Laboratory, Daresbury, U.K.
M. Cliffe, W.R. Flavell, D.M. Graham,
Photon Science Institute, University of Manchester, Manchester, U.K.
D.J. Holder, D. Newton, A. Wolski, Department of Physics, University of Liverpool, Liverpool, U.K.

Abstract

Ultrafast lasers are able to generate THz pulses with >1MV/m field strengths, and with controllable electric field temporal profiles. We report progress on an experiment to demonstrate the use of laser generated THz pulses to manipulate the γ-z correlation of a $\sim$20 MeV electron bunch on a sub picosecond time scale. The manipulation is achieved in free space, without external magnetic fields or undulators, by the interaction of the bunch with the longitudinal electric field of a co-propagating THz pulse in a TEM^{*}_{10}-like mode. We discuss the potential for arbitrary phase space control, including the possibility of correcting temporal jitter and driving electron beams into synchronisation with the laser.

INTRODUCTION

Phase space manipulation with THz pulses has the potential to bridge the time-scale between manipulation with nanosecond period RF, and laser and harmonic manipulation on the femtosecond scale. Laser-driven sources have a demonstrated capability of $> 1\,\mathrm{MV.m^{-1}}$ in the THz frequency range, rising to $100\,\mathrm{MV.m^{-1}}$ for mid-infrared wavelengths[1, 2]; the temporal profile of the THz electric field can be modified or tuned by shaping of the drive laser temporal profile, using well established laser shaping techniques; allowing electric field profile ranging from octave spanning quasi-unipolar pulses through to wavelength tunable narrowband pulses[4].

Here we report progress on an experiment to demonstrate energy modulation on a low energy (10 MeV-25 MeV) electron beam through interaction with a co-propagating THz pulse. The THz pulse is generated with a TEM^{*}_{10} like polarisation, which has a longitudinal component to the electric field on axis. Such modes have been considered before for laser vacuum acceleration (for example [5, 9, 7, 8]). A common conclusion of these past studies is the limiting role played by the faster than c phase velocity of a laser beam near the focus. For THz pulses where the electric field oscillations are of approximately 0.5ps in duration, this constraint is partially relaxed, allowing for an extended interaction region even for relatively low energy beams where it cannot be assumed that $\beta \approx 1$.

EXPERIMENT DESCRIPTION

The experimental concept is shown schematically in Fig.1. Radially-polarised THz pulses are generated using a large area GaAs photo-conductive antenna, and then directed into the electron beam transport line of the ALICE (Accelerator and Lasers in Combined Experiments) accelerator at STFC Daresbury Laboratory [3]. The THz pulse and electron beam are combined by a mirror with a 5 mm radius central aperture, and are free to co-propagate over a region exceeding 2 m in length. The THz beam is focused to a central interaction point approximately 90 cm from the combining mirror. Downstream of the interaction point, imaging of the beam on a YAG:Ce screen in the central dispersive region of the ALICE magnetic compressor is used to characterise the bunch spectrum. The experiment aims to observe a THz induced modulation on this projected energy spread measurement, which requires the accelerator to be operated in a non-standard mode, without the energy chirp needed for magnetic compression.

A YAG:Ce screen for electron bunch transverse imaging, and an intra beamline ZnTe crystal/mirror assembly for in situ electro-optic transverse and temporal THz measurements, are located at the THz focal position. The THz measurements use a laser probe split from the main laser beam and co-propagating down the accelerator beamline with relative THz-probe time delay set by an optical delay line.

As discussed by by Huang et al. [8], the Guoy phase shift of the electromagnetic wave can give rise to cancellation of any energy gain or loss as the beam transits through the focal region. While simulations indicate that for our quasi-single cycle THz pulses a measurable net energy gain or loss can be maintained, we have installed an optional aperture at the focus, allowing the THz-electron beam interaction to be interrupted through scattering of the THz pulse.

THz Source

For our initial experiments we are using a large area photo-conductive antenna. Such antennae have a high conversion efficiency from laser to THz pulse energy, although do not have the electric-field profile shaping capability that is possible with non-linear frequency difference mixing or optical rectification [4] Our antenna consists of a 75 mm diameter, 500 μm thick, GaAs wafer with a radial bias field across the surface. The bias is applied through a hemispher-

ISBN 978-3-95450-123-6

UCLA SEEDED THz FEL UNDULATOR BUNCHER DESIGN

Stephen Gottschalk, Robert Kelly STI Optronics, Washington, USA
Sergei Tochitsky, Chan Joshi, UCLA, California, USA
Sven Reiche, Paul Scherrer Institute, Switzerland

UCLA is planning to build a THz user facility. One is a seeded THz FEL tunable in the range of 0.5 - 3 THz or even 3-9 THz in an optical klystron configuration [1]. Another [2] relies on microbunching at 340 μ using a 3.3-cm undulator or even driving the FEL with an electron beam from a laser-plasma accelerator. These FELs make use of a 2.1-m-long pre-buncher, chicane and shorter, 110-cm-long radiator. Chicane requirements are modest. A round copper waveguide with 4.8-mm ID will be used. We will describe the magnetic design and measured performance of the gap tunable undulators, mechanical design of the entire system, vacuum boxes, waveguides, and expected operational approaches. Both undulators have 33-mm periods and curved poles for two-plane focusing. Discussions will be included on issues associated with fabricating, sorting and shimming curved pole undulators. A new optimization method will be described that was used to meet magnetic requirements with a minimum volume of magnetic material.

INTRODUCTION AND BACKGROUND

The UCLA Neptune lab and STI Optronics have collaborated on undulators for THz operation in the 0.5-9 THz range as well as a potential future FEL based on Laser Wakefield Acceleration [1,2]. Planned first experiments [2] will use a ~kilowatt, 340-μm seed generated by nonlinear difference frequency generation in GaAs using 10.3-μm and 10.6-μm CO_2 lines. A round copper waveguide is used to preserve linear polarization. After passing thru a 1-m undulator, the FEL power is expected to be 300kW. A chicane, or a drift of 1-1.5 meters suffice to convert energy modulation to spatial bunching which will be measured in an X-band RF deflector cavity with a resolution <200 fs.

Future experiments in the THz regime will use an 8- to 14-MeV electron beam from the Neptune photoinjector in a variety of configurations [2]. From 0.5-1.5 THz a 2-m-long, 3.3-cm period undulator would be seeded with a ~1-kw seed laser to reach 2- to10-MW power at saturation. From 1.5-3.0 THz the system would operate as an optical klystron where the first undulator, ~2-m long, is seeded with a 10-100 W laser and then the energy modulation is converted to spatial bunching inside a chicane prior to entering a 1-m long radiator. A third mode is to use HGHG wherein the beam is modulated at 1-3 THz inside a 2-m undulator and then sent into a 1-m radiator tuned to the 3rd harmonic to generate 3-9 THz. All of these situations have been modeled using Genesis 1.3 and confirm the feasibility of multi-MW power output [3]. The UCLA team has built and fully characterized a kW power seed source tunable in the range of 0.5-3 THz [4].

Undulators have been delivered to UCLA after tests at STI. Vacuum boxes, custom optical tables and waveguides have also been delivered to UCLA.

SYSTEM OVERVIEW

The layout for seeded FEL operation in the 1.5 to 3.0-THz wavelength regime is shown in Fig. 1. Both undulators, CAD model of one of the vacuum boxes and kinematic feet hardware are shown. A closeup of the curved poles on the 2-m undulator is in the upper left corner. The 2.1-m long undulator is mounted on kinematic feet and has a motorized gap adjustment with a control system GUI, which is operated by a laptop computer. The 1-m undulator has a manually adjusted gap. It uses 1-μm resolution half-gap micrometers.

The round copper waveguide also has adjusters for x, y, z to help straighten and align the tube. STI designed the waveguide sub-system with UCLA guidance, review and approval of drawings. The UCLA machine shop fabricated it.

UCLA designed the vacuum boxes and STI generated production drawings which were reviewed and approved by UCLA prior to fabrication. Vacuum boxes shown on the right side have vertical and differential micrometer translators for alignment. An off-axis paraboloid reflector with tip, tilt, translation adjusters is used to introduce the seed laser and outcouple the THz radiation. Electron beam passes thru a hole in the center of the paraboloid. Pop-in targets are moved into position with a pneumatic actuator and viewed thru side windows.

MAGNETIC DESIGN

Curved poles with sextupolar focusing [5] are used to minimize the possibility of synchrotron-betatron resonance and provide horizontal focusing in addition to natural vertical wiggler focusing. Unlike an earlier undulator, [6], these two undulators use a more standard approach of changing the gap rather than retracting magnets. For both approaches the focusing depends on gap. This means that the e-beam matching will need to be adjusted as the gap changes and the beam will be elliptical, rather than circular.

When shaping the poles used in the 2-m undulator, we took advantage of the fact that the inner diameter of the round copper waveguide is 4.8 mm. This is a significant issue for 2-m undulator because it means that wide poles are not needed, modest shaping is sufficient and existing spare poles from CHESS could be used. Forces were about 2X lower, which reduced moment loads on linear bearings and required less motor torque. Field quality was

ISBN 978-3-95450-123-6

LUNEX 5 FEL LINE UNDULATORS AND MAGNETIC ELEMENTS

C. Benabderrahmane*, M. Labat, A. Loulergue, F. Marteau, M. Valléau, M.E. Couprie,
Synchrotron SOLEIL, St Aubin, France
G. Le Bec, J. Chavanne, European Synchrotron Radiation Facility, Grenoble, France
C. Evain, PhLAM/ CERLA, Lille, France.

Abstract

LUNEX 5 (free electron Laser Using a New accelerator for the Exploitation of X-ray radiation of 5th generation) aims at investigation the production of short intense and coherent pulses in the soft X-ray region with innovative schemes (such as echo and seeding with harmonics generated in gas) and compact design. The undulators of the FEL line are designed to provide high field short period devices: modulators are in-vacuum undulators with a period of 30 mm and 0.27 m long, radiators are in-vacuum undulators with a period of 15 mm and 3 m long with a cryogenic option, relying on SOLEIL development experience of NdFeB U20 hybrid in-vacuum undulators and 2 m long PrFeB U18 cryogenic undulator operated at 77 K installed on a long straight section of SOLEIL, and ESRF development experience of many in-vacuum undulator and 2 NdFeB U18 cryogenic undulators operating at 150 K. In addition, the line comports electromagnetic quadrupoles for the beam focusing, chicane dipoles for the beam compression and an electromagnetic bending magnet for the beam dump. A prototype of cryo-ready radiator is under design. Variable permanent magnet quadrupoles are under study for the transport of the Laser WakeField Accelerator towards the undulators.

INTRODUCTION

LUNEX5 is a French Free Electron Laser (FEL) test facility project aims at investigating the production of short, intense, and coherent pulses in the soft x-ray region (4-40 nm) [1]. It consists in a Free Electron Laser (FEL) in the seeded configuration (High order Harmonic in Gas seeding and Echo Enable Harmonic Generation) with a 15 mm period in vacuum (potentially cryogenic) undulator of 15 and 30 mm period) [2] using a Conventional Linear Accelerator (CLA) of 400 MeV or a Laser WakeField Accelerator (LWFA) [3] ranging from 0.4 to 1 GeV. The undulators are used either to modulate the electron bunch energy at the external laser seed (modulator) or for the amplification and emission (radiator). The LWFA will be provided first by the 60 TW laser of LOA, by the 10 PW APOLLON laser of ILE (Institut de Lumière Extrême) before a dedicated laser system.

LUNEX5 FEL LINE

Figure 1 presents the LUNEX5 FEL line. It is constituted by short period and high field undulators for the modulators and radiators, electromagnetic quadrupoles for the beam focusing, chicane dipoles for the beam compression and electromagnet bending magnet for the beam dump. Compact and high gradient permanent magnets quadrupoles are needed to focus the high diverging LWFA beam in the transfer line.

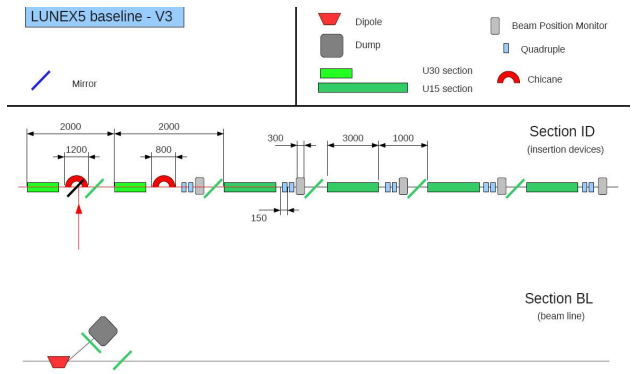

Figure 1: LUNEX5 FEL line.

UNDULATORS

Radiator Undulator

In-vacuum undulator technology is widely used to produce short period small gap undulators. The permanent magnet arrays are mounted on beams inside the vacuum chamber to eliminate the physical limitation of the magnetic gap due to the vacuum chamber [4]. The radiator is an in vacuum undulator with a small gap of 3 mm. The permanent magnet material is NdFeB and the poles material is vanadium permendur. The radiator is a 3 m long undulator with a relatively short period of 15 mm. The magnetic design of the radiator is presented in Figure 2.

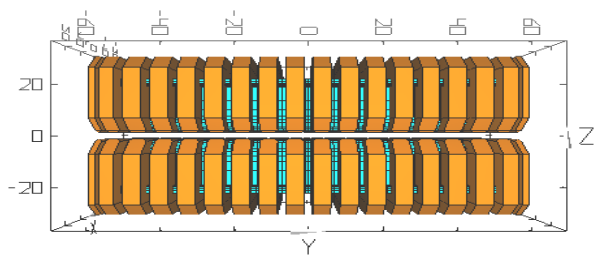

Figure 2: Radiator RADIA [5] model.

The peak magnetic field of the in-vacuum undulators can be increased while operating at cryogenic temperature [6]. When cooling down the NdFeB permanent magnets, the remanence Br increases down to a certain temperature at which the process is limited by the appearance of the Spin Reorientation Transition (SRT) phenomenon [7]. However, when cooling down

*chamseddine.benabderrahmane@synchrotron-soleil.fr

ISBN 978-3-95450-123-6

THE GENERATOR OF HIGH-POWER SHORT TERAHERTZ PULSES

N. Vinokurov#, Budker INP, Novosibirsk, Russia, and KAERI, Daejeon, S. Korea
Y. U. Jeong KAERI, Daejeon, S. Korea

Abstract

The multi-foil cone radiator to generate high field short terahertz pulses with the short electron bunches is described. A round flat conducting foil plates with successively decreasing radius are stacked, comprising a truncated cone with axis *z*. The gaps between foils are equal and filled by some dielectric (it may be vacuum). A short relativistic electron bunch propagates along the *z* axis. At high enough particle energy the energy losses and multiple scattering do not change the bunch shape significantly. Then, passing through each gap between foils, the bunch emits some energy into the gap. After that the radiation pulses propagate radially. For the TEM-like waves with longitudinal (along the *z* axis) electric and azimuthal magnetic field there is no dispersion in these radial lines, therefore the radiation pulses conserve their shapes (time dependence). At the cone outer surface we have synchronous circular radiators. Their radiation field forms the conical wave. The cone angle may be optimized; moreover, the nonlinear dependence of the foil plates radii on their longitudinal coordinate z may be used for the wave front shape control.

INTRODUCTION

The high field short terahertz pulses may be interesting for different applications [1, 2]. The multi-foil cone radiator to generate them using the short electron bunches is described in this proposal. The scheme under consideration is shown in Fig. 1. A round flat conducting foil plates with successively decreasing radius are stacked, comprising a truncated cone with axis *z*. The gaps between foils are equal and filled by some dielectric (it may be vacuum). A short relativistic electron bunch propagates along the *z* axis from left to right. At high enough particle energy the energy losses and multiple scattering do not change the bunch shape significantly. Then, passing through each gap between foils, the bunch emits some energy into the gap. After that the radiation pulses propagates radially, as it is shown in Fig. 1a. For the TEM-like waves with longitudinal (along the *z* axis) electric and azimuthal magnetic field there is no dispersion in these radial lines, therefore the radiation pulses almost conserve their shape (time dependence). At the cone outer surface we have synchronized circular radiators. Their radiation field forms the conical wave (see Fig. 1b).

THE SINGLE GAP EXCITATION

Let us find the radiation field in one gap. We are interested only in TEM waves, having only the longitudinal electric E_z and the azimuthal magnetic H_α fields, which do not depend on *z*. The Maxwell equations for such waves are

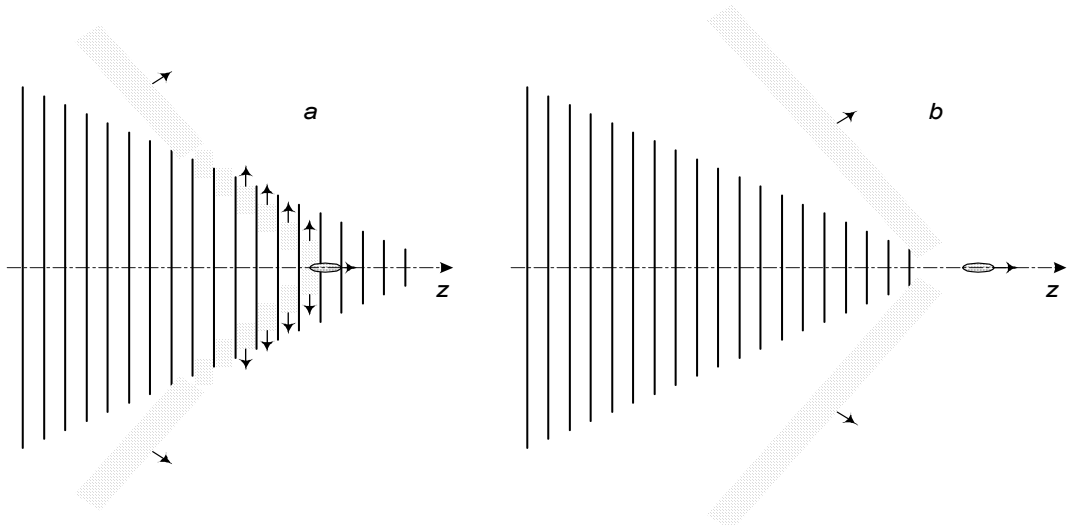

Figure 1: Short electron bunch passes through the conical foil stack. a – after the bunch passed a gap, the wave propagates radially. b – as the pulses reaches the foil boundaries, they are combined to a conical wave.

#vinokurov@inp.nsk.su

ISBN 978-3-95450-123-6

USE OF MONOCAPILLARY X-RAY OPTICS AS A MEANS TO REDUCE LINEWIDTH AND FLUCTUATIONS IN SASE FELS

A. Lin and G. Travish, UCLA Department of Physics & Astronomy, Los Angeles, CA 90095, USA

Abstract

The Self Amplified Spontaneous Emission (SASE) operation of high-gain Free Electron Lasers (FELs) allows for amplification from noise when no suitable seed sources are available. While SASE FELs can achieve high powers and short radiation pulses within the X-ray region, they are hindered by large linewidths and fluctuations in amplitude and temporal profiles. Various approaches have been proposed to clean up the spontaneous emission and produce better effective seed signals. This paper presents the use of monocapillary X-ray optics as an alternative to current methods to improve SASE operation. A monocapillary tube placed at the beginning stages of the undulator can reduce the bandwidth and enhance a narrow band of the spontaneous emission amplified by the FEL. Monocapillary tubes guide radiation due to total external reflection, and the critical angle of the guiding is dependent on the frequency of the radiation (and indirectly on the surface profile and materials). These properties allow for the selection of desired frequencies which are reflected back towards the axis, while all other frequencies are lost through diffraction. The effectiveness of the monocapillary tube was simulated using a simple model for the X-ray mirror. LCLS-like parameters in the hard X-ray regions were simulated and the results are presented.

INTRODUCTION

The radiation produced within a SASE free electron laser is temporally and spectrally noisy, due in part to the incoherence of the shot noise responsible for starting the process. It is beneficial to have the startup radiation be filtered prior to the amplification and bunching processes within the undulator. Current schemes, such as the HXRSS on the Linac Coherent Light Source (LCLS) use a monochrometer to clean-up the radiation after a fixed length of the undulator, and then reintroduces this radiation to the electron bunch later as an effective seeding mechanism [1]. This so-called self seeding process is effective and does give positive results, but the process introduces additional complexity, length and operational constraints. By introducing a finite monocapillary tube, placed at the start of the undulator, it may be possible to effectively clean up the radiation without the redirection of the electron beam and without the use of chicanes. A monocapillary tube, often made of glass due to the surface quality achievable, is a type of cylindrical waveguide whose guiding is based on the principle of total external reflection. The reflectivity of monocapillaries is a function of the frequency of the radiation being guided and the angle at which the radiation impinges on the surface of the tube (Fig. 1). Because the energy of the radiation is dependent on its frequency, the tube can be used to select and preferentially guide certain frequencies of the spontaneous radiation, whose bandwidth is otherwise large. In some SASE applications, it may also be possible to use incident angle filtering. The work presented here is a first attempt to understand this *in situ* filtering and model the process using a numerical code.

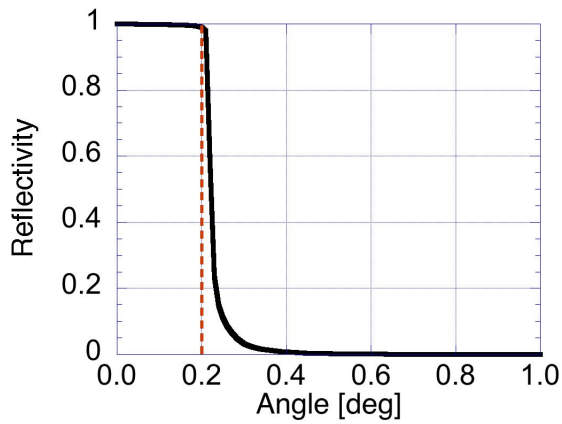

Figure 1: The reflectivity of a silica monocapillary tube over an angular spread at 8 keV. There is a sharp dropoff in the function at $\theta = 0.2\,^{\circ}$, indicating the critical angle of guiding.

MONOCAPILLARY TUBES

Reflection of an electromagnetic wave occurs at the boundary between two regions of differing indices of refraction. Total internal reflection occurs when the first medium has a greater reflective index than the second medium and the incident angle is greater than the critical angle. The value of the critical angle is directly determined from Snell′s law. Because of this, total internal reflection is often used to guide electromagnetic radiation, as seen with optical waveguides and fiber optic cables. However, this method of guiding is not possible for hard X-rays since the refractive indices of all materials are less than unity. The Drude model provides a simple formulation:

$$n(\omega)^2 = 1 - \frac{\omega_p^2}{\omega^2} \tag{1}$$

where

$$\omega_p^2 = \frac{e^2 n_e}{\epsilon_0 m_e} \tag{2}$$

ISBN 978-3-95450-123-6

MEASUREMENT OF THE TRANSVERSE COHERENCE OF THE SASE FEL RADIATION IN THE OPTICAL RANGE USING AN HETERODYNE SPECKLE METHOD

M.D. Alaimo, M. Manfredda, V. Petrillo, M.A.C Potenza, D. Redoglio, L.Serafini
Universita' and INFN-Mi, Milano, Italy
M. Artioli, F. Ciocci, A. Petralia, M. Quattromini, V. Surrenti, A. Torre, C. Ronsivalle
ENEA C.R. Frascati, Frascati, Roma, Italy
L. Giannessi
ENEA C.R. Frascati, Frascati, Roma and Sincrotrone Trieste S.C.p.A., Trieste, Italy
J.V. Rau
ISM-CNR, Roma,Italy
M. Bellaveglia, E. Chiadroni, A. Cianchi, G. Di Pirro, G. Gatti, M. Ferrario, A. Mostacci,
INFN-LNF, Frascati, Roma, Italy

Abstract

We measured the transverse coherence of the SASE radiation an heterodyne speckle method at the SPARC FEL facility. The measure was done at the resonant wavelength $\lambda_R = 400$ nm.

INTRODUCTION

Novel research methods in the investigation of matter permit to reach the spatial resolution at atomic scales. The wave front uniformity and a high degree of transverse coherence (TC) of the radiation are fundamental in the applications where coherence based methods [1], such as intensity fluctuation spectroscopy, phase contrast imaging or holography, are involved. Free-Electron Lasers (FELs) [2, 3, 4] are among the most performing devices for producing radiation with short wavelength, high power, ultra-short time duration and large transverse and temporal coherence.

The transverse quality of the FEL beam, which is high also in the SASE regime and increases during the amplification process, besides being essential for user applications requiring tight focusing of light and intense illumination of the target, can also be used to access information about the FEL dynamics.

The degree of transverse coherence of the SASE FEL radiation, calculated using the statistical theory [7, 8], can be related to the emergence during the growth of specific TEM modes [9].

From an experimental and quantitative point of view, the TC of the FEL radiation has been first estimated by means of the Young's double slit fringes analysis through the Van Citter-Zernicke theorem [10, 13]. Wavefront analysis using the Hartmann technique was then proposed to determine the spatial characteristics of the FEL source in single-shot regime [11] and then demonstrated at the SCSS Test Accelerator using a specifically designed Hartmann Wavefront Sensor [14], and, more recently, on the FEL Fermi at Elettra [12]. Single-shot wavefront measurements were performed directly on the FEL permitting to retrieve information about the FEL dynamics during the amplification, the beam optical quality, the source characteristics and the related instabilities from shot-to-shot.

Other methods of measuring the transverse coherence rely on the speckles generated by a sample of Brownian particles. After Fourier transform and proper normalization, the visibility of the fringes provides the same information as the traditional Young's double slit experiment for a continuous variation of pinhole distances. On the LCLS FEL an evaluation of the transverse coherence in the X ray range has been performed by measuring the homodyne speckle intensity due to coherent diffraction by disordered samples in the low and wide angle configurations (SAXS and WAXS respectively)[15]. By making assumptions about the shape of the beam profile, the first order statistical properties of the speckle patterns are related to the transverse and longitudinal coherence of the incoming radiation field, thus allowing to determine the field correlations and demonstrating the transverse coherence with a number of modes close to 1.

An alternative and powerful technique for the characterization of the two-dimensional transverse coherence has been developed and tested at the ESRF high brilliance undulator beamline ID02 and ID06 based on the measurement of the heterodyne speckle field generated by the scattering from a colloidal suspension of silica particles [16, 6].

In this paper we present the direct measures of the transverse coherence factor of the SASE FEL radiation with the aforementioned method in the optical range.

EXPERIMENTAL SETUP

The experiment was performed at the SPARC FEL facility [4] with an electron beam whose main parameters are summarized in Table1 at the resonant wavelength $\lambda_R = \frac{\lambda_u}{2\gamma^2}(1 + K^2/2) = 400$, nm ($\lambda_u$ being the undulator magnetic field period, $K = eB_u\lambda_u/(2\pi m_e c)$ its deflection pa-

ISBN 978-3-95450-123-6

X-RAY BASED UNDULATOR COMMISSIONING IN SACLA

T. Tanaka*, T. Hatsui, T. Hara, K. Togawa, M. Yabashi, H. Tanaka
RIKEN SPring-8 Center, Koto 1-1-1, Sayo, Hyogo 679-5148, Japan

Abstract

The undulator commissioning such as the precise K value tuning and trajectory correction is the important step toward realization of x-ray free electron lasers. In the SPring-8 Angstrom Compact free electron LAser (SACLA) facility, the undulator commissioning has been carried out by means of characterization of x-ray radiation. The details of the commissioning methods and actual results, together with the evaluation of the achieved accuracy, are presented.

INTRODUCTION

SACLA, the SPring-8 Angstrom Compact free electron LAser, achieved the first lasing in June 2011 at the wavelength of 0.12 nm, which soon got down to 0.08 nm [1]. After further beam tuning aiming at higher laser power and more stable operation, the user operation started in March 2012.

In order to achieve FEL saturation in the angstrom-wavelength region, 18 segments of in-vacuum undulators (IVUs) have been installed in SACLA. Each segment is 5-m long and placed with a 1.15-m long interval to install the devices for electron diagnostics, and steering and quadrupole magnets. Because of such a segmented structure, there exist many error sources that can lead to FEL gain reduction even if each undulator segment is perfect. In addition, the narrow-gap operation of IVUs can lead to unwanted effects that reduce the FEL gain. In order to correct or compensate all these errors and effects, we have to align or tune a number of components related to undulator operation and optimize many parameters so that all the undulator segments work coherently. Such an optimization process is referred to as undulator commissioning.

In SACLA, the undulator commissioning has been carried out based on the characterization of spontaneous or amplified x-ray radiation. In this paper, details of the commissioning procedure and the achieved results are reported.

ERROR SOURCES AND THEIR TOLERANCES

Before describing the details of the undulator commissioning carried out in SACLA, let us first mention the error sources that affect the FEL gain. We have mainly three sources related to utilizing a long undulator composed of more than one segment: trajectory error, K-value discrepancy, and phase mismatch. In addition, the wakefield-induced energy loss is another point to be concerned in SACLA, where narrow-gap IVUs are used. In order to suppress the FEL gain reduction due to these error sources, respective components related to undulator operation should be finely tuned or well aligned. The tolerances specified by a numerical study based on FEL simulations assuming the SACLA beam parameters are summarized in Table 1. Note that all the simulations have been performed with the FEL simulation code SIMPLEX [2].

Table 1: Error Sources and Their Tolerances

Tuning Item		Tolerance
Trajectory		
	BPM Center	2.2 μm
	Injection Angle	0.50 μrad
K Value	Total	5×10^{-4}
	(in Gap)	1.9 μm
	(in Height)	60 μm
Phase Slippage		30 degree
Undulator Taper		10^{-4}/segment

The tolerance of the trajectory error is given in two forms. One gives that of the center of the BPMs installed in the drift sections and the other gives that of the injection angle of the electron beam into undulator segments. As explained later, the injection angle of the electron beam is measured and corrected in SACLA by characterization of monochromatized spontaneous radiation.

The K value deviation, which comes from the tuning error of the gap and misalignment of the undulator height, should be less than 5×10^{-4} in total. Based on the magnetic measurement of the SACLA undulator, this number is converted to the tolerances of 1.9 μm in gap and 60 μm in height.

METHODS AND RESULTS OF COMMISSIONING

In order to align or tune the components within the tolerances as listed in Table 1, characterizations of spontaneous and SASE radiations have been carried out in SACLA. The details are presented in the following sections.

Photon Diagnostics

The photon diagnostics system in SACLA is schematically illustrated in Fig. 1. The slit assembly placed 80 m far from the exit of the last (18th) undulator is used for shaping the photon beam, whose aperture size is variable and

* ztanaka@spring8.or.jp

ISBN 978-3-95450-123-6

OBSERVATION OF HIGH HARMONIC GENERATION FROM 6H-SiC IRRADIATED BY MIR-FEL

K. Yoshida*, H. Zen, K. Okumura, K. Shimahashi, M. Shibata, T. Komai, H. Imon, H. Negm, M. Omer, Y. W. Choi, R. Kinjo, T. Kii, K. Masuda, H. Ohgaki
Institute of Advanced Energy, Kyoto University, Gokasho, Uji, Kyoto 6110011, Japan

Abstract

SiC is attractive as a high power nonlinear optical device [1]. For verifying the possibility of a high harmonic generation from a SiC irradiated by MIR-FEL, we observed the emission from a SiC irradiated by MIR-FEL whose center wavelength was 12 μm. Two measurements observing the second harmonic generation (SHG) and high harmonic generation (HHG) were conducted. As the result, we clearly observed the SHG whose intensity was proportional to the square of MIR-FEL intensity. And emissions corresponding to the wavelength of the high harmonics (9th, 10th, and 11th) of the irradiated MIR-FEL (7.8 μm and 8.6 μm) were observed.

INTRODUCTION

Wide-gap semiconductors such as SiC, ZnO are great interest as they represent the next generation materials for power devices and photocatalyst materials. In addition, SiC and ZnO were attractive as nonlinear optical devices [2, 3]. ZnO is considered as the candidate of the thin film nonlinear optical device because ZnO has a high nonlinear optical susceptibility and an easiness of thin film fabrication [2]. Moreover, SiC has a high nonlinear optical susceptibility as well as a high resistance to the laser induced damage. Therefore, SiC is considered as a candidate of the high power nonlinear optical devices.

In 2010, the high harmonics over 20th from solid material was observed for the first time by using ZnO single crystal [3]. However, in the case of SiC, the harmonics up to only second has been observed by irradiation of Nd-YAG laser [1, 4]. For the development of the high power nonlinear optical devices, verification of the high harmonic generation from SiC is important. Our objective of this paper is to present the observation of the high harmonics from SiC.

For generating the harmonics from nonlinear optical devices, high power laser is essential. FEL is suitable as a light source because the feature of FEL is high power. However, harmonic generation from SiC by using FEL has not been reported. Therefore, at first, we verified the SHG from a SiC irradiated by MIR-FEL. As the next step, we verified the HHG from SiC.

EXPERIMENTAL SET UP

For the verification and observation of the HHG from SiC, two experiments were made; one is the measurement of SHG and the other is the measurement of HHG. The experiments were performed in the atmosphere. SiC (semi-insulator 6H-SiC: Xlamen Powerway Advanced Material Co.,LTD) was used. The size was 15 mm × 15 mm × 0.33 mm. The picture of the used SiC is shown in Fig. 1.

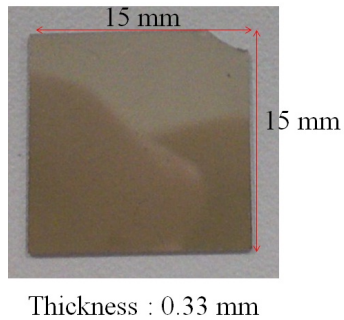

Figure 1: The picture of the used SiC.

The measurement setup for the verification of the SHG was shown in Fig.2. KU-FEL (Kyoto University Free Electron Laser) was used as the laser source. The specification of KU-FEL is reported in the reference [5]. For preventing the 2nd and 3rd harmonics inherently generated by the FEL, the long pass filter (cut-off wavelength of 9 μm, LP-9000 nm, SPECTROGON) was used. In addition, the short pass filter (cut-off wavelength of 7 μm, SP-7150 nm, SPECTROGON) was used to block the fundamental at the wavelength of 12 μm. A Mercury Cadmium Telluride (HgCdTe, MCT) detector (J15D12-M204-S01M-60, Judson Technologies) was used for the detection of the second harmonic light. Moreover, to measure the intensity of the irradiated FEL, a Mercury Cadmium Zinc Telluride (HgCdZnTe, MCZT) detector (VIGO SYSTEM R005-3) was used. Confirmation of the SHG was done by observing the reflected light from SiC. The MIR-FEL whose wavelength was 12 μm was irradiated to SiC. The repetition rate of the FEL was 1 Hz. The macro-pulse energy of FEL was around 2 mJ whose macro-pulse duration was 2 μs.

*k-yoshi@iae.kyoto-u.ac.jp

ISBN 978-3-95450-123-6

BIO-LUMINESCENCE/SCATTERING AND ITS DYNAMICS IN ENCHYTRAEUS JAPONENSIS BY IRRADIATION OF FREE ELECTRON LASER

S. Kurumi, T. Taima, K. Suzuki,
Department of Electrical engineering, Nihon University, Tokyo, Japan
F. Shishikura, School of Medicine, Nihon University, Tokyo, Japan
Y. Hayakawa, K. Hayakawa, T. Tanaka,
LEBRA, Institute of Quantum Science, Nihon University, Chiba, Japan

Abstract

We report on the experiment results of behaviours of the Enchytraeus Japonensis (EJ) which was irradiated a free electron laser (FEL). The focused one shot of the FEL (Power: 300 μJ, Wavelength: 2.9 μm, Micro pulse width: 200 fsec) which resonated with hydroxyl stretching vibration was irradiated to center of the EJ body and we observed it by change coupled device (CCD) camera. As a result, the reactive products from EJ were generated by FEL irradiation. The reactive products were increased in a few milliseconds. More shot of FEL irradiations, the EJ body was broken and we observed emission of laser ablation from the EJ body.

INTRODUCTIONS

Earthworms are well known in whole globe which features are that there is the bottom of the food chain, and they work as the soil improvement agent. Exactly, the soil improvements by earthworms are reported on several papers [1-9]. Earthworms ingest the organic substances and microorganisms in the locality soil. Excretory products from earthworms are promoted effective use as plant growth and good farming land, generally. In addition, there are the earthworms which can ingest the heavy metal (Cd, Pb, Zn etc) [3-9]. These earthworms are expected to detoxifying source for infected soil.

Currently, earth worms which ingested the heavy metal are using for assessment of soil contamination. However, it is required the great care because this assessment method needs large amount of earthworms and processes. To assess the soil contamination by earthworms, first, these earthworms are made to be powders by drying and gridding. After, pollution materials in the soil are analysed by extracted solutions from those powders.

In order to simplify these processes, we focused on the laser ablation techniques [10-11]. The laser ablation is observed from laser irradiation area which wavelength is dependent on the laser irradiated materials. Moreover, laser irradiated materials are excited and emit photoluminescence. These emission spectra are used the qualitative analysis of laser irradiated materials. Therefore, we consider that it is effective method for soil contamination assessment to measure the emission spectra from the earthworm by laser irradiation.

A free electron laser (FEL) is generated by Laboratory for Electron Beam Research and Application (LEBRA), Nihon University [12-14]. This FEL light is irradiated to earthworm as a laser ablation source because this laser wavelength can tune up with the molecular vibration of the chemical component in earthworm, the pulse width of this laser is about a few hundred of femtosecond; Thermally damage is less affect by laser irradiation. The earthworms are used Enchytraeus Japonensis (EJ) [15-16].

In this paper, we report the bioluminescence behaviour from EJ body by LEBA-FEL irradiation.

EXPERIMENTS

Selection of Free Electron Laser Wavelength for the Enchytraeus Japonensis by FT-IR

Infrared light absorption of the EJ was measured by fourier transform infrared spectroscopy (FT-IR). Living EJs were gridded on sappier substrates. Those samples were annealed (Temperature: 200 degree, Time: 10 min) to evaporate the H_2O in EJ. We conducted the FEL wavelength from FT-IR spectrum result.

Free Electron Laser Irradiation to the Echytraeus Japonensis

Figure 1 shows the FEL irradiation system for EJ. A living EJ is put on the quartz substrate as a sample. This sample set up on the X-Y stage. The focused FEL (Power: 300 μJ, Wavelength: 2.9 μm) was irradiated to the EJ. Number of FEL shot was 6 shots. Interval of time between FEL shots was 5 second. Behaviours of laser irradiating EJ were observed by change coupled device (CCD) camera. The quality of FEL is as shown below. Macro pulse interval: 500 ms, Macro pulse width: 7.4 μs, Micro pulse interval: 350 ps, Micro pulse width: about 200 fs. (Micro pulse wide $= 60\ \mu m/C \cong 200$ fs).

RESULTS

Measurement results of Echytraeus Japonensis by FT-IR

Figure 2 shows transmittance result of annealed EJ by FT-IR. Wavelengths about 3.42 μm and 3.50 μm showed clear absorption. These wavelengths were due to

ISBN 978-3-95450-123-6

PIT FORMATION ON DENTAL HARD TISSUES USING TWO DIFFERENT FREE ELECTRON LASER SOURCES, LEBRA-FEL AND KU-FEL

T. Sakae, T. Kuwada, Department of Histology,
School of Dentistry at Matsudo, Nihon University, Chiba, 271-8587, Japan
Y. Hayakawa, T. Tanaka, K. Nakao, M. Inagaki, K. Nogami, K. Hayakawa, I. Sato,
LEBRA, Institute of Quantum Science, Nihon University, Funabashi, 274-8501, Japan
H. Zen, T. Kii, H. Ohgaki, Advanced Energy Generation Division, Quantum Radiation Energy Section, Institute of Advanced Energy, Kyoto University, Kyoto, 611-0011, Japan

Abstract

According to the increased usage and demands of lasers in dentistry, research and development of the more reliable and functional lasers are needed. In the case of caries treatment, the lasers generated by commercial apparatus are not enough to dig the dental enamel and/or dentin tissues. Our previous studies showed that FEL generated at LEBRA has a potential to form pits on these dental hard tissues easily, and that the effective wavelength depends on the tissue types sensitively at about 3000 nm. To progress the FEL study on dental tissues, it is needed to spread the range of wavelengths more than that at LEBRA, between 2000 and 6000 nm. The newly established KU-FEL is able to generate the FEL of wavelength between 5000 and 13000 nm. Combining the two FEL sources, we found a new result that the dental hard tissues were easily dug by 7600 nm KU-FEL, which wavelength has not been presumed before. In the combination of LEBRA-FEL and KU-FEL, the wider knowledge on the FEL action on dental tissues will be achieved.

INTRODUCTION

Lasers in Dentistry

Just after the first ruby laser was developed [1], dental researchers studied possible application of laser energy to dig dental enamel without pain [2]. Now, lasers have been applied in dentistry to sulcular debridemend (Curettage) and reduction of bacterial level, treating periodontitis, root planing, pain control, wound healing, diagnosis of caries, and hard tissue applications using a variety of laser systems including CO2 (10600 nm), Er:YAG (2940 nm), Ho:YAG (2100 nm), Nd:YAG (1064 nm), diode (810, 980 nm), Ar (514, 488 nm).

ADA (American Dental Ass., 2009) stated that while Er:YAG and Er, Cr:YSGG (2780 nm) lasers be an alternative method of removing enamel, dentin and caries, clinicians are encouraged to be cautious and to be aware of the benefits and risks using lasers.

Generally, all the three emission modes (continuous, gated-pulsed, and true-pulsed) used in dental clinical lasers produces the thermal effects [3]. A limited studies on FEL application to dental hard tissues were reported. FEL irradiation, on the other hand, revealed that LEBRA-FEL did not show any apparent heat-effects but did show the formed pit deepness being correlated with the output and wavelength [4].

More recent studies on FEL-dental tissue interaction using KU-FEL showed that dental enamel was dig easily with the other wavelengths than the optimal, 2940 nm. This study aimed to clarify the FEL-dental tissue interaction mechanism using two different FEL sources.

Laser-Tissue Interaction

The principle mechanism of action of laser energy on tissue, known at now, is photothermal, other mechanisms may be secondary to this process [5]. Rapid heating of water molecules within enamel (ca. 96 wt% biological apatite, 2 wt% organic and 2 wt% water) causes rapid vaporization of the water and build-up of steam which causes an expansion that ultimately over comes the crystal strength of the tissue and the materials breaks, by exploding, this process is called ablation. Fig.1 showed the reported FT-IR data for water and hydroxyapatite. Biological apatite, which is the main inorganic component of bone and tooth, is a sub-family of hydroxyapatite, and a chief characteristics is a remarkable carbonate substitutions up to 8 wt% [6]. It is notable that there is a structural OH in the apatite crystal structure, but there is no remarkable absorption around 3000 cm^{-1} in the spectrum.

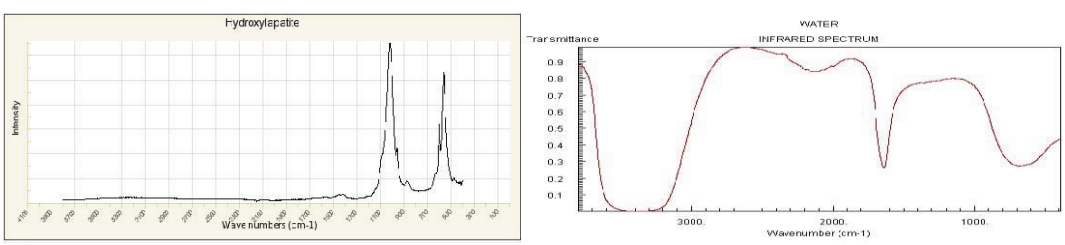

Figure 1: FT-IR data for (left) Hydroxyapatite (RRUFF File), and (right) Water (NIST).

ISBN 978-3-95450-123-6

THE JLAB UV UNDULATOR

Stephen Gottschalk, STI Optronics, Bellevue, WA 98004, USA
Stephen Benson, Wesley Moore, JLAB, Newport News, VA, 23608, USA

Abstract

Recently the JLAB FEL has demonstrated 150 W at 400 nm and 200 W at 700 nm* using a 33-mm period undulator designed and built by STI Optronics. This paper describes the undulator design and performance. Two key requirements were low-phase error, zero steering, and offset end fields and small rms trajectory errors. We will describe a new genetic algorithm that allowed phase error minimization to 1.8 degrees while exceeding specifications. The mechanical design, control system and EPICS interface and lasing results will be summarized.

INTRODUCTION

The UV undulator for JLAB has an interesting history. Originally in 2005 it used the magnetic subsystem consisting of magnets, poles, holders and beams for a 33-mm period undulator built by STI in 1988 for CHESS. In 2011 those parts were returned to CHESS and replaced by an APS "Undulator A" 33-mm period magnetic system originally built by STI in 1998 and used for LEUTL[1]. The LEUTL application was at a fixed gap of 9.35mm. It is the performance of the newer, variable gap system that is described in this paper.

UNDULATOR DESIGN, PERFORMANCE, EPICS SUPPORT AND TUNING

A picture of the device installed at JLAB is shown in Fig. 1. The magnetic design of APS Undulator A 33-mm period has been described elsewhere [2]. Seven poles and magnets were removed from each end to accommodate the existing JLAB vacuum tube. All original shims and other tuning devices were removed by APS prior to shipment to STI. Without shims, phase error was below 5° but trajectory and quadrupoles needed tuning. The specification and performance are summarized in Table 1. A comparison of the original straight-pole CHESS wiggler field strength with the present wedged pole APS wiggler is shown in Fig. 2. The wedged design is 25% stronger and the new wiggler has half the phase error.

The peak-to-peak trajectory error is important since it relates to keeping the electron beam in the middle of the optical mode. When the Rayleigh range is about one third of the wiggler length it is important to keep the electron beam centered on the optical mode to get the best overlap. One can have a mode that has good gain with a plane wave but not with a tight Gaussian mode. In this case we have both. Angular errors can lead to phase errors but they can also compensate field errors to make the phase errors even smaller.

Figure 1: UV wiggler installed at JLAB.

The mechanical design was based on an earlier STI design for the JLAB IR wiggler [3]. Each beam is attached to two trolleys that move on linear guides. A total of four motors are used. A welded steel support frame is used for rigidity. Long bias coils provide ambient field compensation. The IR wiggler had a horizontal B field while the UV has a conventional vertical B-field. The UV wiggler added tilt switches and increased drive power since magnetic forces are larger. A Mitsubishi PLC was included in both systems, but it does not perform motion tasks. It is used as a watchdog to monitor mains, tilt switches, controlled stop, pause and emergency stop functions. The control panel is shown in Fig. 3.

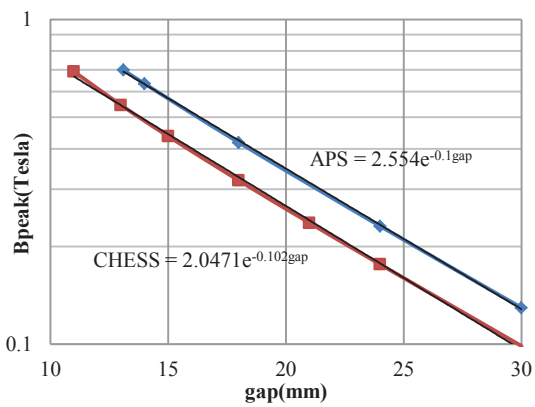

Figure 2: Field strengths of CHESS and APS wigglers.

* S. V. Benson et al., "Beam Line Commissioning of a UV/VUV FEL at Jefferson Lab", presented at the 2011 FEL Conference, Shanghai, China, Aug. 2011

ISBN 978-3-95450-123-6

DESIGN AND PERFORMANCE OF THE NLCTA-ECHO 7 UNDULATORS

Stephen Gottschalk, Robert Kelly, Michael Offenbacker, John Zumdieck STI Optronics, Bellevue, WA 98004, USA

Abstract

The Echo-enabled harmonic generation (EEHG) FEL at SLAC NLCTA has shown coherent radiation in the seventh harmonic (227 nm) of the second seed laser [2]. Earlier experiments demonstrated 3rd and 4th EEHG [1]. We describe design and performance of the 33-mm and 55-mm period undulators built by STI Optronics and used for these experiments. Magnetic design of the 33-mm period undulator was based on an earlier curved-pole, two-plane focusing undulator for the UCLA seeded THz FEL [3]. The 55-mm undulator was identical to the JLAB IR FEL and APS UA U55 designs. A challenge for both these devices was achieving tight normal and skew trajectory excursions (<500 G-cm^2), zero trajectory offset and <10 G-cm steering without end correctors over a 5-mm diameter horizontal and vertical region with a 4-month delivery requirement. We will also describe a new tuning method based on operations research linear programming that was used to help meet these goals over a 2X larger region while maintaining 1° phase errors.

INTRODUCTION

EEG enables seeded X-ray FELs without the shot noise limitation of SASE mode. The theory of EEG is summarized in [1] and advantages of EEG for achieving temporally coherent X-ray operation are described in [2]. The EEG FEL at the NLCTA at SLAC has demonstrated 7th harmonic operation at 227 nm with a 120-MeV electron beam using 795-nm and 1590-nm seed lasers [2]. The experiments utilize multiple chicanes, undulators, and transverse rf cavities. For this project we made undulators U1 (10 periods, 3.3-cm period) and U2 (10 periods, 5.5-cm period) to the specifications shown in Table 1. One device was a modified 33-mm period undulator [3] in which the two-plane sextupolar focusing was replaced by flat pole, one-plane focusing while the 55-mm period device was the same as APS Undulator A, 55 mm and JLAB IR 55 mm. Fig. 1 shows the 55-mm period undulator at NLCTA and the 33-mm period device during scanning at STI.

Table 1: EEHG Undulator Performance

Item	U1 Specification	U1 Actual	U2 Specification	U2 Actual
Type	Hybrid	Hybrid	Hybrid	Hybrid
Magnetic Material	Not specified	Vacodym 890TP Br = 1.164T	Not specified	Shin-etsu N32Z BR = 1.11T
Gap	>10 mm	10.653 mm	>10 mm	25.47 mm
Wiggle Plane	Horizontal	Horizontal	Horizontal	Horizontal
Good Field Region	2.5-mm radius	-3 mm to >5 mm	2.5-mm radius	-4.5 mm to >5 mm
Number of Full Strength Periods	9.5	10.5	9.5	10.5
Period Length	33mm	33.013 mm	55 mm	55.035 mm
K	1.8016	1.8018	2.0724	2.0722
Peak Field	0.5845T	0.5846T	0.4034%	0.40336
First Integrals in Good Field Region	<10 G-cm (x,y)	-5.9 to -6.0 skews +5 to -10 normals	<10 G-cm	-3.0 to -8.0 skews 0 to -6.0 normals
Second Integrals in Good Field Region	<1000 G-cm^2	80 to -50 skews 400 to 0 normals	<1000 G-cm^2	560 to 300 skews 300 to 550 normals
Transverse Rolloff	<1% at 5 mm	0.7%	<1% at 5 mm	0.3%
Pole Width	Not Specified	25.58 MM	Not Specified	55 mm
Phase Error	<20°	0.8°	<20°	1.1°

ISBN 978-3-95450-123-6

DESIGN AND PERFORMANCE OF THE WEDGED POLE HYBRID UNDULATOR FOR THE FRITZ-HABER-INSTITUT IR FEL

S.C. Gottschalk, T.E. DeHart, R.N. Kelly, M.A. Offenbacker, A.S. Valla, STI, Washington, USA
H. Bluem, D. Dowell, J. Rathke, A. M.M. Todd, AES, Princeton, New Yersey, USA
S. Gewinnner, H. Junkes, G. Meijer, W. Schöllkopf, W.Q. Zhang, FHI, Berlin, Germany
U. Lehnert, HZDR, Dresden, Germany

ABSTRACT

An IR and THz FEL with a design wavelength range from 4 to 500 μm has been commissioned at the Fritz-Haber-Institut (FHI) in Berlin, Germany. Lasing at 28 MeV and a wavelength of 16 μm was achieved in February 2012 [1]. We describe the performance of the undulator built and installed at FHI by STI Optronics for use in the mid-IR range (<50 μm) and 15- to 50-MeV beam energy. The undulator was a high-field-strength wedged-pole hybrid (WPH) with 40-mm period, 2.0-m long, and minimum gap 16.5 mm. A new improvement was including radiation resistance in the magnetic design. We will discuss the measured magnetic and mechanical performance, central and zero steering/offset end-field magnetic designs, key features of the mechanical design and gap adjustment system, genetic shimming algorithms, and control system.

INTRODUCTION

The FHI undulator [1] is shown in Fig. 1. FHI chose a hybrid design because they are more radiation resistant than PPM [6] and wedged poles provide higher field strength. Using NdFeB magnetic material does allow repair of magnets damaged by radiation [3] whereas Sm_2Co_{17} magnetic material must be replaced [13]. Magnet homogeneity data was measured and used for sorting. Tuning used a genetic optimizer [4] to satisfy a number of nonlinear, non-smooth constraints. Mechanics and control systems are based on earlier devices [2]. Performance is summarized in Table 1. Factory acceptance testing was completed in 9 months after start of contract.

RADIATION RESISTANT MAGNETIC DESIGN

Radiation has damaged undulators, [3]. The region damaged operated in the 3rd quadrant. In the 1980s, FEL undulators used $SmCo_5$ magnetic material, then as NdFeB improved and synchrotron radiation rings came online in the 1990's, undulators used NdFeB. Since e-beam emittance is larger on FEL's than storage rings, new facilities like FHI are requesting better radiation resistance. The FHI FEL has some energy collimation from the bend but the undulator is the limiting aperture.

Experiments by Bizen [5,6] confirm that coercivity and permeance ($B/\mu_0 H$) are important. Studies with open circuit magnets (room temperature or cryogenic) do not reflect the more challenging undulator magnetic environment. For example, in [6] the lowest permeance was 0.74 but no part of any undulator magnet operates above a permeance of 0.2. Moderators in front of magnets change the particle and energy spectrum as well as the dose pattern making extrapolation to undulators in FEL's questionable.

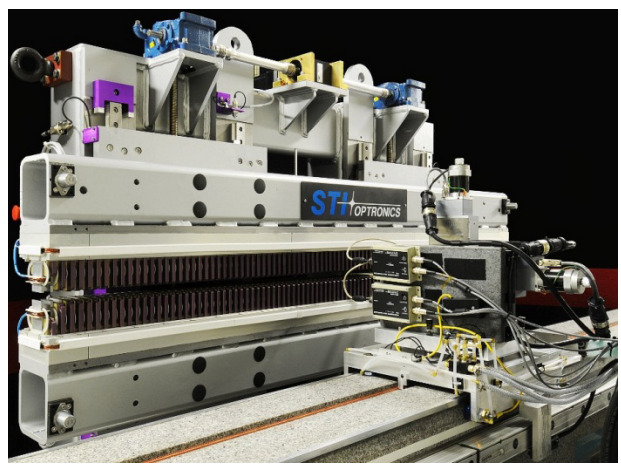

Figure 1: FHI undulator being scanned at minimum gap.

A review of magnet domain theory [9,10] shows that the only mechanism for change of magnetism without melting, baking to Curie temperature or pulverizing magnets is heating above the safe operating temperature for the local permeance. This temperature depends on the anisotropy coefficients for the particular grade and is not directly related to the Curie temperature. When heated, the lowest energy state for the domain becomes a reversed spin orientation [11]. In nucleation magnets like NdFeB, grains enclose domains. Bloch wall energies are sufficiently low that if one domain inside a grain reverses then all domains reverse. Domain sizes range from 5nm to 10 nm and grain sizes are 5-10 μm.

ISBN 978-3-95450-123-6

TUNING AND TESTING OF THE PROTOTYPE UNDULATOR FOR THE EUROPEAN XFEL

U. Englisch, Y.H. Li, J. Pflueger,
European XFEL, Notkestr 85, 22607 Hamburg, Germany

Abstract

The European X-ray Free Electron Laser (EXFEL) uses three undulator systems with a total magnetic length of 455 meters. There are 91 undulator segments each 5m long. They are gap variable use planar hybrid undulator technology. They are currently in production. During the next 2.5 years they will be measured and tuned so that their field complies with the EXFEL specifications.

In order to meet the tight schedule and to reach the high specifications, fast and reliable measurement methods and fine tuning algorithms have been developed and tested so that they can be used for the mass production. In this paper a short description is given. First results of the magnetic tuning preformed on some of the pre-series undulator prototypes, which were built during the past 18 months are given. It is shown that the field quality satisfies all the specifications of the European XFEL. It is also shown that the measurement and tuning process is fairly fast and straightforward to apply.

INTRODUCTION

The European XFEL is currently under construction [1]. It uses the principle of Self-Amplified-Spontaneous-Emission, (SASE), [2, 3]. Three systems will be built: SASE1 and SASE2 will operate in the hard X-ray regime from 0.05 to 0.2nm. SASE3 can be operated in the soft X-ray regime from 0.4 to 5.2 nm.

SASE FELs need long undulator systems: SASE1/2 will each use 35 segments and have a total length of 215m. SASE3 requires 21 segments comprising a total length of 128m. In total, 91 segments will be produced.

Due to the short wavelengths, the magnetic fields of the EXFEL undulator segments need to fulfil demanding specifications in order to provide longitudinal phase synchronization and transverse overlap over the whole length of an undulator system. Since the undulators are gap-tuneable the specifications must be fulfilled over the whole operational gap range. Tuning of the 91 undulator segments is a big challenge. The EXFEL time schedule requires all undulator segments to be finished by the end of 2014.

DESIGN AND SPECIFICATIONS

Two types of magnet structures will be used in EXFEL. The U40 with 40mm period length will be used for the hard X-Ray FELs SASE1 and SASE2. The U68 with a period length of 68 mm is used for the soft X-ray FEL SASE3. All undulator segments are planar hybrid devices using NdFeB magnet material and CoFe soft iron poles. Six so-called pre-series prototypes, four U40s and two U68s were built in 2011 to test the whole production cycle. All devices were tuned following the EXFEL procedures. Two representative devices, one U40 and one U68 are described here.

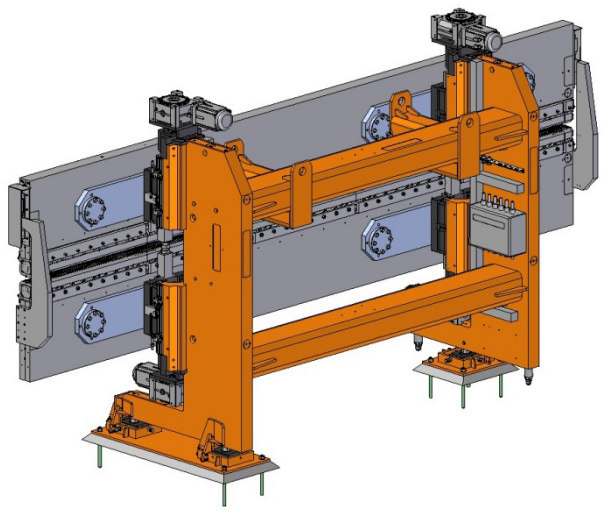

Figure 1: The EXFEL undulator.

All EXFEL magnetic structures have odd symmetry. The end structures have the configuration: ½, -1, 1, …,-1, 1, -½. The sign denotes to the orientation of the magnetization. Due to the opposite signs on the ends systematic gap dependent kicks are self-compensating. There is a small offset in the 2nd field integral, which is, however, below specifications, see Table 1. This configuration has a simple end design, maximizing the number of good poles, and in addition has low gap dependence.

A standardized mechanical support system is used throughout the EXFEL (see Fig. 1). It provides a standard mechanical interface to accommodate either a U40 or an U68 magnet structure. More details are found in [1].

The transverse e^--beam size of the EXFEL in the undulator sections is about 25 microns, smaller than that in storage rings. The required good field regime is therefore more moderate. In addition, e^--beam passes undulator only once in EXFEL. Consequently it makes a big difference to undulators used in storage rings.

For a radiation wavelength of 0.1nm and a normalized emittance of 1.4μm careful studies using Genesis 1.3 [4] have been made to establish tolerable magnetic field errors [5,6]. In these studies the phase jitter is used as a measure of the longitudinal matching of the micro-bunched electron beam with the laser field, and the transverse overlap is calculated to optimize the interaction. Tolerances were determined in such a way

ISBN 978-3-95450-123-6

TECHNICAL OVERVIEW OF THE SWISSFEL UNDULATOR LINE

R. Ganter, M. Aiba, H.-H. Braun, M. Calvi, A. Fuchs, P. Heimgartner, E. Hohmann, R. Ischebeck, H. Joehri, B. Keil, N. Milas, M. Negrazus, S. Reiche, S. Sanfilippo, T. Schmidt, S. Sidorov, P. Wiegand, PSI, Villigen, Switzerland

Abstract

SwissFEL [1] is a hard X-ray FEL facility currently being designed at PSI. It uses a photocathode gun, S-band injector and C-band main linac to drive a hard X-ray undulator line with 100 Hz repetition rate. Beam commissioning of the hard X-ray undulator line called Aramis is scheduled to start in 2016. The Aramis line extends over a length of 177 m, from an energy collimator after the main linac to the electron beam dump. Electrons enter the Aramis line with a maximum energy of 5.8 GeV, a normalized slice emittance below 0.43 µm and a peak current of 3 kA at 200 pC bunch charge. A prototype of an in-vacuum undulator (U15) is currently being assembled. Most of the other beamline components have been designed and for some of them prototypes are already ordered. This paper describes the main beamline components of Aramis (quadrupoles, phase shifters, alignment quadrupoles, mechanical supports, safety components) with particular emphasis on constraints like temperature drifts, stray magnetic field, wakefields and costs. Undulators are however described in details in a companion paper [2].

ENERGY COLLIMATOR AND BEAM STOPPER

At the entrance of Aramis, the electron bunch has a momentum spread of 350 keV for the 200 pC normal operation mode of SwissFEL [1]. The repetition rate is 100 Hz. In order to protect the undulator from beam losses, the electron bunch will pass through an energy collimator (at z= 454 m) having an energy acceptance of 2 % peak to peak. Downstream of the energy collimator chicane the electrons will go through a matching section, where the electron bunch transverse profile is checked with a screen and a wire scanner. During the tuning of the machine the beam is deflected horizontally towards a beam stopper upstream of the 1st undulator (z = 501 m).

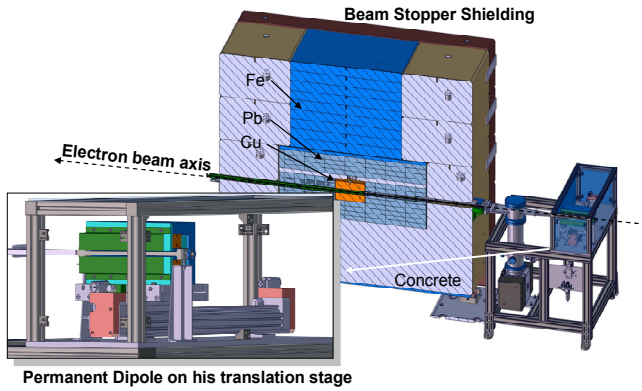

Figure 2: Beam stopper layout assembly: the 5.8 GeV beam is deflected by 0.7 ° when the dipole is inserted.

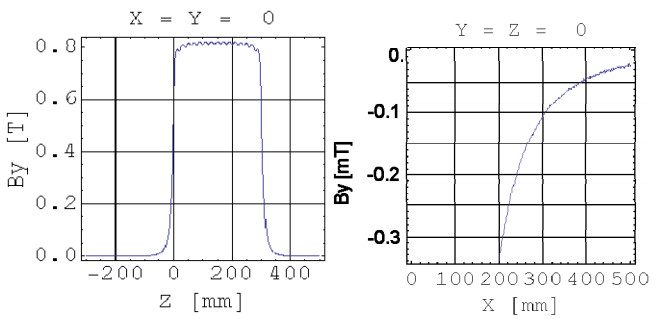

Figure 3: Permanent dipole field profile along axis (left) and transverse stray field at Z=150 mm; Y=0 (right).

This deflection is generated with a permanent dipole magnet. This magnet (which slides transversally) can be moved remotely into the beamline (Fig. 2). When the dipole is retracted 400 mm out of axis the remaining dipole field on axis is less than 0.5 G (Fig. 3), so that the electrons can continue straight to the undulators, with perturbations on the earth magnetic field level. Using an electromagnet instead of a permanent one would have required more space as well as a degauss procedure.

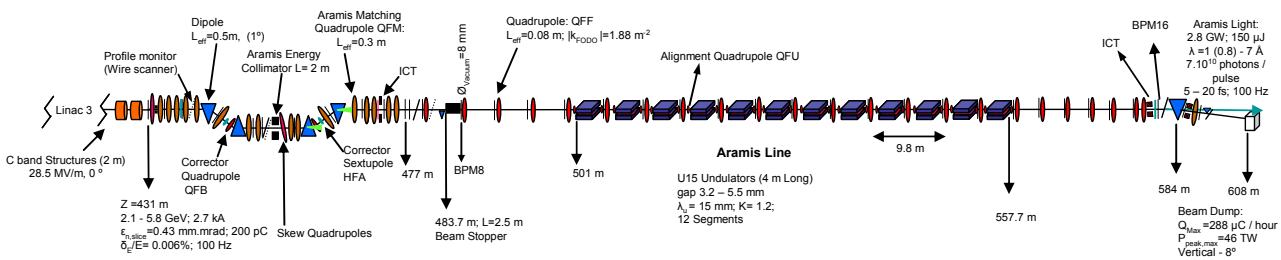

Figure 1: The Aramis hard X-ray SwissFEL undulator line.

ISBN 978-3-95450-123-6

ORIGIN OF SHIFT DEPENDENT MULTIPOLES IN APPLE-II UNDULATORS

M. Kokole, T. Milharčič, M. Zambelli, KYMA TEHNOLOGIJA, Sežna, Slovenia
B. Diviacco, ELETTRA, Basovizza, Italy
G. Soregaroli, M. Tedeschi , EUROMISURE, Pieve S. Giacomo, Italy

Abstract

APPLE-II insertion devices are very flexible devices for production of variably polarized photons. This devices inherently suffer from shift dependent integrated field multipoles that can reach values which can seriously deteriorate quality of the electron beam. Since there is no really effective shimming method for correction of this errors, it is important to understand where they originate. Paper presents a study of integrated field multipoles shift dependency based on deformation of magnetic array due to magnetic forces. We have modeled separately deformations of each magnet keeper in the magnetic array. Model calculations have shown that most of integrated field multipole dependency on the shift is due to mechanical deformation in combination with magnetic effects.

INTRODUCTION

Insertion device should have minimal influence on the electron beam in all modes of operation, consequently requiring a tight control of the integrated magnetic field over the length of the device. Both second and first field integrals should be as close to zero as possible in all operational modes. Also the field integrals mutipoles should be as low as possible and should change as little between different operational modes.

For this reason a lot of design effort was put in the magnetic structure, specifically on the end field terminations [1]. But all this efforts do not solve all the possible errors. It has been shown in multiple cases [2, 3, 4] that mechanical deformations play a critical role in the performance of this devices. Most notably shift dependent multipoles have been observed in the EPUs for FEL-1 and FEL-2 line at FERMI@Elettra [5, 6] and also at other light sources [2]. For these reasons a study of the origin of shift dependent multipoles was prompted.

Even in ideal case it is not possible to keep all the multipoles at zero at all operational modes of an APPLE-II insertion device. Normal dipole is generated in the symmetric field device by default and changes with the shift due to the non zero permeability of magnetic material. Sextupole and its change is also generated by the non zero permeability of the magnetic material. It is possible to limit this changes by proper design of the end field terminations [1].

On the other hand it is not possible to generate the quadrupoles both normal and skew in ideal device. Hence it is believed that they arise for the mechanical deformations. For example a rotation of the horizontally magnetized block around vertical axis [4] can give a rise to a skew quadrupole, which is the most notably observed shift dependent multipole [2, 5, 6]. In the 55 mm periods EPUs for FEL-1 for FERMI@Elettra a large shift dependent skew quadrupole was observed. Largest change of about 400 G was observed at minimum 10 mm gap. Values of multipoles decrease with increasing gap.

To understand which deformations will generate different multipoles and how they change with shift, it is necessary to make a model that includes also deformations for the ideal structure. Following paragraphs contain description and results from such a model.

MAGNETIC MODEL WITH STRUCTURAL DEFORMATIONS DUE TO MAGNETIC FORCES

In order to study how mechanical deformation influence the magnetic performance of the insertion device a special RADIA code was developed without any symmetries allowing a movement and rotation of each magnet block. This code generates an APPLE-II magnetic structure and applies deformations to the structure by displacement and rotation of each block. It is possible to either enter deformations from external files, produced by the mechanical Finite Element Analysis (FEA) of the mechanical structure or the code can also calculate simplified deformations due to magnetic forces.

Magnetic forces

First part of the code will calculate magnetic forces and torques on each magnet block, hence giving an input for the FEA mechanical calculations. For this calculation permeability of material was not taken into account since it does not effect the forces significantly. The largest force is exerted in vertical direction for both horizontally and vertically magnetized block. This force is mostly due to the neighbors in the array. Horizontal and transverse force change with the shift due to the changing neighbors.

At the moment no available computer is able to compute a complete mechanical structure applying forces on each magnet separately. So it is necessary to apply some assumptions. Hence a series of steps were studied in order to get a complete picture. By applying only the deformations from frame and girders no change in multipoles is observed. From this it can be concluded that the multipoles must have an origin in different displacement of each magnet block.

Since FEA can not calculate deformation in a complete mechanical structure for each block separately a approximation approach was taken. Magnetic forces and torques on each magnet were calculated and from this an isotropic

ISBN 978-3-95450-123-6

FEASIBILITY OF DIAGNOSTICS UNDULATOR STUDIES AT ASTA*

A.H. Lumpkin# and M. Wendt, Fermi National Accelerator Laboratory, Batavia, IL 60510 USA
J.M. Byrd, Lawrence Berkeley National Laboratory, Berkeley, CA 94720 USA

Abstract

The Advanced Superconducting Test Accelerator (ASTA) facility is currently under construction at Fermilab. With a 1-ms macropulse composed of up to 3000 micropulses and with beam energies projected from 45 to 800 MeV, the need for non-intercepting diagnostics for beam size, position, energy, and bunch length is clear. In addition to the rf BPMs, optical synchrotron radiation (OSR), and optical diffraction radiation (ODR) techniques already planned, we propose the use of undulator radiation from a dedicated device for diagnostics. with a nominal period of 4-5 cm, a tunable field parameter *K*, and a length of several meters. The feasibility of extending such techniques in the visible regime at a beam energy of 125 MeV into the UV and VUV regimes with beam energies of 250 and 500 MeV will be presented.

INTRODUCTION

One of the challenges of the present-day and proposed superconducting linear accelerators with concomitant high-power beams is the non-intercepting diagnostics of the beam size, energy, bunch length, and phase. The acquisition of a comprehensive set of electron beam properties from a linear accelerator based on undulator radiation emitted from a 5-m long device was demonstrated over two decades ago on a visible wavelength free-electron laser (FEL) [1] driven by a pulse train of 100-μs extent. The high-power electron beams for the Advanced Superconducting Test Accelerator (ASTA) facility involve up to 3000 micropulses with up to 3.2 nC per micropulse in a 1-ms macropulse [2]. With beam energies projected from 45 to 800 MeV the need for non-intercepting diagnostics is clear. Besides the rf BPMs, optical synchrotron radiation (OSR), and optical diffraction radiation (ODR) techniques already considered, we propose the use of the properties of undulator radiation (UR) from a dedicated device for diagnostics with a nominal period of 4-5 cm, a tunable field parameter *K*, and a length of several meters. We propose time resolving the e-beam properties within the macropulse by viewing the UR with standard electronic-shuttered CCDs or gated ICCD's (size and position) and a synchroscan streak camera coupled to an optical spectrometer (energy, bunch length, and phase).

Initial tests could begin at an beam energy of 100-125 MeV with UR in the visible regime and could be extended into the UV and VUV regimes with beam energies of 250 and 500 MeV.

lumpkin@fnal.gov
*Work supported under Contract No. DE-AC02-07CH11359 with the United States Department of Energy.

FACILITY ASPECTS

The ASTA linac with photocathode (PC) rf gun, two booster L-band SCRF accelerators (CC1 and CC2), and beamline is schematically shown in Fig. 1. The L-band accelerating sections will provide 40- to 50-MeV beams before the chicane, and an additional acceleration capability up to a total of 800 MeV will eventually be installed in the form of three cryomodules after the chicane with eight 9-cell cavities with highest possible average gradient (up to ~30 MV/m). The phase of the CC2 section can be adjusted to energy chirp the beam entering the chicane to vary bunch-length compression. Maximizing the far infrared (FIR) coherent transition radiation (CTR) in a detector after the chicane will be used as the signature of generating the shortest bunch lengths. Micropulse charges of 20 to 3200 pC will be used typically as indicated in Table 1. The nominal micropulse format is 3 MHz for 1 ms. This aspect is unique for test facilities in the USA and highly relevant to the next generation of FELs. The macropulse repetition rate will be 5 Hz.

Signal strengths should allow tracking of a subset of the micropulses with standard imaging. The UR pulse length will be measured with the Hamamatsu UV-visible C5680 streak camera, and this length should be correlated with the electron beam bunch length subject to some narrowing when there is SASE gain. The synchroscan streak camera will also allow tracking of the relative phase within the macropulse of sets of micropulses to about 200 fs. At this time we anticipate one would provide optical transport for the signals to the high-energy -end laser lab where a small diagnostics suite of CCD camera, ICCD camera, streak camera, and optical spectrometer would be available on an optics table for characterizing the UR properties and then the deduced electron beam properties. Initial detection could be in the tunnel with local camera stations.

Table 1: Summary of Electron Beam Properties at ASTA

Parameter	Units	Values
Bunch charge	pC	20-3200
Emittance, norm	mm mrad	1-3
Bunch length, rms	ps	3-1
Micropulse Number		1-3000

ISBN 978-3-95450-123-6

STATUS OF PAL-XFEL UNDULATOR SYSTEM

D.E. Kim, H.S. Han, Y.G Jung, H.G Lee, W.W. Lee, K.H. Park, H.S. Suh,
J.Y. Huang, I.S. Ko, M.H. Cho
Pohang Accelerator Laboratory, Pohang, Kyungbuk 790-784, KOREA

Abstract

Pohang Accelerator Laboratory (PAL) is developing 10 GeV, 0.1 nm SASE based FEL for high power, short pulse X-ray coherent photon sources named PAL-XFEL. At the first stage PAL-XFEL needs two undulator lines for photon source. PAL is developing undulator magnetic structure based on EU-XFEL design. The hard X-ray undulator features 7.2 mm min magnetic gap, and 5.0 m magnetic length with maximum effective magnetic field larger than 0.908 T to achieve 0.1nm radiation at 10 GeV electron energy. Soft X-ray undulator system has 8.3 mm undulator gap with 33.4 mm magnetic period. In this report, the status of the undulator project including mechanical design, magnetic design, are summarized.

INTRODUCTION

The Pohang Accelerator Laboratory (PAL) has been developing SASE based light sources since 2011. The key features are 0.1nm class SASE radiation, and 10 GeV class S-band linear accelerator, low emittance (0.5 um) photo cathode RF gun, and EU-XFEL style out vacuum undulator system[1]. It's targeting 60Hz operation with optional 120 Hz operation. In addition to this, 1.0nm~3.0 nm VUV SASE line is also planned. The total length of the PAL-XFEL building will reach 1,100 m including about 120m undulator lines. 22 undulators for X-ray line and 14 undulators for Soft X-ray line is expected. The schematic layout of the linear accelerator and undulator line is shown in Fig. 1. The major parameters of the X-ray FEL and undulator line are shown in Table 1.

Table 1: Major Parameters of the PAL-XFEL Undulator

Symbol	Unit	Min gap	Max gap
E	GeV	10.000	10.000
g	mm	7.20	9.90
λ	mm	24.4	24.4
L_{und}	5	5.0	5.0
λ_r	nm	0.1000	0.0600
B_{eff}	Tesla	0.9076	0.5833
K		2.0683	1.3293
Lg	m	2.88	5.34
Lg/Lg1D		1.36	1.98
Pbeam	TWatt	30.0	30.0
Psat	GWatt	13.7	5.1
Lsat	m	52.8	92.4
Lg	m	2.88	5.34
Lg/Lg1D		1.36	1.98

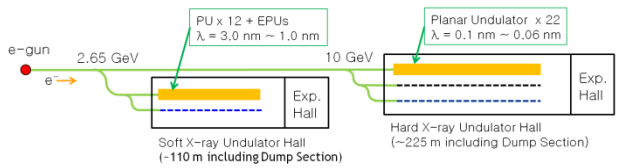

Figure 1: Schematic layout of the PAL-XFEL and undulator line.

EU-FEL UNDULATOR

The key features of the EU-XFEL undulator design are an economic design using standardization and optimization suited for mass serial production [2]. The generator structure of the PAL-XFEL undulator design is shown in Fig. 2 and it is benchmarking the conceptual details of EU-XFEL undulator. It features (a) 4 independent spindle movement for the gap control using easily accessible commercial parts. These 4 motors are electronically synchronized by a control system. (b) strong girder system designed for the worst case magnetic load that can be used for all other cases. (c) unique pole tuning system. The poles can be tuned and locked using tuning studs and notches in the poles. This scheme simplifies the tuning procedure and a big improvement compared to the usual copper shims which are clumsy in nature and tuning range is discrete. With this unique tuning scheme, the supplier can manufacture the undulator meeting the requirements. The detailed tuning and spectrum shimming can be done in house. In this way, the cost can be lowered.

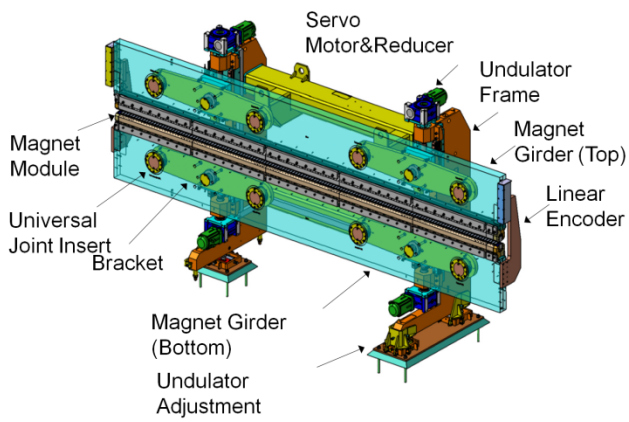

Figure 2: Schematic structure of PAL-XFEL undulator system.

ISBN 978-3-95450-123-6

BEAM DIAGNOSTIC SYSTEM FOR PAL-XFEL

Changbum Kim*, Hyojin Choi, Jae-Young Choi, Jung Yun Huang, Heung-Sik Kang, Do Tae Kim, Byung-Joon Lee, Chang-Ki Min, PAL, Pohang, Korea

Abstract

The XFEL project in Pohang Accelerator Laboratory (PAL) requires low beam-emittance, ultra-short bunch length, high peak current, high stability of beam energy, and measurement and steering of beam trajectory within micrometers. Therefore, beam diagnostics for the self-amplified stimulated emission (SASE) XFEL should be, focused on attaining femto-second precision in the measurement of temporal beam parameters, and sub-micrometer precision in beam position measurement. Charge measurement and energy measurement are important as well. In this work, technical concepts regarding the diagnostic monitors will be summarized and present status of them will be described.

INTRODUCTION

The XFEL[1,2,3,4] is based on the principle of SASE that occurs due to on the generation, acceleration, and transport of unprecedently low-emittance, mono-energetic, high peak current electron bunches through the undulating magnetic field of an undulator array. When the XFEL beam parameters are well matched with XFEL conditions during the electron beam passes through the undulating magnetic field of undulator, the single XFEL mode among the spontaneous emission of synchrotron radiation gains exponential amplification along the undulator magnets. The SASE process is extremely sensitive to the electron beam parameters, so precise beam monitoring and feedback control of the beam parameters are very important in the operation of the XFEL machine. The proposed XFEL project in Pohang Accelerator Laboratory (PAL) requires low beam-emittance (< 1 μm·rad), ultra-short bunch length (~ 50 fs), high peak current (~ 4 kA), high stability of beam energy (< 0.01%), and measurement and steering of beam trajectory within micrometers (< 2 μm) [5].

Therefore, beam diagnostics for SASE XFEL should be, focused on attaining femto-second precision in the measurement of temporal beam parameters, and sub-micrometer precision in beam position measurement. Several beam measurement techniques have been developed for XFEL diagnostics in advanced XFEL study projects. Femtosecond bunch-by-bunch length measurement can be realized using a transverse deflecting cavity. Shot-to-shot variation of bunch length can also be monitored by measuring the coherent synchrotron radiation intensity radiated by femto-second electron bunches. Synchronization between the pump and probe beam for the pump-probe experiments can be achieved with femto-second precision by electro-optic detection of the beam arrival time. For the sub-micrometer beam position measurement, the nanometer beam position monitors (BPMs) developed for the international linear collider (ILC) can be utilized.

For the success of the PAL XFEL project, bunch-by-bunch measurements and control of electron and photon beam parameters must be obtained at critical locations - such as the low energy beam injector, bunch compressors - to achieve optimal tuning of the XFEL. For detailed understanding of the XFEL, beam emittance and beam energy spread should also be measured slice-by-slice along the bunch length. However, the existing diagnostics techniques used for the existing PLS machine, such as single bunch charge measurement, wire scanners, and optical transition radiators for beam size measurement, are also excellent diagnostic tools for the measurements of basic beam parameters in PAL XFEL.

DIAGNOSTICS SYSTEMS

Beam Position

Preservation of beam quality during beam transport, and lasing of the XFEL radiation through the undulator are guaranteed only when the electron beam trajectory is well aligned within the specified tolerance, which is about 10% of the beam size in the undulator. In PAL XFEL, trajectory alignment should be more precise because of the narrow gap (~ 5 mm) in-vacuum undulator. Beam trajectory must be maintained within 10 μm in the linear accelerator and within 2 μm in the undulator array.

The transverse position of the beam in the XFEL can be measured using two different types of BPM: a pickup electrode (stripline or button) BPM, or a cavity BPM. A stripline BPM has a wide dynamic rage with a good resolution and suitable for the use of beam position monitoring in a linac. A cavity BPM has an excellent resolution in a small dynamic range and is widely used in the undulator area. A prototype stripline BPM was developed for the test and installed in the PLS linac.

In the undulator line, because of the tight resolution requirements, cavity BPMs will be used together with the stripline BPM. Cavity BPM has been intensively studied for nanometer beam position measurement for the future International Linear Collider (ILC) [6]. In a cavity BPM, the amplitude of the TM110 mode, excited in the cavity by an off-centered beam, yields a signal proportional to the beam displacement and the bunch charge. Sub-micrometer resolution of the cavity BPM can be achievable, although the measurable range of the cavity BPM is very narrow, typically less than 500 μm.

A prototype cavity BPM has been developed for the ILC (KEK ATF) and XFEL in PAL [7]. A prototype cavity BPM installed in KEK ATF extraction beamline for the

* chbkim@postech.ac.kr

ISBN 978-3-95450-123-6

FAST, ABSOLUTE BUNCH LENGTH MEASUREMENTS IN A LINAC USING AN IMPROVED RF-PHASING METHOD

P. Emma, H. Loos, SLAC, Stanford, CA 94309, USA
C. Behrens, DESY, 22607 Hamburg, Germany

Abstract

There is great demand for a fast, accurate method to measure the absolute bunch length of an electron beam in a linac. Many ideas are available, with one of the most attractive based on the transverse RF deflector [1]. Since this specialized technology can be costly and unavailable, we revive an old method using accelerating RF, but with the same robust characteristics of the transverse deflector (fast, accurate, and absolute). The method is based on the standard "RF zero-phasing" scheme [2], but includes several significant improvements based on experience with the RF deflector method.

INTRODUCTION

Electron bunch length measurements using transverse RF deflectors have become standard in FEL applications and are now quite routine at the *FLASH* [3] and *LCLS* [4] FEL facilities. Although there are actually two separate deflectors at *LCLS*, one before the first bunch compressor (BC1) and one after the second compressor (BC2), there is no deflector between compressors, leaving the intermediate bunch length rarely measured. Similarly, at *FLASH* there is only one deflector at the end of the machine, and future FELs are planning multiple deflectors. In lieu of this costly option, or as a backup method to cover more of the machine, we present a simple method requiring no new hardware, using the existing accelerating RF, and providing a fast (~1 minute), accurate measurement. It is easily calibrated using beam screen data and only the RF frequency needs to be known.

Using a section of linac with nominal off-crest RF phase (standard with bunch compression), the method is first calibrated by fitting the linear slope of beam position, measured on a screen at a dispersive location after the linac, versus small RF phase variations. The dispersed beam size is then measured on the same screen at the nominal off-crest RF phase, then again at nominal, but opposite sign phase, and finally again at crest phase. A parabola is fitted to these three data points and the bunch length is extracted from one of the three fitted parabolic coefficients, using the calibration coefficient.

METHOD

The energy of each electron, $E(z)$, as a function of the bunch length coordinate, z, after a section of linac with peak accelerating voltage V_0 and RF phase φ (with $\varphi = 0$ defined at the crest phase), is

$$E(z) = E_i + eV_0 \cos(\varphi + kz) + E_0 hz \,, \qquad (1)$$

where E_i is the initial electron energy prior to the linac section, k ($= 2\pi/\lambda_{rf}$) is the RF wave number, h is the final linear energy chirp along the bunch, and e is the electron charge. The chirp, h, is the additional linear energy-z correlation (measured in m^{-1}) along the bunch due to the initial correlation (prior to the linac section) and also encompasses any wakefield-induced linear chirp over the linac section. The nominal energy, E_0, after the linac section is

$$E_0 \equiv E_i + eV_0 \cos\varphi_0 \,, \qquad (2)$$

with φ_0 as the nominal (reference) RF phase.

Defining the relative energy deviation as $\delta = (E - E_0)/E_0$, using Eq. (1) and (2) and assuming $k|z| << 1$ (*i.e.*, a short bunch compared to λ_{rf}), we have

$$\delta(z) \approx eV_0[\cos\varphi - \cos\varphi_0 - k\sin\varphi\, z]/E_0 + hz. \qquad (3)$$

At this point it is useful to express these results in terms of a more directly measured quantity, namely the transverse beam position at a dispersive location (*i.e.*, after a bend magnet) following the linac section. Such a location is usually easily identified, since a bunch compressor chicane or other bend system commonly follows such a linac section. The transverse dispersion is defined as η and the transverse position, y, of each on-axis electron is then: $y = \eta\delta$.

Measuring the centroid of the ensemble of particles and using $\langle z\rangle = 0$, the transverse position centroid as a function of the variable RF phase, φ, taken from Eq. (3) is

$$\langle y\rangle = \eta\langle\delta\rangle \approx eV_0\eta[\cos\varphi - \cos\varphi_0]/E_0 \,. \qquad (4)$$

A voltage calibration can then easily be done by measuring the sensitivity of the position centroid, $\langle y\rangle$, using small variations of the RF phase, φ (note that φ_0 is the reference phase and is not variable).

$$\partial\langle y\rangle/\partial\varphi = -eV_0\eta\sin\varphi\,/E_0 \equiv a \qquad (5)$$

Here the calibration slope, a, is defined (see Fig. 1).

Now we express the position of each particle, using the calibration slope, a, at the nominal phase by setting $\varphi = \varphi_0$ in Eq. (3) and again using $y = \eta\delta$.

$$y = (\eta h + ak)z \qquad (6)$$

With $\sigma_y = \langle y^2\rangle^{1/2}$ and $\sigma_z = \langle z^2\rangle^{1/2}$ it is clear that the rms transverse beam size, σ_y, is linearly dependent on the rms bunch length, σ_z, as

$$\sigma_y^2 = (\eta h + ak)^2\sigma_z^2 + \sigma_{y0}^2 \,, \qquad (7)$$

where the chirp, h, is unknown and we introduce σ_{y0} as the non-dispersed (minimum) beam size at the screen.

To eliminate the unknown chirp we note that the sign of a follows the sign of φ, and introduce x as the sign of

ISBN 978-3-95450-123-6

SUB-FEMTOSECOND HARD X-RAY PULSE FROM VERY LOW CHARGE BEAM AT LCLS

V. Wacker*, University of Hamburg, Hamburg, Germany
Y. Ding, J. Frisch, Z. Huang, C. Pellegrini and F. Zhou, SLAC, CA 94025, USA

Abstract

The Linac Coherent Light Source (LCLS) is an x-ray free-electron laser (FEL) at SLAC National Accelerator Laboratory, supporting a wide range of scientific research with an x-ray pulse length varying from a few to several hundred femtoseconds. There is also a large interest in even shorter, single-spike x-ray pulses, which will allow the investigation of matter at the atomic length (Å) and time scale (fs). In this paper, we investigate the FEL performance using 1 pC and 3 pC electron bunches at LCLS, based on the start-to-end simulations. With an optimization of the machine set up, simulations show that single spike, sub-fs, hard x-ray pulses are achievable at such a low charge.

INTRODUCTION

Self-amplified spontaneous emission (SASE) FELs provide tunable, high-power, coherent light sources in the x-ray wavelength range. Several FEL projects worldwide [1, 2, 3] provide users with high peak power, femtosecond long pulses. Nevertheless, a growing interest in even shorter, single-spike pulses with a full longitudinal coherence is evolving within the FEL user community. These ultra-short pulses could open undreamed-of possibilities for experiments in physics and other domains of science.
The generation of single-spike x-ray pulses in SASE mode can be obtained with very short electron bunches, produced by reducing the beam charge, or with using a laser or emittance-spoiling foil to manipulate the long electron bunches [4]. Reducing the bunch charge from nC to pC level is a simple way, as first studied in [5, 6]. At LCLS, a systematic study has been performed with 20 pC [7], and it works very well for providing users of x-ray pulses below 10 fs. In this operation mode, the x-ray pulses typically have a few spikes. It is possilbe to further optimize the machine set up, or to combine the emittance-spoiling foil and taper schemes to achieve a single-spike SASE FEL x-ray pulse at this 20pC charge [8], but the collective effects have to be carefully considered.

In this paper, we study the possibilities of further reducing the charge from 20 pC to 1pC/3pC for producing sub-femtosecond, hard x-ray pulses at LCLS, based on start-to-end simulations. However, the beam diagnostics for such small, low charged bunches are currently challenging topics at LCLS. At such a low charge, the collective effects from the space charge force, the coherent synchrotron radiation, and wake fields are expected to be much smaller. A schematic layout of the LCLS machine is shown in Fig. 1. The compression in the second bunch compressor (BC2) determines the final electron bunch length. By tuning the phase of the L2 linac the compression ratio was adjusted. The start-to-end simulations were made using IMPACT [9] and ELEGANT [10] codes for the tracking of the electron bunch from the photocathode to the beginning of the undulator. From there on the FEL radiation was simulated with GENESIS 1.3 [11]. IMPACT covers the tracking of one million macro-particles from the photocathode to the end of the first dog-leg (DL1) at 135 MeV. The code includes 3D space charge forces allowing detailed modeling at low energies. To reduce the high-frequency numerical noise in the following ELEGANT simulations, the particle output from IMPACT was smoothed in longitudinal dimension [12]. ELEGANT includes a 1D model of incoherent and coherent synchrotron radiation (ISR, CSR) as well as longitudinal space charge (LSC) effects. The generation of the FEL radiation was simulated using GENESIS. This FEL simulation includes LSC effects in the undulator chamber. The influence of resistive wall-wakes is negligible and was not considered.

Our results show that a single-spike pulse with 5 GW peak power and 0.2 fs fwhm is achievable using a bunch charge of 1 pC. The simulations for a bunch charge of 3 pC resulted in about two spikes.

ELECTRON BEAM OPTIMIZATION

In this section the required machine set up for single-spike operation at LCLS is studied. From the photoinjector down to the undulator, we aim for the shortest bunch, the highest current and the smallest transverse emittance possible. In this manner, we obtain high electron beam brightness, the key requirement for FELs.

The condition for the rms bunch length σ_z under which the SASE FEL produces a single-spike pulse was found to be $\sigma_z \leq 2L_{coop}$ [6]. In case of LCLS, the cooperation length L_{coop} is approximately 25 nm, dictating a rms bunch length

$$\sigma_z \leq 50\,\mathrm{nm}. \quad (1)$$

To obtain such a short bunch, shorter bunch length in the injector and almost full-compression in the linac and compression system have been applied, as discussed in the following sections.

Electron Beam Optimization for 1 pC

The photoinjector set up was obtained by IMPACT simulations using one million particles and a bunch charge of 1 pC. The optimized bunch was achieved using a Gaussian

* violetta.wacker@desy.de

ISBN 978-3-95450-123-6

GENERATION OF ULTRA-SHORT ELECTRON BUNCHES AT FLASH*

Juliane Rönsch-Schulenburg†, Hamburg University and CFEL, Hamburg, Germany
Eugen Hass, Alexander Kuhl, Tim Plath, Marie Rehders,
Jörg Rossbach, Hamburg University, Hamburg, Germany
Nicoleta Baboi, Marie Kristin Bock, Michael Bousonville, Christopher Gerth, Karsten Klose, Torsten Limberg, Uros Mavric, Holger Schlarb, Bernhard Schmidt, Siegfried Schreiber, Bernd Steffen, Cezary Sydlo, Stephan Wesch, Silke Vilcins-Czvitkovits, DESY, Hamburg, Germany
Aleksandar Angelovski, Rolf Jakoby, Andreas Penirschke,
Thomas Weiland, TU Darmstadt, Darmstadt, Germany
Sascha Schnepp, ETH Zürich, Zürich, Switzerland

Abstract

In order to produce radiation pulses of a few femtoseconds at FELs like FLASH, different concepts have been proposed. Probably the most robust method is to create an electron bunch, which is in the most extreme case as short as one longitudinal optical mode. For FLASH this translates into a bunch length of a few micrometers only and thus in order to mitigate space charge effects, the bunch charge needs to be about 20 pC. The technical requirements to achieve this goal are discussed. This includes beam dynamics studies to optimize the injection and compression of small charge electron bunches. A reduced photo injector laser pulse duration helps to relax the RF tolerance which scales linear with the compression factor. A new photo injector laser with sub-picosecond pulse duration in combination with a stretcher is used to optimize the initial bunch length. The commissioning of the new laser system and first experiments are described. Limitations of the presently available electron beam diagnostics at FLASH for short, low charge bunches are analyzed. Improvements of the longitudinal phase space diagnostics and the commissioning of a more sensitive bunch arrival time monitor are described.

INTRODUCTION

The users of free-electron lasers (FELs) show a rising interest in very short vacuum ultraviolet (VUV), extreme ultraviolet (XUV) and X-ray pulses in order to study fast process in different areas of science. At FLASH for instance about a quarter of the scheduled user shifts request for pulses with durations below 50 fs (FWHM) [1]. Thus the idea to create electron bunches with lengths of one longitudinal optical mode to create the so-called single spike SASE pulses [2, 3] attracts the interest of several FEL facilities [4, 5, 6]. Such a single spike SASE pulse is bandwidth limited, longitudinally coherent and compared to other concepts (e.g. seeding) no long background signal disturbs the signal. The usage of short pulses also prevents damage of the studied object, since most applications of short-pulses rely on a high photon count [7]. The required electron bunch length (σ_b) has to fulfill the condition $\sigma_b \leq 2\pi L_{coop}$ [2, 3], with L_{coop} the cooperation length.

SINGLE SPIKE OPERATION OF FLASH

FLASH [8] is a single-pass high-gain Self Amplified Spontaneous Emission free-electron laser (SASE-FEL), which operates in a wavelength range from 4.12 to 45 nm. At FLASH typically FEL pulse durations down to 50 fs (FWHM) are generated and bunch charges down to 200 pC are used [8]. A single spike operation at FLASH requires an electron bunch with a duration of a few fs only. In order to create such a short bunch it is mandatory to reduce the charge to avoid the elongation of the bunch by space charge forces. Figure 1 shows as an example a

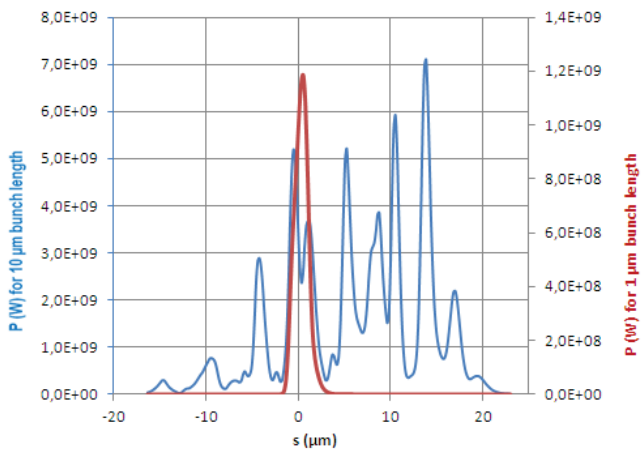

Figure 1: Genesis simulation of the longitudinal distribution of a SASE pulse at FLASH at a wavelength of about 13 nm when applying an electron bunch with a rms bunch length of 10 and 1 μm.

comparison of the longitudinal distribution simulated using Genesis for electron bunches with an rms bunch length of 10μm and 1μm. An rms electron bunch length of about 10μm is about the minimum length which can be achieved during FLASH standard operation when using a charge of 200 pC[9]. This temporal distribution of the SASE-pulse

* The project is supported by the Federal Ministry of Education and Research of Germany (BMBF) under contract No. 05K10GU2 and FSP301
† juliane.roensch@desy.de

ISBN 978-3-95450-123-6

BEAM DYNAMIC STUDIES FOR THE GENERATION OF SHORT SASE PULSES AT FLASH*

M. Rehders†, J. Rossbach, Hamburg University, Germany
J. Rönsch-Schulenburg, Hamburg University and CFEL, Hamburg, Germany
H. Schlarb, S. Schreiber, DESY, Hamburg, Germany

Abstract

Many users at FLASH work on pump-probe experiments, where time resolution is determined by the duration of the SASE pulses. Therefore users have expressed the strong wish for shorter XUV pulses. The shortest possible pulse is a single longitudinal optical mode of the SASE radiation. The most direct way to realize this at FLASH would be to reduce the electron bunch length to only a few μm at the entrance of the undulator section. A bunch charge of 20 pC is sufficient for the generation of such short bunches. Such a small bunch charge reduces space charge in the injector area drastically and thus makes it possible to shorten the bunch duration directly at the photo-cathode [1]. This in turn helps to overcome technical limitations of the bunch compression due to RF induced non-linearities and minimizes collective effects during the compression process. Beam dynamic studies are being performed to optimize the parameters of the photo injector laser, of the accelerating modules, and of the bunch compression. This includes particle tracking starting from the cathode through the accelerating modules with the ASTRA code and through the dipole chicanes using CSRtrack. The expected SASE pulses are being simulated with the Genesis code.

INTRODUCTION

FLASH is a Free Electron Laser user facility in the XUV regime that offers SASE pulses within a wavelength range from 4.1 to 45 nm. At FLASH standard operation, electron bunches with a charge of 0.1 to 1.5 nC produce SASE pulses with pulse durations between 50 and 200 fs (FWHM) [2]. These SASE pulses consist of many optical modes, resulting in a spiky spectrum and temporal distribution.

The time-resolution of pump-probe experiments is determined by the duration of the radiation pulses. Thus in order to be able to time resolve even faster physical and biological processes, one needs to go to shorter SASE pulses. The shortest possible SASE pulse would be of the length of a single longitudinal optical mode. At FLASH this length is in the scale of a few μm. Beam dynamic studies are being done to find out the parameters needed for single spike operation. This paper focusses on a preliminary start-to-end simulation as a starting point for further optimization.

For more information on the progress towards single spike operation at FLASH see also [3].

* The project is supported by the Federal Ministry of Education and Research of Germany (BMBF) under contract No. 05K10GU2 and FSP301.
† marie.rehders@desy.de

SINGLE SPIKE CONDITION

The length of a longitudinal optical mode is determined by the cooperation length L_c [4, 5, 6]. It is the distance spanned by the emitted radiation in its slippage over the electron bunch over one gain length,

$$L_c = \frac{\lambda_r}{4\pi\sqrt{3}\rho} * (1+\eta) \tag{1}$$

where λ_r is the wavelength of the emitted radiation, given by

$$\lambda_r \cong \frac{\lambda_u}{2\gamma^2}(1+K^2) \tag{2}$$

and η is a degradation factor that takes into account 3D effects like radiation diffraction, beam emittance and energy spread, as first introduced by M. Xie [6]. The 1D parameter ρ is the FEL gain parameter, which is a measure of the beam quality. It is defined as

$$\rho = \left[\frac{JJ^2K^2 I_p}{8 I_A k_u{}^2 \gamma^3 \sigma_{tr}}\right]^{1/3} \tag{3}$$

with the undulator parameter K and $k_u = 2\pi\lambda_u$, λ_u being the undulator period length. JJ is the coupling factor between the emitted radiation and the bunch. For planar undulators like FLASH it is just a little below unity. $I_A \approx 17$ kA is the Alfven current. The gain parameter also depends on bunch parameters. Here I_p is the peak current, γ the beam energy in terms of the electron rest mass energy, and σ_{tr} is the transverse beam size.

Another property determined by the gain parameter is the gain length L_g with

$$L_g = \frac{\lambda_u}{4\pi\sqrt{3}\rho}(1+\eta) \tag{4}$$

It determines the distance until SASE radiation power reaches saturation.

Thus by choosing the bunch properties one can control the SASE radiation properties. A bunch with a length of $\sigma_z \leq 2\pi L_c$ would excite only a single longitudinal optical mode [4]. The emitted radiation pulses would not only be extremely short, but also longitudinally coherent.

Due to the wishes of the users to go towards shorter pulse durations, this operation scheme is highly appealing for FLASH.

SHORT BUNCH OPERATION AT FLASH

FLASH uses a two-stage bunch compression scheme to reach the bunch lengths needed for SASE operation. A

ISBN 978-3-95450-123-6

LASER WAVELENGTH TUNING BY VARIABLE-GAP UNDULATORS IN SACLA

Kazuaki Togawa#, Toru Hara, Takashi Tanaka, Hitoshi Tanaka
RIKEN SPring-8 Center, Sayo, Hyogo 679-5148, Japan

Abstract

Wavelength tunability by variable-gap in-vacuum undulators is one of the features of SACLA. To fully utilize this advantage, it is important to suppress gap-dependent magnetic field errors down to the tolerance level, namely sub-microradian per undulator segment, which assures high SASE amplification gain enabling XFEL power saturation. For this purpose, we introduced a "feed-forward correction" scheme, which is a well-known technique in third-generation light sources. However, in linac-based XFELs, it was not easy to make sufficiently accurate correction tables of steering magnets to cancel out error fields due to shot-by-shot beam orbit and energy fluctuations propagating from the accelerator. By using a linear accelerator model, we so far succeeded in suppressing the gap-dependent orbit deviation down to a 10-μm level over the undulator section. Owing to this effort, experimental users at SACLA can quickly change the laser wavelength in a few seconds according to their demands by setting only the undulator K-value. In this paper, we report the present status of wavelength tuning by the undulator gap in SACLA and problems to be solved towards better accuracy.

INTRODUCTION

The Japanese x-ray free-electron laser (XFEL) facility SACLA has started public user operation on March 2012 [1-3]. Currently, high-power stable XFEL light with pulse energies of 100-400 μJ is generated and provided for experimental users in a wavelength range from 5 keV to 15 keV.

Since SACLA adopted variable-gap in-vacuum undulators, a laser wavelength can be changed either by the electron beam energy or the undulator gap. In order to achieve the laser wavelength tuning by controlling the undulator gap, a "feed forward correction" scheme, which is familiar in third-generation light sources, is introduced. In the storage ring, the beam orbit deviation may affect the pointing stability of synchrotron radiation, however intensity of radiation, in principle, does not change. On the other hand in linac-based XFELs, the orbit deviation directly degrades the laser performance. To maintain high SASE amplification gain, the electron beam orbit in the undulator section should be straight and its deviation needs to be less than several-microns [4]. Therefore, the preparation of precise correction tables is indispensable to tune the laser wavelength by the undulator gap.

Here, we report the present status of wavelength tuning by the undulator gap in SACLA, which is the world's first attempt in linac-based SASE FELs.

#togawa@spring8.or.jp

PRECISE MEASUREMENT OF BEAM ORBIT DEVIATION IN UNDULATOR SECTION

For the electron beam orbit measurements, RF cavity type BPMs are used in SACLA [5, 6]. In the undulator section, there are 18 undulators and 17 BPMs are located in between two undulators. In addition, there are 4 BPMs downstream of the undulator section before the beam dump. Although the resolution of these BPMs can reach sub-micron, the dynamic range is limited within ±100 μm. Therefore careful attention should be paid to their usage.

In order to accurately measure the beam orbit deviation in the undulator section, the fluctuation of the injection orbit should be precisely measured for each electron bunch by using two BPMs installed upstream of the first undulator. The two BPMs are separated by a 7.8-m long drift space to determine the position and angle of the injection beam orbit. To eliminate the effect of environmental magnetic fields, the passage of the beam between the two BPMs is magnetically shielded using high-μ metallic-sheets. The components around the drift space are made of low-μ metals. The magnetic fields from ion pumps and cold cathode gauges are confined by iron-plates. After these efforts, the residual magnetic field at the beam passage is suppressed to less than 4 mG, which is 1/100 of the environmental fields. The photograph of the drift space with two BPMs is shown in Fig. 1.

Before the orbit measurements, the bunch charge is reduced to less than 100 pC to avoid BPM signal saturation. Also an orbit and beam energy feedback is applied with an interval of several seconds to suppress slow drift of the injection orbit and beam energy.

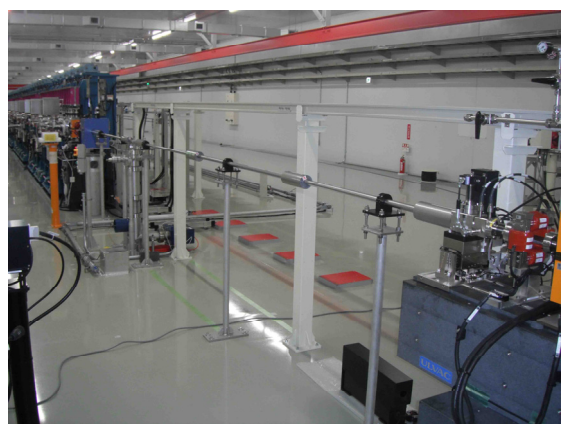

Figure 1: Injection section of the undulator line.

ISBN 978-3-95450-123-6

FEMTOSECOND ELECTRON BUNCH MEASUREMENT USING THz CHERENKOV RADIATION IN DIELECTRIC MATERIALS

K. Kan, J. Yang, A. Ogata, T. Kondoh, T. Toigawa, K. Norizawa, H. Kobayashi, Y. Yoshida,
Institute of Scientific and Industrial Research, Osaka University, Osaka, Japan
M. Hangyo, Institute of Laser Engineering, Osaka University, Suita, Osaka, Japan
R. Kuroda, H. Toyokawa, National Institute of Advanced Industrial Science and Technology,
Tsukuba, Ibaraki, Japan

Abstract

Beam diagnostic for electron bunch length using spectrum analysis of multimode terahertz (THz) -wave on the order of 0.1 THz was investigated. The multimode THz-wave was generated by coherent Cherenkov radiation (CCR) using hollow dielectric tubes and femtosecond/picosecond electron bunches. The spectra of multimode THz-wave depended on electron bunch length, which was measured by a streak camera, resulting in a possibility of a new beam diagnostic based on CCR and a bunch form factor.

INTRUDUCTION

Ultrashort, e. g. femtosecond [1] or picosecond, electron bunches are used in accelerator physics applications such as free electron lasers (FELs), laser-Compton X-ray, and pulse radiolysis [2]. On the other hand, electron bunches with short bunch lengths are also useful for electro-magnetic (EM) radiation production in terahertz (THz) range because the inverse of 1 ps bunch length corresponds to the frequency of 1 THz. A shorter electron bunch can emit EM radiation of higher frequency according to the bunch form factor, which is described by the Fourier coefficients of the bunch distribution [3]. Furthermore, the radiation intensity at lower frequency than the inverse of the bunch length is proportional to the electron number, e. g. $\approx 10^9$ at 1 nC. As the result, an intense THz-wave can be generated by such electron bunches. In the studies on EM radiation emitted from electrons, Cherenkov radiation (CR) has been studied since the 1930s [4] and radiation yield dependence on wavelength and angular distribution was reported. In the 1990s, the bunch form factor [3] and angular distribution of coherent transient radiation (CTR) from electron bunches were measured experimentally. Recently, not only monochromatic THz-wave [5] but also multimode one [6,7] of <0.4 THz were generated by coherent Cherenkov radiation (CCR). Another THz-wave generation method, which utilized a periodic electron bunch distribution, generated narrow-band THz-wave up to ≈0.86 THz for a bunch length diagnostic [8]. Alike THz-wave generated by a laser, that generated by an accelerator would be useful to a probe light, which monitors conductivity due to quasi-free electrons, or imaging for medical and security use.

In this paper, generation of multimode THz-wave using multimode CCR on the order of 0.1 THz was investigated. The multimode CCR was generated by a hollow dielectric tube covered by a metal and femtosecond/picosecond electron bunches from a photocathode RF gun linac. Finally, beam diagnostic for electron bunch length using spectrum analysis of multimode THz-wave was proposed.

EXPERIMENTAL ARRANGEMENT

The photocathode RF gun linac and CCR measurement system are shown in Fig. 1. The details of the linac are discussed in references [9,10,11]. Figure 1(a) shows the linac system. The electron bunch was generated by a 1.6-cell S-band (2856 MHz) RF gun with a copper cathode and a Nd:YLF picosecond laser. The pulse width of the UV pulse from the laser was measured to be 5 ps in FWHM as a Gaussian distribution. The UV light was projected onto the cathode surface at an incident angle of approximately 2° along the electron beam direction. The beam energy at the gun exit was 4.2 MeV. The picosecond electron bunch produced by the RF gun was accelerated up to ~32 MeV by a 2 m long S-band travelling-wave linac with an optimal energy-phase correlation for the bunch compression, in which the head electrons of the bunch have more energy than the bunch tail. Finally, the energy-phase-correlated electron bunch is compressed into femtosecond by rotating the phase space distribution in the magnetic bunch compressor, which is constructed with two 45°-bending magnets (B1 and B2), four quadrupole magnets (Q3, Q4, Q5, and Q6), and two sextupole magnets (S1 and S2). The femtosecond electron bunch was obtained by adjusting the energy modulation in the linac, e. g., compressed bunch length of ~0.2 ps in rms measured by a streak camera at a bunch charge of ~40 pC and a linac phase of 97.5° in this study.

In the experiment, not only the picosecond electron bunch at the linac exit but also the femtosecond one at the compressor exit was used for multimode THz-wave generated by CCR as shown in Fig 1(b). When such electron bunches move on the axis of a hollow dielectric tube covered by a metal, partially periodic electric field, i.e., multimode THz-wave, is induced as shown in Fig. 1(b). This slow-wave structure of the hollow dielectric tube supports modes with phase velocity equal to the beam velocity, which contain fundamental and higher modes. The inner and outer radii of the tube, made of fused silica, were 5 mm and 7 mm, respectively, resulting in the tube wall thickness of 2 mm. The hollow tube was covered by a copper conductive tape for a metal boundary condition, which reflects and stores EM radiation in the tube. In order to measure the intensity and frequency of

ISBN 978-3-95450-123-6

A SIMPLE MODEL FOR THE GENERATION OF ULTRA-SHORT RADIATION PULSES

L.T. Campbell and B.W.J. M^{c}Neil
SUPA, Department of Physics, University of Strathclyde, Glasgow, UK

Abstract

A method for generating a single broadband radiation pulse from a strongly chirped electron pulse is described. The evolution of the chirped electron pulse in an undulator may generate a pulse of coherent spontaneous radiation of shorter duration than the FEL cooperation length. An analytic expression for the emitted radiation pulse is derived and compared with numerical simulation.

INTRODUCTION

Free Electron Lasers based on the SASE mechanism produce intense, uncorrelated radiation pulses of width approximately equal to the FEL cooperation length, l_c [1]. For sufficiently short electron pulses only one single pulse may be emitted. However, such a mode of operation results in output pulses that contain significant temporal jitter. Other methods are being considered to improve the temporal coherence, and to further reduce the temporal width of the radiation pulses [2].

The method discussed here predicts emission of a single radiation pulse of width $< l_c$ from a short, strongly-chirped electron beam evolving in an undulator. The method is described from a general perspective without reference to any specific electron beam source.

A sufficiently strong negative chirp in an electron pulse will cause the pulse to shorten in longitudinal phase space when propogating in an undulator as shown in Fig. 1. After a sufficient propagation distance, the pulse length will come to a minimum, the energy chirp will then become positive and the pulse will start to lengthen.

If the electron pulse length evolves to the order of a resonant FEL wavelength λ_r, it will generate a short pulse of coherent radiation. This coherent spontaneous emission may occur for a number of undulator periods dependent upon the magnitude of the chirp and the length of the electron pulse. For example, for a stronger chirp will cause thee electron pulse to radiate coherently for fewer undulator periods, resulting in a shorter radiation pulse of broader bandwidth.

This is not an FEL effect, rather, it is a coherent effect arising purely from the linear evolution of the electron beam due to the chirp. Nevertheless, an unaveraged system of FEL equations is used to describe the effect, as it is capable of describing both the evolution of the longitudinal shape of the electron pulse, and the consequent emission of CSE from the short electron pulse of length $< \lambda_r$, neither of which can be described using an averaged set of undulator/FEL equations.

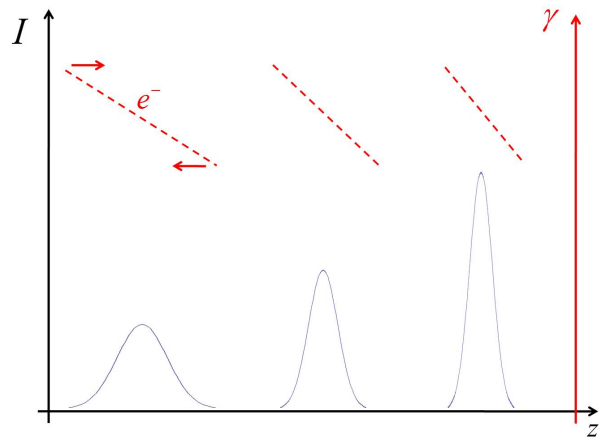

Figure 1: Schematic of the evolution of short negatively chirped electron pulse propagating through an undulator showing the current I and scaled energy γ.

Here, a 1D analytic solution of the expected coherent radiation output from such a chirped electron pulse is derived and compared with both a 1D and 3D numerical simulation using the unaveraged FEL code Puffin [3].

ANALYTIC SOLUTION

An analytic solution is derived from the un-averaged system of FEL equations presented of [4]. These equations are identical to those of the code Puffin [3] in the 1D Compton limit. The electrons are assumed uncoupled from the radiation so that only the wave equation need be solved:

$$\left(\frac{\partial}{\partial\bar{z}}+\frac{\partial}{\partial\bar{z}_1}\right)A(\bar{z},\bar{z}_1)=\frac{1}{\bar{n}_{p\|}}\sum_{j=1}^{N}e^{-i\frac{\bar{z}_1}{2\rho}}\delta(\bar{z}_1-\bar{z}_{1j}), \quad (1)$$

where the scaling of [4] has been used. As in [4], the source term can be put into a more convenient functional form by discretising $\bar{z}_1$ into intervals of width $\Delta\bar{z}_1 << 4\pi\rho$, i.e. much less than a radiation wavelength. In this way, the source term of (1) becomes a sum over discrete intervals:

$$\sum_{n=-\infty}^{\infty}\chi_n\left(\bar{z}\right)e^{-i\frac{\bar{z}_1}{2\rho}}\delta(\bar{z}_1-\bar{z}_{1n})\Delta\bar{z}_1, \quad (2)$$

where: $\chi_n\left(\bar{z}\right)\equiv I_n\left(\bar{z}\right)/I_{pk}$ is the current in the n-th interval scaled with respect to the peak current of the electron pulse at the beginning of the undulator, $\bar{z}=0$. The solution proceeds by then taking the unitary Fourier transform,

ISBN 978-3-95450-123-6

PROGRESS ON A LASER-DRIVEN DIELECTRIC STRUCTURE FOR USE AS A SHORT-PERIOD UNDULATOR

J. Allen, G. Travish, UCLA, Los Angeles, CA 90095, USA
H. Gong, UESTC, Chengdu, Sichuan, China and UCLA, Los Angeles, CA 90095, USA
R. B. Yoder, Manhattanville College, Purchase, NY 10577, USA

Abstract

A laser-powered dielectric structure, based on the Micro Accelerator Platform, has been design and offers undulator periods in the micron to millimeter range. This design was shown previously to potentially support a deflection field strength of several GV/m, equivalent to a magnetic undulator with field strength of about 40 T. In this paper, we address a previous problem in the design involving the junction between half periods of the undulator. Because the structure is resonant, flipping from one deflection direction to the opposite one required controlling the phase of the incident laser and reestablishing a new resonance. One solution to this "phase flipping" problem involves the use of two lasers at different wavelengths to excite adjacent half-periods. This new approach is explored further here along with simulations of the beam trajectory and resulting undulator radiation. We also consider parameter sets that may be possible for these extremely short period undulators.

INTRODUCTION

X-ray sources based on laser undulators have gained increasing interest primarily because their short period makes easier the production of short-wavelength radiation. Thus, these x-ray sources are compact in size, only require low-energy electron beams, and may have low operating costs. Several laser-based undulators have recently been proposed or constructed [1, 2, 3]. These proposed undulators utilize Compton scattering between a free-space laser and a relativistic counter-propagating electron beam. The undulator period is required to be half the laser wavelength; thus, laser power limits the undulator parameter.

To overcome this small undulator parameter, a Bragg structure-based laser undulator has been previously proposed as illustrated in Fig. 1 [4]. The structure is similar to the slab-symmetric acceleration structure that has been investigated at UCLA since 1995 [5, 6, 7, 8]. The top face of the planar structure contains a periodic array of couplers which are incident by a high-powered laser to excite an electromagnetic standing wave in the structure. The undulator provides phase synchronicity between the laser-driven cavity fields and the electron beam as demonstrated in Fig. 2. As an electron travels through the structure, the electron is deflected in one direction by many optical periods within one half undulator-period. In the next half period, the electrons are deflected in the opposite direction. Thus, the undulator parameter is not restricted by the laser wavelength. Also, the structure has previously been shown theoretically capable of producing electron-beam deflection corresponding to an equivalent magnetic field strength of 40T leading to an increased undulator parameter [4].

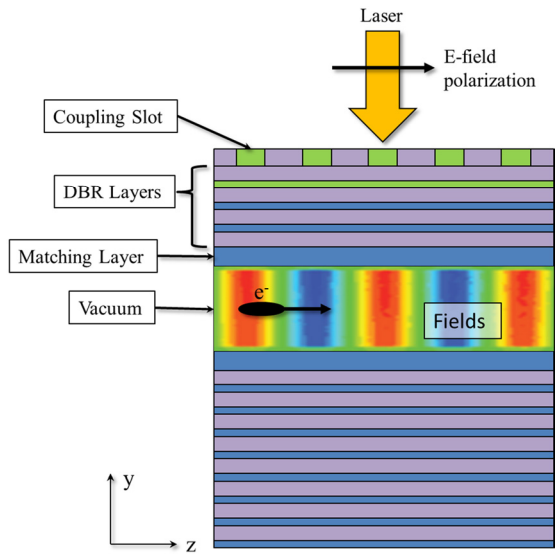

Figure 1: Schematic diagram of the Bragg structure. Five optical periods of the structure are shown; blue represents HfO_2, purple represents SiO_2, and green represents TiO_2.

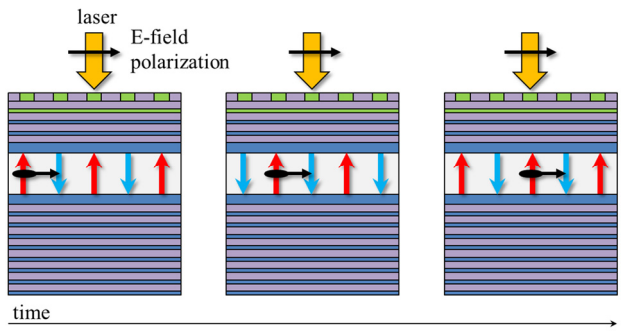

Figure 2: Schematic demonstrating the phase synchronicity between the electron beam and the laser-driven cavity fields. This synchronicity occurs because the electron beam is assumed to travel at velocity $v \approx c$ and the fields evolve at the same rate. Red and blue arrows represent the fields and their directions.

In this study, the problem in the design involving the junction between half periods of the undulator is explored. With this resonant structure, flipping from one deflection direction to the opposite direction requires controlling the phase of the incident laser and re-establishing a new resonance. One approach is the use of two lasers at different wavelengths to excite adjacent half-periods. Additionally, since the fields are not sinusoidal,

ISBN 978-3-95450-123-6

BEAM DYNAMICS AND PERFORMANCE OF ERL-DRIVEN X-RAY FEL*

Yichao Jing†, Vladimir N. Litvinenko, Brookhaven National Lab, Upton, NY 11973, USA

Abstract

In this paper we present a self-consistent concept of ERL generated e-beam to drive an array of X-ray FELs. We use electron-Relativistic Heavy Ion Collider (eRHIC) [1] at BNL as an tool to explore all relevant beam dynamics. First, we study effects of incoherent and coherent synchrotron radiation on the e-beam parameters and present the set of parameters providing for the emittance preservation. Second, we present a single stage bunch compressing scheme with large compression ratio, which suppresses emittance growth caused by CSR. Finally, we present simulation result for soft and hard X-ray FELs driven by such electron beam. We compare projected performance of such facility with world's existing and proposed FEL facilities.

INTRODUCTION

Self-amplified stimulated emission (SASE) free electron laser (FEL) is becoming an attractive source of high-brightness photon beams. Comparing with traditional storage ring based light source, FEL has very narrow bandwidth with highly tunable central frequencies ranging in wavelength from microwaves to hard X-rays. Its peak brightness can be at least ten orders of magnitude higher than the one of storage ring. However, it is also notorious for its low repetition rate and poor stability due to shot to shot noise and fluctuations. In the recent decade, people started to use energy recovery linacs (ERLs) for FEL operation [2, 3, 4]. A single pass or multiple passes ERL can provide high quality electron beam which does not suffer from emittance and energy spread growth through effects of synchrotron radiation and microwave instabilities piling up in storage rings. At the mean time, most of the beam power is recycled before the beam goes to the dump, making a high repetition rate operation of electron beam is now possible. Such a machine could be a perfect candidate for next generation light source.

Among all the radiation wavelengths, X-rays, both soft and hard X-rays, are of great interest for many condensed matter material science and biology experiments. A multi-GeV electron beam with high peak current and low emittance is required for a high-performance X-ray FEL. Many facilities are presently constructed or being proposed while many upgrades are planned in serving this purpose [5, 6, 7, 8]. The future eRHIC ERL [9, 10] can be an excellent platform of providing such high quality electron beam as well. Although the major use of the electron beam in eRHIC is for electron hadron collision, a dedicated

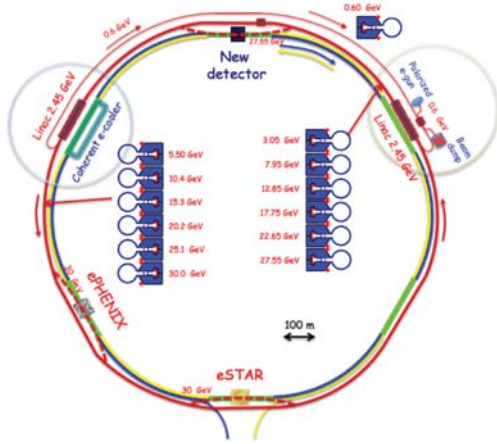

Figure 1: eRHIC layout with a 6 pass 30 GeV ERL. For FEL operation, the bunch compressor will be located at 12 o'clock, while two main linacs are at 2 and 10 o'clock respectively.

FEL operation mode could be planned. In such mode, an electron beam with extremely low emittance, low energy spread and sufficiently large bunch charge would be generated and well preserved through the beam transport to undulator. An array of X-ray FELs could be installed down stream to share the high repetition rate.

LAYOUT OF FEL OPERATION AT ERHIC

As we stated in previous seciton, eRHIC is a multi-pass ERL with a layout shown in Fig. 1. In normal routine operation, the electron beam will be accelerated in 6-pass to reach to its top energy at 30 GeV then collide with ion beams. After the collision, the electron beam energy will be recovered in the same linacs with 180 degree phase difference (decelerating mode) before going to beam dump. The entire machine has a 6-fold symmetry thus six straight sections can be used for linacs (which are located at 2 o'clock and 10 o'clock respectively) and possible experiment interaction regions.

However, for FEL operation, it is not neccessary to have a 30 GeV electron beam to get to the working regime (X-rays) we are interested in. At the mean time, to be accelerated to such a high energy, the electron beam traverses longer distances in circular passes and receives more exposure to synchrotron radiation which will result in having a larger energy spread. We choose a much lower e- beam energy (1.8 GeV – 10 GeV) allowing us to cover X-ray regime with current undulator technology. Electron beam will be injected from a different source with low normal-

* Work supported by Brookhaven Science Associates, LLC under Contract No. DE-AC02-98CH10886 with the U.S. Department of Energy.

† yjing@bnl.gov

ISBN 978-3-95450-123-6

PROGRESS ON THE GENERATION OF UNDULATOR RADIATION IN THE UV FROM A PLASMA-BASED ELECTRON BEAM

G. Lambert, S. Corde, K. Ta phuoc, V. Malka, LOA, ENSTA-CNRS-Ecole Polytechnique, Palaiseau, France
A. Ben Ismail, E. Benveniste, A. Specka, LLR, Ecole polytechnique, Palaiseau, France
M. Labat, A. Loulergue, F. Briquez, M.E. Couprie, Synchrotron Soleil, Gif-sur-Yvette, France

Abstract

Recently, at the Laboratoire d'Optique Appliquée (LOA), progresses have been made for the development of 5th generation light sources based on laser-plasma-accelerator. Electron beam from 100 to 150 MeV was generated at the interaction of a 1 Joule, 30 fs laser focused on a 3 mm long He gas target at an electron density of about $5*10^{18}$ cm^{-3}. Then, the electron beam was focused with a quadrupoles triplet inside a 60 cm long undulator composed of 34 periods of 18 mm. In these conditions, synchrotron radiation light was measured from 450 nm to 230 nm. This constitutes a promising first step in the view of realizing FEL based on plasma acceleration in future.

INTRODUCTION

Synchrotron radiation (SR) and Free-electron laser (FEL) generation processes are well known and understood since many decades. Nowadays, the facilities, which are using these conventional sources, are at the top of the art. Yet, due to the relatively low electric fields (about 30 MV/m) obtained in the classical accelerating structures, huge and high cost installations are necessary.

Advances on laser-plasma acceleration [1-8], in which accelerating fields up to 100 GV/m are created, have motivated the study of the feasibility of synchrotron radiation generation from undulator, in view of realizing a compact FEL. In fact, the number of FEL across the world is rather limited, even if increasing notably recently, and the demand of beam time coming from the user community is highly increasing. Moreover, FEL based on linear accelerator technologies have very limited number of beam lines. As a consequence, performing plasma-based FEL from table-top laser would represent a significant advance and allow to multiply significantly the number of accessible beam lines for studying physics, chemistry and biology.

Actually, this purpose seems quite far from today, but things have to start one day in order to understand better the actual level of possibilities, what has to be improved and in which direction we have to push forward in the coming years. Is the plasma-based electron acceleration mature for this area of activity?

This explains why in LOA, and in other groups all around the world [9-14], in view of getting experience on the way to generate plasma-based FEL, we decided, as a first step, to build a setup for generating synchrotron radiation from electrons wiggling in an undulator [15] and generated in the classical bubble regime.

EXPERIMENTAL SET-UP

The experiment (fig. 1) has been performed with the "salle jaune" Ti: Sa laser facility in LOA. This laser delivers linearly polarized pulses at 800 nm with more than 1 Joule energy, about 30 fs pulse duration and at a maximum of 10 Hz repetition rate. The electrons are generated by focusing the 55 mm aperture laser light with a 1 m length spherical mirror into a supersonic gas target. This latter is a 3 mm long pulsed jet filled with helium gas at pressure about 7 Bars leading to an electron density about $5*10^{18}$ cm^{-3}.

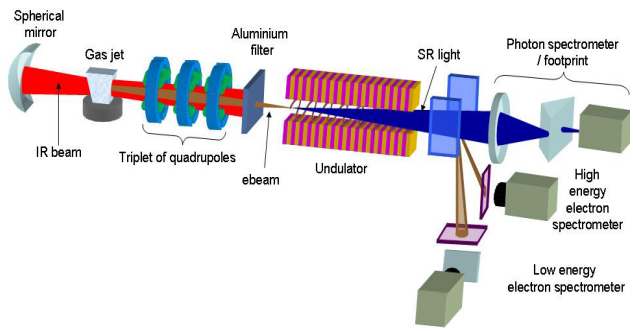

Figure 1: Layout of the experimental setup at LOA for generating synchrotron radiation from laser-plasma acceleration.

With the following conditions, 30 TW pulses focused in a 20 microns (FWHM) spot, the intensity reaches more than $1*10^{18}$ $W.cm^{-2}$ in the gas target, creating a plasma after the ionisation of the gas by the front part of the pulse. In this plasma, the ponderomotive force of the ultra-short laser pushes electrons outward, separates them from the ions and so creates a longitudinal electric field which velocity is close to the speed of light. With these typical electron densities the electric field of the so called "Wakefield" can reach more than 100 GV/m in accelerating structures. After being injected in the wakefield, a few electrons can be accelerated up to energies up to 1 GeV. The regime in which electrons are simply self-injected and accelerated inside the structures is called the "bubble regime". The experiment was performed in this regime.

After the laser-plasma acceleration, the relativistic electrons pass trough a triplet of specially-designed

ISBN 978-3-95450-123-6

NUMERICAL STUDY OF AN FEL BASED ON LWFA ELECTRONS AND A LASER-PLASMA WIGGLER *

R. Lehe†, G. Lambert, A.F. Lifschitz, V. Malka, J.-M. Rax
LOA, Chemin de la Hunière, 91761 PALAISEAU, FRANCE
X. Davoine, CEA, DAM, DIF, 91297 ARPAJON, FRANCE

Abstract

Recent works [1] have suggested that laser-wakefield acceleration (LWFA) may be used to produce the electron beam of an FEL, thereby considerably reducing the size and cost of the device. However, when using conventional magnetic wigglers, the requirements on the beam quality are very stringent, and are still challenging with current LWFA beams.

An interesting alternative may be to use a laser-plasma wiggler (e.g. a plasma wave or a laser beam). Compared to a conventional wiggler, a laser-plasma wiggler has a field amplitude several orders of magnitude higher, as well as a correspondingly shorter wavelength - which may place lower constraints on the beam quality and eliminate the need for transport. Taking into account beam quality, beam transport and wiggler inhomogeneity, we evaluate the range of wiggler properties (field, wavelength) that would make the FEL radiation possible.

From this analysis, the counterpropagating laser wiggler [2] seems to be one of the most promising solutions. We therefore extend the widely-used Ming Xie formula [3] (which was derived for a static, magnetic wiggler) to a counterpropagating laser wiggler. We use this formula to evaluate the potential use of current state-of-the-art lasers.

INTRODUCTION

Over the past ten years, laser-wakefield acceleration (LWFA) has proven to be a successful solution to accelerate electrons to hundreds of MeVs over distances of a few millimeters, which is more than a thousand times shorter than the distance required with a conventional wiggler. As a consequence, replacing the accelerator of an FEL with a laser-wakefield accelerator could drastically reduce the size and cost of the device. Yet, LWFA electrons typically have larger energy spread and divergence than those from a conventional accelerator, so that coupling them to a conventional magnetic wiggler is still challenging. This is due partly to the tight requirements on the beam quality and partly to the difficulty to transport the divergent beam from the accelerator to the wiggler.

Alternatively, the LWFA electrons could be coupled to a wiggler generated by laser-plasma interaction. Previous studies proposed for instance to use a plasma wave [4] or a laser pulse [2] as a wiggler. Such a wiggler has several advantages. First, it can be placed, by proper synchronization, only a few microns behind the accelerator and thereby eliminate the need for transport. Second, its strong field (laser pulses can have magnetic fields in the kiloTesla range) and short wavelength (in the micron range) may place looser constraints on the beam quality. Finally, a laser-plasma accelerator coupled to a laser-plasma wiggler would only be a few millimeters long (without taking into account the size of the laser amplifiers) and therefore extremely compact.

This paper is organized in two sections. In the first one, we evaluate the range of wiggler period and wiggler field strength that would make the FEL mechanism possible, from the point of view of the Ming Xie formula [3]. This section is general and applies to any kind of laser-plasma wiggler. Then, in the second section, we evaluate in more depth the potential of a particular wiggler : that consisting of a CO_2 laser pulse. Further degrading effects like expansion of the electron bunch and longitudinal wiggler non-uniformity – that were not considered in the first section – are taken into account.

RANGE OF PARAMETERS IN WHICH THE FEL MECHANISM IS POSSIBLE

We consider either a static magnetic wiggler or a counterpropagating laser wiggler. In the case of the static wiggler, the fields are of the form

$$\mathbf{E}_{static} = \mathbf{0} \quad (1)$$

$$\mathbf{B}_{static} = a_w \frac{mck_w}{e}(\sin(k_w z)\mathbf{e_x} + \cos(k_w z)\mathbf{e_y}) \quad (2)$$

where a_w is the dimentionless wiggling parameter, c is the speed of light, m and e are the mass and charge of an electron, $k_w = 2\pi/\lambda_w$ with λ_w corresponding to the wiggler period, and where the electron beam propagates along the z-axis in the positive direction. In the case of a laser wiggler

$$\mathbf{E}_{laser} = a_w \frac{mc^2 k_w}{2e}\left(-\cos\left(\frac{k_w(z+ct)}{2}\right)\mathbf{e_x} + \sin\left(\frac{k_w(z+ct)}{2}\right)\mathbf{e_y}\right) \quad (3)$$

$$\mathbf{B}_{laser} = a_w \frac{mck_w}{2e}\left(\sin\left(\frac{k_w(z+ct)}{2}\right)\mathbf{e_x} + \cos\left(\frac{k_w(z+ct)}{2}\right)\mathbf{e_y}\right) \quad (4)$$

* Work partially funded by the European Research Council through the ERC PARIS project.
† remi.lehe@polytechnique.edu

ISBN 978-3-95450-123-6

STEADY STATE MICROBUNCHING FOR HIGH BRILLIANCE AND HIGH REPETITION RATE STORAGE RING-BASED LIGHT SOURCES

Alex Chao, Daniel Ratner, SLAC, Menlo Park, USA
Yi Jiao, IHEP, Beijing, China

INTRODUCTION

Electron-based light sources have proven to be effective sources of high brilliance, high frequency radiation. Such sources are typically either linac-Free Electron Laser (FEL) or storage ring types. The linac-FEL type has high brilliance (because the beam is microbunched) but low repetition rate (see e.g. [1]). The storage ring type has high repetition rate (rapid beam circulation) but comparatively low brilliance or coherence. We propose to explore the feasibility of a microbunched beam in a storage ring that promises high repetition rate and high brilliance. The steady-state-micro-bunch (SSMB) beam in storage ring could provide CW sources for THz, EUV, or soft Xrays. Several SSMB mechanisms have been suggested recently, and in this report, we review a number of these SSMB concepts as promising directions for high brilliance, high repetition rate light sources of the future [2, 3, 4, 5].

The trick of SSMB lies in the RF system, together with the associated synchrotron beam dynamics, of the storage ring. Considering various different RF arrangements, there could be considered a number of scenarios of the SSMB. In this report, we arrange these scenarios more or less in order of the envisioned degree of technical challenge to the RF system, and not in the chronological order of their original references.

Once the stored beam is steady-state microbunched in a storage ring, it passes through a radiator repeatedly every turn (or few turns). The radiator extracts a small fraction of the beam energy as coherent radiation with a wavelength corresponding to the microbunched period of the beam. In contrast to an FEL, this radiator is not needed to generate the microbunching (as required e.g. by SASE FELs or seeded FELs), so the radiator can be comparatively simple and short.

CONVENTIONAL MICROWAVE RF SYSTEM

The simplest SSMB mechanism is the well-known conventional technique of shortening the steady state bunch length by raising the voltage of the RF system. Choosing a higher RF frequency, e.g. to X-band, also helps. Another way not involving RF is to introduce a small momentum compaction factor by the lattice design of the storage ring [6, 7]. Once the steady bunch length is reduced, this simplest SSMB scenario has been suggested to produce THz radiation.

This conventional SSMB scenario can be pushed further by combining the above-mentioned effects (higher RF voltage, higher RF frequency, and low momentum compaction factor). By pushing all three fronts simultaneously, a very short steady state bunch length can be reached [2].

Taking the SPEAR3 storage ring as an example, it was suggested by [2] to reduce the bunch length from 5 mm of the regular user operation mode to 0.3 mm, using a combination of reducing the momentum compaction factor α_p by a factor of 20 from the nominal value together with an application of X-band RF modulation of 7.6 MV applied every 4 turns. This scheme for THz generation has the advantage that it does not impose excessive demand on the usual microwave instability and the coherent synchrotron radiation effects.

LONGITUDINAL BETA BEAT

Pushing the conventional scenario to an extreme with much higher RF voltage and moving towards X-band RF frequency, an additional longitudinal beta-beat effect further shortens the bunch length [2].

We now consider the case when the RF is lumped at one location around the ring. We define the parameter

$$K = \frac{2eV_{mod}\alpha_p C}{E_0 \lambda_{mod}} \tag{1}$$

where C is the storage ring circumference, E_0 is the electron energy, V_{mod} and λ_{mod} are the voltage and wavelength of the RF modulation. Conventionally storage rings have $K \ll 1$, synchrotron oscillation is slow and the synchrotron tune is $\ll 1$. By contrast, in this scenario, K is on the level of 1 and with a localized RF system, it can be shown that the steady state bunch becomes unstable at the origin of phase space when $K > 4$.

Increasing K towards 4, the Courant-Snyder formalism can be used to describe the longitudinal synchrotron motion and electron phase space. The periodic longitudinal beta function β_z beats around the ring, and when K approaches 4, this beat becomes large, with the minimum beta occurring at the location diagonally opposite to the RF (assuming evenly distributed α_p). By locating the radiator at the minimum beta, the bunch gets shorter by an additional factor of $\sqrt{\beta_z}$.This scenario helps shortening a bunch further into the THz range.

The longitudinal beta-function is given by

$$\beta_z = \beta_{max} = \frac{2\alpha_p C}{\sqrt{K(4-K)}} \quad \text{at modulator RF}$$

$$\beta_z = \beta_{min} = \frac{\alpha_p C}{2}\sqrt{\frac{(4-K)}{K}} \quad \text{opposite modulator RF} \tag{2}$$

ISBN 978-3-95450-123-6

DYNAMICS OF A MULTI-BEAM PHOTONIC FREE ELECTRON LASER*

J.H.H. Lee#, M. W. van Dijk, T. Denis, P.J.M. van der Slot, K.-J. Boller,
Laser Physics and Nonlinear Optics, Mesa+ Institute for Nanotechnology,
University of Twente, Enschede, The Netherlands

Abstract

A photonic free-electron laser (pFEL) uses free electrons streaming through a photonic crystal (PhC) to generate tunable coherent radiation. Here, we consider a pFEL driven by a set of three low energy (~ 10 keV), low perveance (< 0.1 μP) electron beams. Using a particle-in-cell code, we numerically study the dynamics and calculate the small-signal growth rate and output power of the various modes. We show that for an appropriate design of the PhC and selective placement of the electron beams, single mode operation is possible. We will also present results on the scaling with the number of electron beams.

INTRODUCTION

In a photonic free-electron laser (pFEL) electrons can stream through the many channels that are available in a photonic crystal (PhC) and produce Cerenkov radiation [1]. The function of the PhC is to slow down the phase velocity of the electromagnetic wave to match the velocity of the co-propagating electrons. More precisely, one of the spatial harmonics that is part of a Bloch mode of the PhC will be phase matched with the co-propagating electrons. For a strong interaction, the field amplitude of the phase-matched spatial harmonic should be as high as possible, and therefore interaction with a low spatial harmonic is desirable [2]. If the Bloch mode possesses an electric field component in the propagation direction of the electrons, then the phase-matched spatial harmonic will bunch the electrons and coherent Cerenkov radiation will be emitted. The many channels that are naturally present in a PhC have the advantage that the total current transmitted through the PhC can be increased by adding more electron beams in parallel and extending the transverse extend of the PhC, while maintaining a low electron density in each beamlet. Consequently, beam quality and transport are greatly improved compared to increasing the total current by increasing the electron density in a single beamlet [3].

On the other hand, extending the transverse size of the PhC may lead to higher-order transverse Bloch modes that can all couple to the electrons and may introduce mode competition. In order to study the dynamics of a multi-beam pFEL, we use a particle-in-cell (PIC) code [4] to model a 3-beam pFEL operating at microwave frequencies. In the following we will present the PhC used in the pFEL and use PIC simulations to determine the starting current and investigate whether mode competition is present or not and how the mode competition is affected by the design of the PhC or placement of the electron beams.

*Work supported by Dutch Technology Foundation STW, applied science division of NWO and the technology program of the Ministry of Economic Affairs
#j.h.h.lee@utwente.nl

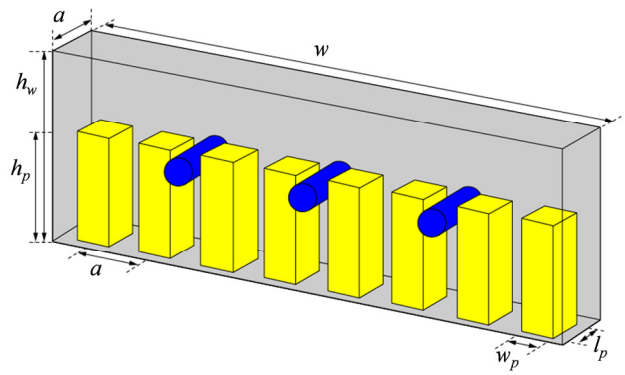

Figure 1: Schematic view of the unit cell of the photonic crystal used for the 3-beam pFEL. See Table 1 for dimensions. The location of the three electron beams used in the PIC simulations are shown as blue cylinders.

PHOTONIC CRYSTAL

The unit cell of the PhC used in this study is schematically shown in Fig. 1, and its dimensions are summarized in Table 1. It consists of a metal waveguide containing a periodic array of metal posts. The PhC is designed to produce microwave radiation around 15 GHz when low energy (~ 10 keV) electrons are used. The metal waveguide is required to guide/confine the microwave radiation.

The PhC effectively allows for seven electron beams to propagate through the structure. A 3-beam electron gun has been designed for use in a pFEL with the PhC [5]. The choice of emitter in this gun however limits the beam-to-beam spacing to 5 mm, hence the beams shown in Fig. 1 fill every other available slot.

Table 1: Dimensions of the PhC Unit Cell

Parameter	Description	Value
w	Width of unit cell / waveguide	20.0 mm
h_w	Height of unit cell /waveguide	7.0 mm
a	Depth of unit cell & distance between posts	2.5 mm
w_p	Width of posts	1.3 mm
l_p	Depth of posts	1.5 mm
h_p	Height of posts	4.0 mm

ISBN 978-3-95450-123-6

TWO-COLOR FEL SCHEMES BASED ON EMITTANCE-SPOILER TECHNIQUE

C. Feng, SLAC National Accelerator Laboratory, Menlo Park, CA 94025, USA,
Shanghai Institute of Applied Physics, CAS, Shanghai 201800, China
Y. Ding, Z. Huang, J. Krzywinski and A. Lutman
SLAC National Accelerator Laboratory, Menlo Park, CA 94025, USA

Abstract

Generation of two-pulse two-color x-ray radiation is attracting much attention within the free-electron laser (FEL) user community. Femtosecond and attosecond x-ray pulses with variable duration and separation can be simply generated by the emittance-spoiler foil method at the Linac Coherent Light Source (LCLS). In this paper, we describe and compare three FEL schemes rely on the emittance-spoiler technique for the generation of two intense x-ray pulses with different colors. With a representative realistic set of parameters of LCLS, numerical simulations confirm that femtosecond x-ray pulses at ten gigawatt level at x-ray wavelengths can be generated by these schemes. The central wavelengths of the output pulses can be easily altered by changing strengths of the undulators.

INTRODUCTION

Two-color operation of Free-electron lasers (FELs) at variable wavelengths in the x-ray regime is of considerable interest in recent days. Applications exist over a broad range of wavelengths involving pump-probe experiments, especially the measurement of the evolution of valence electronic wave packets using Stimulated X-ray Raman Spectroscopy (SXRS) [1]. The SXRS generally requires a pair of ultra-short x-ray pulses with different colors. The first x-ray pulse with carrier wavelength tuned on resonance with a given core hole is used to create a valence electronic wave packet localized in the vicinity of a selected atom. This wave packet is later probed by a window localized on a different atom, selected by the second x-ray pulse with different carrier wavelength. All valence electronic states within the pulse bandwidths can be observed with high spatial and temporal resolution by monitoring the variation of the signal with the delay between the pulses. The atom specificity helps to define where the wave packet of valence electrons is created and where it is probed, which simplifies the analysis of the experiment and aids in understanding the spatial distribution of the valence electron wave packets. It has been proposed in Ref [2] that this kind of two attosecond x-ray pulses with different colors can be produced using the same electron bunch by a two stage seeded FEL scheme, which combine the current enhanced self-amplified spontaneous emission and the echo-enabled harmonic generation technique.

The Linac Coherent Light Source (LCLS) has been in operation since 2009 [3]. An emittance-spoiling foil was added later in the middle of the second bunch compressor for generating femtosecond and attosecond intense x-ray radiation pulses with variable duration and separation [4-6]. At soft x-ray regime, almost single-spike pulses can be generated with using the slotted foil setup, as can be seen in the following examples. If the carrier wavelength of each radiation pulse could be separately controlled, this kind of radiation pulses can also be used for the SXRS experiments.

The emittance-spoiling foil method takes advantage of the fact that the SASE gain process is highly sensitive to the transverse slice emittance. By adding an emittance spoiler foil with vertically oriented narrow slots in the central of the bunch compressor chicane, the emittance of most of the electron beam will be spoiled while leaving only short unspoiled parts to produce x-ray radiation pulses much shorter than the total electron bunch. The central wavelength of each radiation pulse is fixed by the energy of the electron beam γ and the undulator parameter K, and can be written as

$$\lambda_r = \frac{\lambda_u}{2\gamma^2}\left(1+K^2/2\right), \qquad (1)$$

where λ_u is the magnetic period of the undulator and K varies with the undulator gap for the permanent magnet undulators. There are generally two methods that can be used to make the carrier wavelengths of the radiation pulses different: one method is impact an energy chirp on the electron beam to make the central energies of the unspoiled parts of the electron beam different. By using this method, the output wavelengths generated by different parts of the electron beam will be correlated with the separation between the radiation pulses and not easy to separately control. Another method which can be used to overcome this problem is making the electron beam passing through two undulator sections with different undulator parameters, K_1 and K_2, respectively. The output wavelengths of the two pulses can be separately tuned by changing the gaps of the undulators. In this paper, we propose three schemes based on the emittance-spoiler technique and variable gap undulators to generate two-color ultra-short x-ray pulses with variable time delay for user applications such as the SXRS experiment.

METHODS

The layouts of the undulator systems of the three proposed schemes are schematically shown in figure 1. The first two schemes consist of two variable-gap undulator sections separated by a chicane. One may find

ISBN 978-3-95450-123-6

APPLICATION OF LASER-PLASMA ACCELERATOR BEAMS TO FREE-ELECTRON LASERS*

C.B. Schroeder, C. Benedetti, E. Esarey, W.P. Leemans, J. van Tilborg,
LBNL, Berkeley, CA 94720, USA
Y. Ding, Z. Huang, SLAC, Menlo Park, CA 94025, USA
F.J. Grüner, A.R. Maier, CFEL, 22607 Hamburg, Germany

Abstract

Laser-plasma accelerators are able to produce ultra-high accelerating fields, enabling compact accelerators, and ultra-short (fs) beams with high-peak currents. We review recent progress on the development of laser-plasma accelerators and, in particular, recent measurements characterizing the properties of an electron beam generated by a laser-plasma accelerator. It is shown that the 6D beam brightness of a laser-plasma accelerated beam is comparable to state-of-the-art conventional electron beam sources. Given present experimentally achievable laser-plasma accelerator electron beam parameters, we discuss beam decompression as a method of realizing a laser-plasma-accelerator-based free-electron laser.

INTRODUCTION

Laser-plasma accelerators (LPAs) have attracted considerable attention owing to their ability to generate ultra-high accelerating gradients, enabling compact accelerators. Laser-plasma acceleration is realized by using a high-intensity laser to ponderomotively drive a large plasma wave (or wakefield) in an underdense plasma [1]. The plasma wave has relativistic phase velocity, and can support large electric fields in the direction of the laser propagation. When the laser pulse is approximately resonant (pulse duration on the order of the plasma period) and the laser intensity is relativistic, with normalized laser vector potential $a = eA/m_e c^2 \sim 1$, the size of the accelerating field supported by the plasma is on the order of $E_0 = m_e c\omega_p/e$, or $E_0[\mathrm{V/m}] \simeq 96\sqrt{n_0[\mathrm{cm}^{-3}]}$, where $\omega_p = k_p c = (4\pi n_0 e^2/m_e)^{1/2}$ is the electron plasma frequency, n_0 is the ambient electron number density, m_e and e are the electronic mass and charge, respectively, and c is the speed of light in vacuum. For example, an accelerating gradient of $\sim$ 100 GV/m is achieved operating at a plasma density of $n_0 \sim 10^{18}$ cm^{-3}. Owing to these ultra-high accelerating gradients LPAs are actively being researched as compact sources of energetic beams for light sources [2, 3, 4, 5] and future linear colliders [6].

In addition to extremely large accelerating gradients, plasma-based accelerators intrinsically produce ultra-short (fs) electron bunches that are a fraction of the plasma wavelength $\lambda_p = 2\pi/\omega_p$ or $\lambda_p[\mathrm{m}] = 3.3 \times 10^4/\sqrt{n_0[\mathrm{cm}^{-3}]}$. Because of the short beam durations, LPAs are sources of high peak current beams ($\sim$1–10 kA), and, hence, it is natural to consider LPA electron beams as drivers for a free-electron laser (FEL) producing high-peak brightness radiation. LPA electron beams have been coupled into undulators to produce undulator radiation in the visible [7] and soft-x-ray [8]. In this proceedings paper we consider the prospects for applying LPA electron beams to drive an FEL.

* Work supported by the Director, Office of Science, of the U.S. Department of Energy under Contract No. DE-AC02-05CH11231, by the National Science Foundation under Grant and PHY-0917687.

LASER-PLASMA ACCELERATOR BEAM PHASE SPACE

High-quality electron beams up to $\sim$1 GeV have been experimentally demonstrated using 40 TW lasers interacting in centimeter-scale plasma channels [9, 10]. Figure 1 shows a single-shot spectra of a 500 MeV electron beam generated using the LPA at LBNL. In Fig. 1 a 1.5 J, 0.8-μm laser interacts with a 225 μm diameter H-discharge capillary with on-axis density 3.5×10^{18} cm^{-3}. The H-discharge capillary forms a plasma channel for guiding the laser. LPAs are capable of compactly producing 0.5 GeV beams with tens of pC of charge, few percent-level relative energy spread, and mrad divergences, and here we will consider such a beam for driving an FEL.

Recent experimental effort in the plasma-based accelerator community has been focused on improved diagnostics and measurements of the LPA electron beam phase space, and, in particular, measurements of the beam transverse emittance and the beam duration.

Transverse Emittance

The beam transverse size in the plasma wave can be determined by measuring the spectrum of betatron x-rays produced by the beam in the plasma wave [11, 12, 13]. The electron beam undergoes betatron motion in the strong focusing forces ($F_\perp \sim eE_0 k_p r$) of the plasma wave, and emits fs, hard x-rays [14]. The effective wiggler strength parameter $a_\beta = \gamma_z k_\beta r_\beta$ is typically large $a_\beta \gg 1$ (where γ_z is the Lorentz factor of the longitudinal momentum, k_β the betatron wavenumber, and r_β the amplitude of the electron betatron orbit), and the x-ray spectrum is broad. The spectrum is characterized by the critical frequency $\omega_c \simeq 3a_\beta\gamma_z^2 k_\beta c \propto \gamma_z^2 n_0 r_\beta$. Owing to the strength of the transverse focusing force in the plasma wave, the beam emits hard x-rays ($\sim$10 keV). By measuring the spectrum (i.e., ω_c), the amplitude of the betatron oscillation r_β (i.e., the beam radius) may be estimated. This measurement is a non-invasive, in situ, single-shot diagnostic of the

ISBN 978-3-95450-123-6

SWISSFEL U15 MAGNET ASSEMBLY: FIRST EXPERIMENTAL RESULTS

M.Calvi, M.Brügger, S.Danner, A.Imhof, H. Jöhri, T.Schmidt and C.Scoular
Paul Scherrer Institute, CH 5232 Villigen PSI, Switzerland

Abstract

In the framework of the SwissFEL project, an R&D activity concerning in-vacuum undulator technology is ongoing at the Paul Scherrer Institut. The magnetic field configuration of the hard X-ray SwissFEL undulators has been designed on purpose for a single pass machine. Moreover the permanent magnet material (NdFeB) is manufactured following a novel procedure (Dy diffused in the grain boundaries) to improve the coercivity versus remanence. The assembly and tests of a 44 periods hybrid magnetic structure are presented. Procedures for the magnetic field, trajectory and phase optimization are reported versus experimental results.

INTRODUCTION

The SwissFEL is the free electron laser in construction at the Paul Scherer Institute (PSI) in Switzerland. The first beam-line planned is called Aramis and shall deliver photons with wavelengths of 0.7 down to 0.1 nm. It is driven by a linac with a maximum electron energy of 5.8 GeV followed by a chain of in-vacuum permanent magnet undulators (U15). The period length is 15 mm and the K-value can be set between 0.1 and 1.6, changing the gap from 3 up to 20 mm. To meet these requirements NdFeB magnet manufacture should be improved and this is a part of the development ongoing between industries and PSI. Additional changes in the magnetic design were introduced to take advantages from the specific requirements of a linac driven free electron laser with respect to a synchrotron light source.

The undulator line is made of 12 units, each of 4 m length and 267 periods. The design of the frame and the gap drive system is part of the R&D activity ongoing at PSI and details can be found in [1]. A technical overview of the SwissFEL undulator line can be found in [2].

SINGLE MAGNET

The magnetic material selected for the U15 is NdFeB with a remanence of 1.25 T and a coercivity higher than 2300kA/m. With the conventional manufacturing procedure it is not possible to achieve these performances, the Dy used to stabilize the material has the disadvantage to hold a momentum opposite to Nd. As more Dy is added the coercivity continues to increase while remanence decreases. Hitachi Metal Ltd developed a new technique which can be applied to thin magnets. After machining the magnets to the final geometry, they are placed inside a vacuum oven where Dy is vaporized and it diffuses along the grain boundaries. They demonstrate that this approach increases the coercivity of about 320kA/m while the remanence remains substantially invariant. The rational behind this technique is the lower amount of Dy required to stabilize the magnet. The instabilities enucleate at the level of the grains in the material, the presence of Dy in the boundaries is enough to prevent this dynamic and to stabilize the magnet. This new technique has never been applied to undulator magnets and this was one of the reason to spend more effort and build a short prototype to prove the quality and reliability of this approach.

To decrease the spread of the magnetization value and error angles among the magnet production, tighter mechanical tolerances than in the SLS undulators were specified. The results of the Helmholtz coil measurements of the first 1400 magnet produced indicated a momentum spread RMS value of 0.35% and an angular RMS error of 0.185°. The histograms representing the full magnet production are presented in Fig.1.

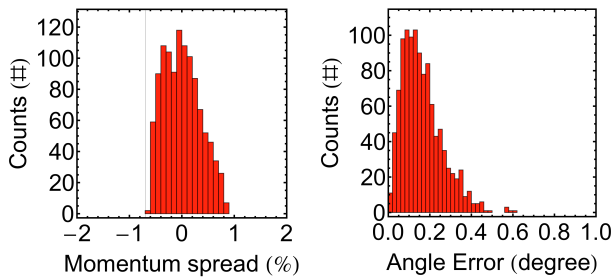

Figure 1: The statistic of the first 1400 magnets produced by Hitachi. On the left the momentum spread and on the right the magnetization angle error.

The assessment of a second magnet manufacture is ongoing to increase the offer in view of the next year production of the magnet for the full undulator line. The first batch has been received recently and a second 44 period short prototype will be assembled.

Within a Swiss program for supporting the local industries in improving their quality and innovation, an R&D activity is ongoing to demonstrate the feasibility of micro-water jet cutting applied to the high quality permanent magnet manufacturing. The first batch of magnet samples has been produced and the mechanical tolerances achieved are beyond the standard quality available on the market. The magnetic measurements of single magnets are ongoing.

MAGNETIC DESIGN

The U15 has a hybrid magnetic structure, made out of permanent magnets and iron (permendur) poles. The standard configuration which consists of one pole and two magnets have been changed into a more cost effective one consisting of a single pole and a single magnet as the

ISBN 978-3-95450-123-6

SWISSFEL U15 PROTOTYPE DESIGN AND FIRST RESULTS

T. Schmidt, P. Böhler, M. Brügger, M. Calvi, S. Danner, P. Huber, A. Imhof, H. Jöhri, A. Keller, M. Locher, T. Stapf, J. Wickstroem, Paul Scherrer Institute, CH 5232 Villigen PSI, Switzerland

Abstract

SwissFEL [1] has in its base line design two undulator lines for the hard- and soft x-ray, U15 in-vacuum and U40 / UE40 APPLE II type undulators with 12 respectively 15 modules of 4m length each. All undulators are equipped with the same frame and gap drive system to profit best from the series production. The frame is built up from two identical bases and side frames made of cast mineral. In this design, the frame transfers its stiffness to the I-beam through a backslash-free wedge based gap drive system. The interfaces to the inner I-beam for the in-vacuum undulator have been rearranged allowing a large reduction in the number of columns. Magnets and poles are carried by an extruded Aluminium block-keeper, which will allow an automatized shimming of the magnet structure. The prototype of the support structure has been built up in 2012 and first mechanical results are presented. The entire prototype shall be ready by the end of 2012.

SWISSFEL UNDUALTOR LINES

SwissFEL will have two undulator lines. The one for hard X-rays from, 7 Å (2 keV) to 1 Å (12.4 keV), with an electron energy of 5.8 GeV, is named Aramis. The second one, covering the entire soft X-ray range, from about 200 eV to 2 keV with full polarization control, is named Athos. In the baseline design, the Aramis line has 12 in-vacuum undulators U15's with 15mm period. However, there are free slots, which can be used i.e. for (self)-seeding. An overview of the Aramis undulator line is given in [2], the magnet array is discussed in detail in [3].

The Athos line will follow in 2020 and has a self-seeding design with 6 planar U40's and 9 APPLE II type UE40's, both with 40mm period. This sums up to 27 undulators. All undulators are 4m long each and have an identical intersection length of 75cm. The design large number of identical undulators for linac driven FELs is well suited for a consequent industrial based small series production.

SPECS AND DESIGN GUIDELINES

The specifications for the SwissFEL undulators can be summarized as follows:

- Short period undulators for Aramis beamline
- Variable polarization for Athos beamline
- Low beam height
- Low costs

SwissFEL has in the pool of hard x-ray FELs with 5.8GeV the lowest electron energy. To achieve photon energies of 12.4keV (1Å wavelength), the undulator period length has to be very small. For SwissFEL it has been optimized to a 15mm period. At a gap of 4.3mm a magnetic flux density of 0.85T provides the design K-value of 1.2. The low electron energy requires in addition small tolerances in all parts of the accelerator and the undulators .

As all forms of transport in SwissFEL tunnel are on the floor (no crane) a common floor level in the entire tunnel is foreseen. The beam height is determined by the undulators and needs to be reduced with respect to the 1.4m beam height at Swiss Light Source. And, of course the costs had to be optimized and as a consequence there is no technical gallery accompanying the undulator hall.

The basic design ideas for the SwissFEL undulators are:

- Modular undulator concept
- O-shape structure
- Use of cast and extruded materials
- Drive system on board
- Remote controlled alignment
- High stability and precise gap drive system.

SUPPORT AND GAP DRIVE

The most demanding undulators with respect to the support structure are the APPLE II type undulators which, when operated in anti-symmetric mode to produce linear inclined polarization, bring in not only vertical forces but also longitudinal and horizontal forces. Therefore the design for a modular undular concept in which the support and gap drive is identical for all types of undulators and only the magnet array with its vacuum system is adapted to the specific undulator type i.e. planar in and out of vacuum and APPLE II. The benefit is reduced engineering, larger series and a common transport concept which overcomes the drawback of partly oversized components.

Support Structure

For maximum stiffness the support structure is not the classical C-structure but a closed O-shape structure. Experience with cryogenic in-vacuum undulators where magnetic measurements inside the vacuum chamber are mandatory lead in recent years to the development of smarter measurement systems where the magnet structure tightly encloses the vacuum chamber a remote alignment required the vacuum chamber to be supported by the undulator itself. Best for series production is cast material, either cast iron or cast mineral which is used in many machine beds. For the SwissFEL undulator supports cast mineral is chosen: it has good internal damping characteristics, is non-magnetic, is cheap in series production and integrated channels for weight reduction can be used as cable traces.

ISBN 978-3-95450-123-6

HIGH DYNAMIC RANGE BEAM IMAGING WITH TWO SIMULTANEOUSLY SAMPLING CCDS*

P. Evtushenko#, D. Douglas, R. Legg, C. Tennant, JLab, Newport News, USA

Abstract

Transverse beam profile measurement with sufficiently high dynamic range (HDR) is a key diagnostic to measure the beam halo, understand its sources and evolution. In this contribution we describe our initial experience with the HDR imaging of the electron beam at the JLab FEL. Contrary to HDR measurements made with wire scanners in counting mode, which provide only two or three 1D projections of transverse beam distribution, imaging allows to measure the distribution itself. That is especially important for non-equilibrium beams in the LINACs. The measurements were made by means of simultaneous imaging with two CCD sensors with different exposure time. Two images are combined then numerically in to one HDR image. The system works as an online tool providing HDR images at 4 Hz. An optically polished YAG:Ce crystal with thickness of 100 μm was used for the measurements. When tested with a laser beam, images with a dynamic range (DR) of about 10^5 were obtained. With the electron beam the DR was somewhat smaller due to the limitations in the time structure of the tune-up beam macro pulse.

MOTIVATION

High current CW SRF LINACs with average current of several mA have been used to provide electron beam for high average brightness, high power IR FELs [1]. It is proposed that LINACs with similar average current and beam energy in the range 0.6 – 1.2 GeV can be used as the drivers for next generation of high average brightness light sources operated in X-ray wavelength range in seeded FEL configuration. The existing pulsed FELs, operating now in the soft and hard X-ray wavelength ranges, utilize average currents many orders of magnitude less than the above-mentioned mA. At the same time, operation of the IR/UV-Upgrade at Jefferson Lab with average current of up to 9 mA has provided an experience base with high-current LINAC operation [1]. The primary operational difference between such high current LINACs and storage rings, even with a few hundred mA of average current, is that LINAC beams have neither the time nor the mechanism to come to equilibrium, in contrast to storage ring beams, which are essentially Gaussian. This has significant operational impact. When a LINAC is setup, by establishing the longitudinal and transverse match, a tune-up beam with small average current is used. Such an accelerator setup is based most frequently on measured mean and RMS parameters such as beam size, bunch length, and energy spread. When going from tune-up mode to higher duty cycle and CW operation, it is frequently found that the "best" RMS-data-based setup must be changed to allow for high current operation to eliminate beam losses. Even when this modification is successful, it is time-consuming process involving some trial and error. It is frequently unclear what the sources of the problem are, and which adjustments to the low-density parts of the phase space distribution were effective in improving performance. This is highly undesirable for any user facility where high availability is required. Also of significance is that the resulting setup does not necessarily provide the best beam brightness and is a compromise between acceptable brightness and acceptably low beam losses.

Contributing to this problem is the fact that the measurements used for machine setup are typically based on methods with a DR of 10^3 or even less. It is not surprising that the relevant (from the high current operation and beam loss point of view) low-intensity and large-amplitude parts of the phase space are simply not visible during machine tuning.

Therefore, we think that the proper solution to the aforementioned tune-up problem is to base the tuning on the measurements with much larger, than routinely used now, DR, such that the very low intensity and large amplitude parts of phase space distribution are taken in to account from the very beginning. We are presently developing such diagnostics at the JLab FEL. The ultimate goal is to be able to measure both the transverse and longitudinal phase space with a DR of about 10^6. Measurements of both phase spaces can be based on the HDR transverse beam profile measurements, which is the first step in our program. One of the techniques we are developing is the HDR beam imaging. Here we present our technique and first results of transverse beam profile measurements with extended DR and its application to emittance and Twiss parameters measurements.

EXPERIMENTAL SETUP

Operation of the JLab FEL relies very heavily on the transverse beam profile measurements made in many places around the machine. Even with a relatively compact footprint the IR and UV recirculators beamlines have 62 viewers and synchrotron light monitors in total. This has allowed us to accumulate a lot of experimental experience with transverse beam profile measurements. From this experience we know the intensity of the beam image on the CCD matrix from OTR or YAG:Ce viewer with the typical beam size and with the amount of beam charge in the tune-up macro pulse. It also agrees well with calculations. Thus one can tell that, for the measurements with the OTR and DR of 10^6 an additional gain in the range between 10 and 100 would be needed, and the measurements with YAG:Ce may not need additional

*Work supported by US DOE office of Basic Energy Sciences under the early career program; DOE award number FWP#JLAB-BES11-05
Pavel.Evtushenko@jlab.org

ISBN 978-3-95450-123-6

PROBING TRANSVERSE COHERENCE WITH THE HETERODYNE SPECKLE APPROACH: OVERVIEW AND DETAILS

M. Manfredda, M.D. Alaimo, M.A.C Potenza
Università degli Studi di Milano & INFN, Milano, Italy
M. Giglio, Università degli Studi di Milano, Milano, Italy

Abstract

Spatial Coherence properties of radiation produced by accelerated relativistic electrons are far from being trivial. The correct assessment of coherence of High-Brilliance X sources (3rd generation Synchrotron or FEL) is of crucial importance both in machine diagnostics and in experiment planning, in the case coherent techniques are used. Classical methods (Young's interferometer) provides a mild knowledge of the spatial coherence.

The Heterodyne Speckle Approach [1],[2] is a valuable alternative that exploits the statistical analysis of light scattered by spherical particles. The technique needs a very essential setup composed only by a water suspension of commercial colloidal particles and a CCD camera. Coherence information are retrieved from the Fourier analysis of the interference pattern generated by the stochastic superposition of the waves scattered by the particles and the unperturbed transmitted beam (heterodyne configuration). The technique a) provides a direct measure of transverse coherence without a-priori assumptions, b) provides full 2D coherence map with single-distance measures, c) has been proved to be capable of time-resolved measures with SR sources (ID06, ESRF), d) is potentially scalable over a wide range of wavelengths (tested 400nm, 0.1nm). It has been used for coherence measures both at the usage point and at the front-end of an undulator source (ID02-ESRF, Grenoble).

INTRODUCTION

Transverse coherence measurement are commonly performed looking at the quality of interference fringes of some kind of ad-hoc engineered device, being Young's interferometer the progenitor of these kind of techniques. The visibility of a given fringe system is proportional to the modulus of the so called Complex Coherence Function, defined as

$$\mu(\vec{r},\Delta\vec{r}) = \frac{\left\langle e_0(\vec{r}) e_0^*(\vec{r}+\Delta\vec{r})\right\rangle}{\sqrt{\left\langle \left|e_0(\vec{r})\right|^2\right\rangle \left\langle \left|e_0^*(\vec{r}+\Delta\vec{r})\right|^2\right\rangle}} \qquad (1)$$

Here the brackets denote the ensemble average over many radiation pulses, since we are dealing with radiation produced by relativistic bunched electrons. In the case of natural thermal sources, like stars, fire and so on, brackets usually denote the time average, so that $\mu(\vec{r_0},\vec{r_0}) = I(\vec{r_0})$ is the classical definition of intensity at $\vec{r_0}$. Notice that the normalization by the mean intensity makes the coherence independent of the intensity profile of the beam, as it must be.

The fact that two points enter the definition of $\mu(\vec{r_0},\vec{r_0})$ means that the mutual degree of coherence of a certain field may vary both with the distance between the probing points $\Delta\vec{r}_{12} = \vec{r}_1 - \vec{r}_2$ and with the position across the beam $\vec{R}_{12} = (\vec{r}_1 + \vec{r}_2)/2$. For homogenous fields the coherence properties are constant all across the beam, so that μ is function of Δr only, regardless of which points are chosen. It must be stated, however, that coherence non-homogeneity can be introduced by beamline optics, so that dropping the dependence on $\vec{R}$ may not be the most recommended solution if one is concerned with optics testing (see for instance [3]).

In providing a 2D map of coherence, the main issue is the capability to explore a wide range of displacements $\vec{r}$ by means of a reasonable experimental setup. Young's interferometer is the simplest but even most inefficient setup, since it requires different pinhole separations and orientation. Other interferometric devices have been developed, in which the modulus of $\Delta\vec{r}$ can be selected by varying the observation distance and its direction by varying the test-plate orientation. But one can do even better, choosing a system in which there is no need to select $\Delta\vec{r}$. at all. The idea is just to write the coherence information corresponding to all the scale lengths on a 2D detector at once, then use Fourier analysis to separate the different spatial spectral contributions.

The system in question is a random distribution of scattering particles in solution. Particles used at visible and Angstrom wavelength are commercial (1um and 0.4um respectively) and are extremely cheap, and no kind of accurate positioning is required.

For a sort of conservation principle, all the efforts that in traditional approach are profused in the development and engineering of complex manufacts, the other one are dedicated to the study and comprehension of a simple physical system. More involved interferometric system than Young's one have been developed. But they all suffer the need of introducing a preferred direction of analysis (or two, in the best cases)

A SIMPLIFIED DESCRIPTION

One-particle and Many Particle

Information about coherence is completely contained in the interference fringes produced by the unperturbed

ISBN 978-3-95450-123-6

THE LUNEX5 PROJECT

M. E. Couprie, C. Benabderrahmane, P. Betinelli, F. Bouvet, A. Buteau, L. Cassinari, J. Daillant, J. C. Denard, P. Eymard, B. Gagey, C. Herbeaux, M. Labat, A. Lestrade, A. Loulergue, P. Marchand, O. Marcouillé, J. L. Marlats, C. Miron, P. Morin, A. Nadji, F. Polack, J. B. Pruvost, F. Ribeiro, J. P. Ricaud, P. Roy, T. Tanikawa, Synchrotron SOLEIL, Saint-Aubin, France
R. Roux, Laboratoire de l'Accélérateur Linéaire, Orsay, France
S. Bielawski, C. Evain, C. Szwaj, PhLAM/ CERLA, Lille, France
G. Lambert, R. Lehe, A. Lifschitz, V. Malka, A. Rousse, K. Ta Phuoc, C. Thaury, LOA, ENSTA-CNRS-Ecole Polytechnique, Palaiseau, France
X. Davoine, CEA-DAM Arpajon, France
A. Dubois, J. Lüning, LCPMR, Paris-VI, France
G. LeBec, L. Farvacque, ESRF, Grenoble, France
G. Devanz, M. Luong CEA/DSM/IRFU/SACM, B. Carré, CEA/DSM/IRAMIS/SPAM, Saclay, France

Abstract

LUNEX5 (free electron Laser Using a New accelerator for the Exploitation of X-ray radiation of 5th generation) aims at investigating the production of short, intense, and coherent pulses in the soft X-ray region. The project consists of a Free Electron Laser (FEL) line enabling the most advanced seeding configurations: High order Harmonic in Gas (HHG) seeding and Echo Enable Harmonic Generation (EEHG) with in-vacuum (potentially cryogenic) undulators of 15 and 30 mm period. Two accelerator types feed this FEL line : a 400 MeV Conventional Linear Accelerator (CLA) using superconducting cavities compatible with a future upgrade towards high repetition rate, for the investigations of the advanced FEL schemes; and a 0.4 - 1 GeV Laser Wake Field Accelerator (LWFA), to be qualified in view of FEL application, in the single spike or seeded regime. Two pilot user experiments for time-resolved studies of isolated species and solid state matter dynamics will take benefit of LUNEX5 FEL radiation and provide feedback of the performance of the different schemes under real user conditions.

INTRODUCTION

X-ray FEL sources open fantastic scientific opportunities but still with a limited access and high cost. LUNEX5 (see fig. 1) aims at proposing a short pulse compact FEL incorporating seeding schemes and new accelerating techniques and at efficiently producing and using stable, coherent, and short X-ray pulses and at extending the national community of X-ray users for the time resolved and coherent imaging studies.

Seeding enables to reduce the saturation length and the jitter, to improve the longitudinal coherence with respect to the Self Amplified Spontaneous Emission (SASE) one [1], which exhibits spiky longitudinal and temporal pulse distributions, apart from single spike operation for low charge regime [2]. FEL can be seeded either with amplified spontaneous emission from first stage undulators sent through a monochromator (so-called self-seeding) [3] or with an external laser or a short wavelength coherent light source, such as HHG [4, 5]. The EEHG [6] scheme with a double electron–laser interaction can extend the spectral range towards shorter wavelengths when operating on a high order harmonic of the seed wavelength.

Laser Wakefield Accelerators (LWFA) using the interacrion of intense laser beams with high electric field in plasmas progress rapidly. They are extremely compact (GeV/cm) and can provide high quality particle beams in extremely short bunches (a few fs) with very high peak currents (a few kA) [7]. FEL application can be viewed as an intermediate qualification [8] of GeV LWFA beams before proceeding to TeV LWFA colliders.

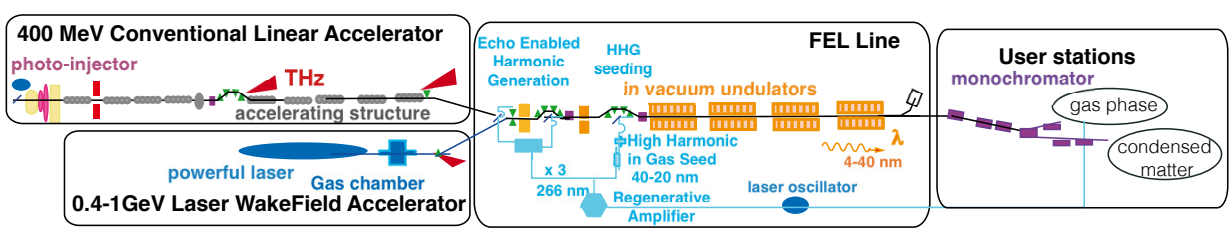

Figure 1: LUNEX5 scheme.

ISBN 978-3-95450-123-6